11-15-2019 10:00 AM

The Epigenetic And Immune Landscapes Of HPV+ Tumor Microenvironments

Steven F. Gameiro, *The University of Western Ontario*

Supervisor: Mymryk, Joe S., *The University of Western Ontario*

A thesis submitted in partial fulfillment of the requirements for the Doctor of Philosophy degree in Microbiology and Immunology

Abstract

Human papillomaviruses (HPVs) are responsible for approximately 4.5% of the global cancer burden. Virtually all cervical cancers (CESC) are caused by HPVs, as well as a subset of head and neck squamous cell carcinomas (HNSC). Our studies began by using data from over 800 CESC and HNSC samples from The Cancer Genome Atlas (TCGA) to test a model proposed from *in vitro* studies of an HPV-dependent deregulation of the *cyclin-dependent kinase inhibitor 2A* (*CDKN2A*) locus. Similar to the proposed models, we found that the HPV+ TMEs—regardless of tissue of origin—expressed significantly higher levels of *KDM6A* which demethylates the repressive tri-methylated lysine 27 on histone 3—critical for tightly regulating expression from the aforementioned locus. Furthermore, we also found that CpG methylation of the *CDKN2A* locus was consistently altered in HPV-positive (HPV+) tumors. We next wanted to test another *in vitro* model that proposed an HPV-dependent transcriptional downregulation of genes that encode for essential products of the class I major histocompatibility complex I (MHC-I) antigen presentation system. Utilizing the same large TCGA cohorts, we unexpectedly found that these genes were expressed at high levels in HPV+ tumors. The high mRNA levels of the MHC-I antigen presentation apparatus could be a consequence of the higher intratumoral levels of interferon-gamma (IFNγ) observed in HPV+ carcinomas, which correlated with signatures of increased infiltration by T- and NK-cells. In addition, we also found increased expression of the class II MHC antigen presentation system in HPV+ HNSC. Furthermore, we observed that HPV+ HNSC TMEs exhibited a strong bias towards a Th1 response which was characterized by increased infiltration with multiple types of immune cells and expression of their effector molecules. Moreover, the HPV+ HNSC TME also expressed high levels of multiple T-cell exhaustion markers that were indicative of a T-cell-inflamed phenotype. Overall, these analyses have provided significant insight into the validity of models proposed from experiments conducted in relatively artificial *in vitro* culture systems. Importantly, these studies have illustrated, in great detail, the strikingly profound differences in both the epigenetic and immune landscapes between the tumor microenvironments of HPV+ and HPV-negative carcinomas.

Summary for Lay Audience

Human papillomaviruses (HPVs) are responsible for approximately 4.5% of the global cancer burden. Virtually all cervical cancers (CESC) are caused by HPVs, as well as a subset of head and neck squamous cell carcinomas (HNSC). CESC and HNSC are the 4th and 7th most common cancers worldwide, respectively. The distinctive etiological factors that are involved in CESC and HNSC tumorigenesis—such as the expression of exogenous oncogenic viral antigens in HPV-positive (HPV+), but not HPV-negative (HPV–), carcinomas—provides us with a unique opportunity to study differences in the tumor microenvironments of HPV+ and HPV– carcinomas in 2 distinct anatomical regions. Much of the existing literature that underpins the foundation for this body of work utilizes artificial *in vitro* model systems. However, their lack of heterogeneity, tumor microenvironment, and infiltrating immune cells severely limit their ability to recapitulate actual human cancers. Therefore, this work capitalizes on genomic and transcriptomic "big" data acquired through next-generation "-omics" technologies from actual human tumors, which allow for an insightful elucidation of mechanistic processes under the influence of a native heterogeneous environment. Utilizing computational methods, this work explores and profiles the epigenetic and immune landscapes between the tumor microenvironments of HPV+ and HPV– carcinomas present in actual human malignancies. The studies presented in this thesis identify strikingly profound differences in the epigenetic and immune landscapes of the tumor microenvironments of these 2 etiologically-distinct carcinomas, regardless of their tissue of origin. Furthermore, they also provide insight into the validity of 2 important models of high-risk HPV-mediated sabotage of intracellular epigenetic and immune networks that were previously proposed from artificial *in vitro* culture studies. In addition, these studies identify potentially useful therapeutic targets and advocate for the utility of novel immunotherapy treatment modalities. Moreover, they also identify potentially predictive biomarkers of clinical outcomes that could have implications for treatment deintensification.

Keywords

Human papillomavirus (HPV), epigenetics, gene expression, methylation, head and neck cancer, cervical cancer, immune checkpoint markers, tumor infiltrating lymphocytes, survival, major histocompatibility complex, antigen presentation, co-stimulatory molecules, survival signals, T-cell, The Cancer Genome Atlas (TCGA), MHC-I, MHC-II, transcriptomics, bioinformatics, *in silico*

Co-Authorship Statement

Chapter 1: The section on The Cancer Genome Atlas was part of a book chapter published in *Methods in Enzymology,* 2019; ISSN 0076-6879. I was the lead author of this manuscript. I co-developed the methodology and co-wrote the manuscript.

Chapter 2: This section of the thesis was published in *Oncotarget*, 2017; 8(42): 72564–72576. I was co-lead author of this manuscript along with Dr. Bart Kolendowski. I participated in study design, development of methodology, data analysis, and writing of the manuscript.

Chapter 3: This section of the thesis was published in *Viruses*, 2017; 9(9): 252. I was the lead author of this manuscript. I participated in study conception and design, development of methodology, data analysis and interpretation, and writing of the manuscript.

Chapter 4: This section of the thesis was published in *OncoImmunology*, 2018; 7(10): e1498439. I was the lead author of this manuscript. I participated in study conception and design, development of methodology, data analysis and interpretation, and writing of the manuscript.

Chapter 5: This section of the thesis was published in *Cancers,* 2019; 11(8): 1129. I was the lead author of this manuscript. I participated in study conception and design, development of methodology, data analysis and interpretation, and writing of the manuscript.

Out of the night that covers me,
Black as the pit from pole to pole,
I thank whatever gods may be
For my unconquerable soul.

In the fell clutch of circumstance
I have not winced nor cried aloud.
Under the bludgeonings of chance
My head is bloody, but unbowed.

Beyond this place of wrath and tears
Looms but the Horror of the shade,
And yet the menace of the years
Finds, and shall find, me unafraid.

It matters not how strait the gate,
How charged with punishments the scroll,
I am the **master of my fate**:
I am the **captain of my soul**.

-Invictus
by William Ernest Henley

Dedication

I dedicate this thesis to Drs. Jeremy Harris, Michael Chu, and Gaetano DeRose. The brilliant cardiac and vascular surgeons that saved my life. Without you none of this would have been possible. Thank you!

I also dedicate this thesis to the countless other doctors, nurses, porters, and technicians that at one point or another played a role in saving me. Thank you!

Finally, I dedicate this thesis to my cousin Nelson Gameiro De Sousa (April 1, 1988 – June 15, 2014). You were more than just my cousin, you were my best friend, and my brother. You were always there for me when I needed you most, and always believed that I would achieve great things, and for that I will always be eternally grateful. Wherever I go, and whatever I do, I will always keep your memory alive. My world has never been the same without you. Until we meet again.

Acknowledgments

First and foremost, I would like to thank my supervisor Dr. Joe Mymryk. You have been an incredible supervisor, mentor, and friend. You have helped me develop into the scientist that I am today. Because of your mentorship, I have learned a lot about science and a random assortment of topics that span from A to Z. I am eternally grateful for your understanding and support throughout the hardships and obstacles that I've had to overcome during my graduate studies. I will surely miss all the fun times in the Mymryk lab and wish you nothing but the best.

I would like to thank Dr. Anthony Nichols and all the past and present members of his lab. It's been a wonderful and productive collaboration between our labs. I would like to specifically acknowledge Dr. John Barrett, you have been a second mentor to me, but more importantly, also a friend.

I would like to thank my other professional mentors, Drs. Greg Dekaban and Jimmy Dikeakos for years of valuable advice and criticism of my work. I've thoroughly enjoyed having the both of you as members of my committee and feel like I have become a better scientist because of it.

I would like to acknowledge past and present members of the Mymryk lab. I've learned a lot from those who were senior to me, and hope that I've been able to teach the junior trainees a thing or two. I have thoroughly enjoyed working and interacting with each and every past and present member in and out of the lab. It's been fun!

I would like to thank my parents and brothers, Natalina, Jose (Gigio), Bruno, and Andre. Your love and unwavering support mean more to me than you'll ever know. Almost 10 years ago, I embarked on a forced journey through the darkest of places without knowing the outcome, but as I look back now, I wouldn't have been able to get through any of it without any of you. You are, and will always be, my light.

Finally, my girlfriend Kaitlyn, thank you for all your love and support during the past year, especially during the writing of this thesis.

Table of Contents

List of Tables

List of Figures

List of Abbreviations

ANRIL	Antisense non-coding RNA in the INK4 locus
APCs	Antigen presenting cells
APOBEC3	Apolipoprotein B messenger RNA-editing, enzyme-catalytic, polypeptide-like 3
BLCA	Bladder urothelial carcinoma
BMI1	B lymphoma Mo-MLV insertion region 1
bp	Base pair
CD74	Cluster of differentiation 74
CDKN2A	Cyclin-dependent kinase inhibitor 2A
CDKN2B	Cyclin-dependent kinase inhibitor 2B
CDKN2B-AS	Cyclin-dependent kinase inhibitor 2B-antisense
CDKs	Cyclin-dependent kinases
CESC	Cervical carcinoma
CI	Confidence interval
CIBERSORT	Cell-type identification by estimating relative subsets of RNA transcripts
CIITA	Class II major histocompatibility complex transactivator
CLIP	Class II-associated invariant chain peptide
COAD	Colon adenocarcinoma
CpG	Cytosine-Guanine dinucleotides

CR	Conserved region
CRPV	Cottontail rabbit papillomavirus
CTLs	Cytotoxic T lymphocytes
DCs	Dendritic cells
DNMT3	DNA methyltransferase 3
E6AP	E6-associated protein
EBI3	Epstein-Barr virus-induced gene 3
EED	Embryonic ectoderm development
ERAP	Endoplasmic reticulum aminopeptidase
EV	Epidermodysplasia verruciformis
EZH2	Enhancer of zeste homolog 2
FDR	False discovery rate
H3K27	Lysine 27 on histone 3
H3K27me3	Tri-methylated lysine 27 on histone 3
H3K36	Lysine 36 on histone 3
H3K36me3	Tri-methylated lysine 36 on histone 3
HDI	Human Development Index
HFKs	Human foreskin keratinocytes
HNSC	Head and neck squamous cell carcinoma
HPV	Human papillomavirus

HPV–	HPV-negative
HPV+	HPV-positive
HPV16	HPV type 16
HPV18	HPV type 18
HR	High-risk
HzR	Hazard ratio
IARC	International Agency for Research on Cancer
ICIs	Immune checkpoint inhibitors
ICOS	Inducible T-cell co-stimulator
IFNγ	Interferon-gamma
Ii	Invariant chain
IQR	Interquartile range
IRF-1	Interferon regulatory factor-1
KDM6A	Lysine demethylase 6A
KDM6B	Lysine demethylase 6B
KDMs	Lysine demethylases
LCR	Long control region
LR	Low-risk
me3	Tri-methylation
MHC-I	Class I major histocompatibility complex

MHC-II	Class I major histocompatibility complex
NCI	National Cancer Institute
NHGRI	National Human Genome Research Institute
NK-cells	Natural killer cells
nm	Nanometer
ORFs	Open reading frames
pRb	Retinoblastoma protein
PRC1	Polycomb repressive complex 1
PRC2	Polycomb repressive complex 2
PRCs	Polycomb repressive complexes
PV	Papillomavirus
PyVs	Polyomaviruses
Rb	Retinoblastoma and related family members
RFX5	Regulatory factor X5
RNA-seq	RNA-sequencing
RSEM	RNA-Seq by Expectation Maximization
SETD2	Su(var)3-9, enhancer-of-zeste and trithorax domain containing 2
SUZ12	Suppressor of zeste 12
SV40	Simian vacuolating virus 40
TAP	Transporter associated with antigen processing

TCGA	The Cancer Genome Atlas
TCR	T-cell receptor
TILs	Tumor-infiltrating lymphocytes
TME	Tumor microenvironment
Tregs	Regulatory T-cells
URR	Upstream regulatory region
VLPs	Virus-like particles
WHO	World Health Organization

Chapter 1

1 Introduction

1.1 A Brief History of Papillomavirus Research

The earliest evidence of human papillomavirus (HPV) infections came from ancient Greek and Roman texts that described lesions akin to present-day genital warts. At the time, such lesions were associated with sexual promiscuity, which hinted at their infectious etiology (Bafverstedt, 1967; zur Hausen, 2009). However, it wasn't until the start of the 20th century that the viral origins and contagious nature of warts were explicitly demonstrated through cell-free transmission experiments conducted in Italy (reviewed in Syrjanen and Syrjanen, 2008). In the 1930s, landmark experiments conducted by Richard Shope identified the first animal papillomavirus (PV)—the cottontail rabbit papillomavirus (CRPV)—through the isolation and characterization of contagious cutaneous papillomas that grew on wild cottontail rabbits (Shope and Hurst, 1933). In addition to causing benign lesions, some CRPV-induced papillomas progressed to carcinomas (Rous and Beard, 1935). This fundamental observation led to the identification of CRPV as the first DNA tumor virus.

Up until the 1950s, CRPV infection of rabbits served as an important model for the study of viral carcinogenesis (reviewed in Syrjanen and Syrjanen, 2008). However, the discovery of polyomaviruses (PyVs) replaced CRPV as a model of virally-induced tumorigenesis, since they were easily propagated in culture, could transform cells *in vitro*, and were tumorigenic to other experimental animals (Javier and Butel, 2008). With the dawn of molecular cloning in the 1970s, scientists were now able to study the biochemical properties of PVs through the cloning of their genomes. Specifically, open reading frames (ORFs) were being identified as putative viral genes, and their functions elucidated through reverse genetics (Chen et al., 1982; Danos et al., 1982).

Anecdotal reports regarding the spontaneous conversion of genital warts into squamous cell carcinomas initiated extensive experiments in which the aim was to establish an association between HPV infection and cancer (zur Hausen, 1977; zur Hausen et al., 1974).

Indeed, in 1982 the first three reports of HPV sequences isolated from human tumors were published (Gissmann et al., 1982; Green et al., 1982; Zachow et al., 1982). Shortly thereafter, *in situ* DNA hybridization experiments on genital cancer biopsies and cervical cancer-derived cell lines identified two novel HPV genotypes—HPV type 16 (HPV16) and HPV type 18 (HPV18)—which were subsequently confirmed to be present in virtually all cervical cancers (Boshart et al., 1984; Durst et al., 1983). These ground-breaking discoveries definitively identified HPV16 and 18 as the causative agents of cervical cancer.

In the 1990s, a large-scale epidemiological study provided evidence that various HPV types—HPV16, 18, 31, 33, and 35—were the main risk factors for cervical cancer (Munoz et al., 1992). In the early 2000s, a seminal paper by Gillison *et al.,* showed evidence of a causal association between HPV infection and a subset of head and neck cancers (Gillison et al., 2000). Today, it is well-established that infection with specific HPV types can give rise to cervical, other anogenital, and head and neck cancers (zur Hausen, 2002). Through almost a century of research initiatives, certain HPV types have emerged as potent human biological carcinogens.

1.2 Papillomaviruses at a Glance

PVs are ubiquitous entities, having successfully infected and co-evolved with at least 54 different non-human host species—mostly mammals, but also birds and reptiles (Rector and Van Ranst, 2013). Their ability to transmit through direct physical contact and general inability to cause fatal disease have allowed PVs to establish successful niches and co-evolve with their host-species (Chen et al., 2018). Typically, infections with PVs—regardless of the host species they infect—causes papillomas (warts), which are simply benign hyperplastic growths of epithelial cells (Rector and Van Ranst, 2013). However, in some instances, papillomas can progress to carcinomas, and this phenomenon of malignant progression is in part responsible for PVs being some of the most intensively researched viruses in the world, specifically those that infect humans.

In humans, there are currently over 200 established HPV types that have been isolated, sequenced, and their clones deposited to the International HPV Reference Center (Muhr et al., 2018). This diverse group of human-specific PVs all share an exclusive tropism for

either cutaneous or mucosal epithelia. The cutaneous HPV types are responsible for the development of common warts (papillomas), which are typically self-limiting, small and grainy growths that occur most often on hands (Mammas et al., 2009). In extremely rare cases, individuals with an autosomal recessive genetic mutation are profoundly susceptible to infection with certain cutaneous HPV types that can lead to a skin disorder that is clinically termed epidermodysplasia verruciformis (EV) (Gewirtzman et al., 2008). Patients with EV have a genetic defect in two genes that are critical for cutaneous immunity, illustrating the importance of the immune system in keeping HPV infections under control (Lane et al., 2003). Symptomatically, patients succumb to a lifelong battle with uncontrollable growth of scaly macules (skin discoloration) and papules (inflamed cutaneous lesions) that can undergo malignant transformation (de Oliveira et al., 2003).

In contrast, mucosal HPV types are responsible for mucosal lesions that occur in the anogenital or oral tracts (Doorbar et al., 2012). These mucosal warts, like their aforementioned cutaneous counterparts, are typically benign or low-grade and are often self-limiting. However, in some instances, infection with certain types of HPVs can lead to the formation of lesions that have a much higher propensity to progress to carcinomas. These epitheliotropic viruses are highly transmissible, with the highest incidence occurring at the onset of sexual activity (Cutts et al., 2007). In fact, mucosal HPVs are the most common sexually transmitted viral infection worldwide and it is estimated that most sexually active individuals, regardless of sex, will acquire it at some point during their life (Crosbie et al., 2013; Dunne et al., 2007). Accordingly, these mucosa-associated HPV types are designated as either low-risk (LR) or high-risk (HR) based on their oncogenic potential (Tommasino, 2014). The prototypical LR HPVs, HPV6 and 11, are responsible for the majority of anogenital and oral warts with about 90% being cleared naturally within 2 years (Bharti et al., 2013). Whereas, the prototypical HR HPV types 16 and 18 are responsible for a small number of mucosal lesions, but the frequency of progression to premalignant lesions that further develop into carcinomas is much higher compared to their low-risk counterparts (Doorbar et al., 2012). Indeed, 12 HR HPV types—including HPV16 and 18— are designated by the World Health Organization's (WHO) International Agency for Research on Cancer (IARC) as Group 1 biological agents: "carcinogenic to humans" (Bouvard et al., 2009). In contrast, LR HPV types are classified by IARC as having

inadequate evidence of carcinogenicity (Group 3). These differences in carcinogenic potential between LR and HR HPV infections can be attributed to variations in viral oncoprotein functions, along with differences in viral promoter activities and gene expression patterns (Doorbar et al., 2012; Klingelhutz and Roman, 2012).

1.3 Human Papillomavirus Biology

HPVs belong to the *Papillomaviridae* family of viruses and are divided into five phylogenetic genera—designated Alpha, Beta, Gamma, Mu, and Nu—based on DNA sequence analysis (Bernard et al., 2010). The majority of research initiatives have focused on the *Alphapapillomaviruses* because of their impact on human health. This genus includes the mucosal wart causing LR types as well as the HR types that cause cancer. At the population level, HPV16 is the most frequently detected *Alphapapillomavirus*, and its high association with carcinogenesis makes this type the most clinically relevant (Schiffman et al., 2016). Indeed, because of its potent carcinogenicity, HPV16 is the best-studied PV and will henceforth be considered in this thesis as the archetypal example.

HPV16 is a small DNA tumor virus with a non-enveloped icosahedral capsid that is approximately 55 nm in diameter (**Figure 1.1A**). This naked capsid is primarily composed of the major capsid protein L1, and to a much smaller extent the minor capsid protein L2. (Doorbar et al., 2015). The virions consist of a single, double-stranded circular DNA genome that is made up of 7,908 base pairs (bp) that contains 8 open reading frames (ORFs) encoded on one DNA strand (**Figure 1.1B**). The genome is organized into 3 major regions: (i) a non-coding region, called the upstream regulatory region (URR)—alternatively called the long control region (LCR)—that contains cis-regulatory elements essential for viral DNA replication and controlling gene expression; (ii) an early region that encodes for the early genes—*E1*, *E2*, *E4*, *E5*, *E6*, and *E7*—that are involved in a plethora of functions including viral replication and cell transformation; and (iii) a late region that encodes for the major (L1) and minor (L2) capsid proteins (Tommasino, 2014). Select functions of the early and late gene products are summarized in **Figure 1.1C**. Furthermore, due to their relatively small genome size and subsequent limited coding capacity, viral gene expression is coordinated by multiple promoters that create a complex configuration of mRNA

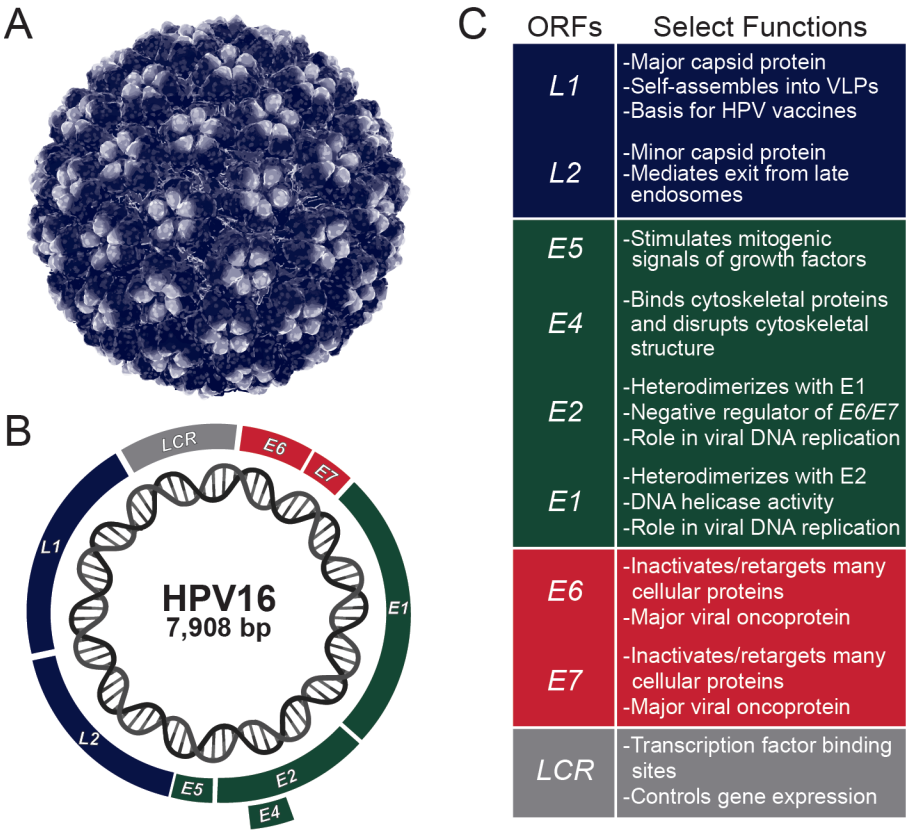

Figure 1.1. The HPV16 capsid and genome organization with select functions highlighted.

Schematic representation of the HPV16 icosahedral capsid (**A**) and genome organization (**B**). Summary of select functions of the viral products encoded by HPV16 (**C**). Regions with similar functions are indicated with similar colors: the non-coding region is in gray, the early region that encodes for the early genes involved in viral replication is in green, the early region that encodes for the early genes involved in cellular transformation is in red, and the late region that encodes for the capsid proteins is in blue. Adapted from Tommasino, 2014.

transcripts that undergo extensive alternative splicing that enables viral gene products to be expressed at different phases throughout the viral replicative cycle (Graham, 2010).

The replicative cycle of HPVs is unique because of the intimate link to the differentiation program of epidermal keratinocytes (**Figure 1.2**). In order for HPVs to successfully replicate, they require access to the basal layer cells of the epithelium through micro-wounds or hair follicles (Doorbar et al., 2012). Once at the basal layer, entry into the host cell is mediated by the viral L1 major capsid protein interacting with heparan sulfate proteoglycans on the cell surface (Shafti-Keramat et al., 2003). This interaction triggers the internalization of the virion via a clathrin-dependent endocytic mechanism (Day et al., 2003). Once internalized, the virus undergoes endosomal transport and subsequent uncoating in the late endosomes. The low pH environment found in late endosomes triggers viral egress by promoting the interaction between the viral L2 minor capsid protein and cellular protein SNX17 (Bergant Marusic et al., 2012). Importantly, the L2 protein—complexed with viral DNA—ensures the correct entry of the viral genome into the host cell nucleus (Doorbar et al., 2012; Schelhaas et al., 2012). Once in the nucleus, there is an initial phase of viral genome amplification that is followed by maintenance of the viral episome at a low-copy number—often proposed to be around 50-200 copies per cell (McBride, 2008; Parish et al., 2006; Pyeon et al., 2009). Viral replication is mediated through the usurpation of the host cells' high-fidelity cellular polymerases. Whereas maintenance of viral genome integrity and accurate segregation to daughter cells during mitosis is ensured by the E1 and E2 viral proteins, which are both necessary and sufficient for PV replication (McBride, 2017).

As the basal layer cells migrate upwards, they begin to differentiate and stop proliferating. During differentiation, the cells undergo several biochemical changes in order to produce the protective, semi-permeable outer layer of skin that is an essential environmental barrier necessary for all terrestrial life (Madison, 2003). It is during this growth-arrested, differentiation stage that the viral E6 and E7 proteins deregulate cell cycle control and force the quiescent cell to re-enter S phase (Bravo and Felez-Sanchez, 2015; Cheng et al., 1995; Sherman et al., 1997). This forced re-entry results in viral genome amplification and

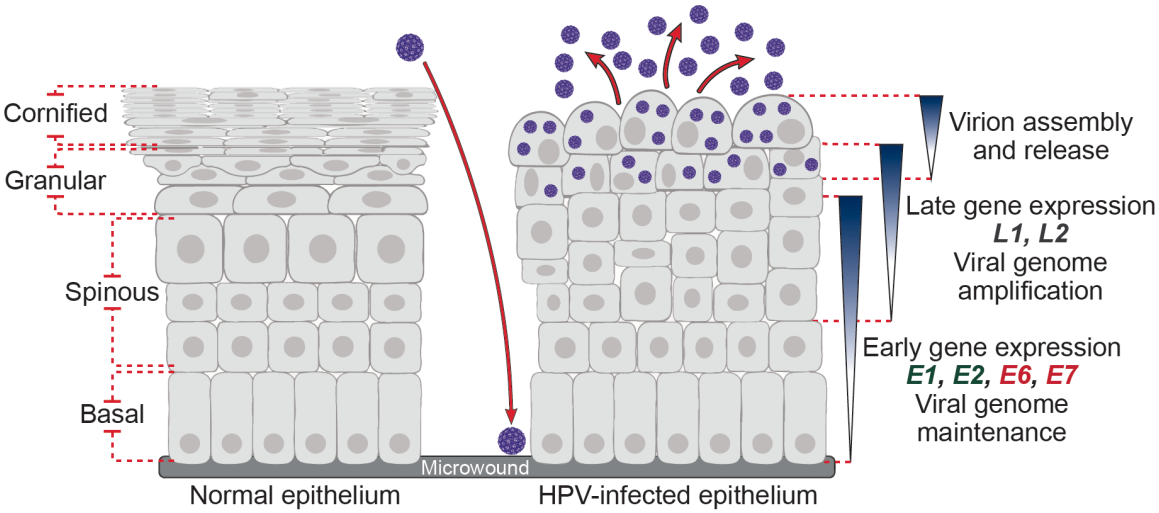

Figure 1.2. The replicative cycle of human papillomaviruses.

HPVs infect keratinocytes present at the basal layer of the epithelium that are exposed through microwounds. Normal epithelium is shown on the left and HPV-infected epithelium is shown on the right. The replicative cycle of HPVs is intimately linked to the differentiation program of epidermal keratinocytes. Once in the basal layer cells, the HPV genome is established in the nucleus as a low-copy number episome. As the basal layer cells migrate upwards, they begin to differentiate and stop proliferating. During this growth-arrested, differentiation stage, the viral E6 and E7 proteins deregulate cell cycle control and force the quiescent cell to re-enter S phase. Following differentiation, the viral genome is amplified to a high-copy number. In the upper layers of the epithelium, the L1 and L2 capsid proteins are produced and the viral genome is encapsidated. Newly assembled virions (purple) are shed into the environment. The different epithelial layers are indicated on the left. Viral progression through the epithelium is indicated on the right. Epithelium was created with BioRender. Adapted from Moody and Laimins, 2010.

hyperproliferation of cells that would have normally exited the cell cycle. Consequently, deregulated cell cycle progression results in the accumulation of mutations that can lead to the development of HPV-associated cancers (Bravo and Felez-Sanchez, 2015). Following differentiation, the expression of *E1*, *E2*, *E4*, and *E5* increases substantially, which results in an amplification of viral genome copy number from 50-200 copies to several 1000s of copies per cell (Bedell et al., 1991). Finally, in the upper layers of the epithelium, the L1 and L2 capsid proteins are produced and the viral genome is encapsidated. Newly assembled virions are shed into the environment through the normal epithelial process of desquamation—shedding of the outermost layer of skin (Bodily and Laimins, 2011; Madison, 2003). This process occurs in the absence of lysis or necrosis, thereby avoiding inflammation and contributing to viral persistence.

1.4 Human Papillomavirus Oncogenes and Transformation

The *E6* and *E7* genes encoded by HR HPVs have been designated as "viral oncogenes" due to their fundamental roles in cellular transformation. The first evidence of their carcinogenic properties came from studies on cell lines derived from cervical cancers (Schwarz et al., 1985). These cervical cancer-derived cells had HR HPV DNA randomly integrated into their genome, with the *E6* and *E7* ORFs intact and several other viral genes disrupted. Their role in carcinogenesis was further highlighted by studies that demonstrated their ability to induce transformation and immortalize both rodent fibroblasts and human keratinocytes (Mansur and Androphy, 1993). Indeed, it is now widely accepted that the products of *E6* and *E7*—often designated as viral oncoproteins—deregulate vital cellular processes, such as differentiation, cell cycle, DNA repair, senescence, and apoptosis (Tommasino, 2014). This deregulation facilitates the accumulation of DNA damage that contributes to the progression of the transformed phenotype. Importantly, the continuous expression of the *E6* and *E7* oncogenes seems necessary to maintain the malignant transformed phenotype, as silencing of *E6* and/or *E7* expression induces rapid growth arrest, senescence, or apoptosis in HPV-positive (HPV+) cervical and oral cancer-derived cell lines. (Goodwin and DiMaio, 2000; Goodwin et al., 2000; Jiang and Milner, 2002; Rampias et al., 2009; Sima et al., 2008).

The *E7* ORF encodes for a small, acidic phosphoprotein of 98 amino acids (Vousden, 1993). This viral oncoprotein has no enzymatic or DNA-binding activities, instead it associates with a wide variety of cellular regulatory proteins to inhibit or retarget their functions (McLaughlin-Drubin et al., 2012; Moody and Laimins, 2010). The HPV E7 oncoprotein is subdivided into three domains: conserved regions 1–3 (CR1–3), based on amino acid sequence similarities between different HPV types (Phelps et al., 1988). The CR1 and CR2 are intrinsically disordered, allowing adaptability in their interactions with a plethora of cellular targets (Dyson and Wright, 2005; Ohlenschlager et al., 2006). Interestingly, CR1 and CR2 are structurally and functionally similar to certain domains found in the otherwise unrelated adenovirus E1A and simian vacuolating virus 40 (SV40) large T antigen (Dyson et al., 1992; Phelps et al., 1988; Vousden and Jat, 1989). Indeed, all 3 contain the LXCXE motif—where X is any amino acid—that is essential for the interaction with the retinoblastoma tumor suppressor and related family members (Rb) (Munger et al., 1989).

The Rb protein (pRb) and related family members, p107 and p130, comprise the "pocket protein" family of cell cycle regulators that control the G1–S phase transition through the regulation of the E2F family of transcription factors (Dyson, 1998). In general, E2F transcription factors will localize and bind to E2F-binding sites that are found within the promoters of numerous genes involved in regulating cell cycle progression, differentiation, and apoptosis (DeGregori and Johnson, 2006). In the context of a normal cell, the Rb pocket protein complex directly binds to the transactivation domain of E2F, thereby repressing transcription from E2F-dependent promoters (Harbour and Dean, 2000). In late G1, the phosphorylation of Rb by cyclin-dependent kinases (CDKs) leads to its disassociation from E2F which results in the transcriptional activation of S phase-specific genes (Stevaux and Dyson, 2002). During HR HPV infection, the E7 oncoprotein will bind to Rb—mediated by the aforementioned LXCXE motif—disrupting the Rb–E2F complex and subsequently targeting Rb for proteasomal degradation through the ubiquitin-dependent pathway (Boyer et al., 1996; Chellappan et al., 1992; Jones et al., 1997). This forced disassociation from E2F results in the constitutive expression of E2F-responsive genes, such as cyclin A and cyclin E, that stimulate premature entry into S phase, thereby reactivating DNA replication (Cheng et al., 1995; Zerfass et al., 1995). Furthermore, E7-

mediated degradation of Rb also abrogates other Rb-specific activities that are fundamentally involved in DNA repair and maintaining host genome integrity (Moody and Laimins, 2010).

In addition, HR HPV E7 also induces epigenetic changes on the host cell transcriptome. Specifically, E7 expression stimulates the activation of the histone methyltransferase EZH2, which catalyzes the tri-methylation (me3) of H3K27 (Holland et al., 2008; Hyland et al., 2011; McLaughlin-Drubin et al., 2011). Furthermore, *in vitro* studies have also observed an E7-dependent activation of the histone demethylases KDM6A and KDM6B that convert H3K27me3 to the di- or mono-methylated forms (Hyland et al., 2011; McLaughlin-Drubin et al., 2011). This E7-mediated induction of KDMs was also shown, *in vitro*, to induce the activation of the tumor suppressor p16, which is a product of the *CDKN2A* locus and functions as a negative regulator of the cell cycle via CDK inhibition (McLaughlin-Drubin et al., 2011; McLaughlin-Drubin et al., 2013; Rayess et al., 2012). Consequently, p16 is found to be expressed at high levels in nearly all HPV-induced tumors, and is therefore used as a surrogate biomarker of HPV status during pathological assessment (Hoffmann et al., 2010; Klaes et al., 2001; Sano et al., 1998). In Chapter 2, we explore the epigenetic landscape by utilizing next-generation "-omics" data from over 800 primary human cervical and head and neck tumors to assess the impact of HPV status on the transcript levels of key regulators of H3K27 methylation, including EZH2, KDM6A, and KDM6B. Additionally, we also examine HPV-specific effects on gene expression and DNA methylation across the entire *CDKN2A* and adjacent *CDKN2B* genomic regions.

The *E6* ORF encodes for a basic and cysteine-rich protein of 158 amino acids. The main structural feature of this oncoprotein is the zinc-binding domains present at both the amino and carboxyl termini (Tommasino, 2014). The two zinc domains, together with an alpha-helical structure in between them, form a binding pocket that strictly binds to cellular targets that contain the LXXLL motif (Nomine et al., 2006; Zanier et al., 2013; Zanier et al., 2012). Interestingly, even though it can bind to a vast number of cellular targets across the entirety of its structured surface, all of its primary interactors contain an LXXLL motif (Vande Pol and Klingelhutz, 2013). The ability to bind to this aforementioned motif is essential for its intracellular functions, as studies have shown that

mutants of E6 that fail to bind LXXLL are rendered functionally defective (Cooper et al., 2003; Zanier et al., 2013). Indeed, this motif plays a central role in E6's best characterized role: the ability to induce the degradation of the tumor suppressor p53 (Scheffner et al., 1990).

A major consequence from the E7-mediated forced re-entry into an unscheduled S phase is the elevation in the levels of p53, which impedes cell growth and induces apoptosis (Demers et al., 1994; Jones et al., 1997). The tumor suppressor p53 is a transcription factor that controls the expression of numerous genes that encode for products that are instrumental in regulating the cell cycle, DNA repair, and apoptosis. During cellular stress, such as DNA damage or hypoxia, p53 will trigger cell cycle arrest or apoptosis in order to safeguard cellular genomic integrity (Levine and Oren, 2009). This strategy of blocking the cell cycle ensures that damaged DNA does not get replicated and allows the cell to repair the damage before entering S phase. In some instances, the accumulated damage may be too great to repair, therefore p53 will induce apoptosis in order to prevent the generation of potentially transformed daughter cells. During an HPV infection, to counteract E7-induced cellular suicide, the E6 oncoprotein will interfere with the functions of p53 (Moody and Laimins, 2010). It accomplishes this feat by binding to the E3 ubiquitin ligase, E6-associated protein (E6AP), via the conserved cellular LXXLL motif and forming a trimeric complex with p53, which ultimately leads to the ubiquitylation and subsequent proteasomal degradation of this indispensable tumor suppressor (Huibregtse et al., 1991; Scheffner et al., 1993; Scheffner et al., 1990). Indeed, this abrogation of p53's function combined with the E7-mediated forced re-entry into S phase, facilitates productive viral replication. However, due to the persistent nature of an HPV infection, it can result in the accumulation of DNA damage—that would have otherwise been repaired—leading to genomic instability that has consequences for tumor development (Moody and Laimins, 2010).

As mentioned previously, the two virally encoded oncoproteins, E6 and E7, are necessary for maintaining the transformed phenotype; however, the functions highlighted above are not sufficient to directly transform infected cells (Moody and Laimins, 2010). Therefore, additional carcinogenic events such as genomic instability must occur for malignant

transformation to develop. Genomic instability can occur over time with a persistent HPV infection due to the accumulation of DNA damage that results from the degradation of tumor suppressor proteins Rb and p53 (White et al., 1994). In addition, genomic instability has also been shown to occur through an anti-HPV response that is mediated by the antiviral apolipoprotein B messenger RNA-editing, enzyme-catalytic, polypeptide-like 3 (APOBEC3) family of DNA cytidine deaminases that inadvertently mutate the host cell genome, resulting in the accumulation of DNA damage over time (Warren et al., 2017). This is in agreement with the prolonged latency observed between initial HPV infection and tumor development (Schiffman et al., 2007). This accidental induction of genomic instability is characteristic of HR HPV-induced malignancies. In fact, the majority of HPV-associated cancers have numerous chromosomal defects such as aneuploidy—gain or loss of entire chromosomes—and chromosomal rearrangements (Moody and Laimins, 2010; White et al., 1994; zur Hausen, 1999). Indeed, this genetic instability is thought to be a precursor to tumor development, occurring before the integration of viral DNA into the host cell genome (Duensing et al., 2001).

One of the fundamental events in facilitating progression to an HPV-mediated transformed phenotype is the integration of HR viral DNA into the host cell genome (Moody and Laimins, 2010). This integration event is generally thought of as a chance event that can cause the disruption of viral genes that are essential for maintaining normal viral gene expression (Doorbar et al., 2012; Thorland et al., 2003). Indeed, the integration breakpoints often occur in the viral genomic area that encodes for the early *E2* gene, which plays a central role in the negative feedback control of the viral oncogenes *E6* and *E7*. Furthermore, the *E6* and *E7* ORFs are consistently found to be preserved in a successful oncogenic-promoting integration event (Parfenov et al., 2014; zur Hausen, 2002) (**Figure 1.3**). Consequently, disruption of *E2* leads to the deregulated expression of the aforementioned oncogenes, subsequently furthering aberrant cellular proliferation through the abrogation of cell cycle checkpoints and fostering the accumulation of DNA damage that accelerates genetic instability. These viral oncoprotein-mediated effects are exacerbated through integration, causing cells to have a selective growth advantage that promotes carcinogenesis (Jeon et al., 1995; McBride and Warburton, 2017). In addition, integration can also lead to the activation of nearby cellular proto-oncogenes or inactivation of tumor

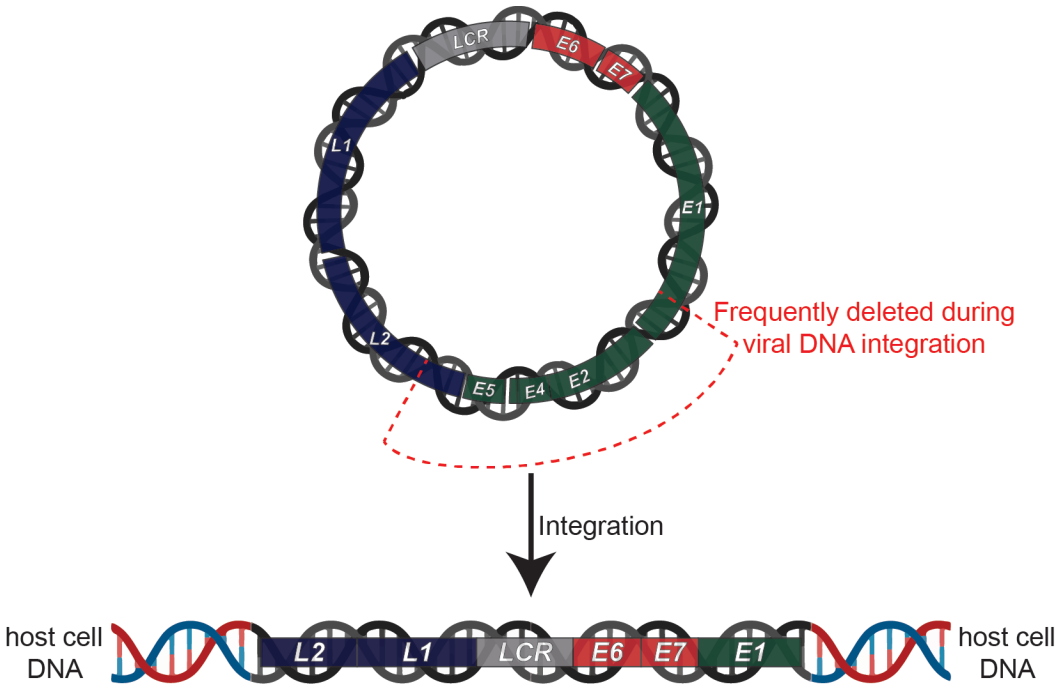

Figure 1.3. Integration of the HPV16 viral genome into host cell DNA.

During progression to a malignant phenotype, the viral DNA genome often integrates into host cell DNA. The integration breakpoints often disrupt the viral genomic areas that encode for *E2, E4, E5,* and *L2*. The non-coding regulatory region *LCR* and the *E6* and *E7* oncogenes are consistently found to be preserved in a successful oncogenic-promoting integration event. Adapted from zur Hausen, 2002.

suppressor genes, as well as aberrant replication issues that lead to the amplification of host genes around the site of integration (Parfenov et al., 2014; Peter et al., 2006; Thorland et al., 2003). Moreover, HPV-associated malignancies become reliant on the expression of the integrated viral oncogenes for sustained proliferation and survival (Goodwin and DiMaio, 2000; Goodwin et al., 2000; Jiang and Milner, 2002; Rampias et al., 2009; Sima et al., 2008). While many HPV+ cancers are found to contain integrated copies of the HPV genome, this is not a universal phenomenon. Indeed, HPV+ carcinomas, such as anogenital and oral cancers, can contain either extrachromosomal HPV DNA, integrated viral DNA, or a combination of both (Kristiansen et al., 1994; McBride and Warburton, 2017). Importantly, unlike other viruses that integrate into the host cell genome, HPV integration is not a part of its normal replicative cycle, instead it is an accidental "dead-end" event that abolishes prospective production of viral progeny (McBride, 2017).

1.5 Human Papillomavirus Cancer and Prevention

The WHO's IARC group have conclusively defined 12 HR HPV types as potent biological human carcinogens—HPV16, 18, 31, 33, 35, 39, 45, 51, 52, 56, 58, and 59 (Bouvard et al., 2009). Of the estimated 14 million cancers that occurred worldwide in 2012, 640,000 were caused by an HPV infection (Plummer et al., 2016). HR HPVs sexually-transmitted mode of infection plays a significant role in causing approximately 4.5% of the global cancer burden, of which more than 80% occur in underdeveloped or developing nations (de Martel et al., 2012). Indeed, persistent infection by HR HPVs are responsible for virtually all cases of cervical cancers and other anogenital cancers that include vaginal, vulvar, penile, and anal carcinomas, as well as a significant fraction of head and neck cancers (Mesri et al., 2014) (**Table 1.1**). Interestingly, the fraction of cancers attributed to HR HPV infection is much higher in women (8.6%) than in men (<1%) because of the unique susceptibility of the cervix to HPV-induced carcinogenesis (Schiffman et al., 2016). Furthermore, the fraction of cancers induced by HPV also varies significantly by geographical region and level of economic development (Roden and Stern, 2018). This variation can be partly explained by the quality of cervical cancer screening initiatives and access to preventative vaccination programs (Schiffman et al., 2016).

Table 1.1. Global estimated fraction of new cancers caused by HPV infection in 2012.

Adapted from Schiffman et al., 2016.

Cancer Site	New cases (n)	Attributable to HPV (n)	Attributable to HPV (%)	Attributable by sex (n)	
				Male	Female
Cervix	528,000	528,000	100	–	528,000
Anus	40,000	35,000	88	17,000	18,000
Vagina and vulva	49,000	20,000	41	–	20,000
Penis	26,000	13,000	51	13,000	–
Oropharynx	96,000	29,000	31	24,000	6,000
Oral cavity and larynx	358,000	9,000	2.4	7,000	2,000

The causal link between HR HPV infection of the cervix and development of cancer is one of the most important scientific discoveries of all time. Indeed, for his seminal work in this ground-breaking discovery, Dr. Harald zur Hausen was awarded the 2008 Nobel Prize in Physiology or Medicine. Worldwide, cervical cancer is the 4th most frequently diagnosed cancer and the 4th leading cause of death in women, with approximately 570,000 new cases and 311,000 deaths in 2018 (Bray et al., 2018). The highest regional incidence and mortality rates are observed in economically disadvantaged areas, such as countries in sub-Saharan Africa. In comparison, there is an estimated 7 to 10 times lower incidence and 18 times lower mortality rates in countries with a high Human Development Index, such as Canada, USA, Australia, and New Zealand (Bray et al., 2018; Small et al., 2017). In fact, there is an inverse correlation between the income level of a country and cervical cancer rates (Schiffman et al., 2016). The main etiological factor is infection with HR HPVs, with 99% of cervical cancers containing HR HPV DNA, of which HPV16 accounts for 50–60%, HPV18 accounts for approximately 20%, and the remaining fraction being caused by the other oncogenic types mentioned above (Roden and Stern, 2018). In countries with state-of-the-art staging and treatment, 3-year local control rates for all stages ranged from 74–95%. In contrast, for many underdeveloped countries the 3- to 5-year survival rate for all stages combined was less than 50% (Small et al., 2017). This huge disparity in prevalence and mortality rates between high-income and low- to middle-income nations, illustrates the need for effective screening and vaccination programs that have the potential to virtually eliminate the burden of cervical cancer from every country, regardless of wealth (Bosch et al., 2016).

Over a decade ago the WHO's IARC group definitively established HR HPVs as being the biological carcinogens responsible for a subset of head and neck squamous cell carcinomas (HNSC) (Gillison et al., 2015). Indeed, since the seminal study that causally linked HPV infection with the development of HNSC was published in 2000 (Gillison et al., 2000), it is now explicitly recognized that infection with HR HPVs causes a significant and increasing fraction of these carcinomas. HNSC is an umbrella term that encompasses a heterogenous group of malignancies in the head and neck region that include the oral cavity, oropharynx, hypopharynx, and larynx (**Figure 1.4**) (Leemans et al., 2018). HNSC

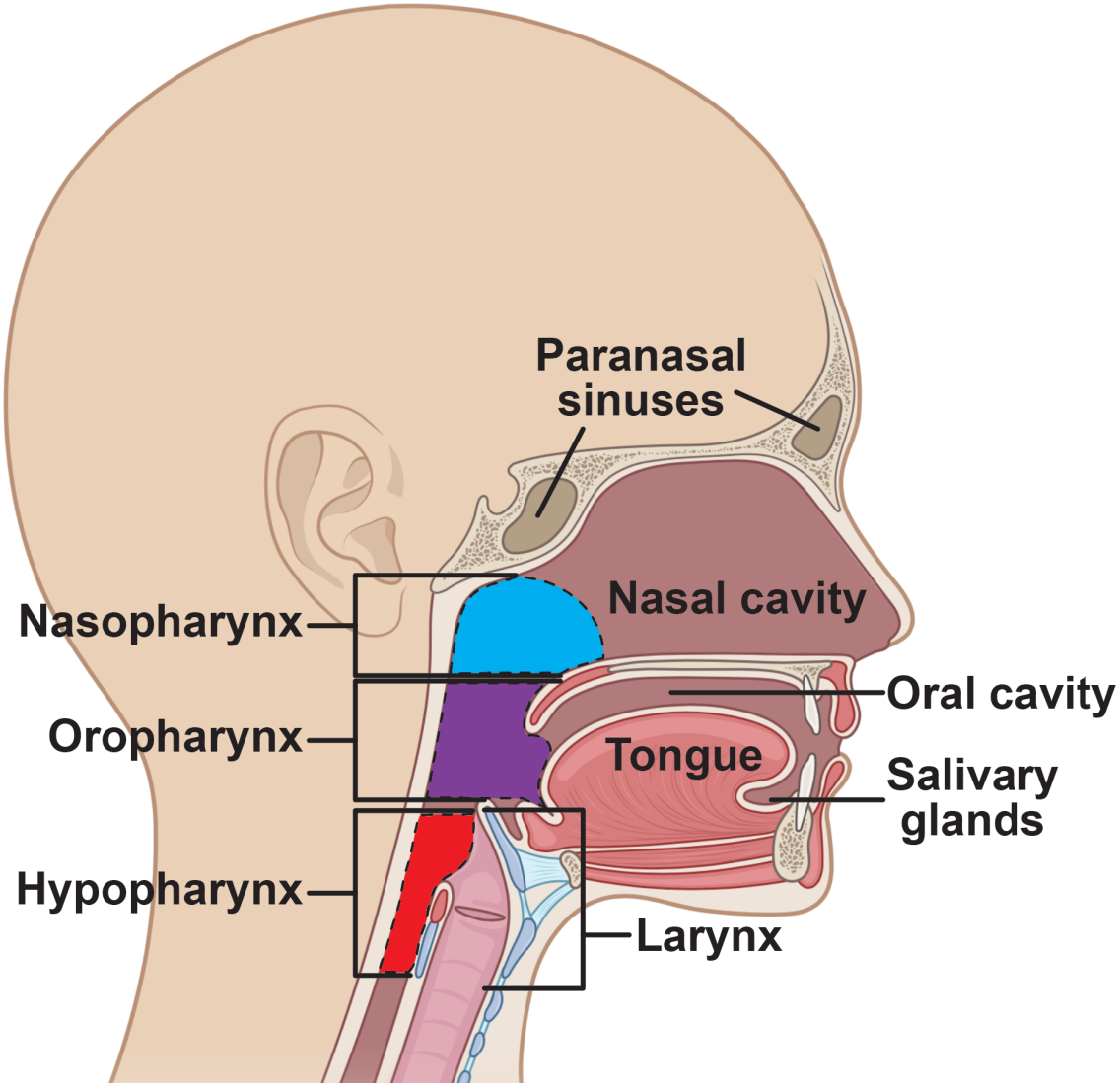

Figure 1.4. Subsites of the head and neck region.

Schematic of the subsites present in the head and neck region. The region of the hypopharynx is highlighted in red, the region of the oropharynx is highlighted in purple, and the region of the nasopharynx is highlighted in light blue. Head template was created with BioRender.

is the 7th most commonly diagnosed cancer worldwide, with approximately 890,000 new cases and 453,000 deaths in 2018 (Bray et al., 2018). The classical etiological agents responsible for the majority of these carcinomas are smoking and excessive alcohol consumption, with HPV infection accounting for approximately 25% of all cases (Kreimer et al., 2005; Leemans et al., 2018). Accordingly, HNSC can be divided into either HPV+ or HPV-negative (HPV–) malignancies based on their respective carcinogenic origins. The majority of HPV+ cases in the head and neck region occur in the oropharynx (30.8%), with a much smaller percentage occurring in the other subsites such as the larynx (2.4%) and oral cavity (2.2%) (de Martel et al., 2017). Furthermore, HPV16 is the most common HPV type associated with these carcinomas, with an estimated 83% of HPV+ HNSC being caused by the potent biological carcinogen (Leemans et al., 2018).

Alarmingly, the global frequency of HPV+ oropharyngeal cancers has increased to epidemic proportions, from 7.2% in the period of 1990–1994 to 32.7% in the period of 2010–2012, which is most likely a consequence of changes in sexual behavior (D'Souza et al., 2007). Interestingly, this increase in HPV+ oropharyngeal cancers has been mostly observed in high-income countries with a concomitant decline in tobacco smoking (Chaturvedi et al., 2011). In agreement, our group has identified a similar epidemic increase in Southwestern Ontario, with the fraction of HPV+ oropharyngeal cancers increasing from 25% in the period of 1993–1999 to 62% in the period of 2006–2011 (Nichols et al., 2013a; Nichols et al., 2013b). In terms of demographic and clinical characteristics, HPV+ HNSC occurs more frequently in males, affects a younger demographic, and generally patients exhibit markedly better clinical outcomes compared to their HPV– counterparts (Kang et al., 2015; Leemans et al., 2018). Indeed, several studies with various cohort sizes have shown that patients with HPV+ HNSC had a 2- to 5-year overall survival rate that ranged from 62–95% (Ang et al., 2010; Fakhry et al., 2008; Lassen et al., 2011; Posner et al., 2011; Rischin et al., 2010). In comparison—from the same aforementioned studies—patients with HPV– HNSC only had a 2- to 5-year overall survival rate that ranged from 35–74%. In essence, HPV+ HNSC is considered a distinct epidemiological, molecular, and clinical entity that is caused by an epitheliotropic sexually transmitted virus and is increasing at an epidemic rate, specifically in the Western world (Kang et al., 2015; Leemans et al., 2018).

In the early 1990s, scientists observed that expression of recombinant HPV L1 proteins—the major capsid protein—in a range of *in vitro* systems, self-assembled into virus-like particles (VLPs) that were devoid of potentially carcinogenic viral DNA (Deschuyteneer et al., 2010; Roden and Stern, 2018). These "ghost particles" were immunologically similar to their native counterparts and were able to elicit high and durable titers of neutralizing antibodies in experimental animal models challenged with infectious, wildtype virus. Furthermore, these studies illustrated that the protection elicited by these VLPs were type-restricted, which indicated that in order to achieve broad protection against other types of HPVs, VLPs generated from several major carcinogenic types were necessary (Breitburd et al., 1995; Suzich et al., 1995). Indeed, these studies provided the proof-of-concept necessary for the development of the first prophylactic HPV vaccine. Since the initiation of those pioneering studies, there have been 3 HPV VLP vaccines licensed: (i) Cervarix (GlaxoSmithKline), a bivalent vaccine targeting both HR HPV16 and 18, which are the two types responsible for most HPV+ cancers; (ii) Gardasil (Merck Inc.), a quadrivalent vaccine that targets HR HPV16 and 18, as well as the two most common LR types that cause the majority of genital warts, HPV6 and 11; and (iii) Gardasil9 (Merck Inc.), a nonavalent vaccine targeting HPV6, 11, 16, 18 and the next 5 most carcinogenic types—HPV31, 33, 45, 52, and 58 (de Martel et al., 2017). All 3 vaccines have been shown to be remarkably safe and highly effective for protection against new infections and precancerous lesions (Schiffman et al., 2016). Furthermore, all 3 vaccines underwent large, phase III randomized controlled trials in young women (15–26 years), where they were shown to be more than 90% effective against genital warts, persistent infections, and precancerous lesions (Castellsague et al., 2011; Lehtinen et al., 2012; Munoz et al., 2010; Schiller et al., 2012). It is estimated that 118 million women aged 10–20 have been targeted by HPV vaccination programs, but unfortunately only 1% of these are in less developed countries (Bruni et al., 2016). Moreover, these HPV vaccines have the ability to prevent 70–90% of all HPV+ cancers and have been projected to dramatically reduce the global burden of cervical cancer after 2050 (de Martel et al., 2017; Jit et al., 2014).

1.6 The Tumor Microenvironment

Normal tissues maintain homeostasis through a dynamic complex of intercellular communication that ensures a strict balance of cellular proliferation and death. In order to achieve and maintain normal physiology a plethora of cells need to work in concert. Each of these cells have an intracellular program that restricts them in their role, location, and number. In contrast, cancers have lost these internal restraints through activating mutations in oncogenes and deactivating mutations in tumor suppressor genes. Nevertheless, these tumor cells are still able to dynamically communicate with diverse non-malignant cellular populations and extracellular infrastructure within their local environment (Joyce and Pollard, 2009). Indeed, as these cancerous cells divide and form tumors, they provoke dramatic molecular, cellular, and physical changes on the surrounding tissue in which they grow, giving rise to the tumor microenvironment (TME). The TME is comprised of a convoluted milieu of stroma that includes blood and lymphatic endothelial cells, fibroblasts, mesenchymal cells, and pericytes, as well as immune cells and the extracellular matrix (Turley et al., 2015). The diverse biological elements within the TME interact intimately with tumor cells, often influencing tumor cell survival, invasiveness, and metastatic dissemination, as well as therapeutic response (Joyce and Pollard, 2009; Nakasone et al., 2012; Polyak et al., 2009).

While the cellular composition of the TME varies across different cancer types, some common features seem to be consistent throughout most solid tumors. For example, most tumors are highly vascularized by disorganized, tortuous and leaky vessels. Furthermore, the TME often contains infiltration from various innate and adaptive immune cell populations that can promote both protumor and antitumor effects (Turley et al., 2015). The utilization of next-generation "-omics" technologies, such as bulk tissue RNA-sequencing (RNA-seq), have deconvoluted the composition of the immune landscape present within the TME (Ali et al., 2016; Aran et al., 2017; Newman et al., 2015). This has led to the broad classification of the TME immune landscape into 2 classes (Binnewies et al., 2018) (**Figure 1.5**). The 1st class is termed infiltrated–excluded, which is defined as lacking cytotoxic T lymphocytes (CTLs) and proinflammatory mediators in the tumor core, instead they contain tumor-associated macrophages along the tumor margins that have been

hypothesized to prevent CTL infiltration (Beatty et al., 2015; Binnewies et al., 2018). These tumors have been classified as being immunologically "cold" or alternatively, non-T-cell-inflamed (Binnewies et al., 2018; Spranger, 2016) (**Figure 1.5A**). The 2nd class is termed infiltrated–inflamed, which is characterized by high infiltration of CTLs that express elevated levels of immune-dampening T-cell exhaustion markers such as LAG3, PD1, TIGIT, and TIM3 (Binnewies et al., 2018; Wherry, 2011). Moreover, they also contain T-cell activation markers and proinflammatory mediators. These types of tumors are considered to be immunologically "hot" or alternatively, T-cell-inflamed (Binnewies et al., 2018; Spranger, 2016) (**Figure 1.5B**). These broad classes of immune landscape classifications of the TME illustrate the possible different dynamic interactions that can occur between malignant and non-malignant cells that can have a substantial impact on both tumor status and therapeutic response (Binnewies et al., 2018). Indeed, characterization of the immune landscape of tumors is helping guide the rational design of therapies that mobilize the immune system to induce long-term remission in cancers previously considered to be terminal (Byrne and Fisher, 2017; Costa et al., 2018; George et al., 2017; Holzel et al., 2013). In Chapters 3, 4, and 5 we utilize large datasets generated by next-generation "-omics" technologies to explore and profile the immune landscapes between HPV+ and HPV– TMEs originating from either the cervical or head and neck regions.

1.7 The Cancer Genome Atlas

Historically, tumor-infiltrating leukocyte (TIL) detection within the TMEs of solid tumors has been primarily performed using immunohistochemistry or flow cytometry (Llosa et al., 2015). Both of these techniques have taught us a great deal about the tumor immune profile, but they require antibodies to specific phenotypic markers of cell type or activation status, can be challenging to standardize, difficult to implement with small tissue samples, and expensive to perform for the dozens of markers necessary for a comprehensive view of the immune landscape of a given TME. More recent alternatives capitalize on the plunging costs of next-generation "-omics" technologies, including next-generation sequencing for genomics and transcriptomics, as well as genome-wide methylome analysis using high-density arrays. Indeed, massive collaborative efforts such as The Cancer Genome Atlas

Figure 1.5. General classification of the types of immune landscapes present in tumor microenvironments.

The tumor microenvironment can be divided into 2 broad classes based on their immune landscape. The tumor core of infiltrated–excluded environments lack cytotoxic T lymphocyte infiltration (CTL) and proinflammatory mediators but contain tumor-associated macrophages (**A**). In contrast, the environments of infiltrated–inflamed are characterized by high infiltration with CTLs that express elevated levels of T-cell exhaustion markers and proinflammatory mediators (**B**). Created with BioRender. Adapted from Binnewies et al., 2018.

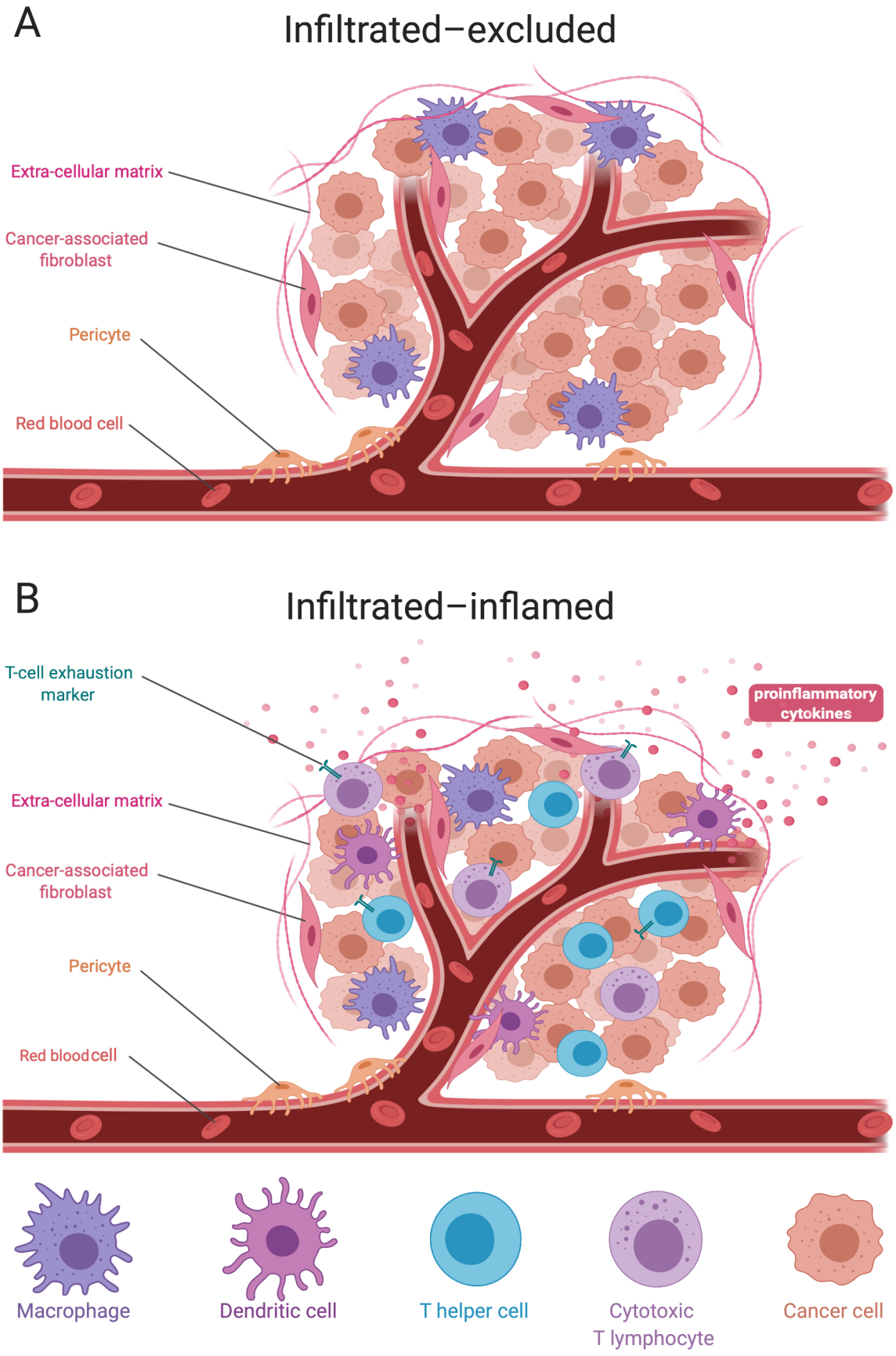
A
Infiltrated–excluded
Extra-cellular matrix
Cancer-associated fibroblast
Pericyte
Red blood cell
B
Infiltrated–inflamed
T-cell exhaustion marker
proinflammatory cytokines
Extra-cellular matrix
Cancer-associated fibroblast
Pericyte
Red blood cell
Macrophage
Dendritic cell
T helper cell
Cytotoxic T lymphocyte
Cancer cell

(TCGA) have generated genomic, transcriptomic, and methylomic data for over 11,000 tumor samples from 33 cancer types and subtypes (Liu et al., 2018). Capitalizing on this freely available data, it is possible to estimate the detailed composition and activation status of tumor-infiltrating immune cells into the TMEs of solid tumors from bulk tissue RNA-seq data using computational approaches based on a set of immune-specific marker genes or expression signatures that correlate with distinct leukocyte populations (Bindea et al., 2013; Danaher et al., 2017; Gameiro et al., 2018; Gameiro et al., 2019; Gameiro et al., 2017; Newman et al., 2015; Rooney et al., 2015; Wolf and Samuels, 2018).

The TCGA was a large-scale collaboration between the National Cancer Institute (NCI) and the National Human Genome Research Institute (NHGRI) to comprehensively characterize the molecular events in primary cancers and provide these data to the public for use by cancer researchers worldwide (Liu et al., 2018). This effort, which ended in 2017, generated publicly available, comprehensive, multidimensional maps of genomic changes in more than 11,000 tumor samples. The TCGA dataset encompasses 33 types of human tumors, all processed via a uniform genomic data analysis pipeline that collected, selected, and analyzed these cancer samples in detail. These analyses included whole exome and/or whole genome sequencing, mRNA sequencing, microRNA sequencing, DNA copy number profiling, DNA methylation profiling, and reverse-phase protein array expression profiling. Although comprehensive clinical annotation was not possible for every TCGA sample, substantial clinical data are available, allowing comparison of many clinical variables and, in most cases, reasonably robust outcomes assessment. Furthermore, the quality and quantity of the TCGA molecular datasets have resulted in studies that have significantly advanced our understanding of cancer biology (The Cancer Genome Atlas Research Network, 2015; The Cancer Genome Atlas Research Network, 2017).

The TCGA project provides an abundant source of free data available for mining by cancer researchers in many different ways. Importantly, many other questions unrelated to tumor immunity can be similarly addressed, such as correlations between gene expression and chemotherapy response, alterations induced by oncogenic pathogens, or expression of markers of differentiation, proliferation, or tumor aggressiveness. Additionally, batch-wise

analysis of this valuable data set for various correlations can also generate novel hypotheses that can be pursued experimentally. Literally, the seeds of thousands of important analyses await discovery in this collection of "big" data.

1.8 Thesis Overview

The work presented in this thesis capitalizes on novel state-of-the-art methods that are being utilized in both the fields of tumor virology and cancer biology. The utilization of next-generation "-omics" provides genomic and transcriptomic data derived from bulk tumors that illuminate the dynamic molecular landscapes of tumors under the influence of their local surroundings. Indeed, these types of analyses provide us with unique insights into the complexities of the TME that would have otherwise been missed by classical 2-dimensional approaches, such as *in vitro* cell culture systems. By utilizing "big" data generated from the TCGA, we ensure a globally-uniform process for patient selection, sample collection, and data acquisition that minimizes artifactual experimental heterogeneity that can often occur without standardized protocols. Instead, the heterogeneity in these datasets are restricted to just the patients and cancers from which they are derived. Utilizing these computational methods, I explore and profile the epigenetic and immune landscapes between the tumor microenvironments of HPV+ and HPV– carcinomas present in actual human malignancies. Furthermore, I hypothesize that the epigenetic and immune landscapes between these 2 etiologically-distinct tumor microenvironments are profoundly different, regardless of their anatomical origins.

As previously detailed above, HR HPVs cause cancer at multiple distinct anatomical locations. Regardless of the tissue of origin, most HPV+ cancers show highly upregulated expression of the p16 product of the *CDKN2A* gene (Klaes et al., 2001; Sano et al., 1998). Paradoxically, HPV+ tumor cells require continuous expression of this tumor suppressor for survival (McLaughlin-Drubin et al., 2013). Thus, restoration of normal p16 regulation has potential therapeutic value against HPV-induced cancers. Normally, p16 transcription is tightly controlled at the epigenetic level via polycomb repressive complex-mediated tri-methylation of H3K27 (Popov and Gil, 2010). Although a mechanism by which HPV induces p16 has been previously proposed based on *in vitro* tissue culture models (McLaughlin-Drubin et al., 2011; McLaughlin-Drubin et al., 2013), it has not been

extensively validated in actual human tumors. Indeed, these cell culture-based experiments have allowed for a detailed elucidation of the biological factors involved in HPV-mediated upregulation of p16; however, an analysis of these HPV-specific epigenetic effects has not been done in any large cohorts of HPV-induced cancers under the influence of their respective native heterogenous environments. Therefore, my objective was to determine if the epigenetic changes involved in p16 upregulation observed in artificial culture systems were recapitulated in actual primary HPV+ tumors from different anatomical locations.

In Chapter 2, I used genomic and transcriptomic data from over 800 human cervical and head and neck tumors from The Cancer Genome Atlas to test this model. I sought out to determine the impact of HPV status on expression from the *CDKN2A* locus, the adjacent *CDKN2B* locus, and transcript levels of key epigenetic regulators of these loci. As expected, HPV+ tumors from both anatomical sites exhibited high levels of *p16*. Furthermore, HPV+ tumors expressed higher levels of *KDM6A*, which demethylates H3K27me3. In addition, analysis of CpG methylation also detected two sites in the *CDKN2A* locus with consistently altered methylation in HPV+ tumors compared to their HPV– counterparts. Taken together, this data validates previous tissue culture studies and identifies remarkable similarities between the effects of HPV on gene expression and DNA methylation in both cervical and head and neck tumors from large human cohorts. Moreover, these results support a model whereby HPV-mediated deregulation of *CDKN2A* transcription requires KDM6A, a potentially druggable target.

I next wanted to use the same computational methodology to validate another tissue culture model that proposed an HPV-mediated transcriptional downregulation of the class I major histocompatibility complex (MHC I) antigen presentation system (Georgopoulos et al., 2000; Heller et al., 2011; Li et al., 2010). Indeed, this proposed downregulation could contribute to viral persistence and allow the infected or transformed cells to evade the adaptive immune response. In Chapter 3, I utilized the same genomic and transcriptomic data from Chapter 2, to determine the impact of HPV status on the mRNA expression of all six MHC-I heavy chain genes (*HLA-A, -B, -C, -E, -F, and -G)*, and the β2 microglobulin light chain in actual HPV-induced carcinomas. Unexpectedly, these genes were all expressed at high levels in HPV+ cancers compared with normal control tissues. Indeed,

many of these genes were expressed at significantly enhanced levels in HPV+ tumors. Similarly, the transcript levels of several other components of the MHC-I peptide-loading complex were also high in HPV+ cancers. The coordinated expression of high mRNA levels of the MHC-I antigen presentation apparatus could be a consequence of the higher intratumoral levels of interferon-gamma (IFNγ) observed in HPV+ carcinomas, which correlated with signatures of increased infiltration by T- and NK-cells. These data, which were obtained from both cervical and head and neck carcinomas in large human cohorts, indicate that HPV oncoproteins do not efficiently suppress the transcription of the MHC-I antigen presentation system in actual human tumors as proposed by *in vitro* cell culture models.

Given the observation of higher levels of intratumoral IFNγ and increased infiltration by T- and NK-cells into the HPV+ TME, a mechanistic and detailed characterization of immune cell presence and status between the 2 anatomically-similar, etiologically-different HNSC types were warranted. In Chapter 4, I utilized an immunogenomic approach on transcriptomic and clinical data to compare the immune landscape between the TMEs of HPV+ and HPV– HNSC and their influence on clinical outcomes. I found that HPV+ HNSC exhibited a strong Th1 response characterized by increased infiltration with multiple types of immune cells—$CD4^+$, $CD8^+$, and regulatory T-cells—and expression of their effector molecules. HPV+ HNSC also expressed higher levels of *CD39* and multiple T-cell exhaustion markers including *LAG3*, *PD1*, *TIGIT*, and *TIM3* compared to their HPV– counterparts. Importantly, patients with higher expression of these exhaustion markers—indicative of a T-cell-inflamed tumor—correlated with markedly improved survival in HPV+, but not HPV–, HNSC. Thus, profound differences exist between the immune landscape of HPV+ and HPV– HNSC. In addition, these results suggest that immune checkpoint inhibitor therapy is a promising treatment strategy for HPV+ HNSC, and that expression of immune checkpoint molecules could also serve as predictive biomarkers of patient outcome.

In the final data chapter of this thesis, I complete my profiling of the immune landscape between the TMEs of HPV+ and HPV– HNSC by determining the impact of HPV status on the expression of class II major histocompatibility complex (MHC-II) genes and related

genes involved in their regulation, antigen presentation, and T-cell co-stimulation. Expression of MHC-II is typically restricted to antigen presenting cells (APCs) (van den Elsen et al., 2004). However, during inflammation, epithelial cells can be induced to express MHC-II and function as accessory APCs (Boss and Jensen, 2003; Collins et al., 1984; Kim et al., 2009). As done previously, I utilized RNA-seq data from over 500 HNSC patients from the TCGA and found that expression of virtually all MHC-II genes was significantly upregulated in HPV+ carcinomas compared to HPV– or normal control tissues. Similarly, genes that encode products involved in MHC-II-specific antigen presentation were also significantly upregulated in the HPV+ cohort. In addition, the expression of *CIITA* and *RFX5*—regulators of MHC-II transcription—were significantly upregulated in HPV+ tumors. This coordinated upregulation of MHC-II genes was found to be correlated with higher intratumoral levels of IFNγ in HPV+ carcinomas. Furthermore, genes that encode for various co-stimulatory molecules involved in T-cell activation and survival were also significantly upregulated in HPV+ tumors. Collectively, these results suggest a previously unappreciated role for epithelial cells in antigen presentation that functionally contributes to the highly immunogenic tumor microenvironment observed in HPV+ HNSC.

Taken together, these analyses have provided insight into the validity of certain models proposed from artificial *in vitro* culture systems, as well as illustrating the profound differences in the epigenetic and immune landscapes between the tumor microenvironments of HPV+ and HPV– carcinomas. These studies also identify a potentially useful therapeutic target in KDM6A and advocate for the use of promising immunotherapy strategies in the treatment of HPV+ HNSC. Furthermore, I also show that expression of immune checkpoint molecules could serve as predictive biomarkers of clinical outcomes that could allow for treatment deintensification. Moreover, the novel hypotheses that have been generated by this work will feedback into the laboratory and allow for further exploration in an experimental setting where relevant models can be generated and biologically manipulated. Lastly, I hope that the accumulated knowledge gained from these studies will advance the field of tumor virology and have a positive impact on patients with these devastating HPV-induced malignancies.

1.9 References

Ali HR, Chlon L, Pharoah PD, et al. (2016) Patterns of Immune Infiltration in Breast Cancer and Their Clinical Implications: A Gene-Expression-Based Retrospective Study. *PLoS Med* 13: e1002194.

Ang KK, Harris J, Wheeler R, et al. (2010) Human papillomavirus and survival of patients with oropharyngeal cancer. *N Engl J Med* 363: 24-35.

Aran D, Hu Z and Butte AJ. (2017) xCell: digitally portraying the tissue cellular heterogeneity landscape. *Genome Biol* 18: 220.

Bafverstedt B. (1967) Condylomata acuminata--past and present. *Acta Derm Venereol* 47: 376-381.

Beatty GL, Winograd R, Evans RA, et al. (2015) Exclusion of T Cells From Pancreatic Carcinomas in Mice Is Regulated by Ly6C(low) F4/80(+) Extratumoral Macrophages. *Gastroenterology* 149: 201-210.

Bedell MA, Hudson JB, Golub TR, et al. (1991) Amplification of human papillomavirus genomes in vitro is dependent on epithelial differentiation. *J Virol* 65: 2254-2260.

Bergant Marusic M, Ozbun MA, Campos SK, et al. (2012) Human papillomavirus L2 facilitates viral escape from late endosomes via sorting nexin 17. *Traffic* 13: 455-467.

Bernard HU, Burk RD, Chen Z, et al. (2010) Classification of papillomaviruses (PVs) based on 189 PV types and proposal of taxonomic amendments. *Virology* 401: 70-79.

Bharti AH, Chotaliya K and Marfatia YS. (2013) An update on oral human papillomavirus infection. *Indian J Sex Transm Dis AIDS* 34: 77-82.

Bindea G, Mlecnik B, Tosolini M, et al. (2013) Spatiotemporal dynamics of intratumoral immune cells reveal the immune landscape in human cancer. *Immunity* 39: 782-795.

Binnewies M, Roberts EW, Kersten K, et al. (2018) Understanding the tumor immune microenvironment (TIME) for effective therapy. *Nat Med* 24: 541-550.

Bodily J and Laimins LA. (2011) Persistence of human papillomavirus infection: keys to malignant progression. *Trends Microbiol* 19: 33-39.

Bosch FX, Robles C, Diaz M, et al. (2016) HPV-FASTER: broadening the scope for prevention of HPV-related cancer. *Nat Rev Clin Oncol* 13: 119-132.

Boshart M, Gissmann L, Ikenberg H, et al. (1984) A new type of papillomavirus DNA, its presence in genital cancer biopsies and in cell lines derived from cervical cancer. *EMBO J* 3: 1151-1157.

Boss JM and Jensen PE. (2003) Transcriptional regulation of the MHC class II antigen presentation pathway. *Curr Opin Immunol* 15: 105-111.

Bouvard V, Baan R, Straif K, et al. (2009) A review of human carcinogens--Part B: biological agents. *Lancet Oncol* 10: 321-322.

Boyer SN, Wazer DE and Band V. (1996) E7 protein of human papilloma virus-16 induces degradation of retinoblastoma protein through the ubiquitin-proteasome pathway. *Cancer Res* 56: 4620-4624.

Bravo IG and Felez-Sanchez M. (2015) Papillomaviruses: Viral evolution, cancer and evolutionary medicine. *Evol Med Public Health* 2015: 32-51.

Bray F, Ferlay J, Soerjomataram I, et al. (2018) Global cancer statistics 2018: GLOBOCAN estimates of incidence and mortality worldwide for 36 cancers in 185 countries. *CA Cancer J Clin* 68: 394-424.

Breitburd F, Kirnbauer R, Hubbert NL, et al. (1995) Immunization with viruslike particles from cottontail rabbit papillomavirus (CRPV) can protect against experimental CRPV infection. *J Virol* 69: 3959-3963.

Bruni L, Diaz M, Barrionuevo-Rosas L, et al. (2016) Global estimates of human papillomavirus vaccination coverage by region and income level: a pooled analysis. *Lancet Glob Health* 4: e453-463.

Byrne EH and Fisher DE. (2017) Immune and molecular correlates in melanoma treated with immune checkpoint blockade. *Cancer* 123: 2143-2153.

Castellsague X, Munoz N, Pitisuttithum P, et al. (2011) End-of-study safety, immunogenicity, and efficacy of quadrivalent HPV (types 6, 11, 16, 18) recombinant vaccine in adult women 24-45 years of age. *Br J Cancer* 105: 28-37.

Chaturvedi AK, Engels EA, Pfeiffer RM, et al. (2011) Human papillomavirus and rising oropharyngeal cancer incidence in the United States. *J Clin Oncol* 29: 4294-4301.

Chellappan S, Kraus VB, Kroger B, et al. (1992) Adenovirus E1A, simian virus 40 tumor antigen, and human papillomavirus E7 protein share the capacity to disrupt the interaction between transcription factor E2F and the retinoblastoma gene product. *Proc Natl Acad Sci U S A* 89: 4549-4553.

Chen EY, Howley PM, Levinson AD, et al. (1982) The primary structure and genetic organization of the bovine papillomavirus type 1 genome. *Nature* 299: 529-534.

Chen Z, DeSalle R, Schiffman M, et al. (2018) Niche adaptation and viral transmission of human papillomaviruses from archaic hominins to modern humans. *PLoS Pathog* 14: e1007352.

Cheng S, Schmidt-Grimminger DC, Murant T, et al. (1995) Differentiation-dependent up-regulation of the human papillomavirus E7 gene reactivates cellular DNA replication in suprabasal differentiated keratinocytes. *Genes Dev* 9: 2335-2349.

Collins T, Korman AJ, Wake CT, et al. (1984) Immune interferon activates multiple class II major histocompatibility complex genes and the associated invariant chain gene in human endothelial cells and dermal fibroblasts. *Proc Natl Acad Sci U S A* 81: 4917-4921.

Cooper B, Schneider S, Bohl J, et al. (2003) Requirement of E6AP and the features of human papillomavirus E6 necessary to support degradation of p53. *Virology* 306: 87-99.

Costa F, Das R, Kini Bailur J, et al. (2018) Checkpoint Inhibition in Myeloma: Opportunities and Challenges. *Front Immunol* 9: 2204.

Crosbie EJ, Einstein MH, Franceschi S, et al. (2013) Human papillomavirus and cervical cancer. *Lancet* 382: 889-899.

Cutts FT, Franceschi S, Goldie S, et al. (2007) Human papillomavirus and HPV vaccines: a review. *Bull World Health Organ* 85: 719-726.

D'Souza G, Kreimer AR, Viscidi R, et al. (2007) Case-control study of human papillomavirus and oropharyngeal cancer. *N Engl J Med* 356: 1944-1956.

Danaher P, Warren S, Dennis L, et al. (2017) Gene expression markers of Tumor Infiltrating Leukocytes. *J Immunother Cancer* 5: 18.

Danos O, Katinka M and Yaniv M. (1982) Human papillomavirus 1a complete DNA sequence: a novel type of genome organization among papovaviridae. *EMBO J* 1: 231-236.

Day PM, Lowy DR and Schiller JT. (2003) Papillomaviruses infect cells via a clathrin-dependent pathway. *Virology* 307: 1-11.

de Martel C, Ferlay J, Franceschi S, et al. (2012) Global burden of cancers attributable to infections in 2008: a review and synthetic analysis. *Lancet Oncol* 13: 607-615.

de Martel C, Plummer M, Vignat J, et al. (2017) Worldwide burden of cancer attributable to HPV by site, country and HPV type. *Int J Cancer* 141: 664-670.

de Oliveira WR, Festa Neto C, Rady PL, et al. (2003) Clinical aspects of epidermodysplasia verruciformis. *J Eur Acad Dermatol Venereol* 17: 394-398.

DeGregori J and Johnson DG. (2006) Distinct and Overlapping Roles for E2F Family Members in Transcription, Proliferation and Apoptosis. *Curr Mol Med* 6: 739-748.

Demers GW, Halbert CL and Galloway DA. (1994) Elevated wild-type p53 protein levels in human epithelial cell lines immortalized by the human papillomavirus type 16 E7 gene. *Virology* 198: 169-174.

Deschuyteneer M, Elouahabi A, Plainchamp D, et al. (2010) Molecular and structural characterization of the L1 virus-like particles that are used as vaccine antigens in Cervarix, the AS04-adjuvanted HPV-16 and -18 cervical cancer vaccine. *Hum Vaccin* 6: 407-419.

Doorbar J, Egawa N, Griffin H, et al. (2015) Human papillomavirus molecular biology and disease association. *Rev Med Virol* 25 Suppl 1: 2-23.

Doorbar J, Quint W, Banks L, et al. (2012) The biology and life-cycle of human papillomaviruses. *Vaccine* 30 Suppl 5: F55-70.

Duensing S, Duensing A, Crum CP, et al. (2001) Human papillomavirus type 16 E7 oncoprotein-induced abnormal centrosome synthesis is an early event in the evolving malignant phenotype. *Cancer Res* 61: 2356-2360.

Dunne EF, Unger ER, Sternberg M, et al. (2007) Prevalence of HPV infection among females in the United States. *JAMA* 297: 813-819.

Durst M, Gissmann L, Ikenberg H, et al. (1983) A papillomavirus DNA from a cervical carcinoma and its prevalence in cancer biopsy samples from different geographic regions. *Proc Natl Acad Sci U S A* 80: 3812-3815.

Dyson HJ and Wright PE. (2005) Intrinsically unstructured proteins and their functions. *Nat Rev Mol Cell Biol* 6: 197-208.

Dyson N. (1998) The regulation of E2F by pRB-family proteins. *Genes Dev* 12: 2245-2262.

Dyson N, Guida P, Munger K, et al. (1992) Homologous sequences in adenovirus E1A and human papillomavirus E7 proteins mediate interaction with the same set of cellular proteins. *J Virol* 66: 6893-6902.

Fakhry C, Westra WH, Li S, et al. (2008) Improved survival of patients with human papillomavirus-positive head and neck squamous cell carcinoma in a prospective clinical trial. *J Natl Cancer Inst* 100: 261-269.

Gameiro SF, Ghasemi F, Barrett JW, et al. (2018) Treatment-naive HPV+ head and neck cancers display a T-cell-inflamed phenotype distinct from their HPV- counterparts that has implications for immunotherapy. *Oncoimmunology* 7: e1498439.

Gameiro SF, Ghasemi F, Barrett JW, et al. (2019) High Level Expression of MHC-II in HPV+ Head and Neck Cancers Suggests that Tumor Epithelial Cells Serve an Important Role as Accessory Antigen Presenting Cells. *Cancers (Basel)* 11.

Gameiro SF, Zhang A, Ghasemi F, et al. (2017) Analysis of Class I Major Histocompatibility Complex Gene Transcription in Human Tumors Caused by Human Papillomavirus Infection. *Viruses* 9.

George S, Miao D, Demetri GD, et al. (2017) Loss of PTEN Is Associated with Resistance to Anti-PD-1 Checkpoint Blockade Therapy in Metastatic Uterine Leiomyosarcoma. *Immunity* 46: 197-204.

Georgopoulos NT, Proffitt JL and Blair GE. (2000) Transcriptional regulation of the major histocompatibility complex (MHC) class I heavy chain, TAP1 and LMP2 genes by the human papillomavirus (HPV) type 6b, 16 and 18 E7 oncoproteins. *Oncogene* 19: 4930-4935.

Gewirtzman A, Bartlett B and Tyring S. (2008) Epidermodysplasia verruciformis and human papilloma virus. *Curr Opin Infect Dis* 21: 141-146.

Gillison ML, Chaturvedi AK, Anderson WF, et al. (2015) Epidemiology of Human Papillomavirus-Positive Head and Neck Squamous Cell Carcinoma. *J Clin Oncol* 33: 3235-3242.

Gillison ML, Koch WM, Capone RB, et al. (2000) Evidence for a causal association between human papillomavirus and a subset of head and neck cancers. *J Natl Cancer Inst* 92: 709-720.

Gissmann L, Diehl V, Schultz-Coulon HJ, et al. (1982) Molecular cloning and characterization of human papilloma virus DNA derived from a laryngeal papilloma. *J Virol* 44: 393-400.

Goodwin EC and DiMaio D. (2000) Repression of human papillomavirus oncogenes in HeLa cervical carcinoma cells causes the orderly reactivation of dormant tumor suppressor pathways. *Proc Natl Acad Sci U S A* 97: 12513-12518.

Goodwin EC, Yang E, Lee CJ, et al. (2000) Rapid induction of senescence in human cervical carcinoma cells. *Proc Natl Acad Sci U S A* 97: 10978-10983.

Graham SV. (2010) Human papillomavirus: gene expression, regulation and prospects for novel diagnostic methods and antiviral therapies. *Future Microbiol* 5: 1493-1506.

Green M, Brackmann KH, Sanders PR, et al. (1982) Isolation of a human papillomavirus from a patient with epidermodysplasia verruciformis: presence of related viral DNA genomes in human urogenital tumors. *Proc Natl Acad Sci U S A* 79: 4437-4441.

Harbour JW and Dean DC. (2000) Chromatin remodeling and Rb activity. *Curr Opin Cell Biol* 12: 685-689.

Heller C, Weisser T, Mueller-Schickert A, et al. (2011) Identification of key amino acid residues that determine the ability of high risk HPV16-E7 to dysregulate major histocompatibility complex class I expression. *J Biol Chem* 286: 10983-10997.

Hoffmann M, Ihloff AS, Gorogh T, et al. (2010) p16(INK4a) overexpression predicts translational active human papillomavirus infection in tonsillar cancer. *Int J Cancer* 127: 1595-1602.

Holland D, Hoppe-Seyler K, Schuller B, et al. (2008) Activation of the enhancer of zeste homologue 2 gene by the human papillomavirus E7 oncoprotein. *Cancer Res* 68: 9964-9972.

Holzel M, Bovier A and Tuting T. (2013) Plasticity of tumour and immune cells: a source of heterogeneity and a cause for therapy resistance? *Nat Rev Cancer* 13: 365-376.

Huibregtse JM, Scheffner M and Howley PM. (1991) A cellular protein mediates association of p53 with the E6 oncoprotein of human papillomavirus types 16 or 18. *EMBO J* 10: 4129-4135.

Hyland PL, McDade SS, McCloskey R, et al. (2011) Evidence for alteration of EZH2, BMI1, and KDM6A and epigenetic reprogramming in human papillomavirus type 16 E6/E7-expressing keratinocytes. *J Virol* 85: 10999-11006.

Javier RT and Butel JS. (2008) The history of tumor virology. *Cancer Res* 68: 7693-7706.

Jeon S, Allen-Hoffmann BL and Lambert PF. (1995) Integration of human papillomavirus type 16 into the human genome correlates with a selective growth advantage of cells. *J Virol* 69: 2989-2997.

Jiang M and Milner J. (2002) Selective silencing of viral gene expression in HPV-positive human cervical carcinoma cells treated with siRNA, a primer of RNA interference. *Oncogene* 21: 6041-6048.

Jit M, Brisson M, Portnoy A, et al. (2014) Cost-effectiveness of female human papillomavirus vaccination in 179 countries: a PRIME modelling study. *Lancet Glob Health* 2: e406-414.

Jones DL, Thompson DA and Munger K. (1997) Destabilization of the RB tumor suppressor protein and stabilization of p53 contribute to HPV type 16 E7-induced apoptosis. *Virology* 239: 97-107.

Joyce JA and Pollard JW. (2009) Microenvironmental regulation of metastasis. *Nat Rev Cancer* 9: 239-252.

Kang H, Kiess A and Chung CH. (2015) Emerging biomarkers in head and neck cancer in the era of genomics. *Nat Rev Clin Oncol* 12: 11-26.

Kim BS, Miyagawa F, Cho YH, et al. (2009) Keratinocytes function as accessory cells for presentation of endogenous antigen expressed in the epidermis. *J Invest Dermatol* 129: 2805-2817.

Klaes R, Friedrich T, Spitkovsky D, et al. (2001) Overexpression of p16(INK4A) as a specific marker for dysplastic and neoplastic epithelial cells of the cervix uteri. *Int J Cancer* 92: 276-284.

Klingelhutz AJ and Roman A. (2012) Cellular transformation by human papillomaviruses: lessons learned by comparing high- and low-risk viruses. *Virology* 424: 77-98.

Kreimer AR, Clifford GM, Boyle P, et al. (2005) Human papillomavirus types in head and neck squamous cell carcinomas worldwide: a systematic review. *Cancer Epidemiol Biomarkers Prev* 14: 467-475.

Kristiansen E, Jenkins A and Holm R. (1994) Coexistence of episomal and integrated HPV16 DNA in squamous cell carcinoma of the cervix. *J Clin Pathol* 47: 253-256.

Lane JE, Bowman PH and Cohen DJ. (2003) Epidermodysplasia verruciformis. *South Med J* 96: 613-615.

Lassen P, Eriksen JG, Krogdahl A, et al. (2011) The influence of HPV-associated p16-expression on accelerated fractionated radiotherapy in head and neck cancer: evaluation of the randomised DAHANCA 6&7 trial. *Radiother Oncol* 100: 49-55.

Leemans CR, Snijders PJF and Brakenhoff RH. (2018) The molecular landscape of head and neck cancer. *Nat Rev Cancer* 18: 269-282.

Lehtinen M, Paavonen J, Wheeler CM, et al. (2012) Overall efficacy of HPV-16/18 AS04-adjuvanted vaccine against grade 3 or greater cervical intraepithelial neoplasia: 4-year end-of-study analysis of the randomised, double-blind PATRICIA trial. *Lancet Oncol* 13: 89-99.

Levine AJ and Oren M. (2009) The first 30 years of p53: growing ever more complex. *Nat Rev Cancer* 9: 749-758.

Li W, Deng XM, Wang CX, et al. (2010) Down-regulation of HLA class I antigen in human papillomavirus type 16 E7 expressing HaCaT cells: correlate with TAP-1 expression. *Int J Gynecol Cancer* 20: 227-232.

Liu J, Lichtenberg T, Hoadley KA, et al. (2018) An Integrated TCGA Pan-Cancer Clinical Data Resource to Drive High-Quality Survival Outcome Analytics. *Cell* 173: 400-416 e411.

Llosa NJ, Cruise M, Tam A, et al. (2015) The vigorous immune microenvironment of microsatellite instable colon cancer is balanced by multiple counter-inhibitory checkpoints. *Cancer Discov* 5: 43-51.

Madison KC. (2003) Barrier function of the skin: "la raison d'etre" of the epidermis. *J Invest Dermatol* 121: 231-241.

Mammas IN, Sourvinos G and Spandidos DA. (2009) Human papilloma virus (HPV) infection in children and adolescents. *Eur J Pediatr* 168: 267-273.

Mansur CP and Androphy EJ. (1993) Cellular transformation by papillomavirus oncoproteins. *Biochim Biophys Acta* 1155: 323-345.

McBride AA. (2008) Replication and partitioning of papillomavirus genomes. *Adv Virus Res* 72: 155-205.

McBride AA. (2017) Mechanisms and strategies of papillomavirus replication. *Biol Chem* 398: 919-927.

McBride AA and Warburton A. (2017) The role of integration in oncogenic progression of HPV-associated cancers. *PLoS Pathog* 13: e1006211.

McLaughlin-Drubin ME, Crum CP and Munger K. (2011) Human papillomavirus E7 oncoprotein induces KDM6A and KDM6B histone demethylase expression and causes epigenetic reprogramming. *Proc Natl Acad Sci U S A* 108: 2130-2135.

McLaughlin-Drubin ME, Meyers J and Munger K. (2012) Cancer associated human papillomaviruses. *Curr Opin Virol* 2: 459-466.

McLaughlin-Drubin ME, Park D and Munger K. (2013) Tumor suppressor p16INK4A is necessary for survival of cervical carcinoma cell lines. *Proc Natl Acad Sci U S A* 110: 16175-16180.

Mesri EA, Feitelson MA and Munger K. (2014) Human viral oncogenesis: a cancer hallmarks analysis. *Cell Host Microbe* 15: 266-282.

Moody CA and Laimins LA. (2010) Human papillomavirus oncoproteins: pathways to transformation. *Nat Rev Cancer* 10: 550-560.

Muhr LSA, Eklund C and Dillner J. (2018) Towards quality and order in human papillomavirus research. *Virology* 519: 74-76.

Munger K, Werness BA, Dyson N, et al. (1989) Complex formation of human papillomavirus E7 proteins with the retinoblastoma tumor suppressor gene product. *EMBO J* 8: 4099-4105.

Munoz N, Bosch FX, de Sanjose S, et al. (1992) The causal link between human papillomavirus and invasive cervical cancer: a population-based case-control study in Colombia and Spain. *Int J Cancer* 52: 743-749.

Munoz N, Kjaer SK, Sigurdsson K, et al. (2010) Impact of human papillomavirus (HPV)-6/11/16/18 vaccine on all HPV-associated genital diseases in young women. *J Natl Cancer Inst* 102: 325-339.

Nakasone ES, Askautrud HA, Kees T, et al. (2012) Imaging tumor-stroma interactions during chemotherapy reveals contributions of the microenvironment to resistance. *Cancer Cell* 21: 488-503.

Network TCGAR. (2015) Comprehensive genomic characterization of head and neck squamous cell carcinomas. *Nature* 517: 576-582.

Network TCGAR. (2017) Integrated genomic and molecular characterization of cervical cancer. *Nature* 543: 378-384.

Newman AM, Liu CL, Green MR, et al. (2015) Robust enumeration of cell subsets from tissue expression profiles. *Nat Methods* 12: 453-457.

Nichols AC, Dhaliwal SS, Palma DA, et al. (2013a) Does HPV type affect outcome in oropharyngeal cancer? *J Otolaryngol Head Neck Surg* 42: 9.

Nichols AC, Palma DA, Dhaliwal SS, et al. (2013b) The epidemic of human papillomavirus and oropharyngeal cancer in a Canadian population. *Curr Oncol* 20: 212-219.

Nomine Y, Masson M, Charbonnier S, et al. (2006) Structural and functional analysis of E6 oncoprotein: insights in the molecular pathways of human papillomavirus-mediated pathogenesis. *Mol Cell* 21: 665-678.

Ohlenschlager O, Seiboth T, Zengerling H, et al. (2006) Solution structure of the partially folded high-risk human papilloma virus 45 oncoprotein E7. *Oncogene* 25: 5953-5959.

Parfenov M, Pedamallu CS, Gehlenborg N, et al. (2014) Characterization of HPV and host genome interactions in primary head and neck cancers. *Proc Natl Acad Sci U S A* 111: 15544-15549.

Parish JL, Bean AM, Park RB, et al. (2006) ChlR1 is required for loading papillomavirus E2 onto mitotic chromosomes and viral genome maintenance. *Mol Cell* 24: 867-876.

Peter M, Rosty C, Couturier J, et al. (2006) MYC activation associated with the integration of HPV DNA at the MYC locus in genital tumors. *Oncogene* 25: 5985-5993.

Phelps WC, Yee CL, Munger K, et al. (1988) The human papillomavirus type 16 E7 gene encodes transactivation and transformation functions similar to those of adenovirus E1A. *Cell* 53: 539-547.

Plummer M, de Martel C, Vignat J, et al. (2016) Global burden of cancers attributable to infections in 2012: a synthetic analysis. *Lancet Glob Health* 4: e609-616.

Polyak K, Haviv I and Campbell IG. (2009) Co-evolution of tumor cells and their microenvironment. *Trends Genet* 25: 30-38.

Popov N and Gil J. (2010) Epigenetic regulation of the INK4b-ARF-INK4a locus: in sickness and in health. *Epigenetics* 5: 685-690.

Posner MR, Lorch JH, Goloubeva O, et al. (2011) Survival and human papillomavirus in oropharynx cancer in TAX 324: a subset analysis from an international phase III trial. *Ann Oncol* 22: 1071-1077.

Pyeon D, Pearce SM, Lank SM, et al. (2009) Establishment of human papillomavirus infection requires cell cycle progression. *PLoS Pathog* 5: e1000318.

Rampias T, Sasaki C, Weinberger P, et al. (2009) E6 and e7 gene silencing and transformed phenotype of human papillomavirus 16-positive oropharyngeal cancer cells. *J Natl Cancer Inst* 101: 412-423.

Rayess H, Wang MB and Srivatsan ES. (2012) Cellular senescence and tumor suppressor gene p16. *Int J Cancer* 130: 1715-1725.

Rector A and Van Ranst M. (2013) Animal papillomaviruses. *Virology* 445: 213-223.

Rischin D, Young RJ, Fisher R, et al. (2010) Prognostic significance of p16INK4A and human papillomavirus in patients with oropharyngeal cancer treated on TROG 02.02 phase III trial. *J Clin Oncol* 28: 4142-4148.

Roden RBS and Stern PL. (2018) Opportunities and challenges for human papillomavirus vaccination in cancer. *Nat Rev Cancer* 18: 240-254.

Rooney MS, Shukla SA, Wu CJ, et al. (2015) Molecular and genetic properties of tumors associated with local immune cytolytic activity. *Cell* 160: 48-61.

Rous P and Beard JW. (1935) The Progression to Carcinoma of Virus-Induced Rabbit Papillomas (Shope). *J Exp Med* 62: 523-548.

Sano T, Oyama T, Kashiwabara K, et al. (1998) Expression status of p16 protein is associated with human papillomavirus oncogenic potential in cervical and genital lesions. *Am J Pathol* 153: 1741-1748.

Scheffner M, Huibregtse JM, Vierstra RD, et al. (1993) The HPV-16 E6 and E6-AP complex functions as a ubiquitin-protein ligase in the ubiquitination of p53. *Cell* 75: 495-505.

Scheffner M, Werness BA, Huibregtse JM, et al. (1990) The E6 oncoprotein encoded by human papillomavirus types 16 and 18 promotes the degradation of p53. *Cell* 63: 1129-1136.

Schelhaas M, Shah B, Holzer M, et al. (2012) Entry of human papillomavirus type 16 by actin-dependent, clathrin- and lipid raft-independent endocytosis. *PLoS Pathog* 8: e1002657.

Schiffman M, Castle PE, Jeronimo J, et al. (2007) Human papillomavirus and cervical cancer. *Lancet* 370: 890-907.

Schiffman M, Doorbar J, Wentzensen N, et al. (2016) Carcinogenic human papillomavirus infection. *Nat Rev Dis Primers* 2: 16086.

Schiller JT, Castellsague X and Garland SM. (2012) A review of clinical trials of human papillomavirus prophylactic vaccines. *Vaccine* 30 Suppl 5: F123-138.

Schwarz E, Freese UK, Gissmann L, et al. (1985) Structure and transcription of human papillomavirus sequences in cervical carcinoma cells. *Nature* 314: 111-114.

Shafti-Keramat S, Handisurya A, Kriehuber E, et al. (2003) Different heparan sulfate proteoglycans serve as cellular receptors for human papillomaviruses. *J Virol* 77: 13125-13135.

Sherman L, Jackman A, Itzhaki H, et al. (1997) Inhibition of serum- and calcium-induced differentiation of human keratinocytes by HPV16 E6 oncoprotein: role of p53 inactivation. *Virology* 237: 296-306.

Shope RE and Hurst EW. (1933) Infectious Papillomatosis of Rabbits : With a Note on the Histopathology. *J Exp Med* 58: 607-624.

Sima N, Wang W, Kong D, et al. (2008) RNA interference against HPV16 E7 oncogene leads to viral E6 and E7 suppression in cervical cancer cells and apoptosis via upregulation of Rb and p53. *Apoptosis* 13: 273-281.

Small W, Jr., Bacon MA, Bajaj A, et al. (2017) Cervical cancer: A global health crisis. *Cancer* 123: 2404-2412.

Spranger S. (2016) Mechanisms of tumor escape in the context of the T-cell-inflamed and the non-T-cell-inflamed tumor microenvironment. *Int Immunol* 28: 383-391.

Stevaux O and Dyson NJ. (2002) A revised picture of the E2F transcriptional network and RB function. *Curr Opin Cell Biol* 14: 684-691.

Suzich JA, Ghim SJ, Palmer-Hill FJ, et al. (1995) Systemic immunization with papillomavirus L1 protein completely prevents the development of viral mucosal papillomas. *Proc Natl Acad Sci U S A* 92: 11553-11557.

Syrjanen S and Syrjanen K. (2008) The history of papillomavirus research. *Cent Eur J Public Health* 16 Suppl: S7-13.

Thorland EC, Myers SL, Gostout BS, et al. (2003) Common fragile sites are preferential targets for HPV16 integrations in cervical tumors. *Oncogene* 22: 1225-1237.

Tommasino M. (2014) The human papillomavirus family and its role in carcinogenesis. *Semin Cancer Biol* 26: 13-21.

Turley SJ, Cremasco V and Astarita JL. (2015) Immunological hallmarks of stromal cells in the tumour microenvironment. *Nat Rev Immunol* 15: 669-682.

van den Elsen PJ, Holling TM, Kuipers HF, et al. (2004) Transcriptional regulation of antigen presentation. *Curr Opin Immunol* 16: 67-75.

Vande Pol SB and Klingelhutz AJ. (2013) Papillomavirus E6 oncoproteins. *Virology* 445: 115-137.

Vousden K. (1993) Interactions of human papillomavirus transforming proteins with the products of tumor suppressor genes. *FASEB J* 7: 872-879.

Vousden KH and Jat PS. (1989) Functional similarity between HPV16E7, SV40 large T and adenovirus E1a proteins. *Oncogene* 4: 153-158.

Warren CJ, Westrich JA, Doorslaer KV, et al. (2017) Roles of APOBEC3A and APOBEC3B in Human Papillomavirus Infection and Disease Progression. *Viruses* 9.

Wherry EJ. (2011) T cell exhaustion. *Nat Immunol* 12: 492-499.

White AE, Livanos EM and Tlsty TD. (1994) Differential disruption of genomic integrity and cell cycle regulation in normal human fibroblasts by the HPV oncoproteins. *Genes Dev* 8: 666-677.

Wolf Y and Samuels Y. (2018) Cancer research in the era of immunogenomics. *ESMO Open* 3: e000475.

Zachow KR, Ostrow RS, Bender M, et al. (1982) Detection of human papillomavirus DNA in anogenital neoplasias. *Nature* 300: 771-773.

Zanier K, Charbonnier S, Sidi AO, et al. (2013) Structural basis for hijacking of cellular LxxLL motifs by papillomavirus E6 oncoproteins. *Science* 339: 694-698.

Zanier K, ould M'hamed ould Sidi A, Boulade-Ladame C, et al. (2012) Solution structure analysis of the HPV16 E6 oncoprotein reveals a self-association mechanism required for E6-mediated degradation of p53. *Structure* 20: 604-617.

Zerfass K, Schulze A, Spitkovsky D, et al. (1995) Sequential activation of cyclin E and cyclin A gene expression by human papillomavirus type 16 E7 through sequences necessary for transformation. *J Virol* 69: 6389-6399.

zur Hausen H. (1977) Human papillomaviruses and their possible role in squamous cell carcinomas. *Curr Top Microbiol Immunol* 78: 1-30.

zur Hausen H. (1999) Immortalization of human cells and their malignant conversion by high risk human papillomavirus genotypes. *Semin Cancer Biol* 9: 405-411.

zur Hausen H. (2002) Papillomaviruses and cancer: from basic studies to clinical application. *Nat Rev Cancer* 2: 342-350.

zur Hausen H. (2009) Papillomaviruses in the causation of human cancers - a brief historical account. *Virology* 384: 260-265.

zur Hausen H, Meinhof W, Scheiber W, et al. (1974) Attempts to detect virus-secific DNA in human tumors. I. Nucleic acid hybridizations with complementary RNA of human wart virus. *Int J Cancer* 13: 650-656.

Chapter 2

2 Human Papillomavirus Dysregulates the Cellular Apparatus Controlling the Methylation Status of H3K27 in Different Human Cancers to Consistently Alter Gene Expression Regardless of Tissue of Origin

2.1 Introduction

Human papillomaviruses (HPV) that infect mucosal tissues are classified as low- or high-risk based on the frequency with which they are associated with cancer. Although both types dysregulate normal cell growth, infection by high-risk HPV is a causative agent for cancers at multiple distinct anatomical subsites (zur Hausen, 1996; zur Hausen, 2002). HPV was first recognized as the cause of virtually all cervical carcinomas and was then subsequently found to contribute to other anogenital cancers as well (Alemany et al., 2016; Crosbie et al., 2013; Guimera et al., 2017; zur Hausen, 2002). More recently, HPV infection was recognized as the agent responsible for an epidemic of oropharyngeal cancers (Gillison et al., 2000; Syrjanen, 2005). HPV has also been suggested to cause a subset of lung, prostate, bladder, and breast cancers (Lawson et al., 2015; The Cancer Genome Atlas Research Network, 2014; Singh et al., 2015; Zhai et al., 2015). Taken together, HPV infection is thought to be responsible for at least 5% of human cancers worldwide (Forman et al., 2012).

HPV encodes two main oncogenes, *E6* and *E7* (Doorbar et al., 2012). Both are constitutively expressed in HPV-positive (HPV+) tumors, and suppression of expression of either of these two viral proteins causes HPV-dependent tumor cells to senesce and die (Deng et al., 2013; Goodwin and DiMaio, 2000; Goodwin et al., 2000; Jiang and Milner, 2002; Rampias et al., 2009; Sima et al., 2008; zur Hausen, 1996). Both E6 and E7 perform multiple functions in an infected and/or cancerous cell. These two viral oncoproteins function by interacting with multiple key cellular regulatory proteins to dysregulate gene expression and growth (Doorbar et al., 2012). For example, p53 is bound and degraded by E6, while the retinoblastoma protein (Rb) and family members are important targets of E7

(Dyson et al., 1992; Kessis et al., 1993). Rb controls exit from the G1 phase of the cell cycle, and the interaction and subsequent degradation of Rb by E7 induces inappropriate cell cycle progression in HPV infected cells (Boyer et al., 1996; Brehm et al., 1998). In high-risk HPV infections, viral oncoproteins function to uncouple cell growth and differentiation and contribute to the formation of epithelial dysplasia, which may progress to carcinoma if the infection is not resolved (Doorbar et al., 2012).

The HPV E7 oncoproteins alter the regulation of many host cellular genes and much effort has been devoted to understanding the mechanisms by which this occurs (Munger et al., 2001). A subset of the effects of E7 on the cellular transcriptome are mediated by epigenetic changes (Durzynska et al., 2017). Specifically, E7 expression has been reported to reduce the global levels of tri-methylated lysine 27 on histone 3 (H3K27me3), a mark of transcriptionally silenced chromatin (McLaughlin-Drubin et al., 2011; McLaughlin-Drubin et al., 2008; Schwartz and Pirrotta, 2007). Paradoxically, several cell culture studies have shown that HPV induces a significant upregulation in the expression level of the enhancer of zeste homolog 2 (EZH2) component of the polycomb repressive complex 2 (PRC2) (Holland et al., 2008; Hyland et al., 2011; McLaughlin-Drubin et al., 2011)—which is the methyltransferase responsible for mono-, di-, and tri-methylation of H3K27 (Popov and Gil, 2010; Schwartz and Pirrotta, 2007). Both studies also observed an HPV-dependent increase in lysine demethylase 6A (KDM6A) or lysine demethylase 6B (KDM6B)—the demethylases that convert H3K27me3 to the di-methylated or mono-methylated forms (Hyland et al., 2011; McLaughlin-Drubin et al., 2011). Thus, HPV increases expression of the enzymes responsible for creating and removing H3K27me3, complicating our understanding of how the global decrease in H3K27me3 is achieved in an HPV infection.

Mechanistic studies of these HPV-dependent changes on epigenetic regulators of gene expression have focused on altered p16 expression, which is present at high levels in nearly all HPV-induced tumors (Klaes et al., 2001; Sano et al., 1998). Indeed, p16 was commonly used as a surrogate marker of HPV status during pathological assessment of tumors, but this method to determine HPV status has largely been superseded by the implementation of molecularly-based diagnostics (Burd, 2016; Hoffmann et al., 2010; Klaes et al., 2001). The p16 and p14 products of the *cyclin-dependent kinase inhibitor 2A* (*CDKN2A*) gene

locus normally function as negative regulators of the cell cycle. The p16 tumor suppressor induces cell cycle arrest and senescence by inhibiting E2F-mediated transcription, whereas p14 induces cell cycle arrest and apoptosis by facilitating p53 function (Zhang et al., 1998). Neither of these products inhibit cell cycle progression in HPV-induced cancers, as the p53 and Rb pathways have been abrogated by E6 and E7, respectively (Dyson et al., 1992; Kessis et al., 1993). However, transcription from the *CDKN2A* locus is tightly regulated by epigenetic changes, with PRC2 serving a key role in repressing expression by catalyzing tri-methylation of H3K27 across this locus. Subsequently, the polycomb repressive complex 1 (PRC1) is recruited to maintain a transcriptionally repressive chromatin environment that is typically reflected by a local increase in DNA methylation (Popov and Gil, 2010). Thus, this well-characterized locus serves as a good model of epigenetic dysregulation induced by HPV infection (Kanao et al., 2004; Schlecht et al., 2015).

In a detailed series of tissue culture-based experiments, evidence was obtained to suggest that the HPV-mediated reduction in H3K27me3 and subsequent transcriptional activation of p16 required E7 to induce expression of the H3K27-specific demethylases KDM6A and KDM6B (McLaughlin-Drubin et al., 2011; McLaughlin-Drubin et al., 2013). Knockdown of either KDM6A or KDM6B in HPV+ cervical carcinoma cell lines not only reduced p16 expression, but also induced cell death (McLaughlin-Drubin et al., 2011; McLaughlin-Drubin et al., 2013). Subsequent experiments showed that E7 expression in cell lines induced an acute dependence on KDM6B for growth. E7 expressing cells were similarly dependent on p16 expression, as treatment with a KDM6 selective small molecule inhibitor was cytotoxic in multiple cervical carcinoma cell lines (McLaughlin-Drubin et al., 2011; McLaughlin-Drubin et al., 2013). Thus, HPV E7 expressing cells are uniquely vulnerable to a targeted agent affecting an epigenetic regulator of cellular gene expression.

While most of this work was done in tissue culture models, similar changes in expression of H3K27me3 regulators were reported in individual cervical carcinomas (Holland et al., 2008; Hyland et al., 2011; McLaughlin-Drubin et al., 2011). An analysis of these effects has not been done in any HPV+ oral cavity tumors or on a large scale for any HPV-induced tumor site. As such, it remains an open question as to whether these changes in epigenetic regulators are specific for distinct subsites of HPV-induced tumors, and how frequently

they occur in clinical samples. This information is clearly relevant, considering that cancerous cells expressing E7 appear preferentially sensitive to KDM6 inhibition (McLaughlin-Drubin et al., 2011; McLaughlin-Drubin et al., 2013), which could represent a new therapeutic approach for their treatment.

In this study, we used data from over 800 human cervical (The Cancer Genome Atlas Research Network, 2017) and head and neck tumors (The Cancer Genome Atlas Research Network, 2015) from The Cancer Genome Atlas (TCGA) to determine how high-risk HPV oncogene expression alters expression of H3K27me3 regulators in human tumors. We assessed the impact of HPV status on the transcript levels of key regulators of H3K27 methylation, including *EZH2*, *KDM6A*, and *KDM6B*. We also examined the effect of HPV status on gene expression and DNA methylation status across the *CDKN2A* genomic region in these two distinct patient cohorts. We found that HPV+ tumors from both anatomical sites exhibited high levels of *p16* and *p14*. Furthermore, HPV+ tumors also expressed higher levels of *EZH2* and *KDM6A*. Analysis of CpG methylation also detected two sites in the *CDKN2A* locus with consistently altered methylation in HPV+ tumors versus HPV-negative (HPV–) samples. Taken together, this data validates conclusions drawn from tissue culture studies and identifies remarkable similarities between the effects of HPV on gene expression and methylation in both cervical and oral tumors in large human cohorts. These results also provide compelling evidence from human tumors that support the current model of HPV dysregulation of H3K27 methylation and cognate gene expression via the upregulation of KDM6A.

2.2 Materials and Methods

2.2.1 RNA expression comparisons and statistical analysis

Level 3 RNA-Seq by Expectation Maximization (RSEM) normalized Illumina HiSeq RNA expression data for the TCGA head and neck cancer (HNSC) and cervical carcinoma (CESC) cohorts was downloaded from the Broad Genome Data Analysis Centers Firehose server (https://gdac.broadinstitute.org/). The use of mRNA expression data that has undergone RSEM normalization via a uniform pipeline allows comparison of samples within and between TCGA cohorts (Li and Dewey, 2011). Effectively, these files represent

tables listing a quantitative RNA-seq read value for each gene or isoform for each TCGA sample. Although rare HPV+ samples have been identified in the TCGA bladder urothelial carcinoma (BLCA) and colon adenocarcinoma (COAD) cohorts, they were not present in sufficient numbers for any useful comparisons. For all genes except *p16* and *p14*, the gene level Firehose dataset was used. For *p16* and *p14*, the gene isoform level Firehose dataset was used (uc003zpk.2 and uc003zpl.2, respectively) to adequately discriminate between these two different products of the *CDKN2A* gene. Normalized expression data was extracted into Microsoft Excel and the HPV status was manually curated based on published datasets (Banister et al., 2017; Bratman et al., 2016; The Cancer Genome Atlas Research Network, 2015; The Cancer Genome Atlas Research Network, 2017). For each gene analyzed, primary patient samples with known HPV status were grouped as HPV+, HPV–, or normal control tissue. Patient samples with unknown HPV status were omitted from our calculations, as were samples obtained from secondary metastatic lesions. This resulted in 73 HPV+, 442 HPV–, and 43 normal control samples with data available for the HNSC gene expression analysis and 278 HPV+, 19 HPV–, and 3 normal control samples available for the CESC gene expression analysis. Boxplot comparison of gene expression was performed using BoxPlotR (http://shiny.chemgrid.org/boxplotr/) and assembled into final form using CorelDRAW. For the box plots, center lines show the medians, box limits indicate the 25th and 75th percentiles as determined by R software and whiskers extend 1.5 times the interquartile range from the 25th and 75th percentiles. Statistical significance was calculated using Graphpad Prism v6.01. *p*-values were assigned using a one-tailed non-parametric Mann-Whitney U test. Post-hoc power calculations were performed with G*Power software version 3.1.9.2 (Faul et al., 2007), using post-hoc t-test family calculations, with effect size selected as 0.8 and $\alpha = 0.05$. All comparisons achieved a power value > 0.8, or demonstrated significant differences, unless otherwise noted in the text.

2.2.2 DNA methylation comparisons and statistical analysis

Level 3 Infinium Human Methylation450 BeadChip array data for the TCGA HNSC and CESC cohorts was downloaded from the Broad Genome Data Analysis Centers Firehose server (https://gdac.broadinstitute.org/). There were 14 methylation probes identified to be

present in the *CDKN2A* and adjacent *CDKN2B* region: cg00718440, cg02400248, cg03079681, cg04026675, cg07562918, cg08390209, cg10848754, cg12840719, cg13601799, cg13926295, cg14069088, cg14430974, cg19133618, cg19481686. Methylation data for all patient samples for these probes were extracted from the Firehose files and assembled into a table using Microsoft Excel. HPV status was manually curated based on published datasets (Banister et al., 2017; Bratman et al., 2016; The Cancer Genome Atlas Research Network, 2015; The Cancer Genome Atlas Research Network, 2017). For each gene analyzed, primary patient samples with known HPV status were grouped as HPV+, HPV–, or normal control tissue. Patient samples with unknown HPV status were omitted from our calculations, as were samples obtained from secondary metastatic lesions. This resulted in 73 HPV+ tumors, 442 HPV– tumors, and 43 normal control samples with data available for the HNSC methylation analysis and 278, 19, and 3 samples, respectively, available for the CESC methylation analysis. The average methylation Beta-value and standard deviation was calculated for each probe for each sample type in each cohort. Data was plotted using Excel and assembled into final form using CorelDRAW. For statistical analysis, Beta-values were converted to M-values using the following equation to improve homoscedasticity of the data:

$$M_i = \log_2\left(\frac{Beta_i}{1 - Beta_i}\right)$$

where M_i and $Beta_i$ are the M-value and Beta-value of the i^{th} interrogated CpG site (Du et al., 2010). The data was analyzed using Graphpad Prism v6.01. The *p*-values were assigned using non-parametric Kruskal-Wallis test and Dunn's multiple comparisons test.

2.3 Results

2.3.1 Impact of HPV status on *CDKN2A* and *CDKN2B* expression in human tumors

The *CDKN2A* and adjacent *cyclin-dependent kinase inhibitor 2B* (*CDKN2B*) loci encode three distinct tumor suppressors: p16 INK4A, p14 ARF, and p15 INK4B. This gene cluster also encodes a long non-coding RNA transcribed in the antisense direction that is referred to as *CDKN2B-AS* or *antisense non-coding RNA in the INK4 locus* (*ANRIL*) (**Figure 2.1**).

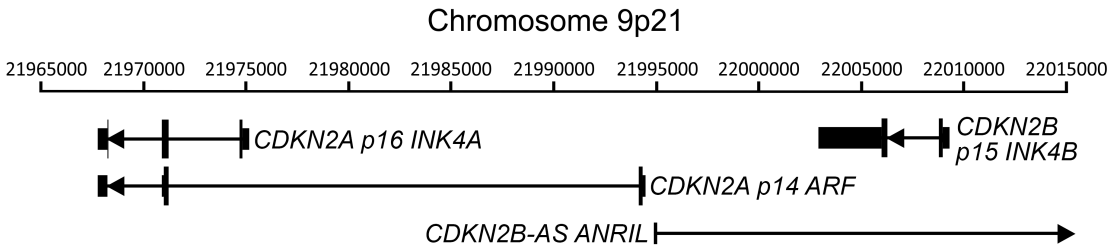

Figure 2.1. Organization of the *CDKN2A* and *CDKN2B* loci.

The *cyclin-dependent kinase inhibitor 2A* (*CDKN2A*) locus encodes two functionally unrelated protein products named p16 INK4A and p14 ARF. The adjacent *CDKN2B* locus encodes p15 INK4B. This gene cluster also encodes a long non-coding RNA transcribed in the antisense direction named *CDKN2B-AS* or *antisense non-coding RNA in the INK4 locus* (*ANRIL*). The position of transcripts (black lines), exons (black vertical bars), coding regions (thick black vertical bars), and orientation (direction of arrowheads) of the major transcripts in this region of chromosome 9 are indicated.

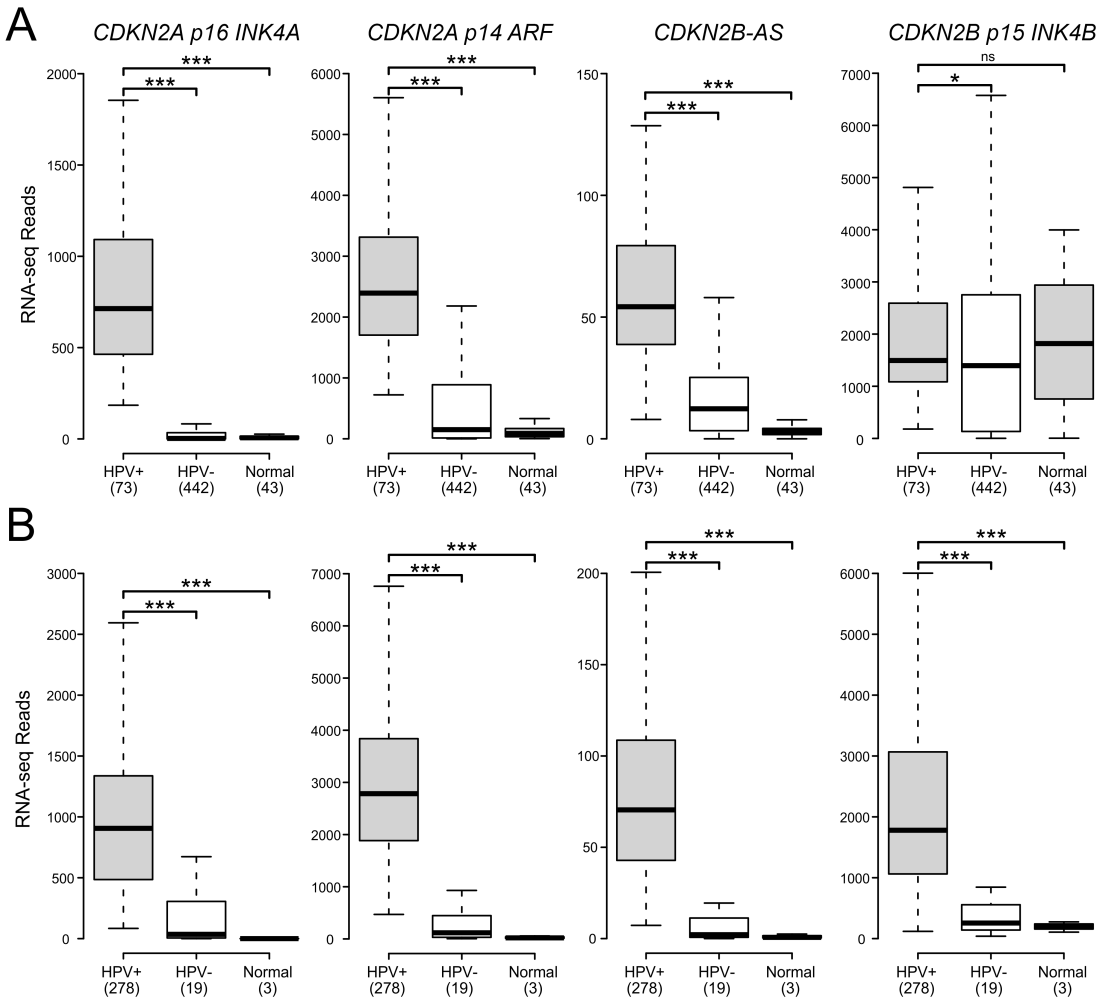

Figure 2.2. HPV perturbation of expression of the *CDKN2A* and *CDKN2B* genes in human head & neck and cervical carcinomas.

Normalized RNA-Seq data extracted from the TCGA database for the HNSC (**A**) and CESC (**B**) cohorts for HPV+, HPV–, and normal control tissues. Numbers in brackets refer to the number of samples included in each analysis. * $p \leq 0.05$, *** $p \leq 0.001$, ns – not significant.

Expression of all three coding genes from this cluster is silenced by PRCs during normal cell growth (Popov and Gil, 2010). While HPV-induced cancers commonly express high levels of the p16 product of the *CDKN2A* locus (Klaes et al., 2001; Sano et al., 1998), the expression levels of *p14*, *p15*, and the non-coding *CDKN2B-AS* RNA have not been studied as extensively. We analyzed the TCGA Illumina HiSeq RNA expression data from the HNSC and CESC cohorts for expression of all four genes (**Figure 2.2**). As expected, HPV+ samples from both the HNSC and CESC cohorts had greatly increased levels of *p16* mRNA expression compared to HPV– tumors and normal control tissue. Like *p16*, a similar upregulation of *p14*, *p15*, and *CDKN2B-AS* was observed in HPV+ cancers with respect to HPV– cancers (**Figure 2.2**). These results indicate that PRC-mediated repression is abrogated across the entire *CDKN2A* and *CDKN2B* regions of the *INK4* locus by HPV infection. The only major difference appears to be the high level of *p15* expression present in the normal control samples for the HNSC cohort, which likely reflects some tissue specific, HPV-independent regulation.

2.3.2 Impact of HPV status on expression of PRC2 components and *BMI1* in human tumors

The H3K27 methyltransferase activity of PRC2 relies on the catalytic subunit EZH2, as well as the embryonic ectoderm development (EED) and suppressor of zeste 12 (SUZ12) components. Multiple studies have reported EZH2 upregulation in HPV+ cancer cell lines, with similarly higher expression reported in small studies of HPV+ cervical carcinomas (Holland et al., 2008; Hyland et al., 2011; McLaughlin-Drubin et al., 2011). Much less is known about the effect of HPV status on the other PRC2 core components. Analysis of TCGA data reveals significantly elevated expression of all three PRC2 core components compared to normal control tissue in both HNSC and CESC (**Figure 2.3**). All but *SUZ12* in the CESC cohort are similarly elevated as compared to HPV– cancers. Thus, the core components of the PRC2 methyltransferase are all consistently transcribed at high levels in HPV+ human tumors. This is in stark contrast to the reported decreases in global H3K27me3 (Hyland et al., 2011; McLaughlin-Drubin et al., 2011) and the upregulation of the *CDKN2A* and *CDKN2B* loci we observe in HPV+ tumors.

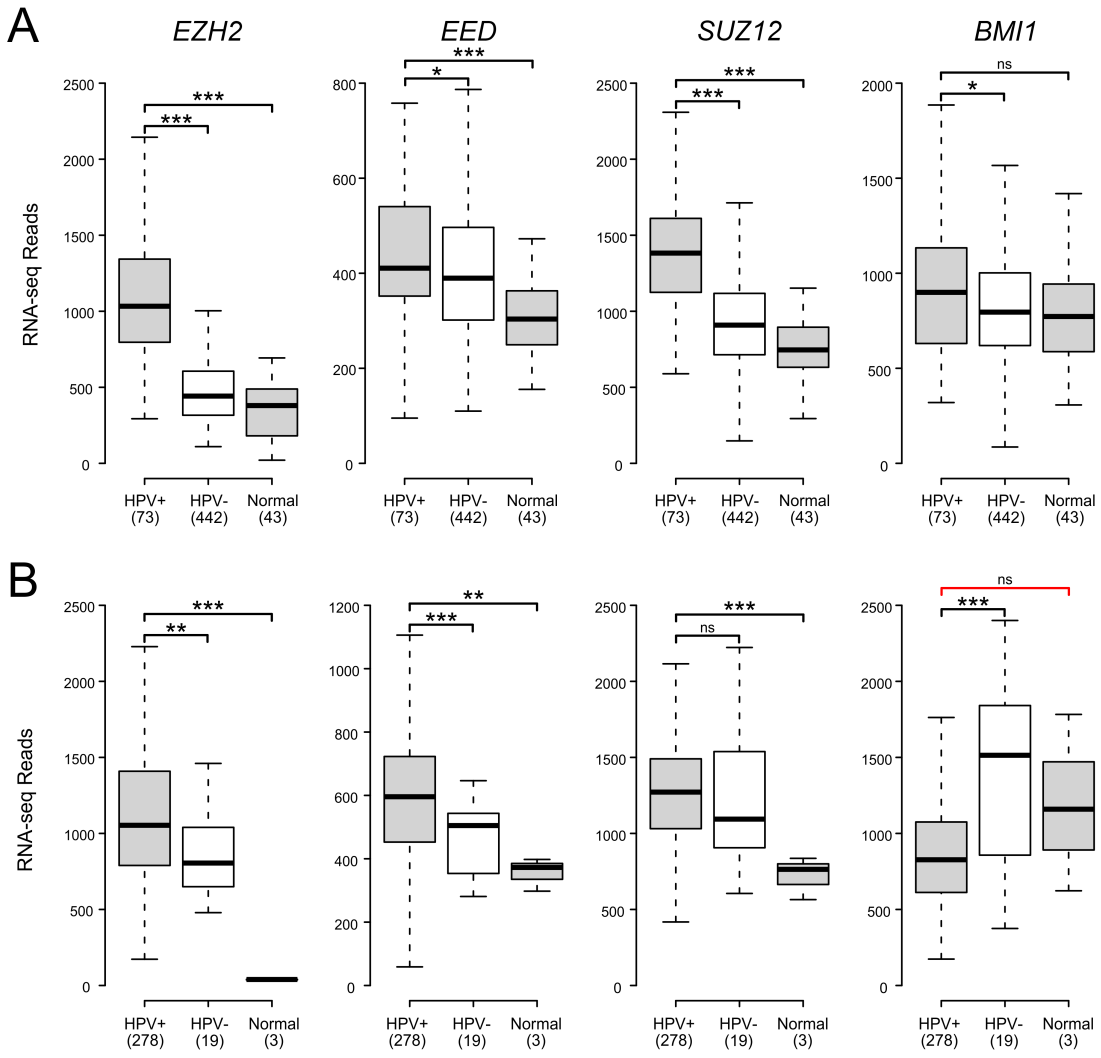

Figure 2.3. HPV perturbation of expression of polycomb components that may regulate *CDKN2A* transcription in human head & neck and cervical carcinomas.

Normalized RNA-Seq data extracted from the TCGA database for the HNSC (**A**) and CESC (**B**) cohorts for HPV+, HPV–, and normal control tissues. Numbers in brackets refer to the number of samples included in each analysis. * $p \leq 0.05$, ** $p \leq 0.01$, *** $p \leq 0.001$, ns – not significant, red bracket indicates a comparison that did not achieve significance with a power value < 0.8.

Tri-methylation of H3K27 by PRC2 is proposed to recruit PRC1 via its B lymphoma Mo-MLV insertion region 1 (BMI1) component to maintain a transcriptionally repressive state (Schwartz and Pirrotta, 2007). A previous study reported that BMI1 expression was reduced by transduction of HPV E6 and E7 into human foreskin keratinocytes (HFKs) (Hyland et al., 2011). A reduction in BMI1 is consistent with a reduction of repression of the *CDKN2A* locus by PRC1. *BMI1* expression in HPV+ CESC tumors was lower than in HPV– or normal control tissues (**Figure 2.3**). However, its expression was generally the same or higher in HPV+ HNSC tumors compared to the HPV– or normal control tissues (**Figure 2.3**). The lack of a consistent reduction in *BMI1* expression in HPV+ tumors suggest that it is not a key factor in HPV activation of *CDKN2A* and *CDKN2B* transcription. This is supported by a smaller independent study that found no correlation between p16 and BMI1 expression in head and neck cancers (Lundberg et al., 2016).

2.3.3 Impact of HPV status on expression of *KDM6A* and *KDM6B* in human tumors

The KDM6A and KDM6B demethylases convert H3K27me3 to the di-methylated or mono-methylated forms (Swigut and Wysocka, 2007). Multiple studies have reported that upregulation of one or both of the KDM6 demethylases occurs in cell lines when HPV E7 is expressed. Furthermore, knockdown of KDM6B or treatment with a small molecule KDM6 inhibitor reduces p16 expression in these models, suggesting a direct causal relationship between KDM6 activity and p16 transcription (McLaughlin-Drubin et al., 2011; McLaughlin-Drubin et al., 2013). Our analysis of the expression of *KDM6A* reveals that it is significantly upregulated in HPV+ tumors compared to HPV– tumors in both the HNSC and CESC cohorts (**Figure 2.4**). In contrast, *KDM6B* expression is significantly reduced in HPV+ cancers compared to HPV– tumors in both the HNSC and CESC tumor types (**Figure 2.4**). Significant changes in *KDM6A* and *KDM6B* expression were similarly noted between HPV+ and normal control tissues for the HNSC samples. However, no significant differences were observed for the CESC samples, which could reflect the limited number of normal control samples in this cohort. Overall, the increased expression of *KDM6A* suggests that it is more likely to play a role in dysregulation of H3K27me3-mediated regulation of transcription in HPV+ cancers.

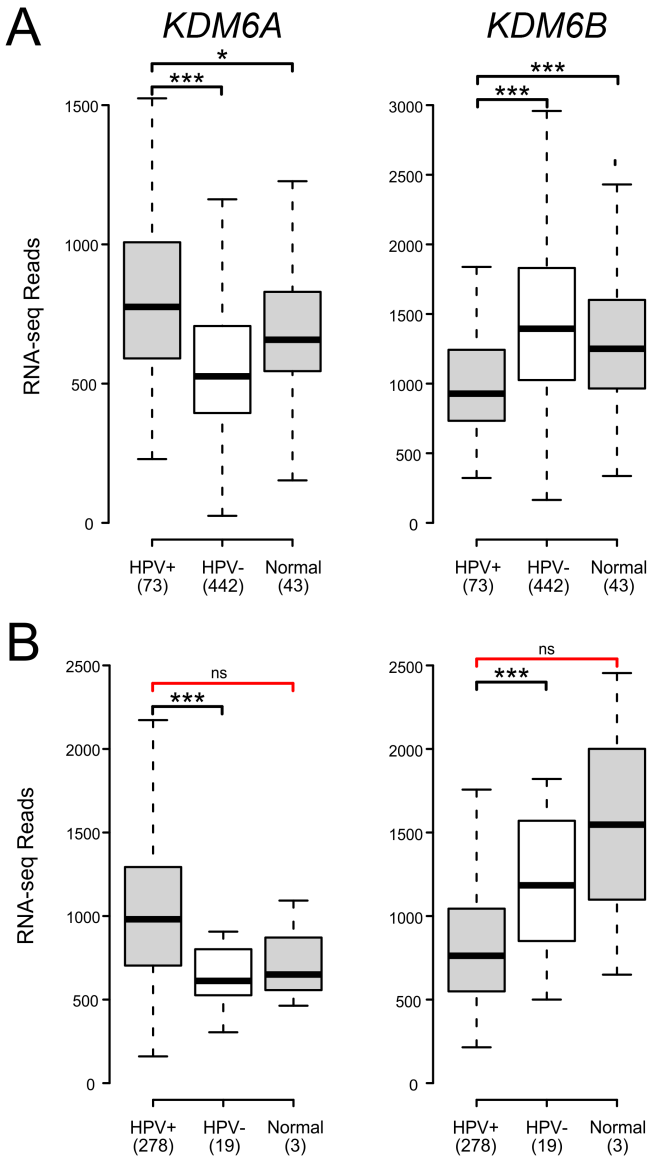

Figure 2.4. HPV perturbation of expression of the lysine demethylases *KDM6A* and *KDM6B* in human head & neck and cervical carcinomas.

Normalized RNA-Seq data extracted from the TCGA database for the HNSC (**A**) and CESC (**B**) cohorts for HPV+, HPV–, and normal control tissues. Numbers in brackets refer to the number of samples included in each analysis. * $p \leq 0.05$, *** $p \leq 0.001$, ns – not significant, red brackets indicate a comparison that did not achieve significance with a power value < 0.8.

2.3.4 Assessment of the DNA methylation status of the *CDKN2A* and *CDKN2B* loci in human tumors

HPV-mediated changes in epigenetic regulation of transcription of the *CDKN2A* and *CDKN2B* genes would be expected to be reflected in methylation status of CpG dinucleotide sequences in or adjacent to these loci. Indeed, a previous report identified altered methylation at 4 CpG loci in this genomic region that correlated with HPV status (Hyland et al., 2011; Schlecht et al., 2015). We analyzed the Infinium HumanMethylation450 BeadChip array data for the TCGA HNSC and CESC cohorts for consistent alterations in DNA methylation in this region of the genome (**Figure 2.5**). A region of DNA upstream of the *p14* transcript (probe cg14069088; see **Figure 2.5A** for location) was consistently identified to be hypomethylated in HPV+ tumors in both the HNSC and CESC cohorts compared to HPV– tumors or normal control tissue. No differences in methylation were detected in the remainder of the probes across the transcribed regions of these loci in HPV+ versus HPV– or normal control samples. In contrast, a hypermethylated region of DNA was identified within the 3'-end of the *CDKN2A* locus (probe cg12840719; see **Figure 2.5A** for location) in HPV+ tumors regardless of anatomical location. Thus, altered methylation is detected at the *CDKN2A* locus in HPV+ tumors, which is consistent with an epigenetic mechanism for transcriptional activation of this locus by HPV infection.

2.4 Discussion

HPV infection and subsequent expression of the *E6* and *E7* oncogenes leads to a large-scale reprogramming of gene expression. This is likely further exacerbated in high-risk HPV+ tumor cells, which typically express higher levels of these powerful viral regulatory proteins compared to levels found in the context of normal infections. Consequently, high-risk HPV transformed cells exhibit many changes in gene expression that contribute to the acquisition and maintenance of cancerous phenotypes unique to viral transformation (Doorbar et al., 2012). In particular, dysregulation of H3K27me3 homeostasis by the E7 proteins from high-risk HPVs contributes to increased expression of loci normally repressed by PRCs, including the *CDKN2A* locus encoding p16 INK4A (McLaughlin

Figure 2.5. HPV perturbation of DNA methylation at the *CDKN2A* and *CDKN2B* loci in human head & neck and cervical carcinomas.

HPV+ cancers exhibit markedly altered methylation from HPV– tumors or normal control tissues at two regions flanking the *CDKN2A* locus. (**A**) Location of the transcripts (black lines), CpG islands, and methylation probes used in this study. Normalized methylation data was extracted from the TCGA database for the HNSC (**B**) and CESC (**C**) cohorts. The mean methylation levels for HPV+, HPV–, and normal control tissues for all probes located in the vicinity of the *CDKN2A* and *CDKN2B* loci are shown. ** $p \leq 0.01$, *** $p \leq 0.001$, **** $p \leq 0.0001$.

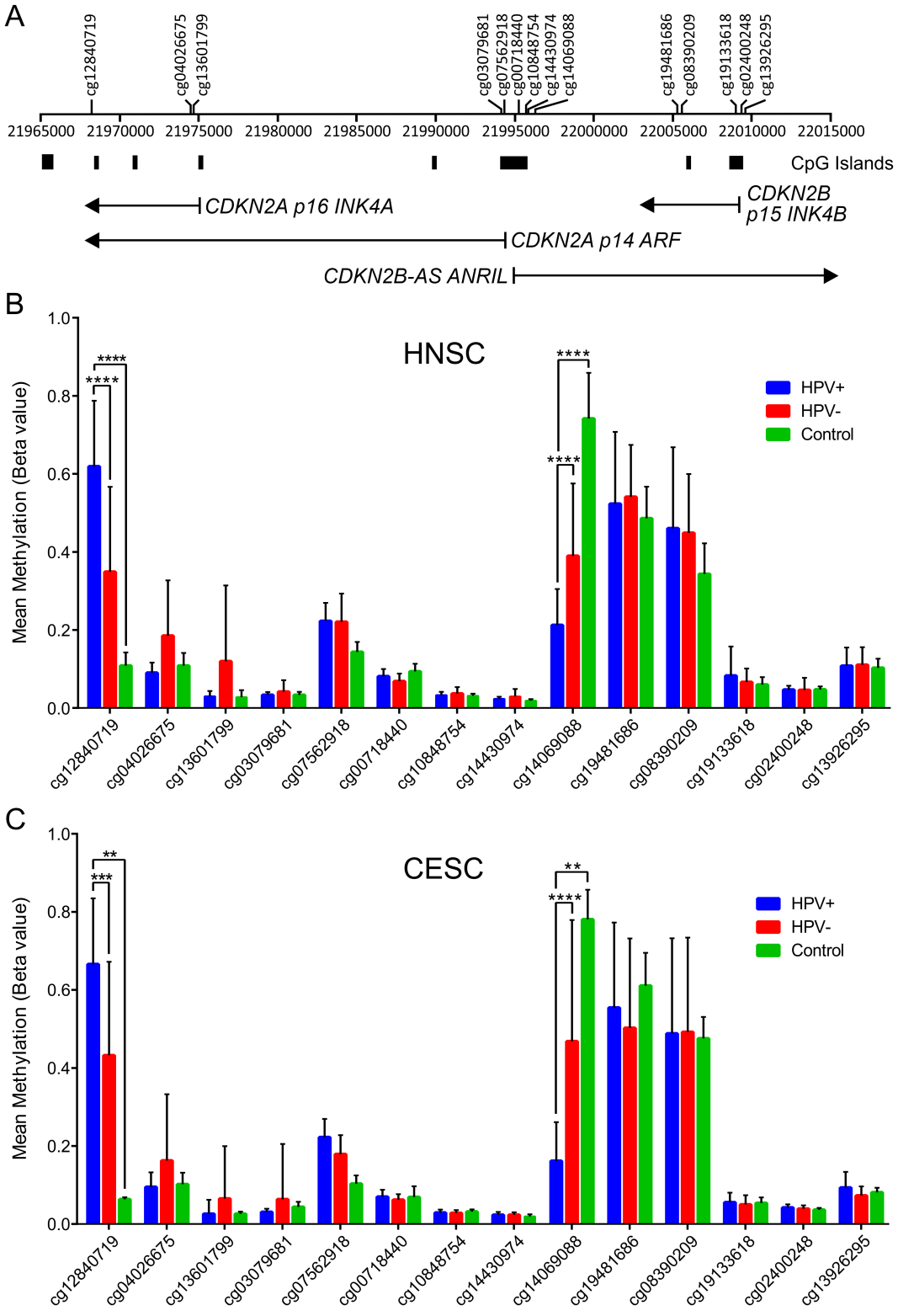
A
cg12840719
cg04026675
cg13601799
cg03079681
cg07562918
cg00718440
cg10848754
cg14430974
cg14069088
cg19481686
cg08390209
cg19133618
cg02400248
cg13926295
21965000
21970000
21975000
21980000
21985000
21990000
21995000
22000000
22005000
22010000
22015000
CpG Islands
CDKN2A p16 INK4A
CDKN2B p15 INK4B
CDKN2A p14 ARF
CDKN2B-AS ANRIL
B
HNSC
Mean Methylation (Beta value)
HPV+
HPV-
Control
C
CESC

Drubin et al., 2011; McLaughlin-Drubin et al., 2008; McLaughlin-Drubin et al., 2013). Interestingly, while strong p16 expression is a near universal hallmark of high-risk HPV+ carcinomas of the cervix or oral cavity (Hoffmann et al., 2010; Klaes et al., 2001; Sano et al., 1998), p16 is not expressed in high-risk HPV+ low-grade lesions and variably expressed in higher grade precancerous lesions (Mills et al., 2015; Woo et al., 2013) or lesions caused by low-risk HPV types (Geissler et al., 2013; Mooren et al., 2014; Sano et al., 1998). Thus, expression of high-risk HPV oncogenes alone is not sufficient to activate high levels of p16 expression, and additional adaptations acquired during tumor development likely contribute to this process.

While cell culture models have allowed detailed analyses of factors involved in virus-mediated activation of *p16* gene expression from the *CDKN2A* locus, far less is known about how similar these effects are to actual HPV+ tumors. In this study, our goal was to determine if the changes in H3K27me3 regulators and their target genes observed in cell culture models of HPV transformation are recapitulated in primary HPV+ tumors from different anatomical locations.

Using data from over 800 primary human tumors, we provide evidence that HPV+ tumors from both the head and neck and cervical sites exhibit remarkably similar alterations in expression of the genes encoded by the *CDKN2A* locus (**Figure 2.2**). It is well established that HPV induces expression of p16 INK4A in both oropharyngeal and cervical carcinomas (Hoffmann et al., 2010; Klaes et al., 2001). While overexpression of the *p14 ARF* gene from this locus has been observed in these cancers (Kanao et al., 2004; Schlecht et al., 2015), this has not been extensively documented. Our observation that *p14* expression, like that of *p16*, is similarly elevated in comparison to HPV– tumors or normal control tissue clearly demonstrates that HPV activates expression of the entire *CDKN2A* locus. Furthermore, this activation extends into the adjacent *CDKN2B* locus, which is also regulated by PRCs (Popov and Gil, 2010). Indeed, both the long non-coding RNA, *CDKN2B-AS ANRIL*, and *p15 INK4B* are induced in HPV+ cervical carcinomas with respect to HPV– tumors and normal control tissue; similarly, high levels of both *CDKN2B* encoded genes are expressed in HPV+ head and neck cancers (**Figure 2.2**). Existing

literature from independent cohorts confirms that p15 is expressed at lower levels in normal cervical tissue compared to cervical carcinomas (Feng et al., 2007; Zhang et al., 2014), supporting our conclusions from the TCGA CESC data. In addition, an independent analysis of a subset of the TCGA HNSC cohort used in our analysis observed similarly high, albeit variable, levels of *p15* in HPV+ and normal control samples (Salyakina and Tsinoremas, 2016). Taken together, the similarities between the normalized expression of all four gene products from the *CDKN2A* and *CDKN2B* gene loci in HPV+ tumors from both the cervix and oropharynx is extraordinary. These results clearly demonstrate the dominant nature of viral reprogramming of cellular gene expression in these cancers with respect to normal control tissue and HPV-negative cancers.

A simple mechanism to explain the observed increase of *CDKN2A* and *CDKN2B* expression in HPV+ cells would be a decreased expression of the proteins necessary for the H3K27 methyltransferase activity of the PRC2. In tissue culture models, expression of the EZH2 methyltransferase is increased by the presence of HPV oncogenes, and no significant change is observed for the EED and SUZ12 core proteins also required for catalytic activity (Hyland et al., 2011; McLaughlin-Drubin et al., 2011). Similarly, in HPV+ tumors from both anatomical sites, we find that these genes are expressed at levels equivalent or even higher than normal control tissue and HPV– samples (**Figure 2.3**). Furthermore, an analysis of ten biopsies of normal cervical tissue, HPV+ high-grade precancerous lesions, and HPV+ cervical carcinomas detected similarly elevated levels of EZH2 protein in the HPV expressing samples (Holland et al., 2008). Thus, there is a remarkably close agreement between the finding reported from tissue culture models and what is observed in human tumors, confirming that a reduction in the overall level of PRC2 expression is not likely responsible for *CDKN2A* and *CDKN2B* activation.

Silencing of euchromatin by PRC2 is stabilized and maintained by PRC1. Cell culture experiments suggest that expression of BMI1, a core component of PRC1, is reduced in E6/E7 transduced HFKs (Hyland et al., 2011) and BMI1 expression is inversely correlated with HPV viral load in cervical carcinomas (Kim et al., 2016). Our analysis of primary human cervical carcinomas indicates that *BMI1* expression is significantly reduced in HPV+ tumors with respect to HPV– tumors. However, this is not the case in head and neck

tumors, where it is modestly upregulated (**Figure 2.3**). For this reason, it seems unlikely that the induction of *CDKN2A* and *CDKN2B* expression observed in both these cancers is related to a reduction in expression of the BMI1 component of PRC1. This is further supported by a study reporting that BMI1 protein expression was lost in less than half of the 40 p16-positive oropharyngeal tumors tested (Lundberg et al., 2016). Thus, a loss of BMI1 expression appears unrelated to increased *p16* transcription, at least in the context of oropharyngeal tumors.

An alternative method of activating the *CDKN2A* and *CDKN2B* loci could be via the removal of the repressive H3K27me3 modification catalyzed by the PRC2 complex. This histone modification is erased by the KDM6A and KDM6B demethylases. Previous work in tissue culture models established that transduction of HPV E7 into HFKs induced KDM6A and/or KDM6B mRNA and protein levels (Hyland et al., 2011; McLaughlin-Drubin et al., 2011). Mechanistically, induction of KDM6B was independent of the interaction of E7 with Rb. More importantly, siRNA knockdown of KDM6B antagonized p16 induction by E7, suggesting that upregulation of these demethylases is the mechanism by which HPV reduces global H3K27me3 levels and activates p16 expression (McLaughlin-Drubin et al., 2011; McLaughlin-Drubin et al., 2013). Our analysis of primary human tumors indicates that *KDM6A* expression is significantly increased in HPV+ head and neck and cervical carcinoma cells with respect to HPV– tumors and likely normal control tissue. However, this is not the case for *KDM6B*, which is significantly reduced (**Figure 2.4**). These data fully support the model proposed from tissue culture experiments, in which enhanced expression of KDM6A, but not KDM6B, by HPV is related to the dysregulation of H3K27me3 homeostasis and subsequent activation of *CDKN2A* and likely *CDKN2B* transcription in both these cancer types. One small study reported that expression of both *KDM6A* and *KDM6B* is substantially reduced in HPV+ mildly dysplastic lesions; however, stepwise increases were observed for both demethylases in precancerous lesions and cervical carcinoma, such that the carcinomas express both demethylases at levels similar to normal control tissues (Iancu et al., 2015). This pattern of re-expression correlates well with the acquisition of p16 expression observed during cervical carcinoma progression.

Accompanying the global reduction in H3K27me3, HPV+ head and neck cancers and cervical carcinomas exhibit numerous alterations in DNA methylation (Lorincz, 2016; van Kempen et al., 2014). Indeed, we recently reported a methylation signature that predicts HPV status in HNSC samples (Papillon-Cavanagh et al., 2017). Our analysis of methylation data for all the probes across the *CDKN2A* and *CDKN2B* loci for the TCGA HNSC and CESC cohorts revealed that there were two consistent alterations in DNA methylation relative to methylation levels present in HPV– tumors and normal tissue (**Figure 2.5**). A hypomethylated region of DNA was identified on the south shore of the CpG island located at the start of the *p14* transcript in HPV+ tumors in both the HNSC and CESC cohorts. Genome-wide studies have clearly shown that methylation in the immediate vicinity of the transcription start site blocks initiation (Jones, 2012). As such, the greatly reduced methylation in HPV+ samples at this region is fully consistent with enhanced *CDKN2A* expression. In addition, we also observed a hypermethylated region of DNA on the north shore of the CpG island closest to the third exon of the *p14* and *p16* transcripts. Hypermethylation at this location has been described in other studies of HPV+ head and neck and cervical carcinomas using alternative probes (Ben-Dayan et al., 2017; Schlecht et al., 2015; Wijetunga et al., 2016). These studies have established that *p16* and *p14* expression in a given tumor sample is strongly correlated with increased methylation at this position in the *CDKN2A* locus (Ben-Dayan et al., 2017; Schlecht et al., 2015). Hypermethylation of gene-bodies has recently been shown to occur during elongation through a mechanism whereby RNA Polymerase II recruits Su(var)3-9, Enhancer-of-zeste and Trithorax domain containing 2 (SETD2), a histone methyltransferase, which then tri-methylates H3K36. DNA Methyltransferase 3 (DNMT3) recognizes and binds H3K36me3, leading to the methylation of CpGs (Baubec et al., 2015; Neri et al., 2017). Thus, along with promoter hypomethylation, gene-body methylation correlates well with the observed enhanced transcription from the *CDKN2A* locus, providing further support for an epigenetic mechanism as the basis for HPV induction of expression from this locus.

Taken together, our analysis of over 350 HPV+ head and neck or cervical carcinomas in comparison with over 450 HPV– cancers from their respective anatomical sites demonstrates that HPV consistently activates expression of both the *CDKN2A* and *CDKN2B* loci in these cancers. Interestingly, this extends beyond just *p16*, with most

tumors expressing the other gene products from these loci including *p14*, *ANRIL*, and *p15*. In these cancers, HPV oncogene expression similarly dysregulates expression of key regulators of H3K27me3, including members of PRC2 and the demethylases KDM6A and KDM6B. As a likely result of these and other alterations in epigenetic regulation, the levels of methylation in the center of the *CDKN2A* and *CDKN2B* loci are significantly decreased in cells expressing high-risk HPV oncogenes.

Importantly, epigenetic reprogramming of gene expression induced by HPV should be reversible and could represent a unique therapeutic target. Paradoxically, cervical carcinoma cell lines or other tumor cell lines expressing HPV E7 from several high-risk HPVs appear to require continuous *p16* expression for survival. Although p16 normally serves as a tumor suppressor, for currently unknown reasons, it becomes necessary for continued growth in cells expressing HPV E7. As HPV+ cells require KDM6 demethylase activity to maintain p16 expression, they are sensitive to small molecule inhibitors of KDM6 in cell culture models (McLaughlin-Drubin et al., 2011; McLaughlin-Drubin et al., 2013). However, it has not been determined if actual primary HPV+ head and neck or cervical carcinoma cells will respond similarly. Our analysis of the epigenetic regulators that control *p16* expression finds many commonalities between the hundreds of tumors making up the TCGA CESC and HNSC cohorts and cell culture models, strongly suggesting that testing of KDM6 inhibitors should be aggressively pursued as a novel therapy of HPV+ cancers.

2.5 References

Alemany L, Cubilla A, Halec G, et al. (2016) Role of Human Papillomavirus in Penile Carcinomas Worldwide. *Eur Urol* 69: 953-961.

Banister CE, Liu C, Pirisi L, et al. (2017) Identification and characterization of HPV-independent cervical cancers. *Oncotarget* 8: 13375-13386.

Baubec T, Colombo DF, Wirbelauer C, et al. (2015) Genomic profiling of DNA methyltransferases reveals a role for DNMT3B in genic methylation. *Nature* 520: 243-247.

Ben-Dayan MM, Ow TJ, Belbin TJ, et al. (2017) Nonpromoter methylation of the CDKN2A gene with active transcription is associated with improved locoregional control in laryngeal squamous cell carcinoma. *Cancer Med* 6: 397-407.

Boyer SN, Wazer DE and Band V. (1996) E7 protein of human papilloma virus-16 induces degradation of retinoblastoma protein through the ubiquitin-proteasome pathway. *Cancer Res* 56: 4620-4624.

Bratman SV, Bruce JP, O'Sullivan B, et al. (2016) Human Papillomavirus Genotype Association With Survival in Head and Neck Squamous Cell Carcinoma. *JAMA Oncol* 2: 823-826.

Brehm A, Miska EA, McCance DJ, et al. (1998) Retinoblastoma protein recruits histone deacetylase to repress transcription. *Nature* 391: 597-601.

Burd EM. (2016) Human Papillomavirus Laboratory Testing: the Changing Paradigm. *Clin Microbiol Rev* 29: 291-319.

Crosbie EJ, Einstein MH, Franceschi S, et al. (2013) Human papillomavirus and cervical cancer. *Lancet* 382: 889-899.

Deng Z, Hasegawa M, Kiyuna A, et al. (2013) Viral load, physical status, and E6/E7 mRNA expression of human papillomavirus in head and neck squamous cell carcinoma. *Head Neck* 35: 800-808.

Doorbar J, Quint W, Banks L, et al. (2012) The biology and life-cycle of human papillomaviruses. *Vaccine* 30 Suppl 5: F55-70.

Du P, Zhang X, Huang CC, et al. (2010) Comparison of Beta-value and M-value methods for quantifying methylation levels by microarray analysis. *BMC bioinformatics* 11: 587.

Durzynska J, Lesniewicz K and Poreba E. (2017) Human papillomaviruses in epigenetic regulations. *Mutat Res Rev Mutat Res* 772: 36-50.

Dyson N, Guida P, Munger K, et al. (1992) Homologous sequences in adenovirus E1A and human papillomavirus E7 proteins mediate interaction with the same set of cellular proteins. *J Virol* 66: 6893-6902.

Faul F, Erdfelder E, Lang AG, et al. (2007) G*Power 3: a flexible statistical power analysis program for the social, behavioral, and biomedical sciences. *Behav Res Methods* 39: 175-191.

Feng W, Xiao J, Zhang Z, et al. (2007) Senescence and apoptosis in carcinogenesis of cervical squamous carcinoma. *Mod Pathol* 20: 961-966.

Forman D, de Martel C, Lacey CJ, et al. (2012) Global burden of human papillomavirus and related diseases. *Vaccine* 30 Suppl 5: F12-23.

Geissler C, Tahtali A, Diensthuber M, et al. (2013) The role of p16 expression as a predictive marker in HPV-positive oral SCCHN--a retrospective single-center study. *Anticancer Res* 33: 913-916.

Gillison ML, Koch WM, Capone RB, et al. (2000) Evidence for a causal association between human papillomavirus and a subset of head and neck cancers. *J Natl Cancer Inst* 92: 709-720.

Goodwin EC and DiMaio D. (2000) Repression of human papillomavirus oncogenes in HeLa cervical carcinoma cells causes the orderly reactivation of dormant tumor suppressor pathways. *Proc Natl Acad Sci U S A* 97: 12513-12518.

Goodwin EC, Yang E, Lee CJ, et al. (2000) Rapid induction of senescence in human cervical carcinoma cells. *Proc Natl Acad Sci U S A* 97: 10978-10983.

Guimera N, Alemany L, Halec G, et al. (2017) Human papillomavirus 16 is an aetiological factor of scrotal cancer. *Br J Cancer* 116: 1218-1222.

Hoffmann M, Ihloff AS, Gorogh T, et al. (2010) p16(INK4a) overexpression predicts translational active human papillomavirus infection in tonsillar cancer. *Int J Cancer* 127: 1595-1602.

Holland D, Hoppe-Seyler K, Schuller B, et al. (2008) Activation of the enhancer of zeste homologue 2 gene by the human papillomavirus E7 oncoprotein. *Cancer Res* 68: 9964-9972.

Hyland PL, McDade SS, McCloskey R, et al. (2011) Evidence for alteration of EZH2, BMI1, and KDM6A and epigenetic reprogramming in human papillomavirus type 16 E6/E7-expressing keratinocytes. *J Virol* 85: 10999-11006.

Iancu IV, Botezatu A, Plesa A, et al. (2015) Histone lysine demethylases as epigenetic modifiers in HPV-induced cervical neoplasia. *Rom Biotechnol Lett* 20: 10236-10244.

Jiang M and Milner J. (2002) Selective silencing of viral gene expression in HPV-positive human cervical carcinoma cells treated with siRNA, a primer of RNA interference. *Oncogene* 21: 6041-6048.

Jones PA. (2012) Functions of DNA methylation: islands, start sites, gene bodies and beyond. *Nat Rev Genet* 13: 484-492.

Kanao H, Enomoto T, Ueda Y, et al. (2004) Correlation between p14(ARF)/p16(INK4A) expression and HPV infection in uterine cervical cancer. *Cancer Lett* 213: 31-37.

Kessis TD, Slebos RJ, Nelson WG, et al. (1993) Human papillomavirus 16 E6 expression disrupts the p53-mediated cellular response to DNA damage. *Proc Natl Acad Sci U S A* 90: 3988-3992.

Kim BW, Cho H, Ylaya K, et al. (2016) Over-expression of BMI1 is associated with favorable prognosis in cervical cancer. *Int J Clin Exp Pathol* 9: 1849-1857.

Klaes R, Friedrich T, Spitkovsky D, et al. (2001) Overexpression of p16(INK4A) as a specific marker for dysplastic and neoplastic epithelial cells of the cervix uteri. *Int J Cancer* 92: 276-284.

Lawson JS, Glenn WK, Salyakina D, et al. (2015) Human Papilloma Viruses and Breast Cancer. *Front Oncol* 5: 277.

Li B and Dewey CN. (2011) RSEM: Accurate transcript quantification from RNA-Seq data with or without a reference genome. *BMC Bioinformatics* 12: 323-339.

Lorincz AT. (2016) Virtues and Weaknesses of DNA Methylation as a Test for Cervical Cancer Prevention. *Acta Cytol* 60: 501-512.

Lundberg M, Renkonen S, Haglund C, et al. (2016) Association of BMI-1 and p16 as prognostic factors for head and neck carcinomas. *Acta Otolaryngol* 136: 501-505.

McLaughlin-Drubin ME, Crum CP and Munger K. (2011) Human papillomavirus E7 oncoprotein induces KDM6A and KDM6B histone demethylase expression and causes epigenetic reprogramming. *Proc Natl Acad Sci U S A* 108: 2130-2135.

McLaughlin-Drubin ME, Huh KW and Munger K. (2008) Human papillomavirus type 16 E7 oncoprotein associates with E2F6. *J Virol* 82: 8695-8705.

McLaughlin-Drubin ME, Park D and Munger K. (2013) Tumor suppressor p16INK4A is necessary for survival of cervical carcinoma cell lines. *Proc Natl Acad Sci U S A* 110: 16175-16180.

Mills AM, Paquette C, Castle PE, et al. (2015) Risk stratification by p16 immunostaining of CIN1 biopsies: a retrospective study of patients from the quadrivalent HPV vaccine trials. *Am J Surg Pathol* 39: 611-617.

Mooren JJ, Gultekin SE, Straetmans JM, et al. (2014) P16(INK4A) immunostaining is a strong indicator for high-risk-HPV-associated oropharyngeal carcinomas and dysplasias, but is unreliable to predict low-risk-HPV-infection in head and neck papillomas and laryngeal dysplasias. *Int J Cancer* 134: 2108-2117.

Munger K, Basile JR, Duensing S, et al. (2001) Biological activities and molecular targets of the human papillomavirus E7 oncoprotein. *Oncogene* 20: 7888-7898.

Neri F, Rapelli S, Krepelova A, et al. (2017) Intragenic DNA methylation prevents spurious transcription initiation. *Nature* 543: 72-77.

Network TCGAR. (2014) Comprehensive molecular characterization of urothelial bladder carcinoma. *Nature* 507: 315-322.

Network TCGAR. (2015) Comprehensive genomic characterization of head and neck squamous cell carcinomas. *Nature* 517: 576-582.

Network TCGAR. (2017) Integrated genomic and molecular characterization of cervical cancer. *Nature* 543: 378-384.

Papillon-Cavanagh S, Lu C, Gayden T, et al. (2017) Impaired H3K36 methylation defines a subset of head and neck squamous cell carcinomas. *Nat Genet* 49: 180-185.

Popov N and Gil J. (2010) Epigenetic regulation of the INK4b-ARF-INK4a locus: in sickness and in health. *Epigenetics* 5: 685-690.

Rampias T, Sasaki C, Weinberger P, et al. (2009) E6 and e7 gene silencing and transformed phenotype of human papillomavirus 16-positive oropharyngeal cancer cells. *J Natl Cancer Inst* 101: 412-423.

Salyakina D and Tsinoremas NF. (2016) Non-coding RNAs profiling in head and neck cancers. *NPJ Genom Med* 1: 15004.

Sano T, Oyama T, Kashiwabara K, et al. (1998) Expression status of p16 protein is associated with human papillomavirus oncogenic potential in cervical and genital lesions. *Am J Pathol* 153: 1741-1748.

Schlecht NF, Ben-Dayan M, Anayannis N, et al. (2015) Epigenetic changes in the CDKN2A locus are associated with differential expression of P16INK4A and P14ARF in HPV-positive oropharyngeal squamous cell carcinoma. *Cancer Med* 4: 342-353.

Schwartz YB and Pirrotta V. (2007) Polycomb silencing mechanisms and the management of genomic programmes. *Nat Rev Genet* 8: 9-22.

Sima N, Wang W, Kong D, et al. (2008) RNA interference against HPV16 E7 oncogene leads to viral E6 and E7 suppression in cervical cancer cells and apoptosis via upregulation of Rb and p53. *Apoptosis* 13: 273-281.

Singh N, Hussain S, Kakkar N, et al. (2015) Implication of high risk human papillomavirus HR-HPV infection in prostate cancer in Indian population--a pioneering case-control analysis. *Sci Rep* 5: 7822.

Swigut T and Wysocka J. (2007) H3K27 demethylases, at long last. *Cell* 131: 29-32.

Syrjanen S. (2005) Human papillomavirus (HPV) in head and neck cancer. *J Clin Virol* 32 Suppl 1: S59-66.

van Kempen PM, Noorlag R, Braunius WW, et al. (2014) Differences in methylation profiles between HPV-positive and HPV-negative oropharynx squamous cell carcinoma: a systematic review. *Epigenetics* 9: 194-203.

Wijetunga NA, Belbin TJ, Burk RD, et al. (2016) Novel epigenetic changes in CDKN2A are associated with progression of cervical intraepithelial neoplasia. *Gynecol Oncol* 142: 566-573.

Woo SB, Cashman EC and Lerman MA. (2013) Human papillomavirus-associated oral intraepithelial neoplasia. *Mod Pathol* 26: 1288-1297.

Zhai K, Ding J and Shi HZ. (2015) HPV and lung cancer risk: a meta-analysis. *J Clin Virol* 63: 84-90.

Zhang Y, Guo L, Xing P, et al. (2014) Increased expression of oncogene-induced senescence markers during cervical squamous cell cancer development. *Int J Clin Exp Pathol* 7: 8911-8916.

Zhang Y, Xiong Y and Yarbrough WG. (1998) ARF promotes MDM2 degradation and stabilizes p53: ARF-INK4a locus deletion impairs both the Rb and p53 tumor suppression pathways. *Cell* 92: 725-734.

zur Hausen H. (1996) Papillomavirus infections--a major cause of human cancers. *Biochim Biophys Acta* 1288: F55-78.

zur Hausen H. (2002) Papillomaviruses and cancer: from basic studies to clinical application. *Nat Rev Cancer* 2: 342-350.

Chapter 3

3 Analysis of Class I Major Histocompatibility Complex Gene Transcription in Human Tumors Caused by Human Papillomavirus Infection

3.1 Introduction

Anti-viral immunity is comprised of multiple levels of defenses that cooperatively block, control, and eliminate infection. Intrinsic and innate immunity function as pre-existing defenses against viral infection, and serve as the first levels of response (Takeuchi and Akira, 2009; Yan and Chen, 2012). In the event that these non-specific immune responses are not sufficient to eliminate an infection, subsequent antigen-specific adaptive immune responses develop. As such, the recognition of intracellularly-derived viral peptides in the context of major histocompatibility complex class I (MHC-I) molecules by cytotoxic T lymphocytes (CTLs) triggers the elimination of virally infected cells (Tscharke et al., 2015), while antibodies specific for virion antigens neutralize viral particles, and block the spread of infection (Dorner and Radbruch, 2007).

Despite the effectiveness of the immune system, many viruses have acquired sophisticated methods to evade anti-viral defenses, including the adaptive CTL response. For example, several viral proteins have been identified that block MHC-I antigen presentation by downregulating the loading of antigen onto MHC-I, the expression of MHC-I itself, and the transport of MHC-I to the cell surface. Viral proteins have also been found to trigger MHC-I internalization and/or degradation (Hansen and Bouvier, 2009). Collectively, these strategies facilitate the evasion of the infected cell from CTL attack, thus allowing the virus to persist.

Human papillomaviruses (HPV) are small, non-enveloped, double-stranded DNA viruses that infect mucosal or cutaneous epithelia and induce cellular proliferation (Doorbar et al., 2015). HPV infections of mucosal tissues are highly prevalent, and infections typically take one to two years to resolve (Munoz et al., 2009). Mucosal HPVs are classified as low- or high-risk based on the frequency with which they are associated with cancer. High-risk

HPVs are causative agents for cancers at multiple distinct anatomical subsites (Doorbar et al., 2015), including the cervix (Crosbie et al., 2013), other anogenital tissues (Alemany et al., 2016; De Vuyst et al., 2009; Guimera et al., 2017), and the oropharynx (Gillison et al., 2000; Mehanna et al., 2013; Syrjanen, 2005). Worldwide, mucosal high-risk HPV infection is responsible for greater than 5% of all human cancers (Forman et al., 2012).

HPV encodes two main oncogenes, *E6* and *E7* (Doorbar et al., 2012), which are constitutively expressed in HPV-positive (HPV+) tumors. The E6 and E7 oncoproteins perform multiple functions in an infected and/or cancerous cell. They interact with key cellular regulatory proteins to dysregulate gene expression and cell growth (Doorbar et al., 2012). For example, E6 binds to and degrades p53, while E7 targets the retinoblastoma protein (Rb) and its family members (Dyson et al., 1992; Scheffner et al., 1990). These events contribute to inappropriate cell cycle progression in HPV-infected cells (Boyer et al., 1996; Brehm et al., 1998). In high-risk HPV infections, viral oncoproteins uncouple cell growth from differentiation. Consequently, this contributes to the formation of epithelial dysplasia, which may progress to carcinoma if the infection is not resolved (Doorbar et al., 2012).

Multiple studies have suggested that HPV oncoproteins contribute to the evasion of the adaptive immune response, which supports a model by which the establishment of a persistent HPV infection contributes to the ability of HPV+ cancers to evade anti-tumor CTL responses (Westrich et al., 2017). Although both E5—a third viral oncoprotein—and E6 from HPV16 have been reported to block MHC-I expression (Ashrafi et al., 2006; Kim et al., 2011), the majority of studies in this area focus on the E7-mediated reduction of MHC-I expression. Specifically, transfection of high-risk HPV E7 into various cell lines represses MHC-I and/or transporter associated with antigen processing (TAP) expression (Georgopoulos et al., 2000; Heller et al., 2011; Li et al., 2010). Reciprocal studies have shown that the knock-down of E7 in some HPV+ cervical cancer cell lines increases MHC-I expression (Bottley et al., 2008; Li et al., 2006). In these studies, the repression of MHC-I appears to be a specific function of high-risk HPV E7 that is not shared by low-risk HPV E7 (Georgopoulos et al., 2000; Heller et al., 2011). Mechanistically, the reduction of MHC-I and TAP expression in these studies occurs at the transcriptional level (Georgopoulos et

al., 2000; Heller et al., 2011; Li et al., 2010). The most detailed studies of the HPV-mediated repression of MHC-I expression report that E7 associates with the promoter of the MHC-I *HLA-A* heavy chain gene, and recruits histone deacetylase activity via residues 70, 80, and 88 of HPV16 E7 (Heller et al., 2011; Li et al., 2006; Li et al., 2009). In addition to repressing the basal transcription of MHC-I, HPV E7 abrogates the interferon regulatory factor-1 (IRF-1) response, thus inhibiting interferon-gamma (IFNγ)-mediated transcriptional induction of MHC-I expression, antigen presentation, and CTL-induced cell death (Park et al., 2000; Perea et al., 2000; Um et al., 2002; Zhou et al., 2013; Zhou et al., 2011).

While the majority of published studies using tissue culture models indicate that HPV oncoproteins such as E7 repress the expression of the antigen presentation apparatus, cognate studies on the effects of HPV in human carcinomas are less consistent. Conflicting reports suggest that HPV+ carcinomas/dysplastic lesions display increased (Jochmus et al., 1993; Torres et al., 1993), decreased (Cromme et al., 1993; Keating et al., 1995; Ritz et al., 2001; van Esch et al., 2014), or the same levels (Djajadiningrat et al., 2015; Ramqvist et al., 2015) of MHC-I or TAP expression when compared with HPV negative (HPV−) tumors or normal control tissues. Some of these differences may be related to different tissue types, stages, and/or grades. The most comprehensive analysis, which examined 109 cervical carcinoma samples, concluded that only about 40% of the samples exhibited MHC-I downregulation (Mehta et al., 2008). However, many types of tumors that are HPV− contain a similar subset that are deficient in MHC-I and/or TAP expression (Garcia-Lora et al., 2003), which suggests that this reduction is not actually virally-mediated. As such, it remains an open question as to whether the E7-mediated changes in the transcription of various MHC-I pathway components observed in tissue culture similarly occur in the context of actual human HPV+ carcinomas. This information is clearly relevant, considering that the activation of an antigen-dependent clearance of tumor cells by the immune system is an extraordinarily effective cancer therapy (Gotwals et al., 2017).

In this study, we used data from over 800 human cervical (The Cancer Genome Atlas Research Network, 2017) and head & neck tumors (The Cancer Genome Atlas Research Network, 2015) from The Cancer Genome Atlas (TCGA). We set out to determine if high-

risk HPV oncogene expression alters the expression of MHC-I heavy chain genes, the β2 microglobulin light chain gene, and other components of the antigen-loading apparatus, which includes: TAP1/2, tapasin, ERp57, calreticulin, calnexin, and ERAP1/2 in human tumors. We found that HPV+ tumors from both anatomical sites expressed substantial levels of mRNA for each of these MHC-I pathway components. Indeed, many of these genes were expressed at significantly higher levels than normal control tissues. Furthermore, an analysis of mutation frequencies in MHC-I genes indicated that the HPV+ and HPV− cancers exhibit similar frequencies of alteration. This is in contrast to *TP53* and *CDKN2A*, which are key regulators of pathways known to be targeted by HPV oncoproteins and are frequently mutated in HPV− but not HPV+ carcinomas. This suggests that the acquisition of somatic mutations in MHC-I genes as a means of evading the anti-tumor CTL response occurs similarly in HPV+ and HPV− cancers, which would not be expected if HPV oncoproteins were effective at repressing MHC-I expression or function. Taken together, this data does not entirely validate conclusions drawn from previous tissue culture studies. Specifically, HPV oncoprotein expression does not repress the transcription of the MHC-I pathway components in cervical carcinomas, although a modest reduction in MHC-I mRNA levels was observed in HPV+ vs. HPV− head & neck cancers.

3.2 Materials and Methods

3.2.1 RNA expression comparisons and statistical analysis

Level 3 RNA-Seq by Expectation Maximization (RSEM) normalized Illumina HiSeq RNA expression data for the TCGA head & neck cancer (HNSC) and cervical carcinoma (CESC) cohorts was downloaded from the Broad Genome Data Analysis Center's Firehose server (https://gdac.broadinstitute.org/). For all of the genes, the gene level Firehose dataset was used. Normalized expression data was extracted into Microsoft Excel, and the HPV status was manually curated based on published datasets (Banister et al., 2017; Bratman et al., 2016; The Cancer Genome Atlas Research Network, 2015; The Cancer Genome Atlas Research Network, 2017). For each gene analyzed, primary patient samples with known HPV status were grouped as HPV+, HPV−, or normal control tissue. Patient samples with unknown HPV status were omitted from our calculations, as were samples obtained from secondary metastatic lesions. This resulted in 73 HPV+, 442 HPV−, and 43 normal control

samples with data available for the HNSC gene expression analysis and 278 HPV+, 19 HPV−, and 3 normal control samples available for the CESC gene expression analysis. Boxplot comparison of gene expression was performed using GraphPad Prism v7.0 (Graphpad Software, Inc., San Diego, California, USA) and assembled into final form using CorelDRAW (Corel, Ottawa, Ontario, Canada). For the boxplots, center lines show the medians, box limits indicate the 25th and 75th percentiles as determined by Graphpad Prism, and whiskers extend from the minimum to maximum values. Statistical significance was calculated using Graphpad Prism. *p*-values were assigned using a one-tailed non-parametric Mann–Whitney U test. Post-hoc power calculations were performed with G*Power software version 3.1.9.2 (Faul et al., 2007), using post-hoc t-test family calculations, with effect size selected as 0.8 and $\alpha = 0.05$. All comparisons achieved a power value > 0.8, or demonstrated significant differences, unless otherwise noted in the text.

3.2.2 Somatic mutation frequency comparisons and statistical analysis

Somatic mutations present in selected genes of the tumor samples in the TCGA, HNSC, and CESC cohorts were downloaded as the DNA Mutation Packager Calls dataset from the Broad Genome Data Analysis Center's Firehose server (https://gdac.broadinstitute.org/), and manually annotated for HPV status. This resulted in 67 HPV+ and 431 HPV− samples for the HNSC cohort, and 181 HPV+ and 10 HPV– samples for the CESC cohort. Differences in the frequencies of DNA mutations in selected genes were calculated between HPV+ and HPV− samples using the maftools package (Mayakonda et al., 2018) in R statistical environment (Version 3.4.0). Silent mutations were excluded from the analysis, and samples with multiple mutations in a gene were counted as one for the calculations. Statistical significance ($p < 0.05$) was determined using Fisher's exact test.

3.3 Results

3.3.1 Impact of HPV status on MHC-I heavy chain expression in human tumors

MHC-I is a heterodimer comprised of a heavy chain encoded by one of three classical (*HLA-A, -B,* and *-C*) or non-classical (*HLA-E, -F,* and *-G*) genes and the invariant *β2 microglobulin light chain* (Hansen and Bouvier, 2009). We analyzed the Illumina HiSeq RNA expression data from the TCGA head & neck squamous cell carcinoma (HNSC) and cervical carcinoma (CESC) cohorts for expression of *HLA-A*, *HLA-B*, and *HLA-C*, the three classical genes (**Figure 3.1**). Unexpectedly, HPV+ samples from both the HNSC and CESC cohorts expressed high levels of mRNA for all three genes, as shown by the normalized RNA-seq absolute read count values, which averaged in the range of 25,000–50,000. The HPV+ samples from the HNSC cohort expressed significantly elevated levels of *HLA-A*, *HLA-B*, and *HLA-C* compared with normal control tissue. In the CESC cohort, although the median RNA-seq values for the HPV+ samples appeared at least as high as those for normal control samples, there was insufficient power to exclude the possibility that the expression of *HLA-A*, *HLA-B*, or *HLA-C* was not different. In the HNSC cohort, levels in HPV+ samples were slightly lower than HPV− samples, whereas HPV+ samples in the CESC cohort had substantially higher levels of expression versus HPV− samples. Nevertheless, all tumor subsets expressed high absolute levels of the mRNAs for each of the classical MHC-I heavy chain genes.

Similarly, higher or comparable levels of expression of the non-classical genes, *HLA-E*, *HLA-F*, and *HLA-G*, were observed in HPV+ cancers with respect to normal control tissues in the HNSC cohort (**Figure 3.2**). Again, a comparison of the HPV+ samples to normal control samples in the CESC cohort was insufficiently powered to allow us to exclude the possibility that the expression of *HLA-E*, *HLA-F,* or *HLA-G* was not altered by the presence of HPV oncogenes. However, *HLA-E* and *HLA-F* were expressed at relatively high levels based on the absolute normalized read values. As noted by others (Cicchini et al., 2017), *HLA-E* was expressed at significantly reduced levels in HPV+ samples compared with HPV− samples in the HNSC cohort. However, this was not a consistent effect in all HPV+ carcinomas, as *HLA-E* was expressed at much higher levels in the HPV+ samples compared

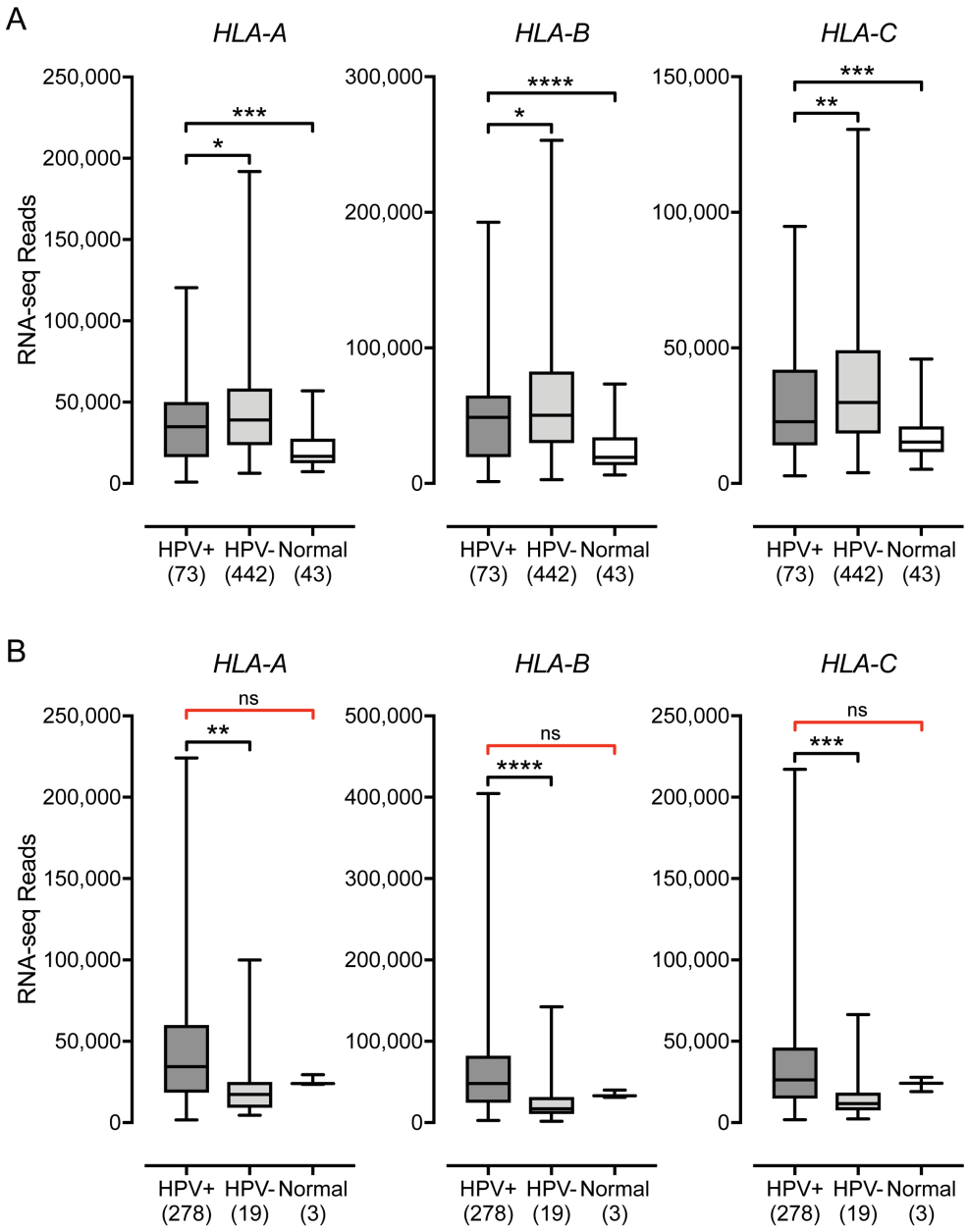

Figure 3.1. Expression of classical MHC-I heavy chain genes in head & neck or cervical carcinomas stratified by HPV status.

Normalized RNA-seq data for the indicated MHC-I heavy chain genes was extracted from The Cancer Genome Atlas (TCGA) database for the head & neck cancer (HNSC) (**A**) and cervical carcinoma (CESC) (**B**) cohorts for HPV+, HPV−, and normal control tissues. Numbers in brackets refer to the number of samples included in each analysis. * $p \leq 0.05$, ** $p \leq 0.01$, *** $p \leq 0.001$, **** $p \leq 0.0001$, ns – not significant, red brackets indicate a comparison that did not achieve significance with a power value < 0.8.

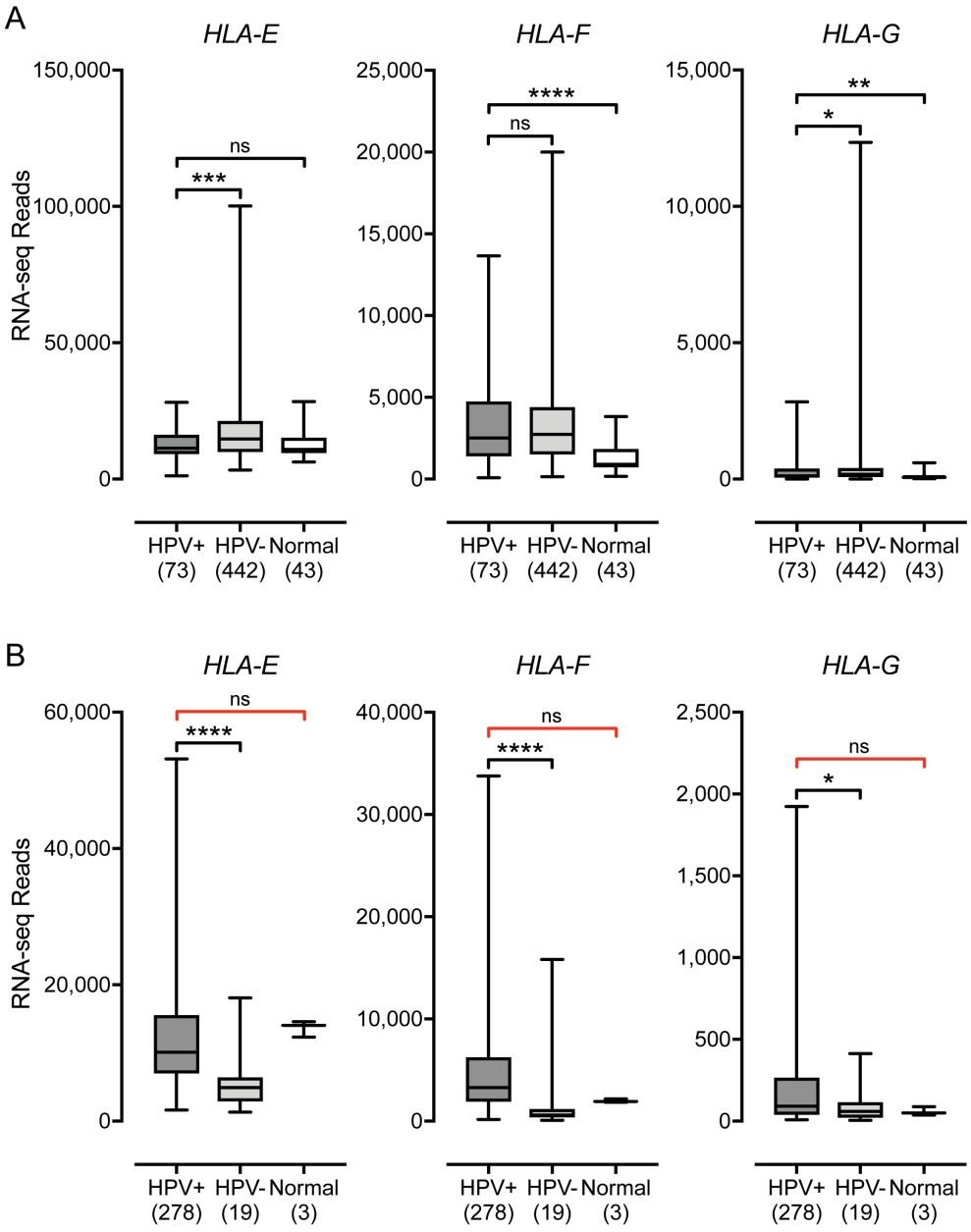

Figure 3.2. Expression of non-classical MHC-I heavy chain genes in head & neck or cervical carcinomas stratified by HPV status.

Normalized RNA-seq data for the indicated MHC-I heavy chain genes was extracted from the TCGA database for the HNSC (**A**) and CESC (**B**) cohorts for HPV+, HPV−, and normal control tissues. Numbers in brackets refer to the number of samples included in each analysis. * $p \leq 0.05$, ** $p \leq 0.01$, *** $p \leq 0.001$, **** $p \leq 0.0001$, ns – not significant, red brackets indicate a comparison that did not achieve significance with a power value < 0.8.

with the HPV− samples in the CESC cohort. Although *HLA-G* was expressed at lower overall levels than the other heavy chain genes, it was also expressed at comparable or elevated levels in HPV+ samples versus HPV− or normal control samples (**Figure 3.2**). Collectively, these results indicate that the expression of HPV oncogenes in actual human tumors is not correlated with strong repression of the MHC-I loci, in contrast to what is reported in tissue culture-based models. Indeed, the average expression of the mRNA for these genes is consistently higher or equivalent in HPV+ samples versus the normal control.

3.3.2 Impact of HPV status on the expression of other components of the antigen presentation apparatus in human tumors

The MHC-I heavy chain folds and assembles with the β2 microglobulin light chain within the endoplasmic reticulum, in a process dependent on binding to a peptide antigen (Hansen and Bouvier, 2009). The MHC-I peptide-loading complex consists of MHC-I, the peptide transporter TAP, the bridging factor tapasin, the endoplasmic reticulum aminopeptidase (ERAP), and the chaperones: calreticulin, calnexin, and ERp57. Several studies have reported the downregulation of TAP in HPV+ cancer cell lines (Georgopoulos et al., 2000; Li et al., 2010). Much less is known about the effect of HPV status on the expression of the other components necessary for MHC-I antigen presentation, so we examined the impact of HPV status on all mRNA expression for all components of the MHC-I peptide-loading complex. Analysis of TCGA data revealed high levels of transcripts for the *B2M* gene encoding β2 microglobulin, the *TAP1* and *TAP2* genes encoding the TAP heterodimer, and the genes encoding ERAP, tapasin, calreticulin, calnexin, and ERp57 (*ERAP1/2*, *TAPBP*, *CALR*, *CANX*, and *PDIA3* respectively) in HPV+ samples in head & neck (**Figure 3.3**) and cervical (**Figure 3.4**) carcinomas. All genes were expressed at higher levels in HPV+ samples with respect to normal control tissue in the HNSC cohort, with the sole exception of *CANX*, which was expressed at a comparable level. There were no consistent differences in expression with respect to HPV+ and HPV− samples in the HNSC cohort. *B2M* and *TAP1* were expressed at equivalent levels; *TAP2*, *CANX*, *CALR*, and *PDIA3* were reduced; while *TAPBP*, *ERAP1*, and *ERAP2* were increased (**Figure 3.3**). In the CESC cohort, nearly all of these genes were expressed at elevated or comparable levels

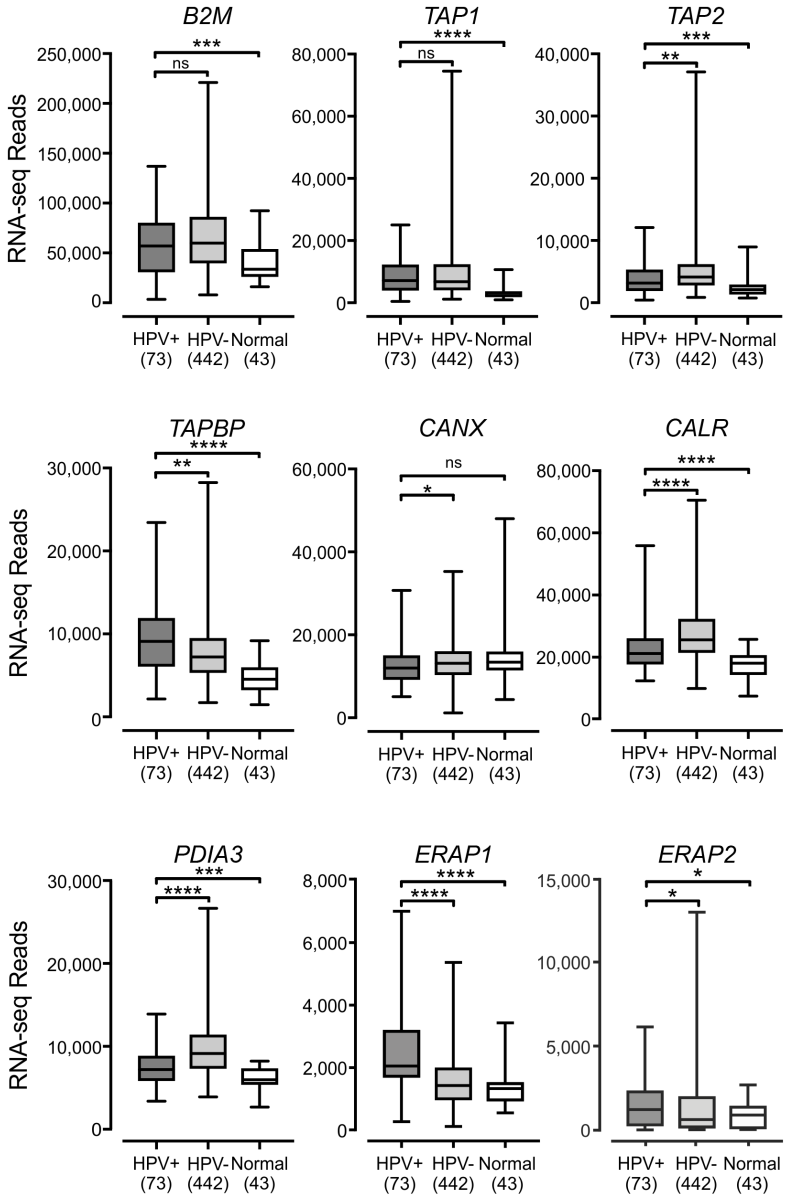

Figure 3.3. Expression of the MHC-I light chain and other genes involved in MHC-I-dependent antigen presentation in head & neck carcinomas stratified by HPV status. Normalized RNA-seq data for the indicated genes involved in MHC-I-dependent antigen presentation was extracted from the TCGA database for the HNSC cohort for HPV+, HPV−, and normal control tissues. Numbers in brackets refer to the number of samples included in each analysis. * $p \leq 0.05$, ** $p \leq 0.01$, *** $p \leq 0.001$, **** $p \leq 0.0001$, ns – not significant.

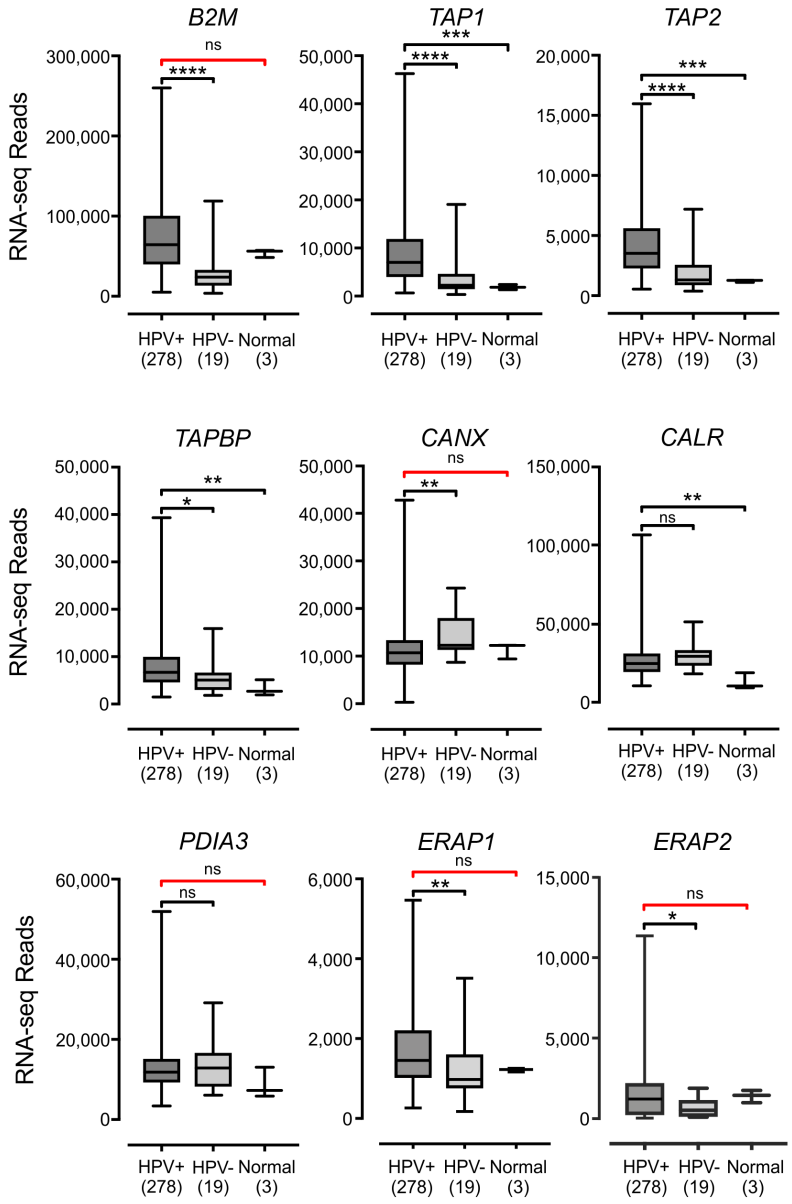

Figure 3.4. Expression of the MHC-I light chain and other genes involved in MHC-I-dependent antigen presentation in cervical carcinomas stratified by HPV status.

Normalized RNA-seq data for the indicated genes involved in MHC-I-dependent antigen presentation was extracted from the TCGA database for the CESC cohort for HPV+, HPV−, and normal control tissues. Numbers in brackets refer to the number of samples included in each analysis. * $p \leq 0.05$, ** $p \leq 0.01$, *** $p \leq 0.001$, **** $p \leq 0.0001$, ns – not significant, red brackets indicate a comparison that did not achieve significance with a power value < 0.8.

to normal control tissue or HPV− samples, although some comparisons were limited based on insufficient sample numbers. The sole exception was *CANX*, which was expressed at a lower level in HPV+ versus HPV− samples (**Figure 3.4**). Thus, most components of the MHC-I loading complex were transcribed in HPV+ human tumors at levels that appear similar or significantly higher than normal control tissue. This again contrasts with the reported decreases in *TAP* transcription reported in tissue culture models.

3.3.3 Higher levels of lymphocytes and interferon γ are present in HPV+ human tumors

IFNγ, the product of the *IFNG* locus, can coordinately induce higher levels of transcription in many of the genes involved in antigen processing and presentation by MHC-I, and provides enhanced immune surveillance under inflammatory conditions (Boehm et al., 1997). Given our observation that mRNA levels of all MHC-I loading and presentation genes were expressed at higher or at least similar levels in HPV+ tumors compared with HPV− and normal control tissues, we hypothesized that infiltrating lymphocytes producing IFNγ could be present at higher levels in HPV+ tumors versus HPV− tumors or normal control tissues.

We first assessed the relative proportion of T- and NK-cells in these samples, which are the primary producers of IFNγ. Similarly to what has been done by others (Becht et al., 2016), we analyzed the mRNA expression levels of the genes encoding CD3 (*CD3D*, *CD3E,* and *CD3G*) and CD16a (*FCGR3A*), as surrogate markers for T- and NK-cells, respectively (**Figure 3.5**). HPV+ samples from both the HNSC and CESC cohorts showed significantly increased expression of all three genes encoding subunits of CD3 versus HPV− samples. For the HNSC cohort, *CD3* expression in HPV+ samples were also consistently higher than normal control tissues. No significant differences in *CD3* levels were observed between HPV+ samples and normal control tissues in the CESC cohort, but this comparison was not powered sufficiently to confirm this result. For the NK-cell marker CD16a, expression of *FCGR3A* was readily detected and significantly higher in HPV+ cells versus normal control tissue from both the HNSC and CESC cohorts. No difference in *FCGR3A* levels were apparent between HPV+ and HPV− samples from either cohort,

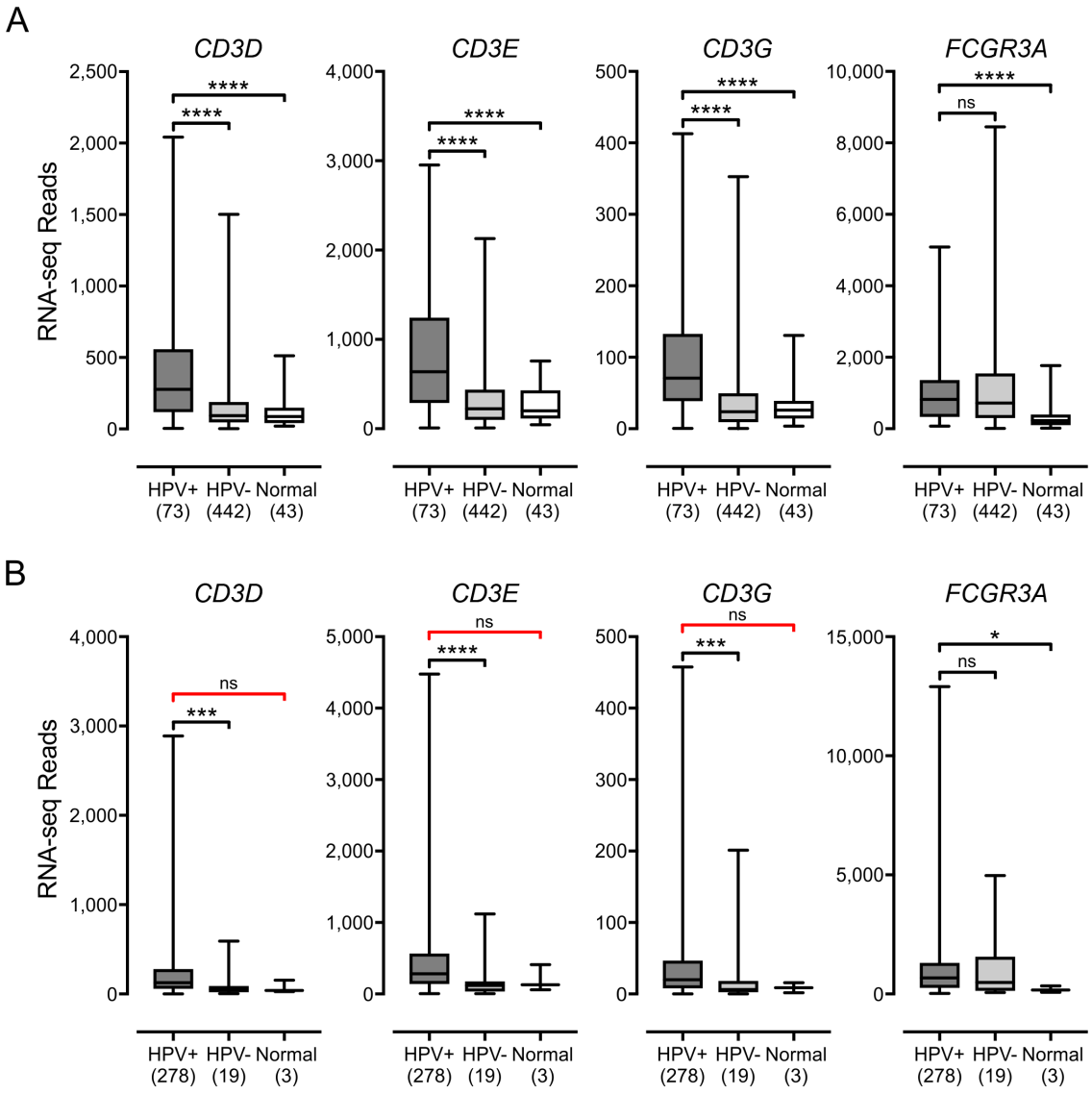

Figure 3.5. Detection of tumor infiltrating T-cells and NK-cells in head & neck and cervical carcinomas stratified by HPV status.

Normalized RNA-seq data for genes indicative of tumor-infiltrating T-cells (*CD3D*, *CD3E*, and *CD3G*) or NK-cells (*FCGR3A*) was extracted from the TCGA database for the HNSC (**A**) and CESC (**B**) cohorts for HPV+, HPV−, and normal control tissues. Numbers in brackets refer to the number of samples included in each analysis. * $p \leq 0.05$, *** $p \leq 0.001$, **** $p \leq 0.0001$, ns – not significant, red brackets indicate a comparison that did not achieve significance with a power value < 0.8.

which indicated that infiltration by NK-cells is similar in both HPV+ and HPV− samples. Taken together, these results suggest that there is significant infiltration of both cervical and head & neck tumors with T-cells and likely NK-cells, which could be stimulating the tumor cells to upregulate MHC-I. Notably, the absolute normalized RNA-seq read levels for genes derived from these infiltrating lymphocytes were much lower than any of the other genes we analyzed, with the exception of the weakly expressed *HLA-G*. This was as expected, as the lymphocytes are expected to represent only a fraction of the tumor mass (Aran et al., 2015).

We next looked for IFNγ mRNA to determine whether these lymphocytes were producing this proinflammatory cytokine (**Figure 3.6**). Although the expression of IFNγ mRNA in these samples was low, it was detectable, and significantly higher in HPV+ samples versus HPV− or normal control tissues in both the HNSC and CESC cohorts (**Figure 3.6**). Taken together, these results indicate that HPV+ carcinomas have a significant level of infiltrating lymphocytes that appear to be producing some IFNγ. Thus, the upregulated expression of the MHC-I loading and presentation genes observed in these carcinomas may be a consequence of exposure to IFNγ.

3.3.4 Genes encoding components of the antigen presentation apparatus are frequently mutated in HPV+ human tumors

Precancerous cells undergo strong selection for properties that are advantageous for growth and survival, leading to clonal evolution and cancer formation. As such, tumor cells frequently acquire somatic mutations that activate oncogenes or inactivate growth inhibitory genes. In HPV-dependent cancers, the expression of virally-derived oncogenes should eliminate the need for somatic mutations in the key cellular regulatory pathways they target. Thus, if high-risk HPV E7 repressed MHC-I expression and function, the frequency of mutations in MHC-I that would allow tumor escape from the immune system should be reduced in HPV+ versus HPV− carcinomas.

To validate this concept, we first analyzed the frequency of mutations in *TP53* and *CDKN2A* (**Figures 3.7A, B, left panels**). *TP53* encodes the p53 tumor suppressor protein, which is targeted by the E6 oncoproteins of high-risk HPVs. *CDKN2A* encodes the p16

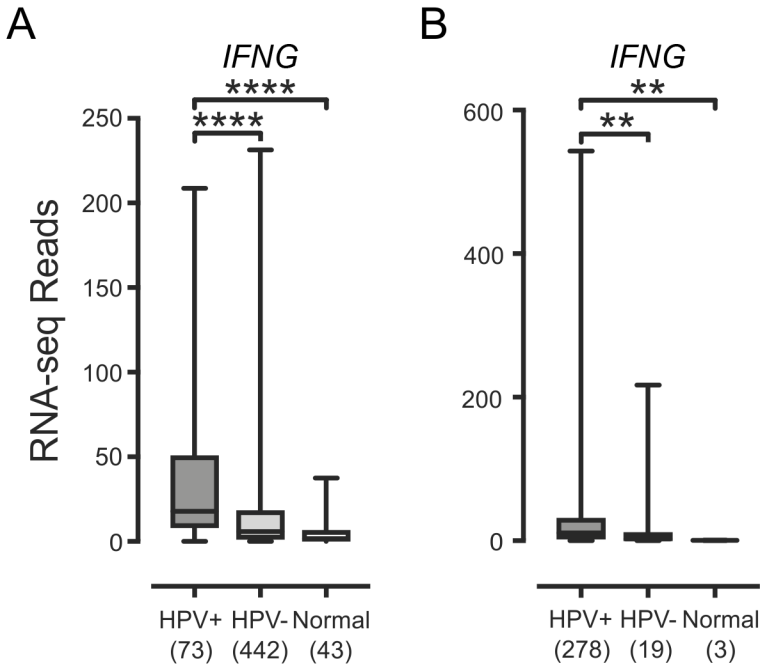

Figure 3.6. Detection of IFNγ mRNA in head & neck and cervical carcinomas stratified by HPV status.

Normalized RNA-seq data for the IFNγ gene produced by tumor-infiltrating lymphocytes was extracted from the TCGA database for the HNSC (**A**) and CESC (**B**) cohorts for HPV+, HPV−, and normal control tissues. Numbers in brackets refer to the number of samples included in each analysis. ** $p \leq 0.01$, **** $p \leq 0.0001$.

tumor suppressor, a key regulator of the Rb pathway targeted by the E7 oncoprotein of high-risk HPVs (Boyer et al., 1996; Sherr and McCormick, 2002). There were dramatic differences in the frequency of somatic mutations in *TP53* and *CDKN2A* in HPV+ versus HPV− samples from both the TCGA HNSC and CESC cohorts, although the frequencies in the CESC cohort were not statistically different due to a smaller sample size. The mutation load for *TP53* was much higher in HPV− samples, with a 55-fold (HNSC) and 5.2-fold (CESC) increase compared with their HPV+ counterparts. For *CDKN2A*, a fold increase could not be calculated for the HNSC cohort, as no mutations were present in the HPV+ samples. However, 26% of HPV− HNSC samples contained *CDKN2A* mutations. In the CESC cohort, there was an 18-fold increase in *CDKN2A* mutations in HPV− compared with HPV+, respectively. These observations were expected, as high-risk HPV E6 targets p53 for degradation, while high-risk HPV E7 targets Rb. Thus, these viral oncoproteins functionally inactivate these critical anti-cancer pathways without the need for the somatic mutations acquired by HPV− carcinomas during tumor evolution.

We next compared the frequency of somatic mutations in all of the genes encoding MHC-I and the antigen-loading complex in HPV+ samples versus HPV− samples in the TCGA HNSC and CESC cohorts (**Figures 3.7A, B, right panels**). As noted by others (The Cancer Genome Atlas Research Network, 2015; The Cancer Genome Atlas Research Network, 2017), mutations in the genes encoding MHC-I heavy chains were the most frequent. However, mutations in *B2M*, *TAP1/2*, or other components of the MHC-I loading complex were also present at lower frequencies. To simplify this analysis, we compared the mutation frequency in both classical and non-classical MHC-I genes as a group, as well as all of the components of the MHC-I and associated loading complex, collectively. This second comparison should be valid, as the inactivation of any single component of this pathway could be sufficient to impair antigen presentation (Hansen and Bouvier, 2009). Indeed, one comprehensive study in a small cohort of cervical carcinomas found that 15 out of 16 tumors exhibited an impaired expression of at least one component of the MHC-I antigen presentation apparatus (Ritz et al., 2001). Our inspection of the TCGA data reveals that both HPV+ and HPV− carcinomas in the HNSC or CESC cohorts acquire relatively frequent somatic mutations in the components of the MHC-I antigen presentation pathway,

Figure 3.7. Comparison of the somatic mutation frequency in genes involved in MHC-I-dependent antigen presentation in head & neck and cervical carcinomas stratified by HPV status.

The presence or absence of somatic mutations in selected genes of the tumor samples in the TCGA HNSC and CESC cohorts was obtained from the Broad Genome Data Analysis Center's Firehose server. The frequency of mutations in individual genes or groups of genes in HPV+ versus HPV− samples was calculated to determine whether they were influenced by HPV status. Analysis of *TP53* and *CDKN2A* (left panels) revealed a significantly reduced frequency of somatic mutations in HPV+ versus HPV− samples in both the TCGA HNSC (**A**) and CESC (**B**) cohorts. No significant decrease was observed for somatic mutation frequency in the MHC-I heavy chain genes, or a collective grouping of all genes involved in MHC-I-dependent antigen presentation between HPV+ and HPV− samples in either the TCGA HNSC (**A**) or CESC (**B**) cohorts. Numbers in brackets refer to the number of samples included in each analysis. * $p \leq 0.05$, ns – not significant.

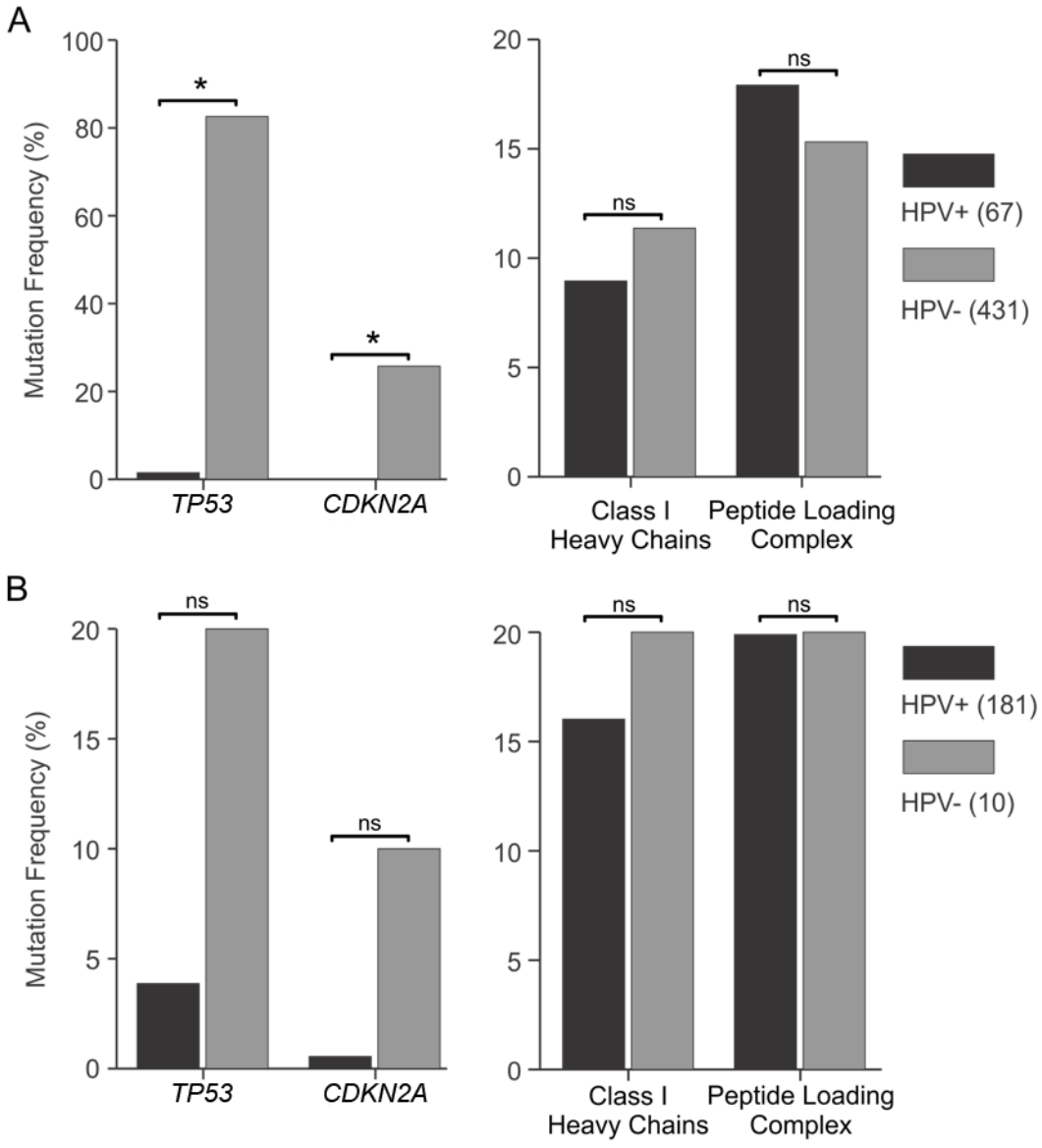
A
Mutation Frequency (%)
100
80
60
40
20
0
*
*
TP53
CDKN2A
20
15
10
5
0
ns
ns
Class I Heavy Chains
Peptide Loading Complex
HPV+ (67)
HPV- (431)
B
Mutation Frequency (%)
20
15
10
5
0
ns
ns
TP53
CDKN2A
ns
ns
Class I Heavy Chains
Peptide Loading Complex
HPV+ (181)
HPV- (10)

presumably as a means of immune escape. There was no difference in the frequency of somatic mutations in genes encoding MHC-I or the antigen-loading apparatus between HPV+ and HPV− samples in either cohort (**Figures 3.7A, B, right panels**). Thus, the presence of HPV oncogenes has no impact on the frequency of somatic mutations in genes related to MHC-I antigen presentation. This is consistent with the conclusion that HPV oncogenes do not effectively reduce antigen presentation by MHC-I, which would have eliminated the need for HPV+ carcinomas to acquire mutations in this pathway.

3.4 Discussion

The stable surface expression of MHC-I requires loading of the heavy chain/light chain dimer with an antigenic peptide in the endoplasmic reticulum. The loading complex consists of multiple essential factors, including the peptide transporter TAP, the bridging factor tapasin, and the chaperones: calreticulin, calnexin, and ERp57. Reduced expression or mutation of any of these components can compromise MHC-I-dependent antigen presentation, and allow the infected or cancerous cell to escape T-cell recognition and clearance (Hansen and Bouvier, 2009).

HPV infection and subsequent expression of the viral oncoproteins leads to a large-scale reprogramming of gene expression. Multiple studies have reported that the high-risk HPV E7 oncoprotein contributes to the evasion of the adaptive immune response; this process occurs through transcriptional downregulation of the MHC-I heavy chain genes or other components necessary for antigen loading and presentation (Georgopoulos et al., 2000; Heller et al., 2011; Li et al., 2010). This mechanism has been proposed to support the establishment of persistent HPV infection and contribute to the ability of HPV+ cancers to evade anti-tumor CTL responses. Additional downregulation of MHC-I is mediated by the high-risk HPV E5 oncoprotein. This occurs via a non-transcriptional mechanism in which the classical heavy chains are trapped in the Golgi apparatus and not transported to the cell surface (Ashrafi et al., 2006).

While cell culture models have allowed detailed studies on the mechanism of E7-mediated transcriptional downregulation of components in the MHC-I antigen presentation

apparatus, far less is known about how similar these effects are to actual HPV+ tumors. In this study, our goal was to determine whether the transcriptional reduction in MHC-I components mediated by E7 is recapitulated in primary HPV+ tumors from different anatomical locations.

Using data from over 800 primary human tumors, we provide evidence that HPV+ tumors from both the head & neck and cervical sites display high mRNA levels for MHC-I components, including heavy and light chains, as well as all factors required for MHC-I loading. Indeed, HPV+ head & neck carcinomas exhibit significant increases, rather than decreases, in mRNA levels for many MHC-I components compared with normal control tissue, and this trend continues in the cervical carcinoma cohort (**Figures 3.1–3.4**). These unexpected results contradict the existing paradigm of virally-mediated immune evasion and suggest that in the context of an *in vivo* tumor setting, the presence of HPV may actually result in enhanced expression of mRNA encoding MHC-I-dependent antigen presentation components.

As our results specifically addressed the question of whether HPV oncoproteins repress expression of the MHC-I genes at the transcriptional level, they do not eliminate the possibility that other post-transcriptional mechanisms, such as those mediated by high-risk HPV E5, can reduce antigen presentation. However, a comprehensive analysis of MHC-I protein expression by immunohistochemical detection indicated that only a subset of about 40% of HPV+ cervical carcinomas have reduced expression of one or more components at the protein level (Mehta et al., 2008). As only a minority of carcinomas have reduced antigen presentation apparatus, it appears that the HPV-mediated reduction of MHC-I is not absolutely necessary for tumorigenesis.

Our results also do not rule out the possibility that E7 could mediate a reduction in MHC-I transcription in non-cancerous or pre-cancerous lesions, as all samples in this study are carcinomas. However, a purpose for the reacquisition of expression of MHC-I during the progression of a non-neoplastic lesion to a carcinoma is difficult to reconcile with current models of tumorigenesis.

Further evidence supporting our conclusion that HPV oncoproteins are unable to functionally antagonize MHC-I-dependent antigen presentation in human carcinomas is provided by our comparison of somatic mutation frequencies between HPV+ and HPV− samples (**Figure 3.7**). The anticipated sharp reduction in the occurrence of mutations in genes encoding MHC-I or antigen-loading complex components was not observed in HPV+ samples. This is in stark contrast to what was observed for *TP53*, which encodes p53, a known target of the high-risk HPV E6 oncoproteins (Scheffner et al., 1990) or *CDKN2A*, which encodes the p16 component of the Rb pathway targeted by high-risk HPV E7 oncoproteins (Boyer et al., 1996).

Furthermore, HPV utilizes multiple other strategies to evade the adaptive immune response, which suggests that a simple reduction in MHC-I transcription is unlikely to be sufficient to escape surveillance by the immune system. These include the ability of E5 to block MHC-I transport to the cell surface (Ashrafi et al., 2006), the preferential utilization of low-abundance codons to ensure minimal translation of viral antigens (Zhao and Chen, 2011), and the induction of the ERAP1 protease to partially degrade and attenuate the presentation of viral antigenic epitopes (Steinbach et al., 2017).

A simple mechanism to explain the lack of MHC-I repression would be a failure of these tumors to express the HPV E7 oncogene, which has been reported to be necessary and sufficient for the downregulation of transcription from at least some of these genes (Bottley et al., 2008; Georgopoulos et al., 2000; Heller et al., 2011; Li et al., 2006; Li et al., 2009; Li et al., 2010). This is clearly not the case, as all HPV+ samples were reported to express detectable levels of *E6* and *E7* mRNAs (The Cancer Genome Atlas Research Network, 2015; The Cancer Genome Atlas Research Network, 2017). In addition, a lack of E7 would not be expected to lead to the observed increase in MHC-I expression, but rather cause equivalent expression to that of HPV− cervical carcinoma samples.

An alternative method of activating expression of MHC-I and components of the antigen-loading complex could be via the activation of the JAK/STAT/IRF-1 signal transduction pathway by exposure to IFNγ. However, multiple studies done in tissue culture models have shown that HPV E7 abrogates the IRF-1 response, thus inhibiting the IFNγ induction

of MHC-I expression, antigen presentation, and CTL-induced cell death (Park et al., 2000; Perea et al., 2000; Um et al., 2002; Zhou et al., 2013; Zhou et al., 2011). Our analysis reveals low but detectable levels of mRNA for IFNγ in HPV+ samples, which are higher than HPV− samples or normal control tissue in both TCGA cohorts (**Figure 3.6**). In addition, we searched for the presence of mRNAs that should be unique to infiltrating lymphocytes that can express IFNγ (**Figure 3.5**). Using these surrogate markers, we found evidence for significant infiltration by T-cells and NK-cells in both HPV+ and HPV− carcinomas. Indeed, the levels of infiltrating lymphocytes were significantly higher in HPV+ vs. HPV− samples for both TCGA cohorts, which could have resulted from detection of foreign virally-derived antigens. Taken together, the high absolute levels of mRNAs encoding MHC-I components expressed in HPV+ head & neck and cervical carcinomas provide good evidence that high-risk HPV E7 is unable to efficiently block the IFNγ induction of transcription of these genes in actual human tumors. Although this contrasts with the results of the studies listed above, our work agrees with other studies showing that various cervical cancer cell lines upregulate MHC-I in response to IFNγ (Bornstein et al., 1997; Evans et al., 2001; Mora-Garcia Mde et al., 2006), and the treatment of HPV+ pre-cancerous cervical lesions in patients increased expression of at least HLA-B in a majority of cases (Sikorski et al., 2004). It should be noted that the levels of MHC-I heavy chain mRNAs are statistically lower in HPV+ vs HPV− samples in the HNSC cohort (**Figure 3.1**), despite the increased levels of IFNγ (**Figure 3.6**). This may indicate that HPV is able to modestly impact IFNγ activation in these tissues, but this was not observed in the CESC cohort.

Our analysis of over 350 HPV+ head & neck or cervical carcinomas in comparison with over 450 HPV− cancers demonstrates subtle differences in the effect of HPV on MHC-I transcription between the two anatomical sites. Specifically, HPV does not repress the transcription of MHC-I heavy chain genes in cervical carcinomas, which exhibit high levels with respect to both HPV− carcinomas and normal control tissue. In contrast, a statistically significant but modest reduction in MHC-I heavy chain mRNA levels was observed in HPV+ vs HPV− head & neck cancers. However, transcription of these genes was nevertheless substantially elevated with respect to normal control tissues. Interestingly, our observations with the MHC-I heavy chain genes extend to many of the other genes

involved in MHC-I loading. These results are in sharp contrast to much of the existing literature derived from tissue culture-based experiments, possibly because of the complex interplay between the MHC-I antigen presentation apparatus and cytokines produced by infiltrating lymphocytes present in actual tumors. This differs markedly from our previous study on the effects of HPV on numerous regulators of H3K27 methylation and the expression of multiple downstream targets of these regulators, in which we showed that tissue culture models faithfully recapitulate what is observed in human tumors (Gameiro et al., 2017).

Importantly, MHC-I-dependent antigen presentation is critical for $CD8^+$ T-cell responses, which are essential for the control and clearance of virally-infected or cancerous cells. This is particularly important as recent advances in cancer immunotherapy using immune checkpoint blockades rely on reactivating antigen-dependent clearance of tumor cells (Postow et al., 2015). Although we detect high levels of MHC-I mRNA in HPV+ tumors, this may not necessarily translate into high levels of expression of these proteins. In addition, a functional defect in any component of the MHC-I antigen presentation apparatus could compromise the detection and clearance of HPV+ carcinomas by the adaptive immune system (Hansen and Bouvier, 2009). Thus, the utility of immune checkpoint blockade therapy in HPV-dependent cancers remains to be determined. Nevertheless, it is intriguing to speculate that the expression of non-self-derived viral antigens, combined with intact MHC-I presentation and increased levels of infiltrating T-cells, may contribute to the well-established observation that patient outcomes using conventional therapies are markedly better for HPV+ versus HPV− carcinomas in both the head & neck and cervix (Ang et al., 2010; Gotwals et al., 2017).

3.5 References

Alemany L, Cubilla A, Halec G, et al. (2016) Role of Human Papillomavirus in Penile Carcinomas Worldwide. *Eur Urol* 69: 953-961.

Ang KK, Harris J, Wheeler R, et al. (2010) Human papillomavirus and survival of patients with oropharyngeal cancer. *N Engl J Med* 363: 24-35.

Aran D, Sirota M and Butte AJ. (2015) Systematic pan-cancer analysis of tumour purity. *Nat Commun* 6: 8971.

Ashrafi GH, Haghshenas M, Marchetti B, et al. (2006) E5 protein of human papillomavirus 16 downregulates HLA class I and interacts with the heavy chain via its first hydrophobic domain. *Int J Cancer* 119: 2105-2112.

Banister CE, Liu C, Pirisi L, et al. (2017) Identification and characterization of HPV-independent cervical cancers. *Oncotarget* 8: 13375-13386.

Becht E, Giraldo NA, Lacroix L, et al. (2016) Estimating the population abundance of tissue-infiltrating immune and stromal cell populations using gene expression. *Genome Biol* 17: 218.

Boehm U, Klamp T, Groot M, et al. (1997) Cellular responses to interferon-gamma. *Annu Rev Immunol* 15: 749-795.

Bornstein J, Lahat N, Kinarty A, et al. (1997) Interferon-beta and -gamma, but not tumor necrosis factor-alpha, demonstrate immunoregulatory effects on carcinoma cell lines infected with human papillomavirus. *Cancer* 79: 924-934.

Bottley G, Watherston OG, Hiew YL, et al. (2008) High-risk human papillomavirus E7 expression reduces cell-surface MHC class I molecules and increases susceptibility to natural killer cells. *Oncogene* 27: 1794-1799.

Boyer SN, Wazer DE and Band V. (1996) E7 protein of human papilloma virus-16 induces degradation of retinoblastoma protein through the ubiquitin-proteasome pathway. *Cancer Res* 56: 4620-4624.

Bratman SV, Bruce JP, O'Sullivan B, et al. (2016) Human Papillomavirus Genotype Association With Survival in Head and Neck Squamous Cell Carcinoma. *JAMA Oncol* 2: 823-826.

Brehm A, Miska EA, McCance DJ, et al. (1998) Retinoblastoma protein recruits histone deacetylase to repress transcription. *Nature* 391: 597-601.

Cicchini L, Blumhagen RZ, Westrich JA, et al. (2017) High-Risk Human Papillomavirus E7 Alters Host DNA Methylome and Represses HLA-E Expression in Human Keratinocytes. *Sci Rep* 7: 3633.

Cromme FV, Meijer CJ, Snijders PJ, et al. (1993) Analysis of MHC class I and II expression in relation to presence of HPV genotypes in premalignant and malignant cervical lesions. *Br J Cancer* 67: 1372-1380.

Crosbie EJ, Einstein MH, Franceschi S, et al. (2013) Human papillomavirus and cervical cancer. *Lancet* 382: 889-899.

De Vuyst H, Clifford GM, Nascimento MC, et al. (2009) Prevalence and type distribution of human papillomavirus in carcinoma and intraepithelial neoplasia of the vulva, vagina and anus: a meta-analysis. *Int J Cancer* 124: 1626-1636.

Djajadiningrat RS, Horenblas S, Heideman DA, et al. (2015) Classic and nonclassic HLA class I expression in penile cancer and relation to HPV status and clinical outcome. *J Urol* 193: 1245-1251.

Doorbar J, Egawa N, Griffin H, et al. (2015) Human papillomavirus molecular biology and disease association. *Rev Med Virol* 25 Suppl 1: 2-23.

Doorbar J, Quint W, Banks L, et al. (2012) The biology and life-cycle of human papillomaviruses. *Vaccine* 30 Suppl 5: F55-70.

Dorner T and Radbruch A. (2007) Antibodies and B cell memory in viral immunity. *Immunity* 27: 384-392.

Dyson N, Guida P, Munger K, et al. (1992) Homologous sequences in adenovirus E1A and human papillomavirus E7 proteins mediate interaction with the same set of cellular proteins. *J Virol* 66: 6893-6902.

Evans M, Borysiewicz LK, Evans AS, et al. (2001) Antigen processing defects in cervical carcinomas limit the presentation of a CTL epitope from human papillomavirus 16 E6. *J Immunol* 167: 5420-5428.

Faul F, Erdfelder E, Lang AG, et al. (2007) G*Power 3: a flexible statistical power analysis program for the social, behavioral, and biomedical sciences. *Behav Res Methods* 39: 175-191.

Forman D, de Martel C, Lacey CJ, et al. (2012) Global burden of human papillomavirus and related diseases. *Vaccine* 30 Suppl 5: F12-23.

Gameiro SF, Kolendowski B, Zhang A, et al. (2017) Human papillomavirus dysregulates the cellular apparatus controlling the methylation status of H3K27 in different human cancers to consistently alter gene expression regardless of tissue of origin. *Oncotarget* 8: 72564-72576.

Garcia-Lora A, Algarra I and Garrido F. (2003) MHC class I antigens, immune surveillance, and tumor immune escape. *J Cell Physiol* 195: 346-355.

Georgopoulos NT, Proffitt JL and Blair GE. (2000) Transcriptional regulation of the major histocompatibility complex (MHC) class I heavy chain, TAP1 and LMP2 genes by the human papillomavirus (HPV) type 6b, 16 and 18 E7 oncoproteins. *Oncogene* 19: 4930-4935.

Gillison ML, Koch WM, Capone RB, et al. (2000) Evidence for a causal association between human papillomavirus and a subset of head and neck cancers. *J Natl Cancer Inst* 92: 709-720.

Gotwals P, Cameron S, Cipolletta D, et al. (2017) Prospects for combining targeted and conventional cancer therapy with immunotherapy. *Nat Rev Cancer* 17: 286-301.

Guimera N, Alemany L, Halec G, et al. (2017) Human papillomavirus 16 is an aetiological factor of scrotal cancer. *Br J Cancer* 116: 1218-1222.

Hansen TH and Bouvier M. (2009) MHC class I antigen presentation: learning from viral evasion strategies. *Nat Rev Immunol* 9: 503-513.

Heller C, Weisser T, Mueller-Schickert A, et al. (2011) Identification of key amino acid residues that determine the ability of high risk HPV16-E7 to dysregulate major histocompatibility complex class I expression. *J Biol Chem* 286: 10983-10997.

Jochmus I, Durst M, Reid R, et al. (1993) Major histocompatibility complex and human papillomavirus type 16 E7 expression in high-grade vulvar lesions. *Hum Pathol* 24: 519-524.

Keating PJ, Cromme FV, Duggan-Keen M, et al. (1995) Frequency of down-regulation of individual HLA-A and -B alleles in cervical carcinomas in relation to TAP-1 expression. *Br J Cancer* 72: 405-411.

Kim DH, Kim EM, Lee EH, et al. (2011) Human papillomavirus 16E6 suppresses major histocompatibility complex class I by upregulating lymphotoxin expression in human cervical cancer cells. *Biochem Biophys Res Commun* 409: 792-798.

Li H, Ou X, Xiong J, et al. (2006) HPV16E7 mediates HADC chromatin repression and downregulation of MHC class I genes in HPV16 tumorigenic cells through interaction with an MHC class I promoter. *Biochem Biophys Res Commun* 349: 1315-1321.

Li H, Zhan T, Li C, et al. (2009) Repression of MHC class I transcription by HPV16E7 through interaction with a putative RXRbeta motif and NF-kappaB cytoplasmic sequestration. *Biochem Biophys Res Commun* 388: 383-388.

Li W, Deng XM, Wang CX, et al. (2010) Down-regulation of HLA class I antigen in human papillomavirus type 16 E7 expressing HaCaT cells: correlate with TAP-1 expression. *Int J Gynecol Cancer* 20: 227-232.

Mayakonda A, Lin DC, Assenov Y, et al. (2018) Maftools: efficient and comprehensive analysis of somatic variants in cancer. *Genome Res* 28: 1747-1756.

Mehanna H, Beech T, Nicholson T, et al. (2013) Prevalence of human papillomavirus in oropharyngeal and nonoropharyngeal head and neck cancer--systematic review and meta-analysis of trends by time and region. *Head Neck* 35: 747-755.

Mehta AM, Jordanova ES, Kenter GG, et al. (2008) Association of antigen processing machinery and HLA class I defects with clinicopathological outcome in cervical carcinoma. *Cancer Immunol Immunother* 57: 197-206.

Mora-Garcia Mde L, Duenas-Gonzalez A, Hernandez-Montes J, et al. (2006) Up-regulation of HLA class-I antigen expression and antigen-specific CTL response in

cervical cancer cells by the demethylating agent hydralazine and the histone deacetylase inhibitor valproic acid. *J Transl Med* 4: 55.

Munoz N, Hernandez-Suarez G, Mendez F, et al. (2009) Persistence of HPV infection and risk of high-grade cervical intraepithelial neoplasia in a cohort of Colombian women. *Br J Cancer* 100: 1184-1190.

Network TCGAR. (2015) Comprehensive genomic characterization of head and neck squamous cell carcinomas. *Nature* 517: 576-582.

Network TCGAR. (2017) Integrated genomic and molecular characterization of cervical cancer. *Nature* 543: 378-384.

Park JS, Kim EJ, Kwon HJ, et al. (2000) Inactivation of interferon regulatory factor-1 tumor suppressor protein by HPV E7 oncoprotein. Implication for the E7-mediated immune evasion mechanism in cervical carcinogenesis. *J Biol Chem* 275: 6764-6769.

Perea SE, Massimi P and Banks L. (2000) Human papillomavirus type 16 E7 impairs the activation of the interferon regulatory factor-1. *Int J Mol Med* 5: 661-666.

Postow MA, Callahan MK and Wolchok JD. (2015) Immune Checkpoint Blockade in Cancer Therapy. *J Clin Oncol* 33: 1974-1982.

Ramqvist T, Mints M, Tertipis N, et al. (2015) Studies on human papillomavirus (HPV) 16 E2, E5 and E7 mRNA in HPV-positive tonsillar and base of tongue cancer in relation to clinical outcome and immunological parameters. *Oral Oncol* 51: 1126-1131.

Ritz U, Momburg F, Pilch H, et al. (2001) Deficient expression of components of the MHC class I antigen processing machinery in human cervical carcinoma. *Int J Oncol* 19: 1211-1220.

Scheffner M, Werness BA, Huibregtse JM, et al. (1990) The E6 oncoprotein encoded by human papillomavirus types 16 and 18 promotes the degradation of p53. *Cell* 63: 1129-1136.

Sherr CJ and McCormick F. (2002) The RB and p53 pathways in cancer. *Cancer cell* 2: 103-112.

Sikorski M, Bobek M, Zrubek H, et al. (2004) Dynamics of selected MHC class I and II molecule expression in the course of HPV positive CIN treatment with the use of human recombinant IFN-gamma. *Acta Obstet Gynecol Scand* 83: 299-307.

Steinbach A, Winter J, Reuschenbach M, et al. (2017) ERAP1 overexpression in HPV-induced malignancies: A possible novel immune evasion mechanism. *Oncoimmunology* 6: e1336594.

Syrjanen S. (2005) Human papillomavirus (HPV) in head and neck cancer. *J Clin Virol* 32 Suppl 1: S59-66.

Takeuchi O and Akira S. (2009) Innate immunity to virus infection. *Immunol Rev* 227: 75-86.

Torres LM, Cabrera T, Concha A, et al. (1993) HLA class I expression and HPV-16 sequences in premalignant and malignant lesions of the cervix. *Tissue Antigens* 41: 65-71.

Tscharke DC, Croft NP, Doherty PC, et al. (2015) Sizing up the key determinants of the CD8(+) T cell response. *Nat Rev Immunol* 15: 705-716.

Um SJ, Rhyu JW, Kim EJ, et al. (2002) Abrogation of IRF-1 response by high-risk HPV E7 protein in vivo. *Cancer Lett* 179: 205-212.

van Esch EM, Tummers B, Baartmans V, et al. (2014) Alterations in classical and nonclassical HLA expression in recurrent and progressive HPV-induced usual vulvar intraepithelial neoplasia and implications for immunotherapy. *Int J Cancer* 135: 830-842.

Westrich JA, Warren CJ and Pyeon D. (2017) Evasion of host immune defenses by human papillomavirus. *Virus Res* 231: 21-33.

Yan N and Chen ZJ. (2012) Intrinsic antiviral immunity. *Nat Immunol* 13: 214-222.

Zhao KN and Chen J. (2011) Codon usage roles in human papillomavirus. *Rev Med Virol* 21: 397-411.

Zhou F, Chen J and Zhao KN. (2013) Human papillomavirus 16-encoded E7 protein inhibits IFN-gamma-mediated MHC class I antigen presentation and CTL-induced lysis by blocking IRF-1 expression in mouse keratinocytes. *J Gen Virol* 94: 2504-2514.

Zhou F, Leggatt GR and Frazer IH. (2011) Human papillomavirus 16 E7 protein inhibits interferon-gamma-mediated enhancement of keratinocyte antigen processing and T-cell lysis. *FEBS J* 278: 955-963.

Chapter 4

4 Treatment-naïve HPV+ Head and Neck Cancers Display a T-cell-inflamed Phenotype Distinct from their HPV– Counterparts that has Implications for Immunotherapy

4.1 Introduction

Recent advances in understanding the basics of tumor immunology have paved the way for development of therapies that can induce effective anti-tumor immune responses. Many of these are based on immune checkpoint inhibition, in which normal negative regulatory mechanisms, which keep immune responses in check, are overcome (Pardoll, 2012; Topalian et al., 2015). Current immuno-oncology therapies can demonstrate tremendous efficacy and induce long-term remission in patients (Del Paggio, 2018). However, responses to immunotherapy are often restricted to a subset of cancers, for reasons that are not entirely understood.

Head and neck squamous cell carcinomas (HNSC) represent the 6th most common human cancer type (Ferlay et al., 2010) and are often characterized by aggressive local invasion and overall poor prognosis (Baxi et al., 2012). In addition to mortality, both the disease and its treatment often result in significant patient morbidity. Indeed, treatments for HNSC often impact the most personal characteristics of an individual, including facial appearance and the ability to eat and speak.

Infection with human papillomavirus (HPV) is a major etiological factor for tumors located in the oropharynx. Indeed, HPV-positive (HPV+) HNSC is increasing at an epidemic pace (Marur et al., 2010; Nichols et al., 2013). Importantly, HPV-negative (HPV–) and HPV+ HNSC are molecularly distinct, with a different spectrum of mutations (The Cancer Genome Atlas Research Network, 2015). HPV+ HNSC also constitutively express viral oncogenes that deregulate cell growth and gene expression (Mittal and Banks, 2017). In addition, clinical outcomes for HPV+ HNSC are far superior to those in HPV– cases (Ang et al., 2010; Fakhry et al., 2008).

Both HPV+ and HPV– HNSC display a comparable frequency of somatic mutations, a major source of tumor specific neoantigens that can be recognized and targeted by anti-tumor immunity (The Cancer Genome Atlas Research Network, 2015). However, HPV+, but not HPV–, HNSC express exogenous antigenic viral proteins that may be the source of a key difference in the tumor immune landscape between these two types of HNSC and may contribute to the superior clinical outcomes associated with HPV+ HNSC. Several studies have compared various immunological parameters between HPV+ and HPV– HNSC and have commonly concluded that HPV+ HNSC are immune "hot" tumors, with markedly more immune infiltration and higher levels of $CD8^+$ T-cell activation than HPV– HNSC (Mandal et al., 2016; Solomon et al., 2018). These and other studies suggest that a detailed comparison of the immunological differences between HPV+ and HPV– HNSC provides an opportunity to identify immunological determinants that contribute to successful treatment in HNSC that may be broadly applicable to cancer treatment in general (Feng et al., 2017; Lyford-Pike et al., 2013; Montler et al., 2016).

In this study, we used RNA-sequencing data from over 500 HNSC samples from The Cancer Genome Atlas (TCGA) to compare the immune landscape between HPV+, HPV–, and normal-adjacent control tissue. Importantly, these samples were treatment-naïve prior to surgical resection, avoiding any confounding effects of exposure to chemotherapy or radiation on the immune-status of these tumors. Such analysis can provide scientific rationale for treating HNSC patients with immune checkpoint inhibitors (ICIs) as first-line therapy.

We determined that HPV+ HNSC tumors exhibit a strong Th1 response, characterized by increased infiltration with dendritic cells (DCs), $CD4^+$ and $CD8^+$ T-cells. HPV+ HNSC also expressed higher levels of *CD39* and multiple T-cell exhaustion markers including *LAG3*, *PD1*, *TIGIT*, and *TIM3* compared to HPV– HNSC. This gene expression profile is consistent with a "T-cell-inflamed" phenotype, one that is dominated by T-cell markers and chemokines associated with effector T-cell recruitment (Gajewski et al., 2013). Importantly, higher expression of these T-cell exhaustion genes correlated with markedly improved patient survival in HPV+, but not HPV–, HNSC. These results illustrate the profound differences between the immune landscape of HPV+ and HPV– HNSC tumors

and its association with patient outcome. Furthermore, the presence of high expression levels of multiple immune inhibitory genes in HPV+ HNSC suggests that these cancers will exhibit strong beneficial responses to immunotherapy, providing a strong rationale for using ICIs as single treatment or combination therapies in first-line treatment of HPV+ HNSC. This would save patients from disfiguring surgery, or the toxicities associated with conventional chemotherapy or radiation treatment.

4.2 Materials and Methods

4.2.1 Data collection

Patient data from The Cancer Genome Atlas (TCGA), including Merged Clinical data (build 2016012800) and Level 3 RSEM-normalized Illumina HiSeq RNA expression data (build 2016012800) for the HNSC cohort, was downloaded from the Broad Genome Data Analysis Centers Firehose server (https://gdac.broadinstitute.org/). Written informed consents were obtained from the patients (or their families) by the TCGA project. CIBERSORT immune fraction data (TCGA.Kallisto.fullIDs.cibersort.relative.tsv) and Leukocyte Fraction (TCGA_all_leuk_estimate.masked.20170107.tsv) data from the Pan-Cancer Atlas was downloaded from the National Cancer Institute Cancer Genome Commons (https://gdc.cancer.gov/about-data/publications/panimmune).

4.2.2 RNA expression comparisons

RNA-Seq by Expectation Maximization (RSEM)-normalized expression data was extracted into Microsoft Excel and the HPV status was manually curated based on published datasets as described (Gameiro et al., 2017a). Primary patient samples with known HPV status were grouped as HPV+, HPV–, or normal control tissue. This classification agrees completely with work done by others (Chakravarthy et al., 2016), with the exception of sample TCGA-BB-7862-01A. That sample had minimal reads aligning to the HPV genome, none of which aligned to the HPV16 *E6* or *E7* oncogenes, and we classified this sample as HPV– rather than HPV+. Patient samples with unknown HPV status were omitted from our calculations, as were samples obtained from secondary metastatic lesions. This resulted in 73 HPV+, 442 HPV–, and 43 normal control samples with data available for the HNSC gene expression analysis. This surgically managed cohort

was considered treatment-naïve, as only 9 patients received neoadjuvant radiation or chemotherapy treatment (2 HPV+, 7 HPV–). Boxplot comparison of gene expression was performed using GraphPad Prism v7.0 (Graphpad Software, Inc., San Diego, California, USA) and assembled into final form using Adobe Illustrator. For the boxplots, center lines show the medians, box limits indicate the 25th and 75th percentiles as determined by Graphpad Prism, and whiskers extend 1.5 times the interquartile range from the 25th and 75th percentiles. Statistical significance was calculated using Graphpad Prism. *p*-values were assigned using a one-tailed non-parametric Mann-Whitney U test. Selected genes were compared in a pairwise fashion and concordance calculated using Spearman's Rho analysis. Differences were considered to be statistically significant for $p < 0.05$.

4.2.3 Immune fraction estimates

The relative fractions of 22 leukocyte types as calculated using CIBERSORT (Newman et al., 2015) was previously reported for all TCGA samples as part of the Pan-Cancer Atlas (Thorsson et al., 2018). Only those HNSC samples with a CIBERSORT $p < 0.01$ were included in our analysis, which resulted in 28 HPV+, 209 HPV–, and 17 normal control samples used in this analysis. The total leukocyte fraction was also previously reported for all TCGA samples as part of the Pan-Cancer Atlas. The HNSC values were extracted from this data and annotated for HPV status as described above.

4.2.4 Survival analysis

Five-year overall survival outcomes and disease-free progression were compared in both HPV+ and HPV– subsets of patients as dichotomized by median expression of *LAG3*, *PD1*, *TIGIT*, *TIM3*, or *CD39*. A second set of survival outcomes were done to compare tumors expressing high levels of each combination of two of these markers. Log-rank statistical *p*-values were calculated for each Cox survival model. Univariate survival analysis was done through R statistical environment (version 3.4.0) based on a Cox Proportional Hazard Model using survival package (version 2.41-3). Stepwise bidirectional multivariate analysis was then carried out with clinical variables (sex, age, smoking history, subsite, T stage, N stage, Overall stage, and HPV type), *LAG3*, *PD1*, *TIGIT*, *TIM3*, and *CD39* expression. The *p*-values derived from the Wald test on survival coefficients were reported

for investigated variables. The derived log-rank *p*-values for all tested genes (**Table 4.1**) were assessed for significance after correcting for false discovery rate (FDR) using the Benjamini–Hochberg method, and an FDR threshold of 0.1 was set for significance.

4.3 Results

4.3.1 HPV+ and HPV– head & neck carcinomas exhibit differences in some leukocyte populations

To identify and understand differences in the immune landscape between HPV+ and HPV– HNSC, we conducted a preliminary analysis using the CIBERSORT deconvolution algorithm in order to elucidate the immune cell populations present in each sample (Newman et al., 2015). This computational method is based on the differential expression of 547 genes to estimate the relative fraction of 22 leukocyte populations in each of the samples for the TCGA HNSC cohort (**Figure 4.1**). Our comparison of the HPV+ and HPV– samples revealed a number of differences, including an increased percentage of $CD8^+$ T-cells and $CD4^+$ T-regulatory cells (Tregs) in HPV+ samples compared to HPV– samples. HPV+ samples were also estimated to contain a greatly decreased level of uncommitted (M0) and anti-inflammatory (M2) macrophages as compared to HPV– samples. Increased levels of follicular helper $CD4^+$ T-cells, but not other types of $CD4^+$ T-cells, were present in HPV+ versus HPV– HNSC samples, as well increased levels of naïve and memory B-cells, but not plasma cells. These data indicate a difference between the immune landscape of HPV+ and HPV– HNSC tumors that requires further investigation.

Given the observed differences in the various leukocyte populations, we also compared the total leukocyte fraction between the HPV+ and HPV– samples in the TCGA HNSC cohort using a previously defined DNA methylation signature that is highly specific for leukocytes (Hoadley et al., 2018). However, no significant differences were detected between the overall leukocyte fraction of HPV+ versus HPV– HNSC (**Figure 4.2**).

4.3.2 HPV+ head & neck carcinomas exhibited a Th1 $CD4^+$ helper T-cell phenotype

CIBERSORT identified a number of differences between HPV+ and HPV– HNSC samples for multiple classes of T-cells, however, cancer-induced dysregulations and immune

Table 4.1. Analysis of significance between gene expression and survival (overall and disease-free) after correcting for false discovery rate (FDR).

Gene	All HNSC				HPV+ HNSC				HPV– HNSC			
	Overall Survival		Disease-free Survival		Overall Survival		Disease-free Survival		Overall Survival		Disease-free Survival	
	p value	FDR	*p* value	FDR	*p* value	FDR	*p* value	FDR	*p* value	FDR	*p* value	FDR
CD8A	0.031	0.091	0.620	0.730	0.023	0.087	0.821	0.937	0.481	0.795	0.955	0.955
CD8B	0.118	0.208	0.426	0.566	0.009	0.058	0.614	0.912	0.538	0.795	0.653	0.912
FOXP3	0.014	0.052	0.007	0.093	0.039	0.115	0.380	0.912	0.154	0.454	0.016	0.209
TBX21	0.277	0.367	0.927	0.927	0.004	0.047	0.814	0.937	0.280	0.634	0.777	0.935
CD6	0.002	0.014	0.204	0.403	0.027	0.090	0.647	0.912	0.011	0.200	0.696	0.912
CD3D	0.015	0.052	0.488	0.623	0.069	0.164	0.711	0.912	0.136	0.449	0.917	0.955
CD3E	0.001	0.014	0.091	0.269	0.005	0.047	0.576	0.912	0.042	0.343	0.429	0.846
CD3G	0.002	0.014	0.264	0.463	0.076	0.165	0.582	0.912	0.091	0.449	0.881	0.954
SH2D1A	0.010	0.043	0.202	0.403	0.035	0.107	0.603	0.912	0.145	0.449	0.726	0.912
TRAT1	0.028	0.087	0.055	0.210	0.003	0.047	0.383	0.912	0.517	0.795	0.724	0.912
XCL1	0.755	0.805	0.659	0.752	0.271	0.385	0.423	0.912	0.536	0.795	0.499	0.854
XCL2	2.4e-04	0.005	0.278	0.463	0.073	0.164	0.432	0.912	0.021	0.267	0.484	0.854
NCR1	0.008	0.037	0.144	0.325	0.095	0.175	0.694	0.912	0.111	0.449	0.186	0.626
KIR2DL3	0.091	0.169	0.078	0.263	0.498	0.589	0.044	0.912	0.336	0.693	0.158	0.626
KIR3DL1	0.005	0.026	0.009	0.093	0.258	0.381	0.923	0.968	0.049	0.357	0.261	0.678
KIR3DL2	0.025	0.082	0.042	0.171	0.020	0.083	0.385	0.912	0.979	0.982	0.671	0.912
IL21R	0.032	0.091	0.013	0.093	0.049	0.127	0.365	0.912	0.283	0.634	0.239	0.675
FPR1	0.726	0.786	0.067	0.241	0.690	0.729	0.068	0.912	0.804	0.886	0.291	0.701
NCAM1	0.005	0.026	0.178	0.385	0.701	0.729	0.364	0.912	0.034	0.316	0.179	0.626
MS4A2	0.002	0.014	0.017	0.113	0.405	0.510	0.734	0.912	0.004	0.200	0.009	0.203
CD84	0.357	0.446	0.095	0.269	0.004	0.047	0.569	0.912	0.888	0.962	0.036	0.293
LAG3	0.245	0.346	0.227	0.433	0.047	0.127	0.343	0.912	0.706	0.846	0.927	0.955
CD19	2.1e-05	0.001	0.042	0.171	0.134	0.229	0.630	0.912	0.012	0.200	0.405	0.823
CD103	0.693	0.763	0.008	0.093	0.257	0.381	0.219	0.912	0.622	0.843	0.009	0.203
ITGB7	0.015	0.052	0.314	0.495	0.028	0.090	0.277	0.912	0.025	0.271	0.156	0.626
KLRB1	1.2e-04	0.004	0.028	0.139	0.006	0.048	0.847	0.947	0.012	0.200	0.322	0.720
CD4	0.057	0.126	0.007	0.093	0.073	0.164	0.598	0.912	0.500	0.795	0.033	0.293
TIM3	0.875	0.903	0.081	0.263	0.019	0.083	0.151	0.912	0.582	0.822	0.498	0.854
PDCD1	0.076	0.160	0.818	0.872	0.013	0.075	0.265	0.912	0.399	0.740	0.816	0.936
GATA3	0.496	0.608	0.367	0.508	0.305	0.421	0.744	0.912	0.691	0.846	0.330	0.720
STAT6	0.561	0.663	0.114	0.296	0.397	0.510	0.525	0.912	0.763	0.885	0.186	0.626
XCR1	0.085	0.167	0.001	0.048	0.512	0.594	0.530	0.912	0.132	0.449	0.003	0.163
CD141	0.258	0.357	0.577	0.708	0.415	0.510	0.472	0.912	0.798	0.886	0.291	0.701
IRF8	0.316	0.402	0.140	0.325	0.097	0.175	0.621	0.912	0.716	0.846	0.254	0.678
CD137	0.088	0.168	0.012	0.093	0.416	0.510	0.422	0.912	0.778	0.886	0.090	0.534
FCGR3A	0.952	0.964	0.272	0.463	0.134	0.229	0.100	0.912	0.635	0.843	0.484	0.854
IL6R	0.238	0.346	0.243	0.450	0.082	0.172	0.953	0.968	0.454	0.795	0.353	0.741
IL10RB	0.244	0.346	0.351	0.495	0.706	0.729	0.729	0.912	0.161	0.455	0.196	0.626
IL12A	0.192	0.297	0.489	0.623	0.898	0.898	0.996	0.996	0.510	0.795	0.744	0.912
IL12B	0.042	0.104	0.703	0.788	0.272	0.385	0.289	0.912	0.532	0.795	0.870	0.954
CD11A	0.034	0.092	0.205	0.403	0.016	0.081	0.701	0.912	0.662	0.846	0.689	0.912
CD11B	0.646	0.737	0.093	0.269	0.089	0.175	0.081	0.912	0.958	0.982	0.090	0.534
CD11C	0.124	0.212	0.398	0.539	0.345	0.458	0.335	0.912	0.177	0.472	0.736	0.912
IDO1	0.040	0.104	0.122	0.304	0.664	0.729	0.233	0.912	0.524	0.795	0.946	0.955
BIN1	0.820	0.860	0.629	0.730	0.340	0.458	0.441	0.912	0.697	0.846	0.707	0.912
IFNG	0.047	0.112	0.787	0.855	0.095	0.175	0.930	0.968	0.141	0.449	0.801	0.936
TNF	0.079	0.160	0.789	0.855	0.015	0.079	0.807	0.937	0.182	0.472	0.675	0.912
RORC	0.102	0.185	0.102	0.275	0.554	0.632	0.111	0.912	0.070	0.449	0.036	0.293
RORA	0.148	0.247	0.009	0.093	0.694	0.729	0.107	0.912	0.338	0.693	0.015	0.209

Table 4.1. (continued). Analysis of significance between gene expression and survival (overall and disease-free) after correcting for false discovery rate (FDR).

Gene	All HNSC				HPV+ HNSC				HPV– HNSC			
	Overall Survival		Disease-free Survival		Overall Survival		Disease-free Survival		Overall Survival		Disease-free Survival	
	p value	FDR	*p* value	FDR	*p* value	FDR	*p* value	FDR	*p* value	FDR	*p* value	FDR
CXCR3	0.002	0.014	0.011	0.093	0.005	0.047	0.664	0.912	0.215	0.537	0.143	0.626
STAT4	0.658	0.738	0.342	0.495	0.685	0.729	0.254	0.912	0.692	0.846	0.202	0.626
CCR5	0.058	0.126	0.145	0.325	0.002	0.047	0.720	0.912	0.579	0.822	0.709	0.912
CCL3	0.532	0.641	0.312	0.495	0.189	0.313	0.395	0.912	0.610	0.843	0.126	0.626
CCL4	0.964	0.964	0.845	0.885	0.043	0.122	0.097	0.912	0.930	0.975	0.556	0.912
CXCL1	0.182	0.288	0.332	0.495	0.096	0.175	0.546	0.912	0.397	0.740	0.332	0.720
CXCR6	0.001	0.014	0.267	0.463	0.007	0.048	0.950	0.968	0.093	0.449	0.955	0.955
CXCL2	0.200	0.303	0.022	0.127	0.020	0.083	0.537	0.912	0.923	0.975	0.112	0.606
TIGIT	0.005	0.026	0.351	0.495	0.027	0.090	0.581	0.912	0.127	0.449	0.726	0.912
CD39	0.011	0.043	0.038	0.171	0.001	0.047	0.649	0.912	0.100	0.449	0.078	0.534
GZMA	0.157	0.255	0.913	0.927	0.218	0.346	0.860	0.947	0.366	0.720	0.821	0.936
GZMB	0.306	0.398	0.624	0.730	0.237	0.366	0.245	0.912	0.135	0.449	0.737	0.912
PRF1	0.052	0.120	0.538	0.672	0.192	0.313	0.909	0.968	0.260	0.625	0.626	0.912
PDL1	0.591	0.686	0.862	0.890	0.430	0.518	0.355	0.912	0.341	0.693	0.457	0.854
IL23A	0.005	0.026	0.027	0.139	0.051	0.127	0.390	0.912	0.097	0.449	0.230	0.675
EBI3	0.266	0.360	0.330	0.495	0.813	0.826	0.800	0.937	0.982	0.982	0.845	0.947

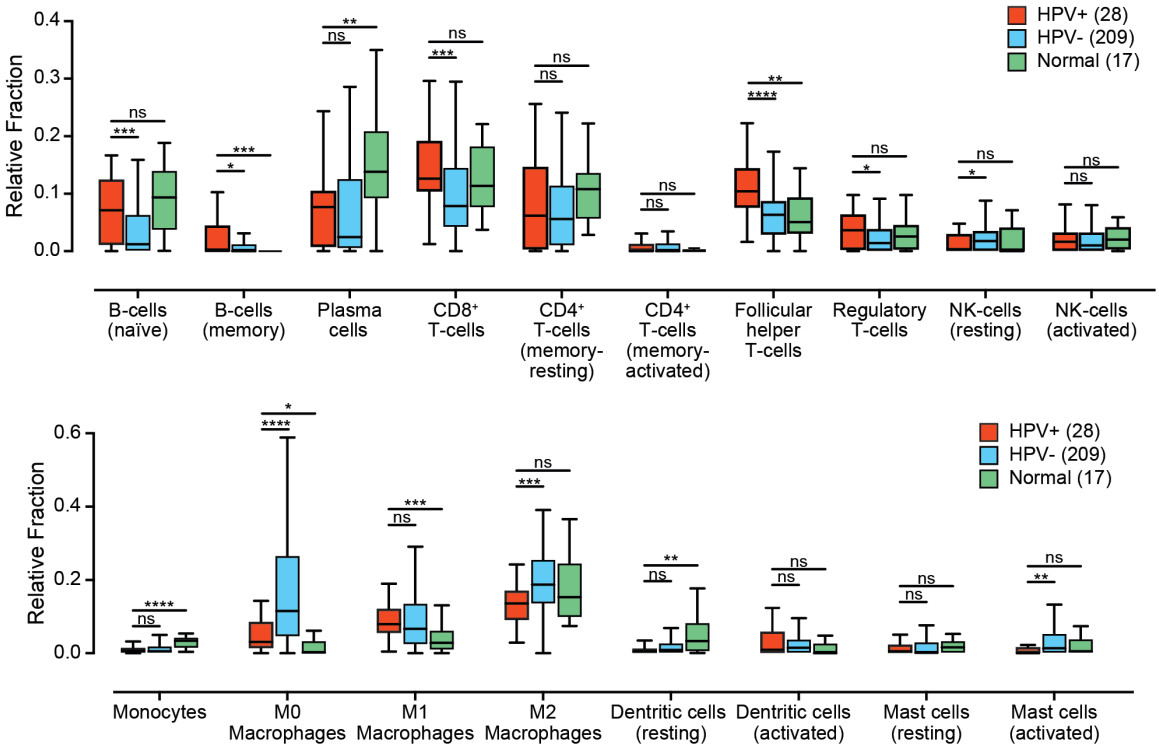

Figure 4.1. The relative fraction of immune cell populations in head & neck carcinomas stratified by HPV status.

The relative population of 22 leukocyte types present in the tumor microenvironment was determined by the CIBERSORT algorithm and compared between HPV+, HPV–, and normal control samples. Four leukocyte types (neutrophils, eosinophils, naïve $CD4^+$ T-cells, and gamma delta T-cells) are not shown, as they were undetectable in this cohort. * $p \leq 0.05$, ** $p \leq 0.01$, *** $p \leq 0.001$, **** $p \leq 0.0001$, ns – not significant.

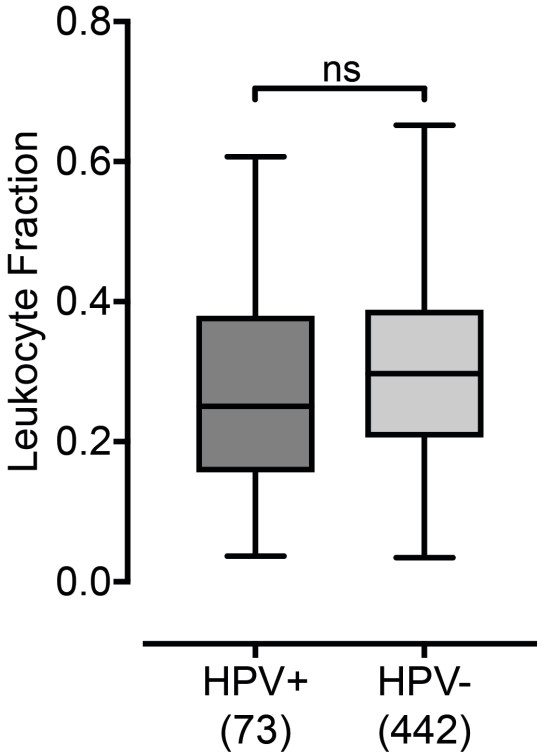

Figure 4.2. No differences in total leukocyte fraction were detected between HPV+ and HPV– HNSC samples.

Total leukocyte fraction as estimated by a DNA methylation signature was extracted for all HNSC samples in the TCGA dataset and annotated for HPV status. Numbers in brackets refer to the number of samples included in each analysis. ns – not significant.

cell phenotypic plasticity can limit the ability of CIBERSORT to accurately characterize immune components of the tumor microenvironment (Newman et al., 2015). Therefore, we began a detailed and mechanistically oriented comparison of the immune responses in HPV+ versus HPV– HNSC. $CD4^+$ helper T-cells are instrumental in establishing the type of response triggered by immune activation, whether it be a cell-mediated Th1 response, a humorally-biased Th2 response, or the proinflammatory Th17 response necessary to maintain the immunological integrity of mucosal barriers (Mucida and Salek-Ardakani, 2009). Each of the $CD4^+$ subsets are characterized by a distinct transcriptional program regulated by specific master regulatory transcription factors (Fang and Zhu, 2017). To examine the tumor immune landscape of HPV+ and HPV– HNSC, we analyzed the TCGA Illumina HiSeq RNA expression data from the HNSC cohort for expression of *TBX21* (Th1), *GATA3* and *STAT6* (Th2), and *RORA* and *RORC* (Th17) (**Figure 4.3**). As expected, a strong Th17 signature was observed in normal control samples, and that signature expression profile was markedly reduced in HPV+ and HPV– carcinomas (**Figure 4.3A**). HPV+ samples had significantly increased levels of *TBX21* as compared to HPV– and normal control samples, indicative of a polarization toward a Th1 response (**Figure 4.3B**). A modest increase in *GATA3* accompanied by a reduction in *STAT6* was observed in HPV+ samples versus normal control samples (**Figure 4.3C**). Taken together, these results indicate that a strong shift in the normal Th17 bias towards Th1 occurred in HNSC, with a significantly accentuated Th1 signature in HPV+ versus HPV– carcinomas.

4.3.3 Higher levels of $CD4^+$ and $CD8^+$ T-cells were present in HPV+ head & neck carcinomas

We next assessed the relative proportion of $CD4^+$ and $CD8^+$ T-cells in these samples, based on relative expression of the lineage defining *CD4* and *CD8A*/*CD8B* marker genes, respectively (**Figures 4.4A and B**). HPV+ samples showed significantly increased expression of all three genes versus HPV– HNSC or normal control samples, confirming that enhanced T-cell infiltration is a common feature of HPV+ HNSC. We also observed significantly higher *FOXP3* expression in HPV+ HNSC compared to HPV– HNSC and normal control samples. *FOXP3* is associated with Tregs infiltrating into these tumor

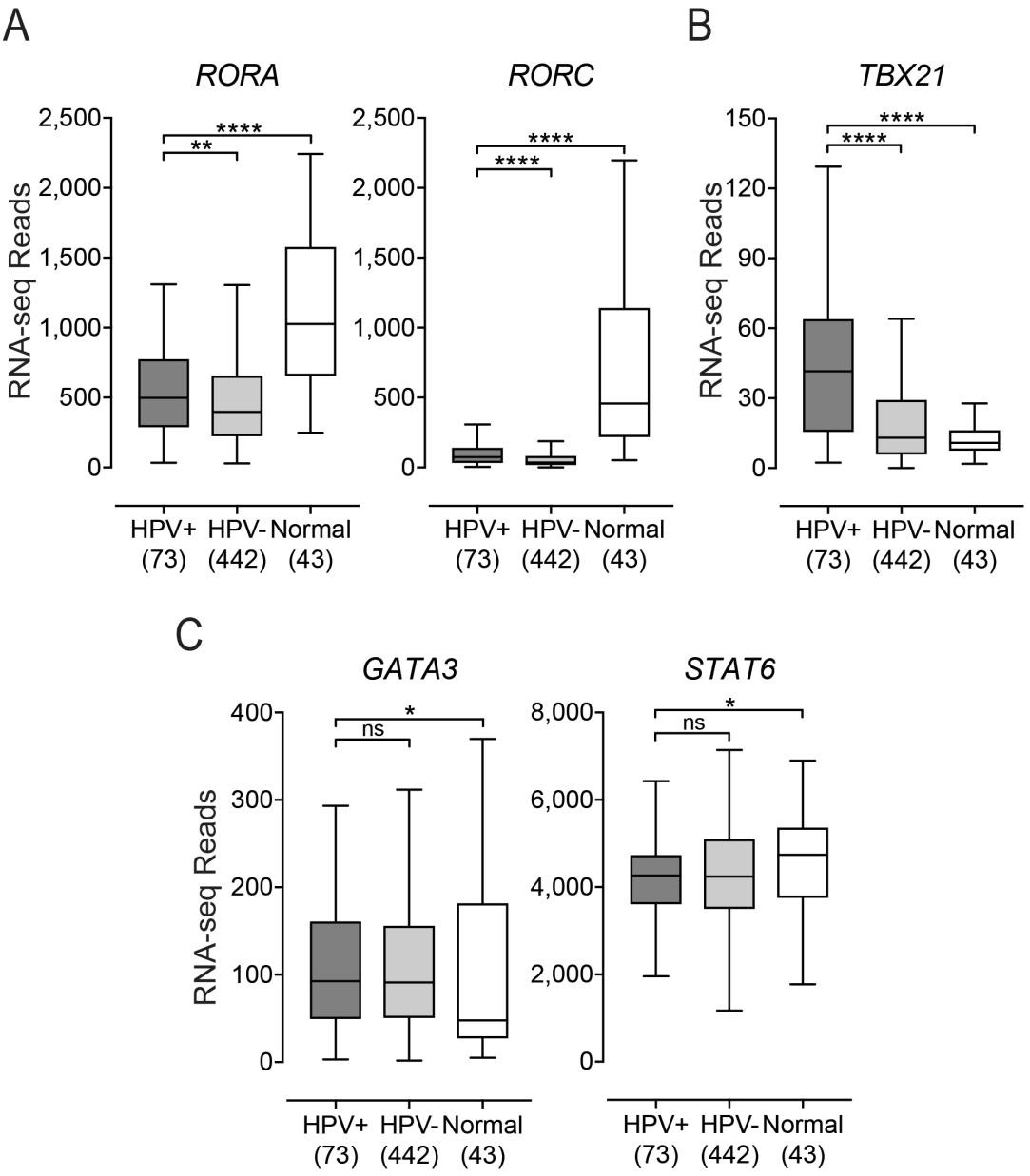

Figure 4.3. Expression of marker genes indicating CD4$^+$ helper T-cell subsets present in head & neck carcinomas stratified by HPV status.

Normalized RNA-seq data for *RORA* and *RORC* (Th17) (**A**), *TBX21* (Th1) (**B**), and *GATA3* and *STAT6* (Th2) (**C**) was extracted from The Cancer Genome Atlas (TCGA) database for the head & neck cancer (HNSC) cohort for HPV+, HPV−, and normal control tissues. Numbers in brackets refer to the number of samples included in each analysis. * $p \leq 0.05$, ** $p \leq 0.01$, **** $p \leq 0.0001$, ns – not significant.

(**Figure 4.4C**). Furthermore, analysis of the expression of *CD137* (4-1BB), an activation-induced costimulatory molecule present primarily on $CD8^+$ T-cells, detected significantly higher levels in HPV+ versus HPV– or normal control samples, suggesting a higher overall level of T-cell activation and effector function in HPV+ disease (**Figure 4.4D**).

Activated cytotoxic $CD8^+$ T-cells produce various effector molecules, including IFNγ and TNF. Although expression of IFNγ mRNA (*IFNG*) in these samples was low, it was detectable at significantly higher levels in HPV+ samples versus HPV– HNSC or normal control tissues. No significant difference was observed for *TNF* (**Figure 4.4E**). HPV+ HNSC tumors also expressed significantly higher levels of cytotoxic mediators, including granzyme A (*GRZA*), granzyme B (*GRZB*), and perforin (*PRF1*) compared to both HPV– HNSC or normal control tissues (**Figure 4.5A**). Taken together, these results indicate $CD8^+$ T-cells are not only present at higher levels in HPV+ HNSC, but are concomitantly more active and producing effector molecules such as IFNγ, granzyme A, granzyme B, and perforin, but not TNF. We also observed low—but significantly higher than in HPV– HNSC or normal control tissues—expression levels of genes associated with natural killer (NK)-cells (*SH2D1A*, *XCL2*, *NCR1*, *KIR2DL3*, *KIR3DL1*, and *KIR3DL2*) and B-cells (*IL21R* and *CD19*) in HPV+ tumors indicating higher infiltration of these immune cells into HPV+ HNSC (**Figures 4.5B and C, respectively**). While many of these observations agree with the CIBERSORT estimations (**Figure 4.1**), there are some differences. In some cases, this may be related to the use of different marker genes, or to the fact that CIBERSORT divides some classes of leukocytes into multiple subcategories based on a gene signature that can be affected by disease dysregulation.

4.3.4 Interferon γ-induced immunomodulatory genes are expressed at higher levels in HPV+ head & neck carcinomas

An expected consequence of higher levels of infiltrating $CD8^+$ T-cells producing IFNγ would be induction of expression of interferon response genes in tumor cells in close proximity to the infiltrating T-cells. Indeed, we previously reported that multiple interferon responsive components of the MHC-I antigen presentation apparatus were upregulated in HPV+ HNSC (Gameiro et al., 2017b). We extended those studies to *PDL1* and *IDO1*, two immunomodulatory genes known to be expressed by tumor cells in response to IFNγ

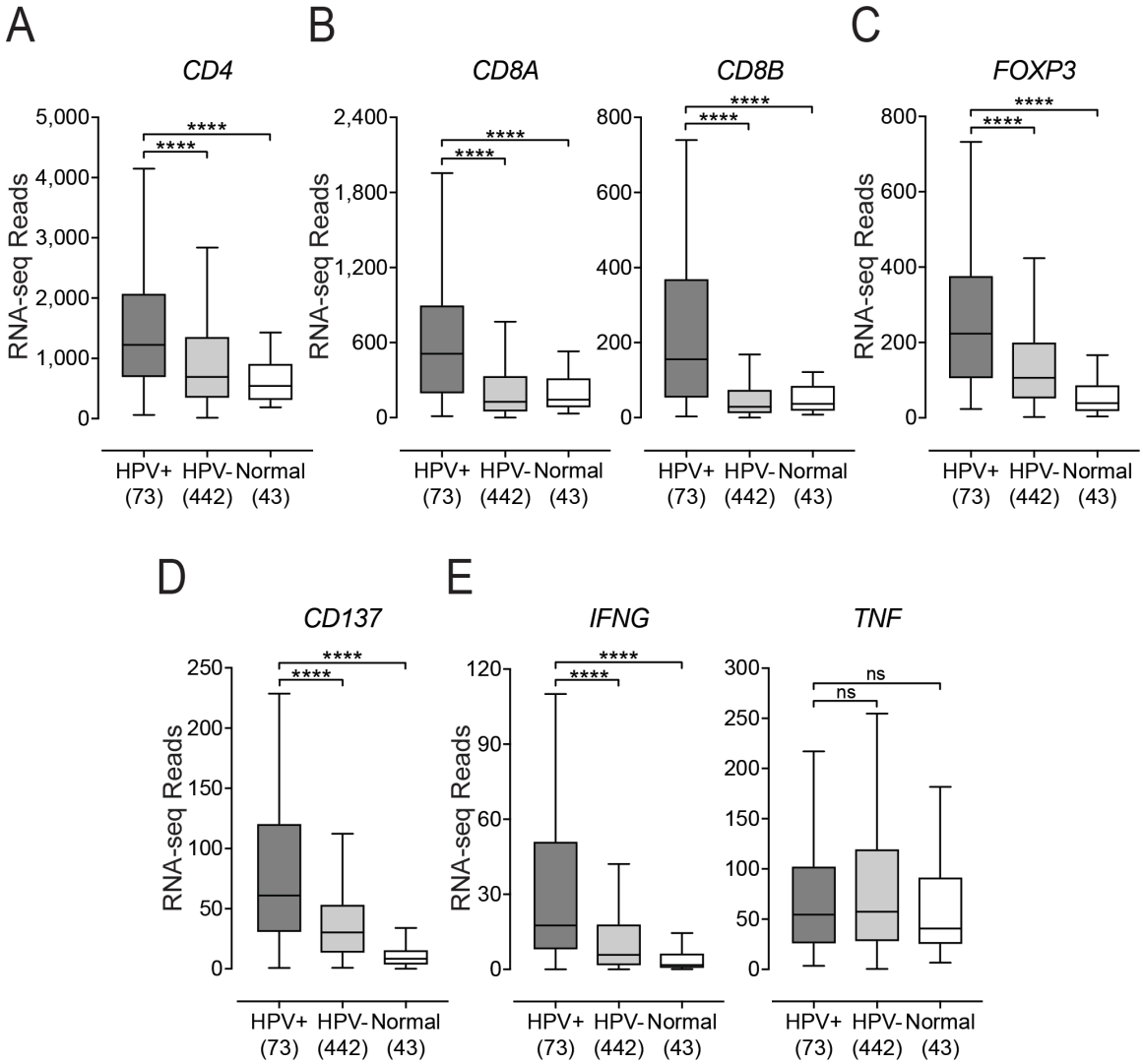

Figure 4.4. Detection of tumor infiltrating T-cells and their activation status in head & neck carcinomas stratified by HPV status.

Normalized RNA-seq data for genes indicative of tumor infiltrating $CD4^+$ (*CD4*) (**A**), $CD8^+$ (*CD8A* and *CD8B*) (**B**), or regulatory (**C**) T-cells and their activation status (*CD137*, *IFNG*, and *TNF*) (**D, E**) was extracted from the TCGA database for the HNSC cohort for HPV+, HPV–, and normal control tissues. Numbers in brackets refer to the number of samples included in each analysis. **** $p \leq 0.0001$, ns – not significant.

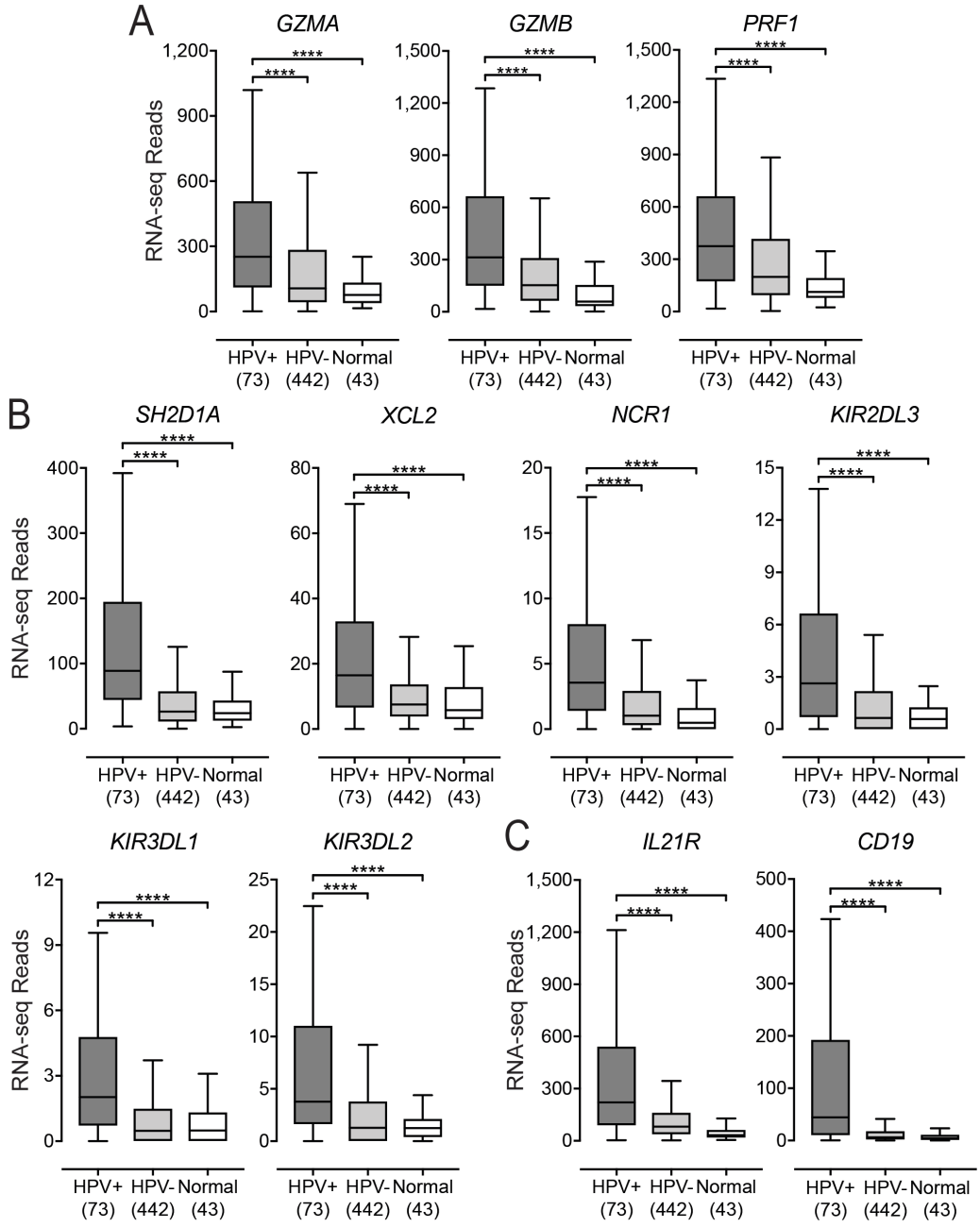

Figure 4.5. Detection of immune effector molecules and tumor-infiltrating NK-cells and B-cells in head & neck carcinomas stratified by HPV status.

Normalized RNA-seq data for genes indicative of tumor infiltrating: Effector molecules (*GZMA*, *GZMB*, and *PRF1*) (**A**), NK-cells (*SH2D1A*, *XCL2*, *NCR1*, *KIR2DL3*, *KIR3DL1*, and *KIR3DL2*) (**B**), and B-cells (*IL21R* and *CD19*) (**C**) was extracted from the TCGA database for the HNSC cohort for HPV+, HPV–, and normal control tissues. Numbers in brackets refer to the number of samples included in each analysis. **** $p \leq 0.0001$.

(**Figure 4.6**). Both *PDL1* and *IDO1* were significantly upregulated in HPV+ HNSC compared to normal control samples. While *IDO1* was also significantly upregulated compared to HPV– HNSC, no significant difference was observed between PDL1 expression in HPV+ versus HPV– carcinomas. Interestingly, *BIN1* expression was significantly downregulated in HPV+ compared to both HPV– HNSC and normal control samples (**Figure 4.6**). As BIN1 is a negative regulator of IDO expression and deletion of BIN1 increases IFNγ stimulation of *IDO1* gene expression, these results are consistent with the higher levels of *IDO1* observed in both HPV+ and HPV– HNSC (Muller et al., 2005). Taken together, these data (**Figures 4.4–4.6**) indicate that HPV+ HNSC, in treatment-naïve patients, shows a T-cell-inflamed phenotype (Gajewski et al., 2013).

4.3.5 Dendritic cell signatures are elevated in HPV+ head & neck carcinomas

Because HPV+ HNSC displayed a T-cell-inflamed phenotype and DCs play a key role as professional antigen-presenting cells to stimulate T-cell function, we performed an analysis of DC signatures in these tumors. Using the expression of mRNA encoding CD103 and CD11C to detect DCs in tumor samples, we found that both genes are expressed at higher levels in HPV+ HNSC compared to normal control samples (**Figure 4.7A**). While *CD103* was expressed at significantly higher levels in HPV+ versus HPV– carcinomas, *CD11C* was not. We also determined that there was a modest but significant correlation between *CD103* and *CD11C* in individual tumors (**Figure 4.7A**; r = 0.56, p = 2.6e-07). This suggested that these markers tended to be coordinately expressed, although the link was not strong enough to lead to increased *CD11C* expression in HPV+ carcinomas in accord with increased *CD103*.

A key anti-tumor role for DCs is to express effector cytokines such as IL12 and IL23 that mediate $CD8^+$ T-cell activation and IFNγ production. While *IL12A* mRNA levels in HPV+ samples were not significantly induced versus normal control tissue, they were elevated compared to HPV– HNSC (**Figure 4.7B**). IL12 activates STAT4 signaling, which is critical for anti-tumor immunity (Lund et al., 2004). Notably, *STAT4* expression levels were higher in HPV+ HNSC tumors (**Figure 4.7B**). Activated DCs also produce IL23—

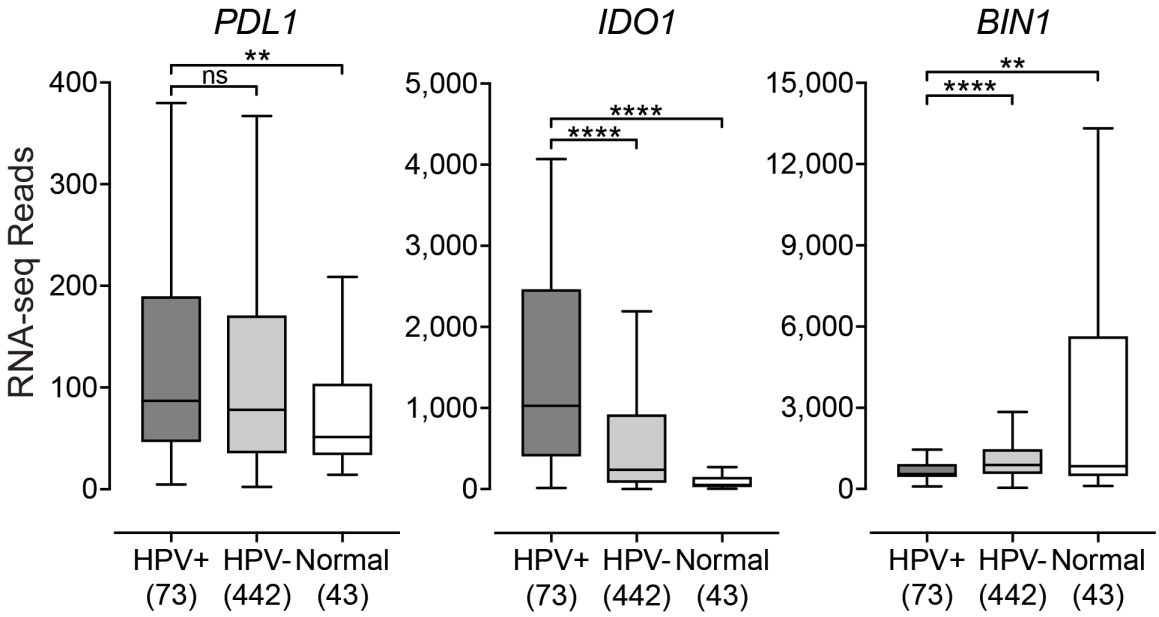

Figure 4.6. Transcript levels of tumor-derived IFNγ-responsive immunomodulatory genes in head & neck carcinomas stratified by HPV status.

Normalized RNA-seq data for genes associated with tumor cell mediated immune-modulation including *IDO1*, its negative regulator *BIN1*, and *PDL1* was extracted from the TCGA database for the HNSC cohort for HPV+, HPV–, and normal control tissues. Numbers in brackets refer to the number of samples included in each analysis. ** $p \leq 0.01$, **** $p \leq 0.0001$, ns – not significant.

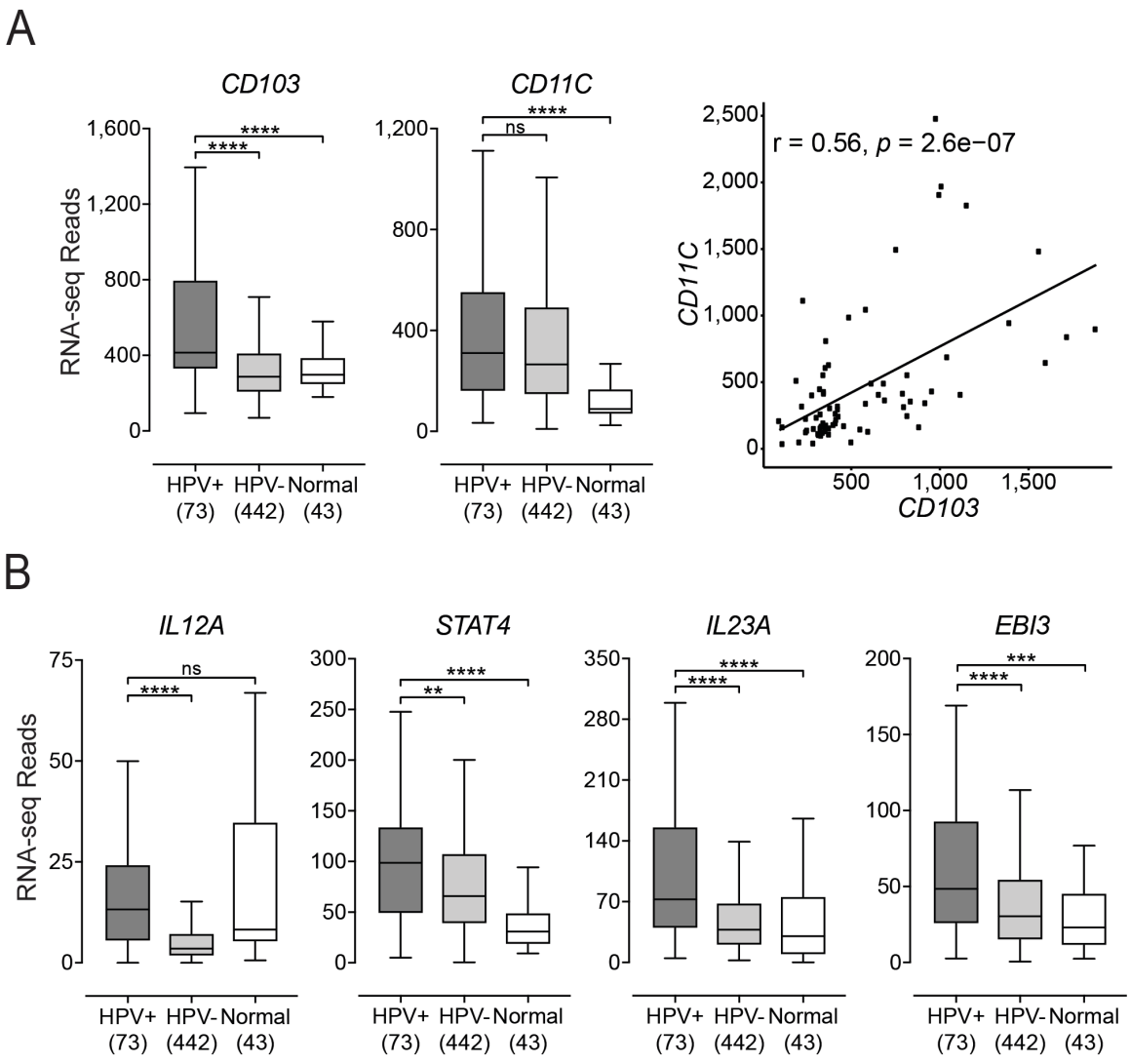

Figure 4.7. Detection of dendritic cells and their effector cytokines in head & neck carcinomas stratified by HPV status.

Normalized RNA-seq data for genes indicative of tumor infiltrating dendritic cells (*CD103* and *CD11C*) (**A**) and genes encoding cytokines indicative of dendritic cell activation status (*IL12A*, *STAT4*, *IL23A*, and *EBI3*) (**B**) was extracted from the TCGA database for the HNSC cohort for HPV+, HPV–, and normal control tissues. Numbers in brackets refer to the number of samples included in each analysis. ** $p \leq 0.01$, *** $p \leq 0.001$, **** $p \leq 0.0001$, ns – not significant.

a proinflammatory cytokine—that induces IFNγ secretion from activated $CD4^+$ T-cells (Shi et al., 2015). *IL23A* levels were higher in HPV+ HNSC than HPV– tumors and normal control samples (**Figure 4.7B**). Moreover, *Epstein-Barr virus-induced gene 3* (*EBI3*) transcripts that encode a component of IL27—a cytokine that synergizes with IL12 and induces IFNγ production by naïve $CD4^+$ T-cells (Pflanz et al., 2002)—were significantly higher in HPV+ than HPV– tumors and normal control samples (**Figure 4.7B**). We were not able to analyze the other two genes within the IL12 family of cytokines—*IL12B* and *IL27A*—because their RNA transcripts were not detectable in the majority of tumor and normal control samples. Finally, we looked at a number of inflammatory chemokines and chemokine receptors that are crucial for DC and T-cell recruitment to tumors (Castellino et al., 2006; Chen et al., 2018a; Mikucki et al., 2016; Mitchell et al., 2015). *CCR5*, *CCL4*, and *CXCR3* were highly expressed in HPV+ HNSC compared to HPV– tumors and normal control samples, while *CCL3* expression was elevated in HPV+ HNSC compared to normal control samples (**Figure 4.8**). Overall, these results indicate a higher level of DC involvement in HPV+ than in HPV– HNSC, with higher levels of effector cytokines that could be responsible for the elevated levels of T-cell infiltration of these samples.

4.3.6 HPV+ head & neck carcinomas expressed high levels of multiple T-cell exhaustion markers

Once activated, T-cells upregulate expression of multiple cell surface receptors that negatively regulate their proliferation and moderate their level of activation. These so-called “exhaustion markers” include LAG3, PD1, TIGIT, and TIM3 (Anderson et al., 2016). They are important targets for immune checkpoint blockade therapies that are approved or under development. Notably, all four of these checkpoint genes were significantly upregulated in HPV+ compared with HPV– HNSC or normal control samples (**Figure 4.9**). We also determined that individual tumors expressing high levels of any one of these T-cell inhibitory genes generally co-expressed high levels of the other exhaustion markers (r values ranging from 0.78 to 0.9), suggesting that these genes are coordinately expressed (**Figure 4.10**). We also examined the expression of the immunosuppressive molecule CD39 (Jie et al., 2013) in this cohort of patients. CD39 was recently shown to be exclusively expressed on tumor antigen-specific $CD8^+$ T-cells and not bystander $CD8^+$

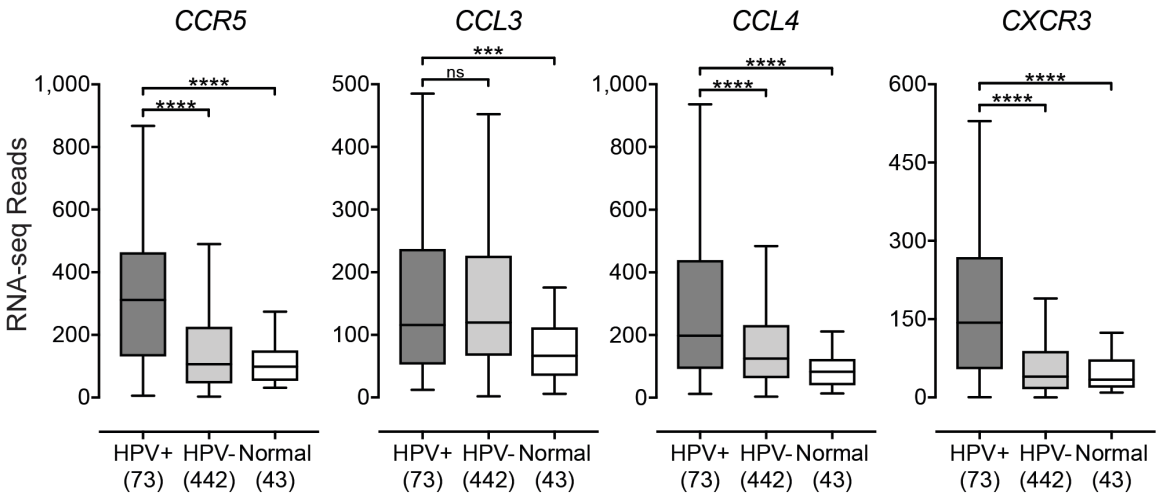

Figure 4.8. Detection of dendritic cell-associated chemokines and receptors in head & neck carcinomas stratified by HPV status.

Normalized RNA-seq data for genes indicative of dendritic cell-associated chemokines and receptors (*CCR5*, *CCL3*, *CCL4*, and *CXCR3*) was extracted from the TCGA database for the HNSC cohort for HPV+, HPV–, and normal control tissues. Numbers in brackets refer to the number of samples included in each analysis. *** $p \leq 0.001$, **** $p \leq 0.0001$, ns – not significant.

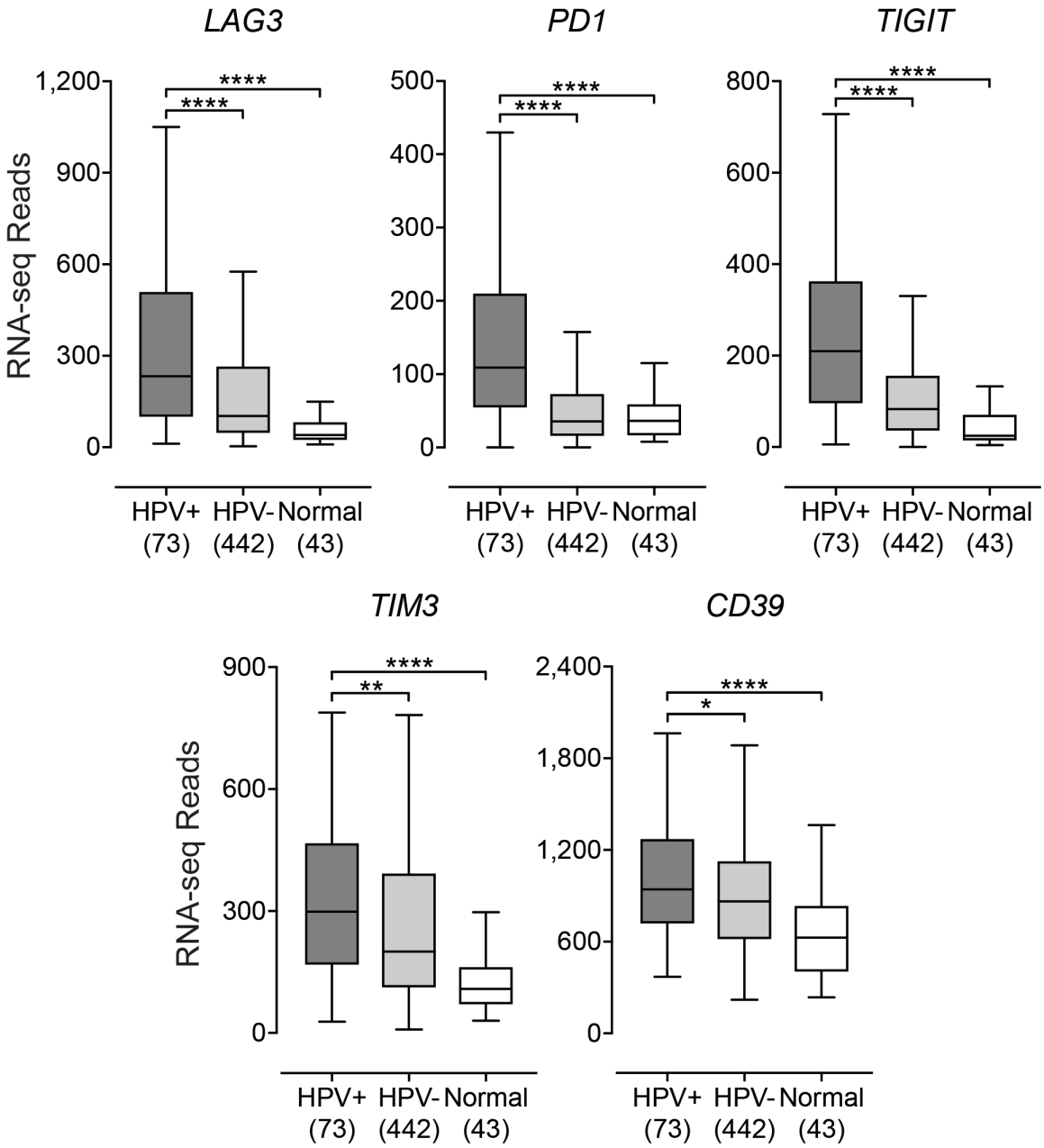

Figure 4.9. Transcript levels of T-cell exhaustion marker genes and *CD39* in head & neck carcinomas stratified by HPV status.

Normalized RNA-seq data for genes associated with T-cell exhaustion (*LAG3*, *PD1*, *TIGIT*, and *TIM3*) and *CD39* was extracted from the TCGA database for the HNSC cohort for HPV+, HPV–, and normal control tissues. Numbers in brackets refer to the number of samples included in each analysis. * $p \leq 0.05$, ** $p \leq 0.01$, **** $p \leq 0.0001$.

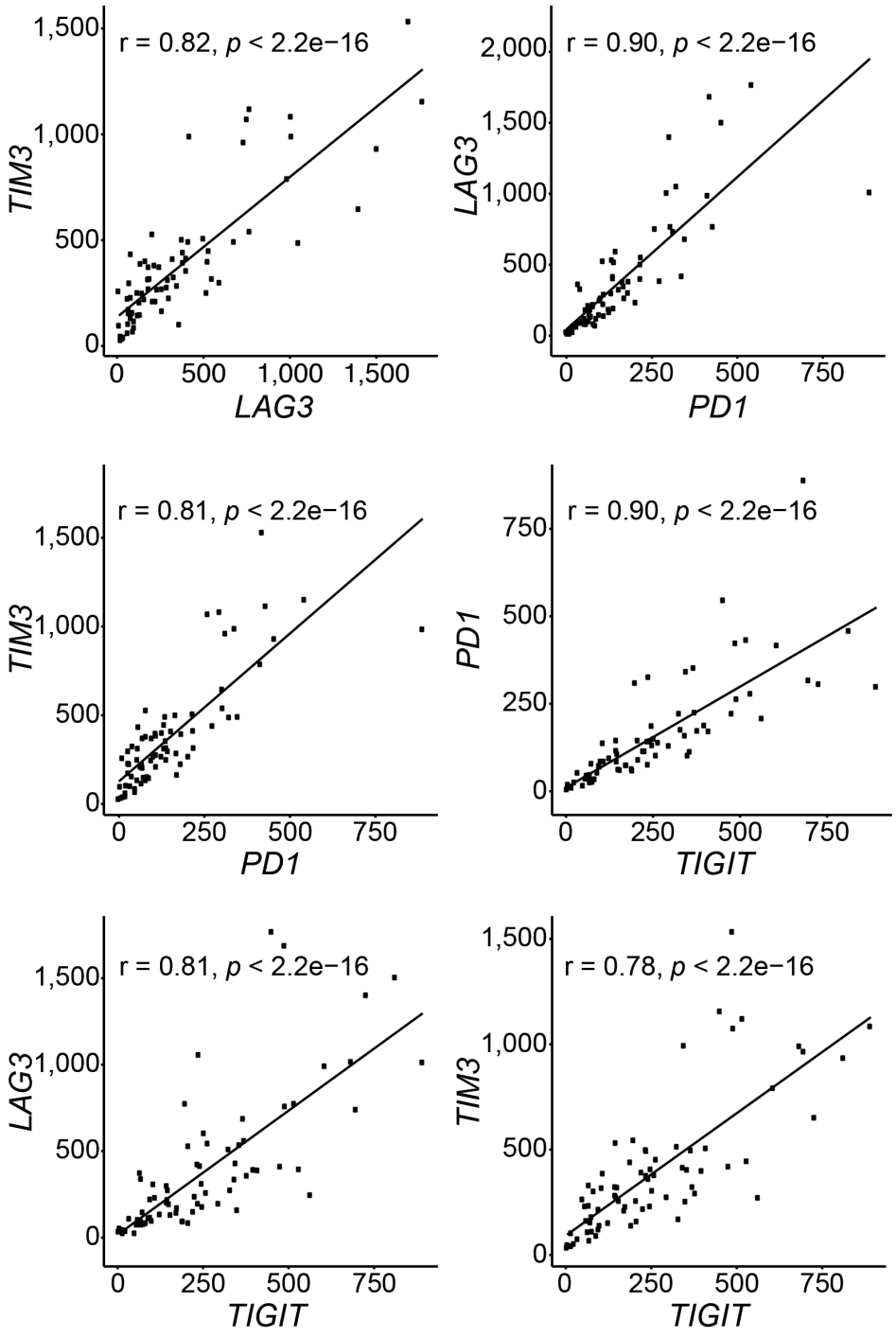

Figure 4.10. HPV+ head & neck carcinomas concordantly express multiple markers of T-cell exhaustion.

Normalized RNA-seq data for *LAG3*, *PD1*, *TIGIT*, and *TIM3* was compared in a pairwise fashion in HPV+ HNSC samples and concordance calculated by Spearman's Rho analysis.

T-cells in colorectal and lung tumors (Simoni et al., 2018). Notably, *CD39* showed significantly higher RNA expression levels in HPV+ HNSC tumors compared to HPV– HNSC samples (**Figure 4.9**). Interestingly, individual tumors expressing high levels of *CD39* also co-expressed high levels of the four exhaustion markers (r values ranging from 0.37 to 0.62), suggesting that these genes are coordinately expressed (**Figure 4.11**). Taken together, HPV+ HNSC display a markedly different immune signature from HPV– HNSC, indicative of sustained $CD8^+$ T-cell activation in HPV+ HNSC.

4.3.7 High levels of T-cell exhaustion markers correlated with improved survival of HPV+ head & neck carcinomas

High $CD8^+$ T-cell infiltration into HNSC tumors has been previously linked to better patient outcome (de Ruiter et al., 2017). Moreover, expression of checkpoint molecules such as PD1 on circulating $CD8^+$ T-cells is a biomarker of tumor antigen specificity (Gros et al., 2016). We therefore dichotomized the HPV+ HNSC data set based on median *LAG3*, *PD1*, *TIGIT*, or *TIM3* expression and calculated the impact of high versus low expression on overall patient survival (**Figure 4.12, black and red curves**). Higher than median expression of any of these genes predicted markedly improved survival in HPV+ HNSC over those patients with tumors expressing these markers at levels below the median. This sharp overall increase in clinical outcome was also statistically significant following correction for multiple testing in all the assessed genes, with the exception of *LAG3* (**Table 4.1**). In contrast, a similar analysis did not reveal any survival advantage for HPV– samples expressing higher levels of *LAG3*, *PD1*, *TIGIT*, or *TIM3* (**Figure 4.12, green and purple curves**).

Given our observation that HPV+ tumors expressing high levels of *LAG3*, *PD1*, *TIGIT*, or *TIM3* transcripts generally displayed higher levels of at least one more of these exhaustion markers (**Figure 4.10**), we repeated the survival analysis by comparing HPV+ HNSC samples that were above the median expression for each combination of two markers to those below the median for both markers (**Figure 4.13, black and red curves**). Remarkably, overall survival for patients with high expression of any combination of two of the T-cell exhaustion markers identified individuals with a virtual certainty of long-term

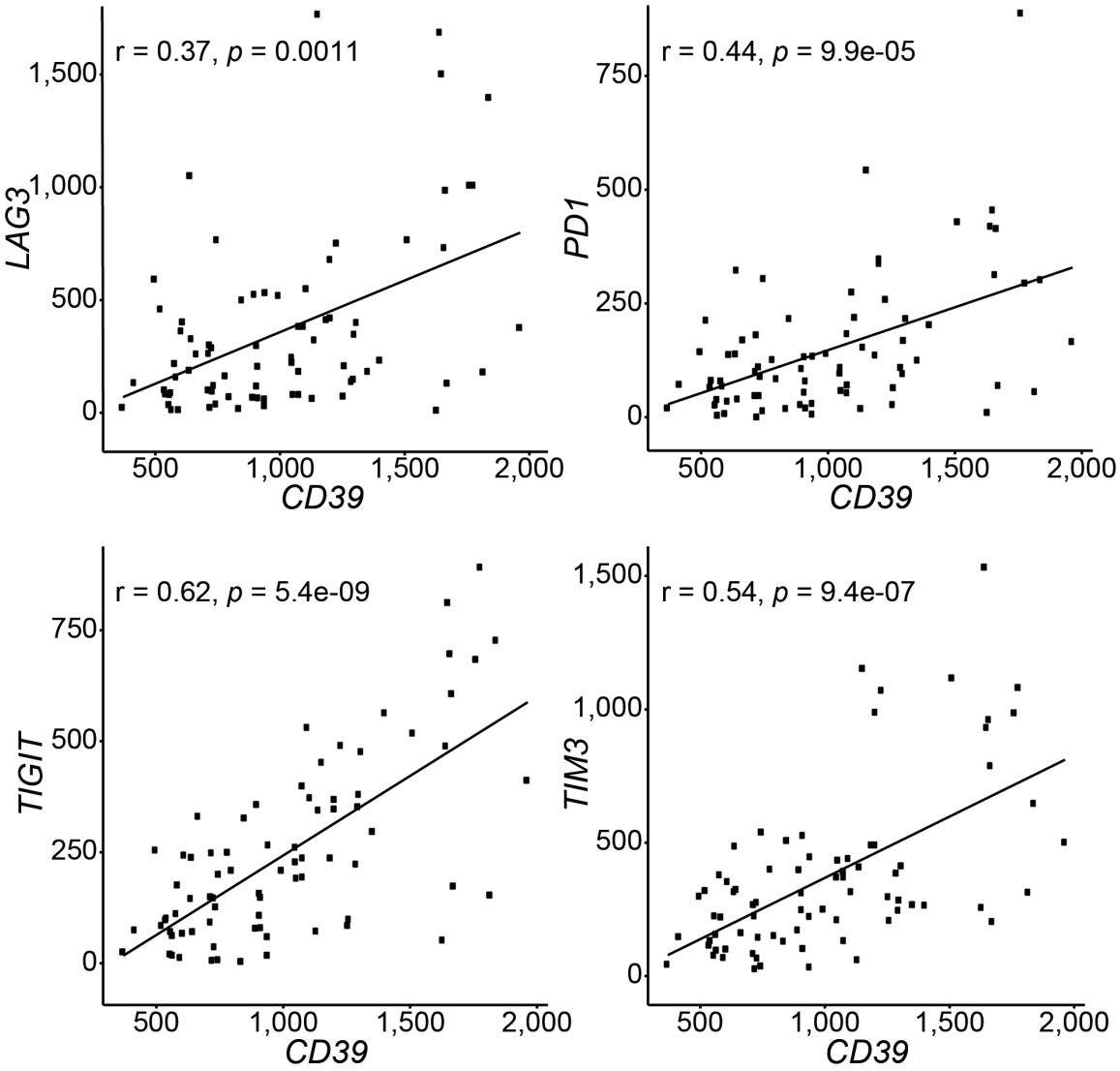

Figure 4.11. HPV+ head & neck carcinomas express *CD39* concordantly with multiple markers of T-cell exhaustion.

Normalized RNA-seq data for *CD39* was compared in a pairwise fashion to *LAG3*, *PD1*, *TIGIT*, and *TIM3* in HPV+ HNSC samples. Concordance was calculated by Spearman's Rho analysis.

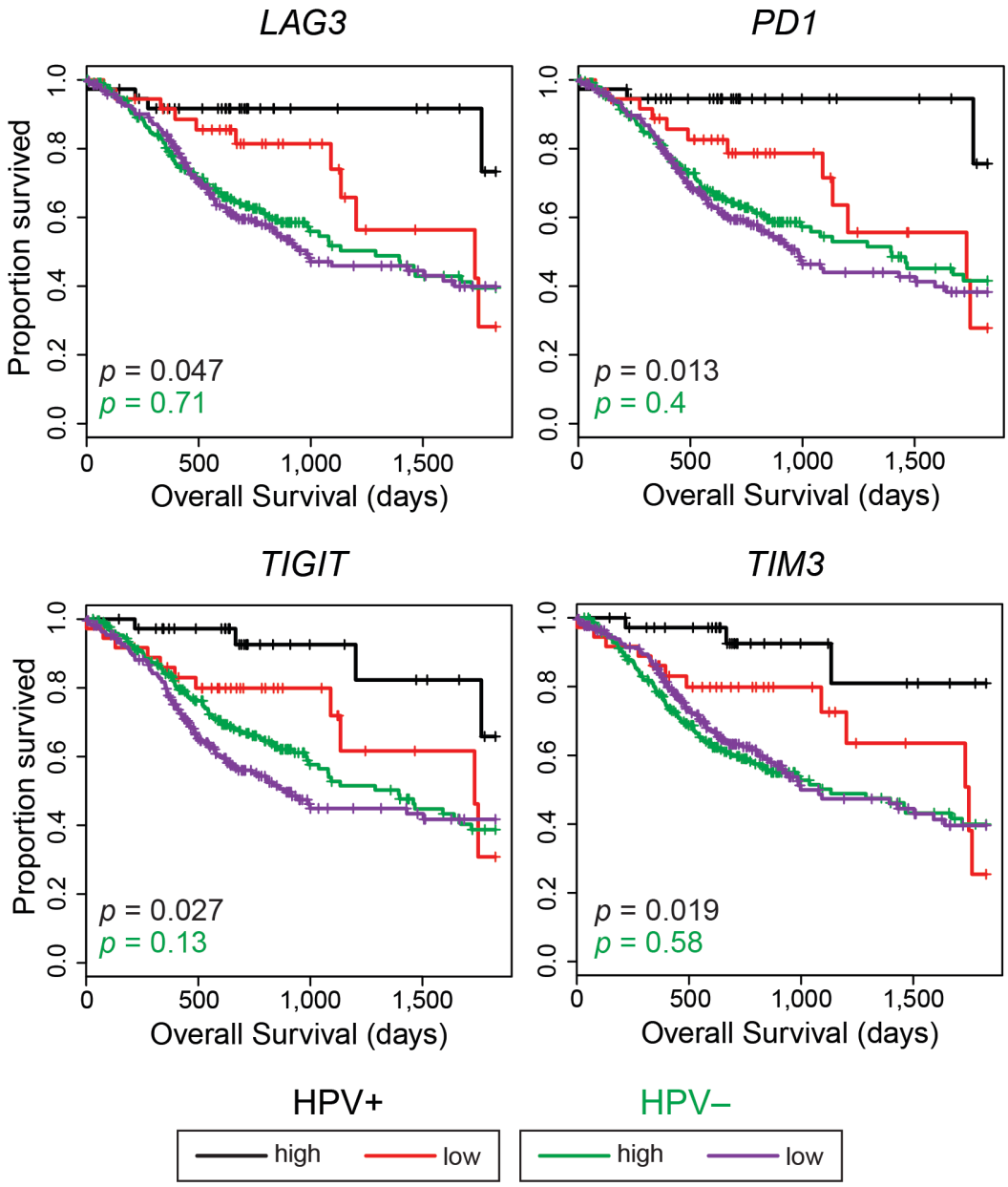

Figure 4.12. High *LAG3*, *PD1*, *TIGIT*, or *TIM3* gene transcript levels are strongly associated with improved survival in treatment naïve patients with HPV+ but not HPV– head & neck carcinomas.

Overall survival of patients within the HPV+ cohort dichotomized by median expression of *LAG3*, *PD1*, *TIGIT*, or *TIM3*. Comparison between groups was made by the 2-sided log-rank test. Red = low expression of the indicated gene in HPV+ samples, Black = high expression of the indicated gene in HPV+ samples, Purple = low expression of the indicated gene in HPV– samples, Green = high expression of the indicated gene in HPV– samples.

Figure 4.13. Concordant levels of multiple markers of T-cell exhaustion is strongly associated with survival in patients with HPV+ head & neck carcinomas.

Overall survival of patients within the HPV+ cohort dichotomized by median transcript levels of the indicated pairs of T-cell exhaustion markers. Comparison between groups was made by the 2-sided log-rank test. Red = low expression of the indicated gene in HPV+ samples, Black = high expression of the indicated gene in HPV + samples, Purple = low expression of the indicated gene in HPV– samples, Green = high expression of the indicated gene in HPV– samples.

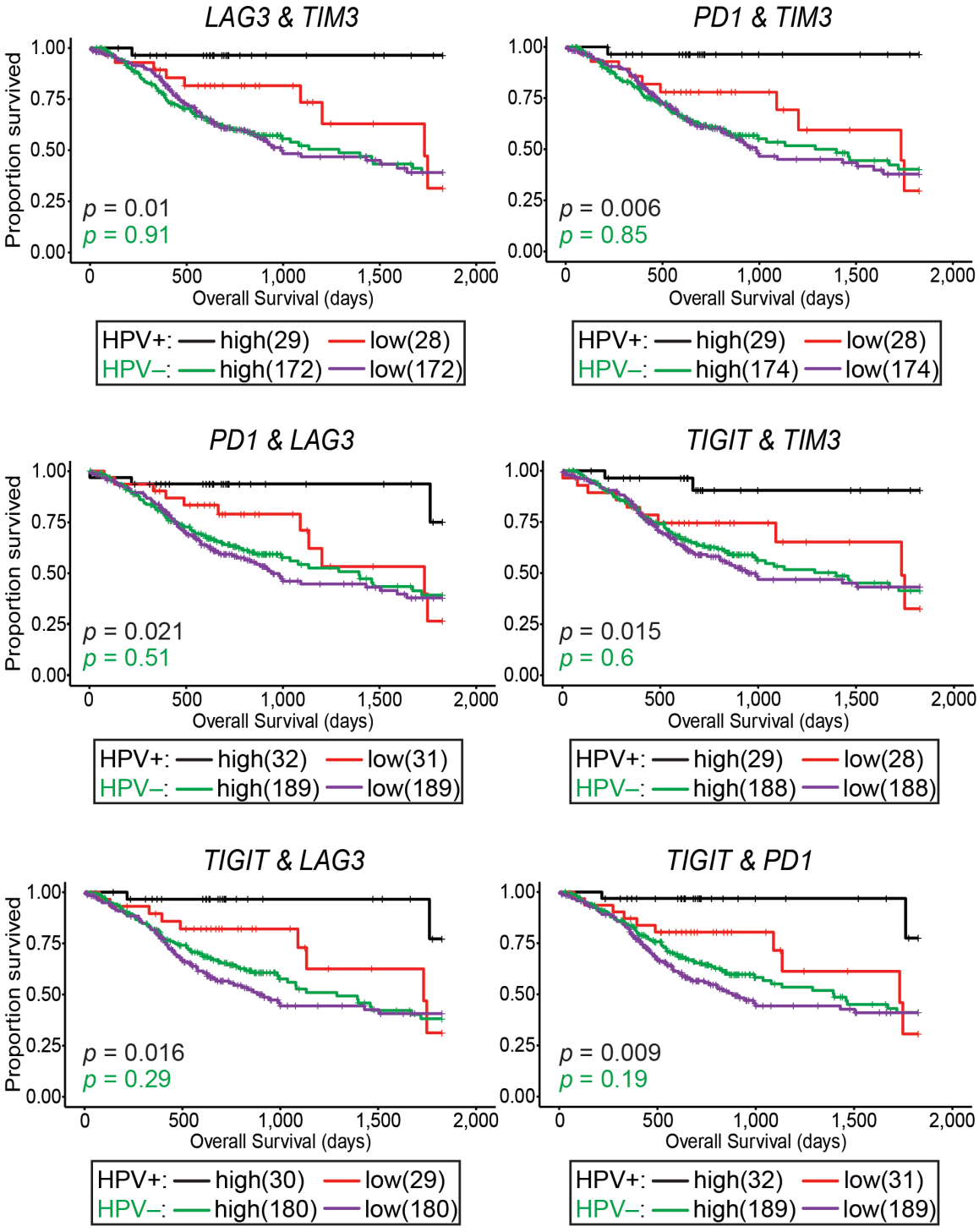
LAG3 & TIM3
Proportion survived
1.00
0.75
0.50
0.25
0.00
p = 0.01
p = 0.91
0
500
1,000
1,500
2,000
Overall Survival (days)
HPV+: high(29) low(28)
HPV–: high(172) low(172)
PD1 & TIM3
p = 0.006
p = 0.85
HPV+: high(29) low(28)
HPV–: high(174) low(174)
PD1 & LAG3
p = 0.021
p = 0.51
HPV+: high(32) low(31)
HPV–: high(189) low(189)
TIGIT & TIM3
p = 0.015
p = 0.6
HPV+: high(29) low(28)
HPV–: high(188) low(188)
TIGIT & LAG3
p = 0.016
p = 0.29
HPV+: high(30) low(29)
HPV–: high(180) low(180)
TIGIT & PD1
p = 0.009
p = 0.19
HPV+: high(32) low(31)
HPV–: high(189) low(189)

survival. No improvement was seen when a similar analysis was performed using the HPV– HNSC cohort (**Figure 4.13, green and purple curves**). These results suggest that the co-expression of high levels of *LAG3*, *PD1*, *TIGIT*, and *TIM3* in HPV+ HNSC reflect the successful development of T-cell-based anti-tumor immunity and a T-cell-inflamed phenotype, which contributed to long-term remission. This immune signature could be used as a predictive biomarker of HPV+ HNSC patient outcome after surgery.

4.3.8 High levels of *CD39* correlated with improved survival of HPV+ head & neck carcinomas

We also dichotomized the HPV+ and HPV– HNSC data set based on median *CD39* expression and calculated the impact of high versus low expression on overall patient survival (**Figure 4.14**). Higher than median expression of *CD39* predicted markedly improved survival in HPV+ HNSC over those patients with tumors expressing this marker at levels below the median. This sharp overall increase in clinical outcome was also statistically significant. Similar to our previous analysis (**Figure 4.13**), a combination of *CD39* and any of the T-cell exhaustion markers identified long-term survivors in HPV+ HNSC (**Figure 4.14**).

We next applied the Cox Proportional Hazards model to identify clinical variables and immunological markers predictive of overall survival (**Table 4.2**). By univariate analysis high expression of *TIGIT*, *TIM3*, *PD1*, and *CD39* were correlated with favorable prognosis (HzR = 0.29, 0.24, 0.22, and 0.15 respectively, $p < 0.05$), while an HPV type other than HPV16 was associated with a markedly poorer survival (HzR = 3.22, $p = 0.03$). Oral cavity tumors had significantly worse survival compared those in the oropharyngeal subsite (HzR = 3.05, $p = 0.03$). There was a trend towards improved outcome with high expression of *LAG3* (HzR = 0.32, $p = 0.06$). Stepwise regression analysis was used to identify the best multivariate model of survival, and the final model included N stage, HPV type, and *CD39*. Notably, *CD39* (HzR = 0.07, $p = 0.0007$), and HPV type (HzR = 9.23, $p = 0.001$) remained as significant predictors of survival in the multivariate model.

Figure 4.14. High *CD39* gene transcript level is strongly associated with improved survival in treatment naïve patients with HPV+ head & neck carcinomas.

Overall survival of patients within the HPV+ and HPV– cohorts were dichotomized by median expression of *CD39* (**A**). Concordant levels of *CD39* and multiple markers of T-cell exhaustion was strongly associated with survival in patients with HPV+ head & neck carcinomas (**B**). Overall survival of patients within the HPV+ cohort dichotomized by median transcript levels of the indicated pairs of T-cell exhaustion markers with *CD39*. Comparison between groups was made by the 2-sided log-rank test. Red = low expression of the indicated gene in HPV+ samples, Black = high expression of the indicated gene in HPV+ samples, Purple = low expression of the indicated gene in HPV– samples, Green = high expression of the indicated gene in HPV– samples.

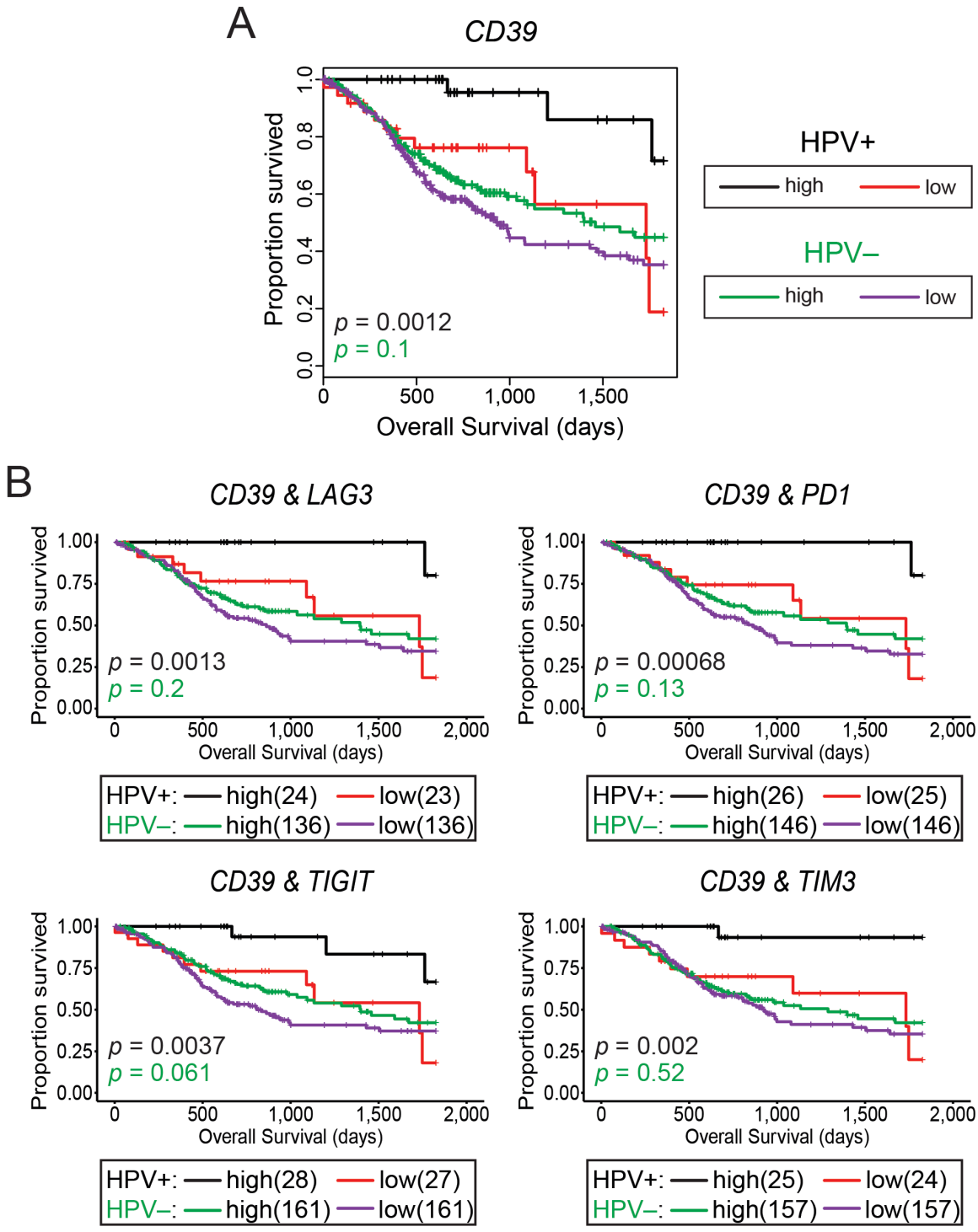
A
CD39
Proportion survived
1.0
0.8
0.6
0.4
0.2
0.0
p = 0.0012
p = 0.1
0
500
1,000
1,500
Overall Survival (days)
HPV+
high
low
HPV–
high
low
B
CD39 & LAG3
Proportion survived
1.00
0.75
0.50
0.25
0.00
p = 0.0013
p = 0.2
0
500
1,000
1,500
2,000
Overall Survival (days)
HPV+: high(24) low(23)
HPV–: high(136) low(136)
CD39 & PD1
Proportion survived
1.00
0.75
0.50
0.25
0.00
p = 0.00068
p = 0.13
0
500
1,000
1,500
2,000
Overall Survival (days)
HPV+: high(26) low(25)
HPV–: high(146) low(146)
CD39 & TIGIT
Proportion survived
1.00
0.75
0.50
0.25
0.00
p = 0.0037
p = 0.061
0
500
1,000
1,500
2,000
Overall Survival (days)
HPV+: high(28) low(27)
HPV–: high(161) low(161)
CD39 & TIM3
Proportion survived
1.00
0.75
0.50
0.25
0.00
p = 0.002
p = 0.52
0
500
1,000
1,500
2,000
Overall Survival (days)
HPV+: high(25) low(24)
HPV–: high(157) low(157)

Table 4.2. Univariate and multivariate analysis of the association of clinical characteristics and *LAG3*, *PD1*, *TIGIT*, *TIM3*, and *CD39* expression and overall survival in HPV+ HNSC.

Variables		Univariate Analysis		Multivariate Analysis	
		HzR (95% CI)	*p* value	HzR (95% CI)	*p* value
Sex	Male vs Female	0.95 (0.21 – 4.29)	0.95		
Age	per every additional year	0.99 (0.94 – 1.05)	0.77		
Smoking	Light vs Non-Smoker	0.84 (0.16 – 4.39)	0.84		
	Heavy vs Non-Smoker	1.99 (0.54 – 7.38)	0.30		
Subsite	Oral cavity vs Oropharynx	3.05 (1.09 – 8.49)	**0.03**		
	Larynx vs Oropharynx	1.46e-08 (0 – Inf)	Inf		
	Hypopharynx vs Oropharynx	1.57e-08 (0 – Inf)	Inf		
T Stage	T3-4 vs T1-2	1.06 (0.37 – 2.99)	0.92		
N Stage	N2b-N3 vs N0-N2a	0.35 (0.12 – 1.05)	0.06	0.24 (0.08 – 0.81)	**0.02**
Overall Stage	IV vs I-III	0.80 (0.27 – 2.36)	0.69		
HPV Type	Other vs 16	3.22 (1.10 – 9.45)	**0.03**	9.23 (2.45 – 34.7)	**0.001**
LAG3	High vs Low Expression	0.32 (0.10 – 1.04)	0.06		
PD1	High vs Low Expression	0.22 (0.06 – 0.81)	**0.02**		
TIGIT	High vs Low Expression	0.29 (0.09 – 0.93)	**0.04**		
TIM3	High vs Low Expression	0.24 (0.07 – 0.87)	**0.03**		
CD39	High vs Low Expression	0.15 (0.04 – 0.56)	**0.004**	0.07 (0.02 – 0.34)	**0.0007**

4.4 Discussion

Although evading anticancer immunity is one of the hallmarks of cancer, immunotherapy—also referred to as immuno-oncology—harnesses the power of the immune system to destroy cancer cells. Durable responses to immunotherapy among cancer patients are what sets immunotherapy apart from conventional oncology therapies, including chemotherapy, radiotherapy, and targeted therapy. Cancer immunotherapy is now widely recognized as having the potential to revolutionize cancer treatment. Despite the recent "tsunami of immunotherapy in oncology" and many reports of immunotherapy treatment resulting in near-miraculous cures in cases of highly refractory cancers, in general only a subset of patients respond to these treatments. The underlying reasons for response, or lack thereof, remain an intense area of investigation (Routy et al., 2018).

Based on their somatic mutation prevalence (Sadelain et al., 2017), tumors can be categorized as immunologically "cold" or immunologically "hot". Immunologically hot tumors such as melanoma and smoking-induced lung cancer, often respond more favorably to immune checkpoint inhibition therapy than cold tumors. Therefore, a partial explanation for immune checkpoint inhibitor response appears to be related to high mutation burden, which leads to higher levels of tumor-derived neoantigens. Indeed, a significant correlation exists between immune checkpoint inhibitor response and mutational load across cancer sites (Yarchoan et al., 2017).

A variety of studies have compared various immunological parameters between HPV+ and HPV– HNSC and generally concluded that HPV+ HNSC are immune "hot" tumors, with markedly more immune infiltration and higher levels of $CD8^+$ T-cell activation than HPV– HNSC (Chen et al., 2018b; Keck et al., 2015; Mandal et al., 2016; Solomon et al., 2018). Although this is thought to contribute to the improved prognosis of HPV+ HNSC, the mutational loads in HPV+ and HPV– HNSC are similar therefore the immune hot and cold model cannot explain the survival differences observed among HNSC patients. However, HPV+, but not HPV–, HNSC express exogenous antigenic viral oncoproteins that may represent a key difference in the tumor immune landscape between these two types of HNSC, giving HPV+ HNSC a T-cell-inflamed phenotype that can at least partially explain

the better patient outcome in HPV+ HNSC compared to HPV– HNSC. Furthermore, HPV+ HNSC tumors are different from HPV– HNSC tumors at the epigenetic and genomic levels, but viral etiology alone may not be sufficient to confer favorable outcome in HNSC (Chakravarthy et al., 2016). Therefore, the substantial differences observed in anti-tumor immunity between HPV+ and HPV– cancers could be the major source of improved prognosis in HPV+ tumors.

In this study, for the first time, we report the detailed immune characteristics of T-cell-inflamed HPV+ HNSC compared to non-T-cell-inflamed HPV– HNSC. We performed a mechanistic analysis of the tumor immune landscape in treatment-naïve HNSC using the TCGA cohort, which allows a detailed and direct comparison between HPV+ and HPV– HNSC and normal-adjacent control tissue. However, examination of only the RNA expression levels limits the ability to accurately confirm expression levels on each cell type. To address this limitation, we primarily used immune lineage-specific markers or examined co-expression correlations for markers that are expressed by more than one cell type. We found that HPV+ HNSC has a predominant Th1 immune phenotype (**Figure 4.3**) with a significant increase in $CD8^+$ and $CD4^+$ T-cell infiltration compared to HPV– HNSC (**Figure 4.4**). Interestingly, higher T-cell infiltration into HPV+ tumors was accompanied with greater T-cell activation, as shown by high *CD137* (4-1BB) gene transcript levels.

Mononuclear cells isolated from patients with advanced head and neck cancer have been reported to be defective in IFNγ production *in vitro* (Conti-Freitas et al., 2012). Given the high *CD137* RNA levels in HPV+ HNSC samples, we expected higher effector cytokine production by T-cells in these samples. Indeed, HPV+ HNSC expressed significantly higher levels of IFNγ, granzyme A, granzyme B, and perforin compared to HPV– HNSC or normal control samples, indicating that there remains some T-cell effector functionality in these tumors. Moreover, the higher levels of *CD137* and multiple effector molecules in HPV+ HNSC could be a consequence of higher infiltration of these tumors with antigen-specific tumor-infiltrating lymphocytes (TILs). In contrast, we did not observe differences in TNF transcript levels—a critical cytokine for anti-tumor immunity (Calzascia et al., 2007)—between HPV+ and HPV– HNSC, indicating T-cell dysfunction in these samples. Given the role of IFNγ in inducing MHC-I expression in tumor cells, these findings explain

our previous observation that HPV+ HNSC tumors had significantly higher levels of expression of MHC-I apparatus (Gameiro et al., 2017b). Furthermore, high IFNγ transcript levels in HPV+ HNSC were associated with significantly higher levels of IFN-responsive gene transcripts, including *IDO* and *PD-L1* (**Figure 4.6**). These observations provide a scientific rationale for combining immunotherapy of HPV+ HNSC with ICIs and IDO inhibitors in treatment-naïve patients. Currently the only phase II study of such a combination (NCT03325465) has been canceled in light of the recent failure of combined IDO inhibition and pembrolizumab in showing advantage in progression-free survival over pembrolizumab monotherapy in melanoma patients. However, that study (NCT03325465) was not focused specifically on HPV+ HNSC, which we show here express higher levels of IDO compared to HPV– HNSC.

The observed increased numbers of $CD8^+$ and $CD4^+$ T-cells in HPV+ HNSC can likely be explained by the ability of DCs to migrate to these tumors, pick up antigens, and present those antigens to T-cells (Spranger et al., 2015). Indeed, we observed not only high levels of transcripts from DC-associated genes, but also molecules expressed by activated DCs, including chemokines that attract DCs and T-cells into tumors (**Figure 4.7 and Figure 4.8**). We also observed less M2 macrophages in HPV+ HNSC samples (**Figure 4.1**) indicative of less immunosuppressive activity in these tumors compared to HPV– HNSC. These observations provide a mechanistic insight into the processes that shape the immune structure of HPV+ HNSC as a T-cell-inflamed tumor.

T-cell-inflamed tumors show high levels of immune regulatory genes including *IDO* and *PD-L1*, and high infiltration of FoxP3+ Tregs (Gajewski et al., 2017), secondary to cytotoxic T-cell infiltration into those tumors. The presence of these immunosuppressive events in a T-cell-inflamed microenvironment is often accompanied by increased levels of multiple T-cell immune checkpoint molecules and T-cell anergy (Gajewski et al., 2017). Our findings show that HPV+ HNSC, but not HPV– HNSC, have similarly high levels of multiple immune checkpoint molecules (*LAG3*, *TIM3*, *PD1*, and *TIGIT*; **Figure 4.9**), suggesting that combined immunotherapy with drugs that target more than one of these inhibitory molecules can be effective in overcoming resistance to anti-tumor immunity in HPV+ HNSC tumors. There are no such trials currently under way, but these findings

strongly indicate that initiation of such clinical studies is justified. CD39 is an immunosuppressive molecule that can be expressed on intratumoral Tregs (Jie et al., 2013) and tumor-specific $CD8^+$ TILs, but not bystander $CD8^+$ T-cells (Simoni et al., 2018). *CD39* RNA expression was higher in both HPV+ and HPV– HNSC tumors compared to normal control samples (**Figure 4.9**). Of note, *CD39* expression in HPV+ HNSC was significantly higher than HPV– tumors. *CD39* alone or in combination with any of the T-cell exhaustion markers analyzed above was also a predictive biomarker of survival in HPV+ HNSC (**Figure 4.14**). Therefore, *CD39* may represent a useful biomarker of survival in HPV+ HNSC. Our findings warrant the initiation of prospective trials in determining the predictive value of this gene as a potential genomic biomarker correlated with improved overall survival in HPV+ HNSC.

High T-cell infiltration into HNSC, regardless of HPV status, has been reported as a positive prognostic factor (Nguyen et al., 2016). We observed that high levels of transcripts from one or any combination of two genes expressing immune checkpoint molecules (*PD1*, *TIM3*, *TIGIT*, *LAG3*) in HPV+, but not HPV–, HNSC can predict patient survival after surgery. These findings require confirmation by prospective clinical studies to—we anticipate—pave the way for the development of immune-predictive biomarkers for HPV+ HNSC patients that will ultimately lead to treatment deintensification in this patient population.

Taken together, this study provides clear evidence, for the first time, that the immune landscape of HPV+ HNSC represents a T-cell-inflamed phenotype that is very different from HPV– HNSC. Of prime importance, we demonstrate that multiple mechanisms that negatively regulate the anti-tumor immune response are significantly upregulated in the majority of HPV+ HNSC cases, that is secondary to $CD8^+$ T-cell infiltration and IFNγ production in HPV+ HNSC. Therefore, high levels of such gene transcripts—*PD1*, *TIM3*, *LAG3*, and *TIGIT*—correlate strongly with improved clinical outcome. Crucially, many of these negative regulators of the immune response are targets of clinically-approved immune checkpoint inhibitors or inhibitors under investigation in current clinical trials. Thus, HPV+ HNSC has many immunological features that suggest that it would be highly amenable to immune checkpoint inhibition therapy. Based on these data, we propose that

HPV+ HNSC is a T-cell-inflamed disease and should be treated differently in the clinic than HPV– HNSC, specifically with combinations of immune checkpoint inhibitors.

4.5 References

Anderson AC, Joller N and Kuchroo VK. (2016) Lag-3, Tim-3, and TIGIT: Co-inhibitory Receptors with Specialized Functions in Immune Regulation. *Immunity* 44: 989-1004.

Ang KK, Harris J, Wheeler R, et al. (2010) Human papillomavirus and survival of patients with oropharyngeal cancer. *N Engl J Med* 363: 24-35.

Baxi S, Fury M, Ganly I, et al. (2012) Ten years of progress in head and neck cancers. *J Natl Compr Canc Netw* 10: 806-810.

Calzascia T, Pellegrini M, Hall H, et al. (2007) TNF-alpha is critical for antitumor but not antiviral T cell immunity in mice. *J Clin Invest* 117: 3833-3845.

Castellino F, Huang AY, Altan-Bonnet G, et al. (2006) Chemokines enhance immunity by guiding naive CD8+ T cells to sites of CD4+ T cell-dendritic cell interaction. *Nature* 440: 890-895.

Chakravarthy A, Henderson S, Thirdborough SM, et al. (2016) Human Papillomavirus Drives Tumor Development Throughout the Head and Neck: Improved Prognosis Is Associated With an Immune Response Largely Restricted to the Oropharynx. *J Clin Oncol* 34: 4132-4141.

Chen F, Yin S, Niu L, et al. (2018a) Expression of the Chemokine Receptor CXCR3 Correlates with Dendritic Cell Recruitment and Prognosis in Gastric Cancer. *Genet Test Mol Biomarkers* 22: 35-42.

Chen X, Yan B, Lou H, et al. (2018b) Immunological network analysis in HPV associated head and neck squamous cancer and implications for disease prognosis. *Mol Immunol* 96: 28-36.

Conti-Freitas LC, Foss-Freitas MC, Mamede RC, et al. (2012) Interferon-gamma and interleukin-10 production by mononuclear cells from patients with advanced head and neck cancer. *Clinics (Sao Paulo)* 67: 587-590.

de Ruiter EJ, Ooft ML, Devriese LA, et al. (2017) The prognostic role of tumor infiltrating T-lymphocytes in squamous cell carcinoma of the head and neck: A systematic review and meta-analysis. *Oncoimmunology* 6: e1356148.

Del Paggio JC. (2018) Immunotherapy: Cancer immunotherapy and the value of cure. *Nat Rev Clin Oncol* 15: 268-270.

Fakhry C, Westra WH, Li S, et al. (2008) Improved survival of patients with human papillomavirus-positive head and neck squamous cell carcinoma in a prospective clinical trial. *J Natl Cancer Inst* 100: 261-269.

Fang D and Zhu J. (2017) Dynamic balance between master transcription factors determines the fates and functions of CD4 T cell and innate lymphoid cell subsets. *J Exp Med* 214: 1861-1876.

Feng Z, Bethmann D, Kappler M, et al. (2017) Multiparametric immune profiling in HPV-oral squamous cell cancer. *JCI insight* 2: 93652.

Ferlay J, Shin HR, Bray F, et al. (2010) Estimates of worldwide burden of cancer in 2008: GLOBOCAN 2008. *Int J Cancer* 127: 2893-2917.

Gajewski TF, Corrales L, Williams J, et al. (2017) Cancer Immunotherapy Targets Based on Understanding the T Cell-Inflamed Versus Non-T Cell-Inflamed Tumor Microenvironment. *Adv Exp Med Biol* 1036: 19-31.

Gajewski TF, Schreiber H and Fu YX. (2013) Innate and adaptive immune cells in the tumor microenvironment. *Nat Immunol* 14: 1014-1022.

Gameiro SF, Kolendowski B, Zhang A, et al. (2017a) Human papillomavirus dysregulates the cellular apparatus controlling the methylation status of H3K27 in different human cancers to consistently alter gene expression regardless of tissue of origin. *Oncotarget* 8: 72564-72576.

Gameiro SF, Zhang A, Ghasemi F, et al. (2017b) Analysis of Class I Major Histocompatibility Complex Gene Transcription in Human Tumors Caused by Human Papillomavirus Infection. *Viruses* 9: 252.

Gros A, Parkhurst MR, Tran E, et al. (2016) Prospective identification of neoantigen-specific lymphocytes in the peripheral blood of melanoma patients. *Nat Med* 22: 433-438.

Hoadley KA, Yau C, Hinoue T, et al. (2018) Cell-of-Origin Patterns Dominate the Molecular Classification of 10,000 Tumors from 33 Types of Cancer. *Cell* 173: 291-304.

Jie HB, Gildener-Leapman N, Li J, et al. (2013) Intratumoral regulatory T cells upregulate immunosuppressive molecules in head and neck cancer patients. *Br J Cancer* 109: 2629-2635.

Keck MK, Zuo Z, Khattri A, et al. (2015) Integrative analysis of head and neck cancer identifies two biologically distinct HPV and three non-HPV subtypes. *Clin Cancer Res* 21: 870-881.

Lund RJ, Chen Z, Scheinin J, et al. (2004) Early target genes of IL-12 and STAT4 signaling in th cells. *J Immunol* 172: 6775-6782.

Lyford-Pike S, Peng S, Young GD, et al. (2013) Evidence for a role of the PD-1:PD-L1 pathway in immune resistance of HPV-associated head and neck squamous cell carcinoma. *Cancer Res* 73: 1733-1741.

Mandal R, Senbabaoglu Y, Desrichard A, et al. (2016) The head and neck cancer immune landscape and its immunotherapeutic implications. *JCI insight* 1: e89829.

Marur S, D'Souza G, Westra WH, et al. (2010) HPV-associated head and neck cancer: a virus-related cancer epidemic. *Lancet Oncol* 11: 781-789.

Mikucki ME, Skitzki JJ, Frelinger JG, et al. (2016) Unlocking tumor vascular barriers with CXCR3: Implications for cancer immunotherapy. *Oncoimmunology* 5: e1116675.

Mitchell DA, Batich KA, Gunn MD, et al. (2015) Tetanus toxoid and CCL3 improve dendritic cell vaccines in mice and glioblastoma patients. *Nature* 519: 366-369.

Mittal S and Banks L. (2017) Molecular mechanisms underlying human papillomavirus E6 and E7 oncoprotein-induced cell transformation. *Mutat Res Rev Mutat Res* 772: 23-35.

Montler R, Bell RB, Thalhofer C, et al. (2016) OX40, PD-1 and CTLA-4 are selectively expressed on tumor-infiltrating T cells in head and neck cancer. *Clin Transl Immunology* 5: e70.

Mucida D and Salek-Ardakani S. (2009) Regulation of TH17 cells in the mucosal surfaces. *J Allergy Clin Immunol* 123: 997-1003.

Muller AJ, DuHadaway JB, Donover PS, et al. (2005) Inhibition of indoleamine 2,3-dioxygenase, an immunoregulatory target of the cancer suppression gene Bin1, potentiates cancer chemotherapy. *Nat Med* 11: 312-319.

Network TCGAR. (2015) Comprehensive genomic characterization of head and neck squamous cell carcinomas. *Nature* 517: 576-582.

Newman AM, Liu CL, Green MR, et al. (2015) Robust enumeration of cell subsets from tissue expression profiles. *Nat Methods* 12: 453-457.

Nguyen N, Bellile E, Thomas D, et al. (2016) Tumor infiltrating lymphocytes and survival in patients with head and neck squamous cell carcinoma. *Head Neck* 38: 1074-1084.

Nichols AC, Palma DA, Dhaliwal SS, et al. (2013) The epidemic of human papillomavirus and oropharyngeal cancer in a Canadian population. *Curr Oncol* 20: 212-219.

Pardoll DM. (2012) The blockade of immune checkpoints in cancer immunotherapy. *Nat Rev Cancer* 12: 252-264.

Pflanz S, Timans JC, Cheung J, et al. (2002) IL-27, a heterodimeric cytokine composed of EBI3 and p28 protein, induces proliferation of naive CD4+ T cells. *Immunity* 16: 779-790.

Routy B, Le Chatelier E, Derosa L, et al. (2018) Gut microbiome influences efficacy of PD-1-based immunotherapy against epithelial tumors. *Science* 359: 91-97.

Sadelain M, Riviere I and Riddell S. (2017) Therapeutic T cell engineering. *Nature* 545: 423-431.

Shi Q, Yin Z, Zhao B, et al. (2015) PGE2 Elevates IL-23 Production in Human Dendritic Cells via a cAMP Dependent Pathway. *Mediators Inflamm* 2015: 984690.

Simoni Y, Becht E, Fehlings M, et al. (2018) Bystander CD8(+) T cells are abundant and phenotypically distinct in human tumour infiltrates. *Nature* 557: 575-579.

Solomon B, Young RJ, Bressel M, et al. (2018) Prognostic Significance of PD-L1(+) and CD8(+) Immune Cells in HPV(+) Oropharyngeal Squamous Cell Carcinoma. *Cancer Immunol Res* 6: 295-304.

Spranger S, Bao R and Gajewski TF. (2015) Melanoma-intrinsic beta-catenin signalling prevents anti-tumour immunity. *Nature* 523: 231-235.

Thorsson V, Gibbs DL, Brown SD, et al. (2018) The Immune Landscape of Cancer. *Immunity* 48: 812-830.

Topalian SL, Drake CG and Pardoll DM. (2015) Immune checkpoint blockade: a common denominator approach to cancer therapy. *Cancer Cell* 27: 450-461.

Yarchoan M, Hopkins A and Jaffee EM. (2017) Tumor Mutational Burden and Response Rate to PD-1 Inhibition. *N Engl J Med* 377: 2500-2501.

Chapter 5

5 High Level Expression of MHC-II in HPV+ Head and Neck Cancers Suggests that Tumor Epithelial Cells Serve an Important Role as Accessory Antigen Presenting Cells

5.1 Introduction

High-risk human papillomaviruses (HPVs) are small, non-enveloped, double-stranded DNA viruses that are responsible for an estimated 5% of all human cancers (Doorbar et al., 2015; Forman et al., 2012). These biological carcinogens are the causative agents of virtually all cervical cancers and a subset of head and neck squamous cell carcinomas (HNSC) (Doorbar et al., 2015). HNSC are a heterogenous group of malignancies caused by multiple distinct etiologies. Infection with high-risk HPVs is responsible for approximately 85,000 of the 600,000 global annual cases of HNSC, making it the second most common cause of HPV-induced cancers (Gillison et al., 2014; Gillison et al., 2000; Syrjanen, 2005). HPV-positive (HPV+) tumors are distinct from their HPV-negative (HPV−) counterparts from a molecular perspective, with distinct genetic, epigenetic, and protein expression profiles (Gameiro et al., 2018; Gameiro et al., 2017a; Gameiro et al., 2017b; Seiwert et al., 2015; Sepiashvili et al., 2015; Worsham et al., 2013). Interestingly, patients with HPV+ HNSC tumors have markedly better clinical outcomes compared to those with HPV− tumors, leading to the recognition of HPV+ HNSC as unique clinical entities (Ang et al., 2010; Fakhry et al., 2008; Psyrri et al., 2014).

We and others have noted significant differences in the immune landscape between the tumor microenvironments of HPV+ and HPV− HNSC (Baruah et al., 2019; Chen et al., 2018; Gameiro et al., 2018; Gameiro et al., 2017b; Mandal et al., 2016; Nguyen et al., 2016; Solomon et al., 2018). Specifically, HPV+ tumors express higher levels of class I major histocompatibility complex (MHC-I) compared to their HPV− counterparts, which could be a consequence of the higher intratumoral levels of interferon-gamma (IFNγ) observed in the tumors of the HPV+ cohort (Gameiro et al., 2017b). Utilizing an

immunogenomic approach, we have also shown that HPV+ HNSC tumors exhibited a strong Th1 response characterized by increased infiltration with multiple types of T-cells—$CD4^+$, $CD8^+$, and regulatory T-cells—and expression of their effector molecules (Gameiro et al., 2018). In addition, HPV+ HNSC also expressed higher levels of *CD39* and multiple T-cell exhaustion markers including *LAG3*, *PD1*, *TIGIT*, and *TIM3* compared to HPV− HNSC. Importantly, patients with higher expression of these exhaustion markers—indicative of a T-cell-inflamed tumor—exhibited markedly improved survival in HPV+, but not HPV−, HNSC (Gameiro et al., 2018).

In order for an effective T-cell-specific anti-tumor response to occur, a tumor associated antigen must be presented in either the context of MHC-I or class II MHC (MHC-II) (Rock et al., 2016). This process is dependent on the initial acquisition of specific antigenic peptides by surveilling antigen presenting cells (APCs). APCs present these exogenous peptides on their cell surface in the context of major histocompatibility complex-II (MHC-II) to activate cognate $CD4^+$ helper T-cells in an antigen-specific fashion (Roche and Furuta, 2015). This crosslinking of T-cell receptor (TCR) with its cognate antigen-MHC-II complex is the initial step in the activation of T-cells. The next step is the crosslinking of co-stimulatory molecules between T-cell and APCs that will provide the appropriate signals to initiate T-cell proliferation and survival (Chen and Flies, 2013). Once activated, $CD4^+$ T-cells then stimulate the proliferation of $CD8^+$ cytotoxic T-cells (CTLs) that recognize and respond to the initial antigenic peptide. CTLs subsequently target tumor cells for lysis based on presentation of the cognate endogenously derived antigenic peptides on the tumor cell surface in the context of MHC-I (Luckheeram et al., 2012; Zhang and Bevan, 2011).

Although the ability of HPV to suppress MHC-I expression in cell culture systems is well known (Ferris, 2015; Heller et al., 2011), this is not likely the case in actual human tumors. Indeed, we previously reported that HPV+ head and neck cancers express higher levels of MHC-I than HPV− tumors (Gameiro et al., 2017b). Thus, HPV+ tumor cells may be more effective at displaying endogenously derived viral or neo-antigenic peptides, making them more easily targeted for CTL lysis. Expression of MHC-II molecules is typically restricted to professional APCs, such as dendritic cells (DCs), macrophages, and B-cells (van den

Elsen et al., 2004). However, epithelial cells can be stimulated by proinflammatory cytokines—specifically IFNγ—to express MHC-II and function as accessory APCs to stimulate T-cell responses (Boss and Jensen, 2003; Collins et al., 1984; Kim et al., 2009). As mentioned above, MHC-II proteins play a key role in presenting exogenously-derived peptide antigens that ultimately lead to an effective CTL response, and it is likely that the induced tumor-specific MHC-II expression on epithelial cells may accentuate this process. Indeed, the role of tumor cell-derived MHC-II in anti-tumor immunity has become increasingly appreciated (Axelrod et al., 2019), with accumulating evidence suggesting that tumor-specific MHC-II expression is correlated with favorable outcomes in melanoma, classic Hodgkin's lymphoma, breast cancer, and oropharyngeal cancers (Axelrod et al., 2019; Cioni et al., 2019; Forero et al., 2016; Johnson et al., 2016; Roemer et al., 2018).

In this study, we used RNA-seq data from over 500 human head and neck tumors from The Cancer Genome Atlas (TCGA) to determine if the presence of oncogenic HPV is associated with altered expression of all classical MHC-II genes and other key genes involved in their regulation, antigen presentation, and T-cell co-stimulation. We found that expression of virtually all classical MHC-II genes was significantly upregulated in HPV+ tumors compared to their HPV− counterparts or normal control tissue. Similarly, genes that encode products that are fundamental to proper antigen loading and presentation were also significantly upregulated in HPV+ tumors. Importantly, the relative level of expression of these inducible MHC-II genes was far beyond those genes associated with professional APCs. Furthermore, the expression of *class II major histocompatibility complex transactivator* (*CIITA*) and *regulatory factor X5* (*RFX5*)—essential master regulators of the MHC-II transcriptional control system—were significantly upregulated in the HPV+ cohort. This coordinated upregulation of the mRNA levels of genes involved in the MHC-II antigen presentation pathway and their regulation were correlated with the higher intratumoral levels of IFNγ observed in HPV+ carcinomas. In addition, genes that encode various T-cell co-stimulatory molecules involved in T-cell activation and survival were found to be significantly upregulated in HPV+ tumors compared to HPV− tumors and normal control tissue. Taken together, these results suggest a previously unappreciated role

for epithelial cells in antigen presentation that functionally contributes to the highly immunogenic tumor microenvironment observed in HPV+ HNSC. This further illustrates the profound differences in the immune landscape between the tumor microenvironments of HPV+ and HPV− HNSC and may in part contribute to the superior clinical outcomes that are associated with HPV+ HNSC.

5.2 Materials and Methods

5.2.1 TCGA RNA-seq boxplot comparisons

Level 3 RNA-Seq by Expectation Maximization (RSEM)-normalized Illumina HiSeq RNA expression data for the TCGA head and neck cancer (HNSC) cohort was downloaded from the Broad Genome Data Analysis Centers Firehose server (https://gdac.broadinstitute.org/). The normalized, gene level Firehose dataset was utilized for all the genes analyzed. RSEM-normalized RNA-Seq data was extracted into Microsoft Excel and the HPV status was determined based on published datasets (Banister et al., 2017; Bratman et al., 2016; The Cancer Genome Atlas Research Network, 2015; The Cancer Genome Atlas Research Network, 2017). For all genes analyzed in this study, patient samples from primary tumors with known HPV status were grouped as HPV+, HPV−, or normal control samples. Patient samples with undetermined HPV status or samples from secondary metastatic lesions were omitted from our calculations. This resulted in 73 HPV+, 442 HPV−, and 43 normal control samples with RNA-Seq data available for gene expression analysis. Oropharynx-only gene reanalysis was performed by utilizing patient samples that were isolated from the tissues of the oropharynx (tonsils, base of tongue, or oropharynx) for both HPV+ and HPV− samples. This resulted in 53 HPV+ and 26 HPV− samples with RNA-Seq data available for gene expression analysis. Graphpad Prism v7.0 (Graphpad Software, Inc., San Diego, California, USA) was used to generate boxplot comparisons of gene expression between the indicated HPV+, HPV−, and normal control samples as well as the oropharynx-only reanalysis between HPV+ and HPV− samples. For each boxplot, the center line indicates the median, the lower and upper box limits represent Q1 (25th percentile) and Q3 (75th percentile), respectively, and the whiskers extend 1.5 times the interquartile range (IQR) from Q1 (lower whisker) and Q3 (upper whisker). An unpaired, two-tailed non-parametric Mann–Whitney U test was

utilized to assign *p*-values. G*Power Software version 3.1.9.2 (Faul et al., 2007) was used to perform post-hoc power calculations, with effect size selected as 0.8 and α = 0.05. All boxplot comparisons achieved a power value > 0.8. Figures were assembled into final form using Adobe Illustrator CS6.

5.2.2 Correlation matrix

Level 3 RSEM-normalized RNA-seq data for the genes listed above were extracted from the TCGA database and processed as detailed above. For the HPV+ (upper triangle) and HPV− samples (lower triangle), pairwise spearman correlation was performed for each gene involved in the MHC-II transcriptional control system. Hierarchical clustering was utilized to group genes based on strength of correlation. Correlations and clustering were performed using R statistical environment (version 3.4.0) utilizing packages ggplot2 and reshape2. Correlation matrix figure was assembled into final form using Adobe Illustrator.

5.3 Results

5.3.1 Classical MHC class II α- and β-chain genes are expressed at higher levels in HPV+ head & neck carcinomas

Constitutive expression of classical MHC-II molecules is typically restricted to professional antigen presenting cells—DCs, macrophages, and B-cells (van den Elsen et al., 2004). However, in non-immune cells that lack constitutive expression, such as those of the epithelia, their expression can be induced through exposure to proinflammatory cytokines (Boss and Jensen, 2003; Collins et al., 1984; Steimle et al., 1994). In humans, the genes that encode the three classical polymorphic MHC-II molecules HLA-DP, HLA-DQ, and HLA-DR are expressed as α- and β-chains that form heterodimers on the cell surface (van den Elsen et al., 2004). We began by analyzing the Illumina HiSeq RNA expression data from the TCGA HNSC cohort for expression of *HLA-DPA1*, *-DPB1*, *-DQA1*, *-DQA2*, *-DQB1*, *-DQB2*, *-DRA*, *-DRB1*, *-DRB5*, and *-DRB6* genes, encoding the various α- and β-chains for all three classical isotypes (**Figure 5.1**). Uniformly, all HPV+ patient samples expressed significantly higher levels of mRNA for all 10 MHC-II genes analyzed compared to HPV− patient samples and virtually all normal control tissues—with

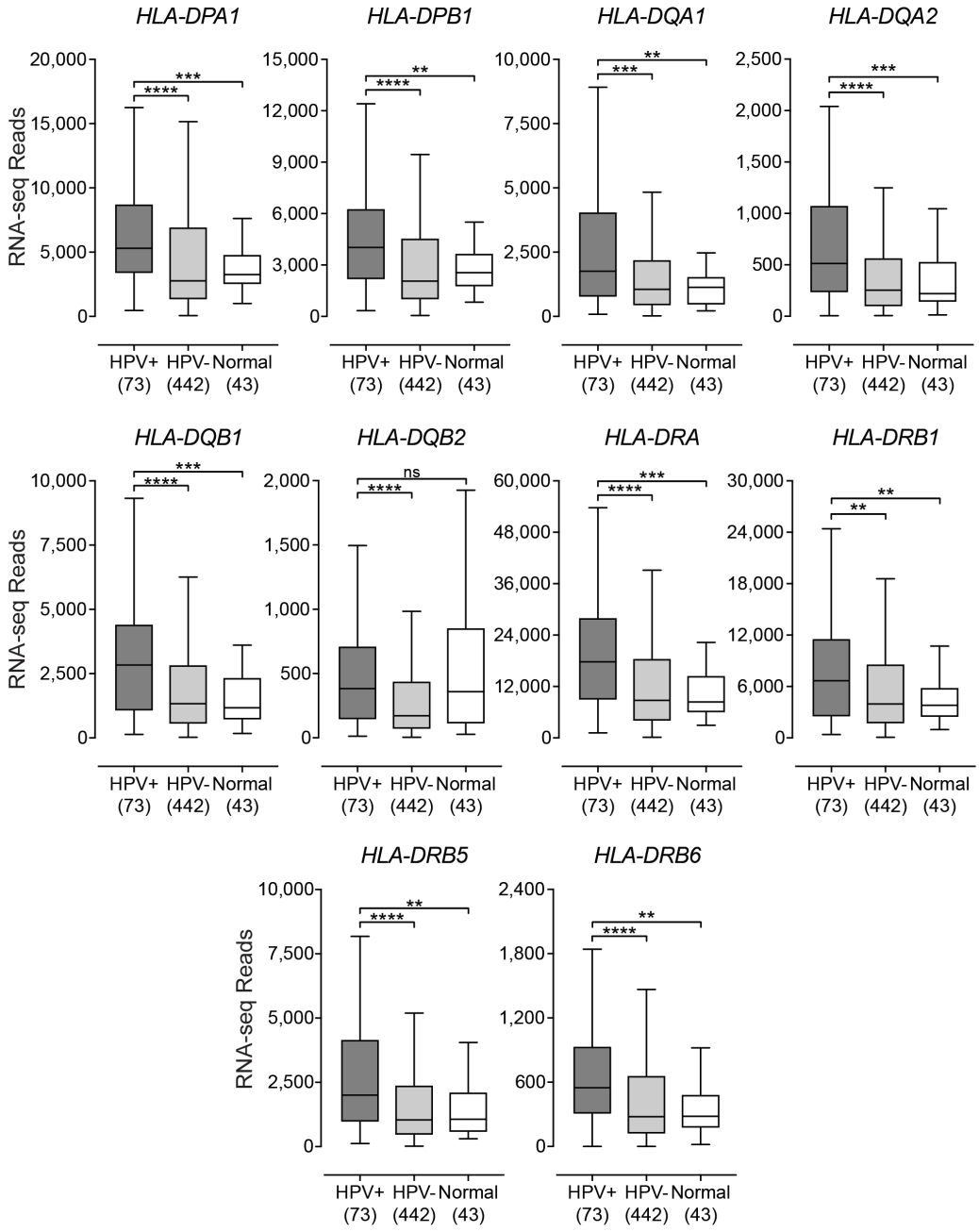

Figure 5.1. Expression of classical MHC-II α- and β-chain genes in head & neck squamous cell carcinomas stratified by high-risk HPV status.

RSEM-normalized RNA-seq data for the indicated MHC-II genes was extracted from the TCGA database for the HNSC cohort for HPV+, HPV–, and normal control tissues. Numbers in brackets refer to the number of samples included in each analysis. Statistical analysis was performed using a two-tailed non-parametric Mann–Whitney U test. ** $p \leq 0.01$, *** $p \leq 0.001$, **** $p \leq 0.0001$, ns – not significant.

the exception of *HLA-DQB2* (HPV+ versus Normal). As the majority of the HPV+ samples are from the oropharynx subsite, we repeated this analysis with HPV+ and HPV− samples that occur only in the oropharynx. Similarly, to the analysis including all subsites, HPV+ oropharyngeal tumors expressed significantly higher levels of MHC-II α- and β-chain genes compared to their HPV− oropharyngeal tumor counterparts (**Figure 5.2**). Collectively, these results indicate that HPV+ head and neck tumors express high levels of the mRNAs encoding the α- and β-chain heterodimers of the classical MHC-II molecules versus HPV− tumors or normal control tissues. It is noteworthy that based on the normalized read levels, all of these genes are expressed at levels several orders of magnitude above any markers of professional APCs, such as *CD19* (B-cells) (Wang et al., 2012), *CCL13* (DCs) (Danaher et al., 2017), and *CD84* (macrophages) (Zaiss et al., 2003) (**Figure 5.3A**). However, these normalized read levels are comparable to that of an established epithelial cell marker, E-cadherin (*CDH1*) (Gall and Frampton, 2013) (**Figure 5.3B**). Thus, it is likely that these genes are being expressed by epithelial cells within the actual tumor.

5.3.2 Genes encoding key components of the MHC-II antigen presentation pathway are expressed at higher levels in HPV+ head & neck carcinomas

In the endoplasmic reticulum, newly synthesized MHC-II α- and β-chains form a trimeric complex with a non-polymorphic protein called the invariant chain (Ii), which is encoded by the *HLA-DR antigens-associated invariant chain* or *Cluster of Differentiation 74* (*CD74*) gene (Cresswell, 1996). This association with the Ii chain prevents premature peptide loading and also dictates the trafficking of the Ii-MHC-II complex to the endosomal-lysosomal antigen-processing compartments, which contain the antigenic peptides (Roche and Cresswell, 1990; Roche and Furuta, 2015). Once in this compartment, Ii is proteolytically cleaved, leaving only a small fragment in the peptide-binding groove called the class II-associated invariant chain peptide (CLIP). Similarly, to the genes encoding the classical MHC-II α- and β-chains, *CD74* was found to be significantly upregulated in HPV+ HNSC compared to their HPV− counterparts or normal control tissues (**Figure 5.4**).

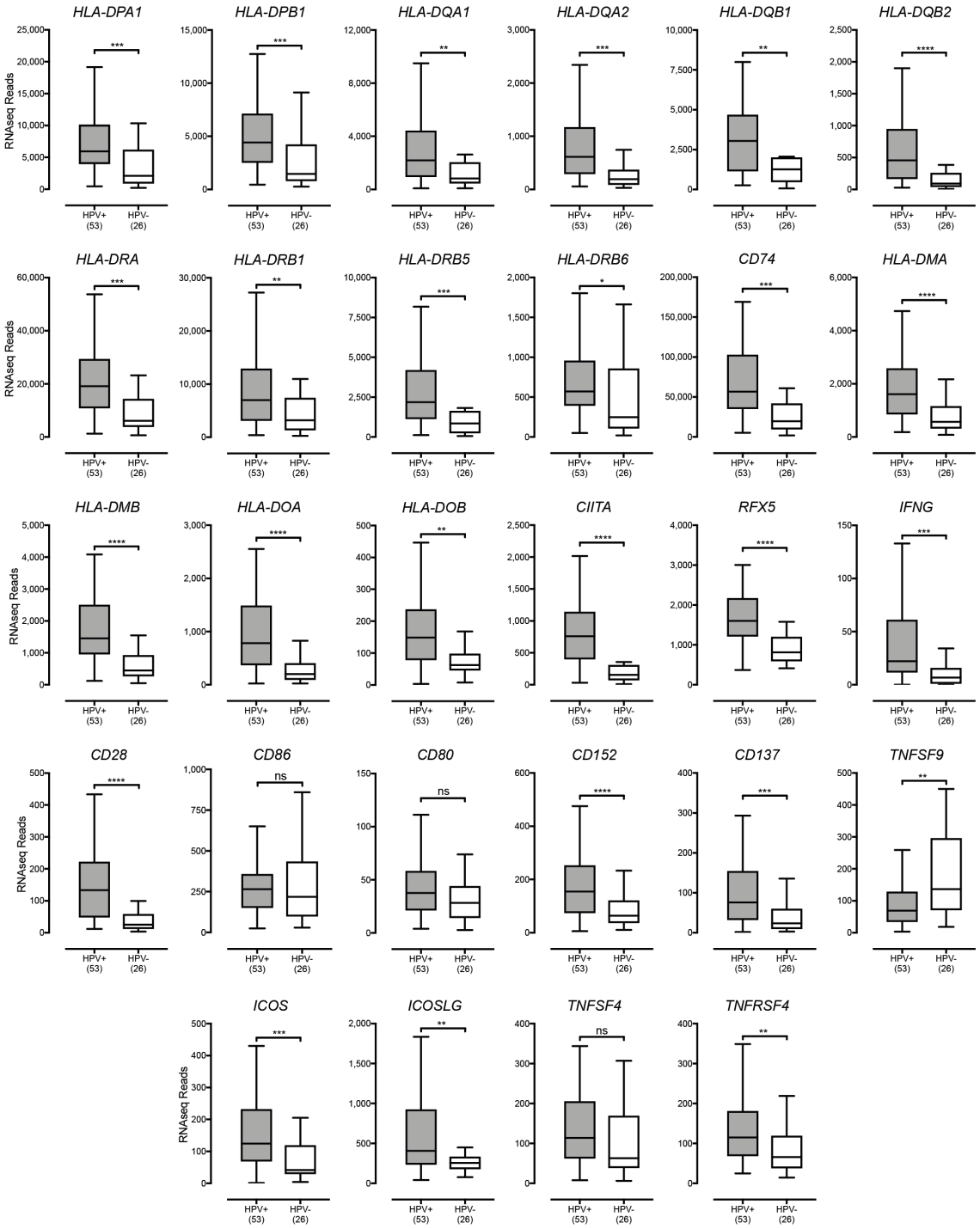

Figure 5.2. Gene expression reanalysis in the oropharynx.

RSEM-normalized RNA-seq data for tumors occurring in the oropharynx was extracted from the TCGA database for the HNSC cohort for HPV+ (53) and HPV– (26) samples. Statistical analysis was performed using a two-tailed non-parametric Mann-Whitney U test. * $p \leq 0.05$, ** $p \leq 0.01$, *** $p \leq 0.001$, **** $p \leq 0.0001$, ns – not significant.

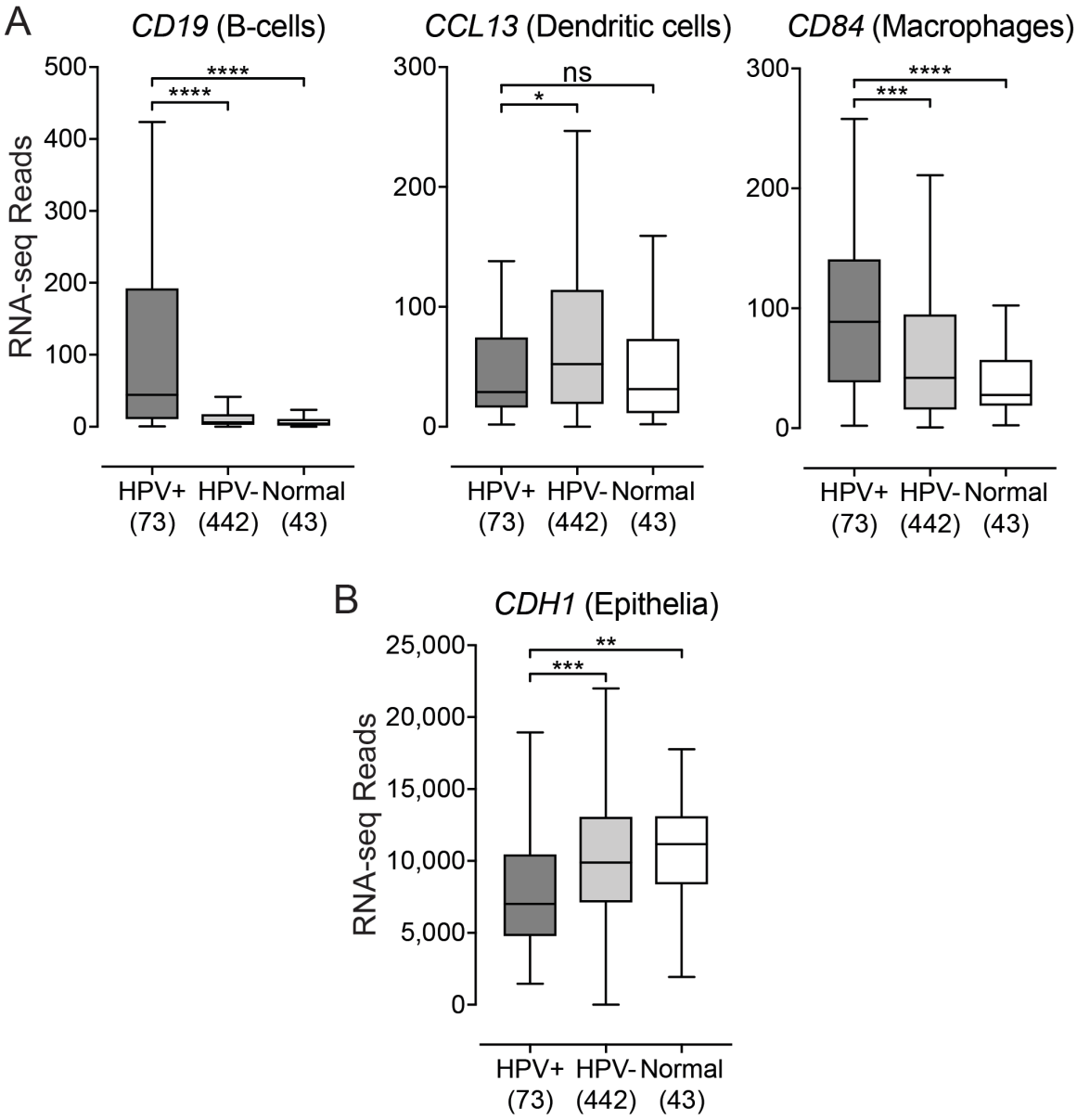

Figure 5.3. Expression of markers associated with APCs or epithelia.

RSEM-normalized RNA-seq data for genes associated with APCs (**A**) or epithelia (**B**) was extracted from the TCGA database for the HNSC cohort for HPV+, HPV–, and normal control tissues. Statistical analysis was performed using a two-tailed non-parametric Mann-Whitney U test. Numbers in brackets refer to the number of samples included in each analysis. * $p \leq 0.05$, ** $p \leq 0.01$, *** $p \leq 0.001$, **** $p \leq 0.0001$, ns – not significant.

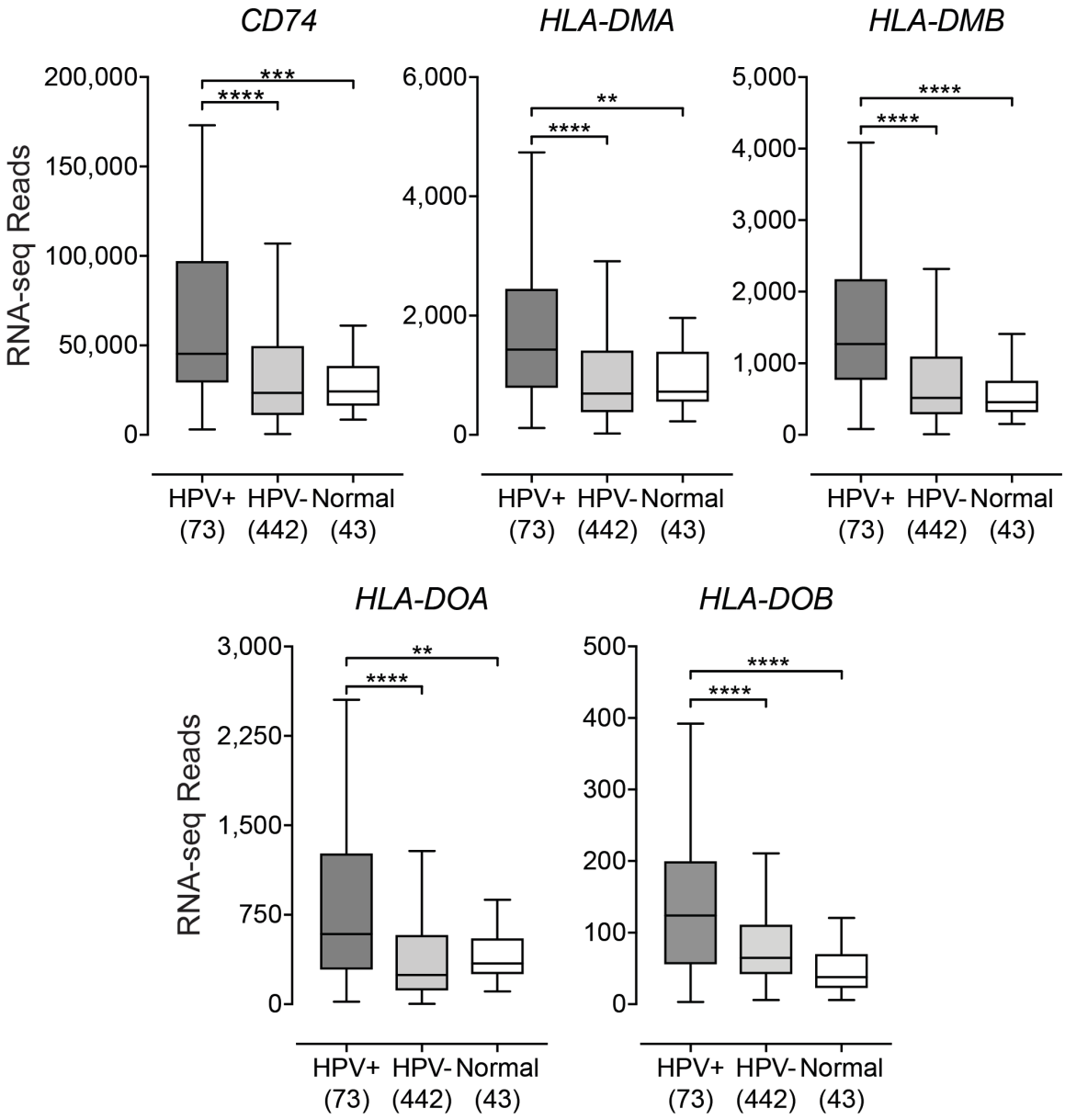

Figure 5.4. Expression of the invariant chain and MHC class II-like genes in head & neck carcinomas stratified by HPV status.

RSEM-normalized RNA-seq data for the indicated genes involved in MHC-II-dependent antigen processing and presentation was extracted from the TCGA database for the HNSC cohort for HPV+, HPV–, and normal control tissues. Numbers in brackets refer to the number of samples included in each analysis. Statistical analysis was performed using a two-tailed non-parametric Mann–Whitney U test. ** $p \leq 0.01$, *** $p \leq 0.001$, **** $p \leq 0.0001$.

In order for antigenic peptide-binding to occur, CLIP must be removed from the peptide-binding groove (Cresswell, 1996; Roche and Furuta, 2015). The enzymatic removal of CLIP is mediated by the MHC class II-like heterodimer, HLA-DM. After HLA-DM-mediated removal of CLIP, the class II molecules can now bind lysosomally generated antigenic peptides (Busch et al., 2005; Roche, 1995). The binding of antigenic peptides is influenced by another MHC class II-like heterodimer, HLA-DO, which regulates the MHC-II peptide repertoire by modulating the activity of HLA-DM (Denzin et al., 2005; Poluektov et al., 2013). The α- and β-chains of these dimeric class II-like molecules are encoded by the *HLA-DMA*, *HLA-DMB*, *HLA-DOA*, and *HLA-DOB* genes. Like the classical MHC-II genes, all four genes encoding the class II-like MHC molecules are similarly upregulated in HPV+ HNSC versus HPV− tumors or normal control tissues (**Figure 5.4**).

When repeated only considering the oropharynx subsite, HPV+ oropharyngeal tumors expressed significantly higher levels of the invariant chain and MHC-II-like genes compared to their HPV− oropharyngeal tumor counterparts (**Figure 5.2**). Taken together, the upregulation of the genes encoding the MHC-II invariant chain and class II-like genes, suggests that key components of the MHC-II antigen presentation pathway are transcribed in HPV+ HNSC at levels that are significantly higher than observed in HPV− tumors or normal control tissues. Furthermore, these genes are also expressed at very high levels, with the exception of *HLA-DOB*, that are indicative of being expressed by epithelial cells within the actual tumor.

5.3.3 Impact of HPV status on the expression of transcriptional regulators of MHC-II gene expression

Transcriptional control of MHC-II genes and the related genes that encode key components of the MHC-II antigen presentation pathway is among one of the best understood systems in mammals. It is a complex transcriptional system with a unique method of regulation that is completely dependent on the master transcriptional regulator CIITA (Boss and Jensen, 2003; van den Elsen, 2011). In agreement with the high levels of MHC-II genes and related genes, analysis of the TCGA data reveals significantly higher levels of *CIITA* in HPV+

samples compared to HPV− or normal control tissues (**Figure 5.5**). In addition, *RFX5*—another important transcriptional regulator of MHC-II genes (Boss and Jensen, 2003)—was similarly expressed at significantly higher levels in HPV+ samples with respect to HPV− tumors or normal control tissues (**Figure 5.5**). Again, these differences were also observed when only considering the expression of these genes in the oropharynx (**Figure 5.2**).

Expression of MHC-II genes and related genes are restricted to APCs, however non-hematopoietic cells such as fibroblasts, endothelial cells, and epithelial cells can be stimulated by IFNγ to express MHC-II molecules and related proteins involved in the antigen presentation pathway (Boss and Jensen, 2003; Collins et al., 1984; Steimle et al., 1994). We analyzed the expression level of the IFNγ gene (*IFNG*) (**Figure 5.5**). As expected, the relative level of *IFNG* expression was similar in magnitude to that of other leukocyte specific genes (**Figure 5.3A**). However, *IFNG* was expressed at significantly higher levels in HPV+ tumors compared to its HPV– counterpart or normal control tissues (**Figure 5.5**). In addition, when only considering the oropharynx, the expression of the IFNγ gene was significantly higher in HPV+ samples compared to HPV− oropharyngeal tumors (**Figure 5.2**).

To further illustrate the IFNγ-specific coordinated upregulation of MHC-II genes and related genes that encode products essential for antigen processing and presentation, we generated a correlation matrix for both HPV+ (**Figure 5.6: upper triangle**) and HPV− samples (**Figure 5.6: lower triangle**). As expected, regardless of HPV status, we found that expression of all MHC-II antigen presentation-specific genes were correlated in a pairwise fashion in each patient sample.

Thus, the upregulated expression of *CIITA*, *RFX5*, and subsequent expression of all the classical MHC-II genes and related genes required for antigen loading and presentation observed in HPV+ head and neck carcinomas are likely a consequence of IFNγ exposure. Furthermore, the correlation matrix illustrates the unique simultaneous coordination of the MHC-II transcriptional control system that has been shown to be dictated by the master transcriptional regulator CIITA (Boss and Jensen, 2003; van den Elsen, 2011).

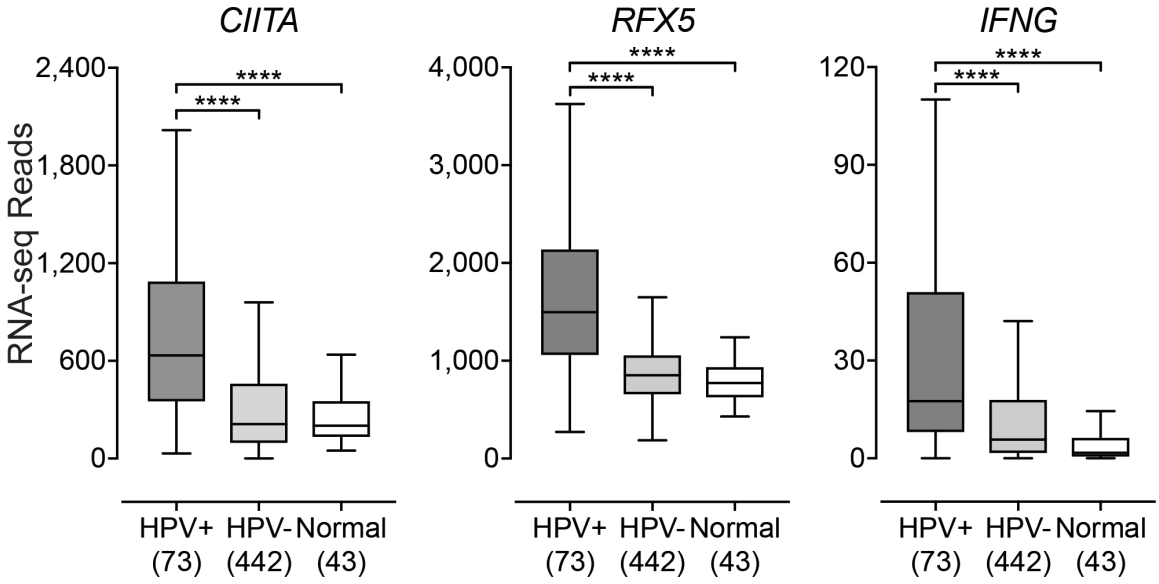

Figure 5.5. Expression of *CIITA*, *RFX5*, and *IFNG* mRNA in head & neck carcinomas stratified by HPV status.

RSEM-normalized RNA-seq data for the *CIITA*, *RFX5*, and *IFNG* genes were extracted from the TCGA database for the HNSC cohort for HPV+, HPV−, and normal control tissues. Numbers in brackets refer to the number of samples included in each analysis. Statistical analysis was performed using a two-tailed non-parametric Mann–Whitney U test. **** $p \leq 0.0001$.

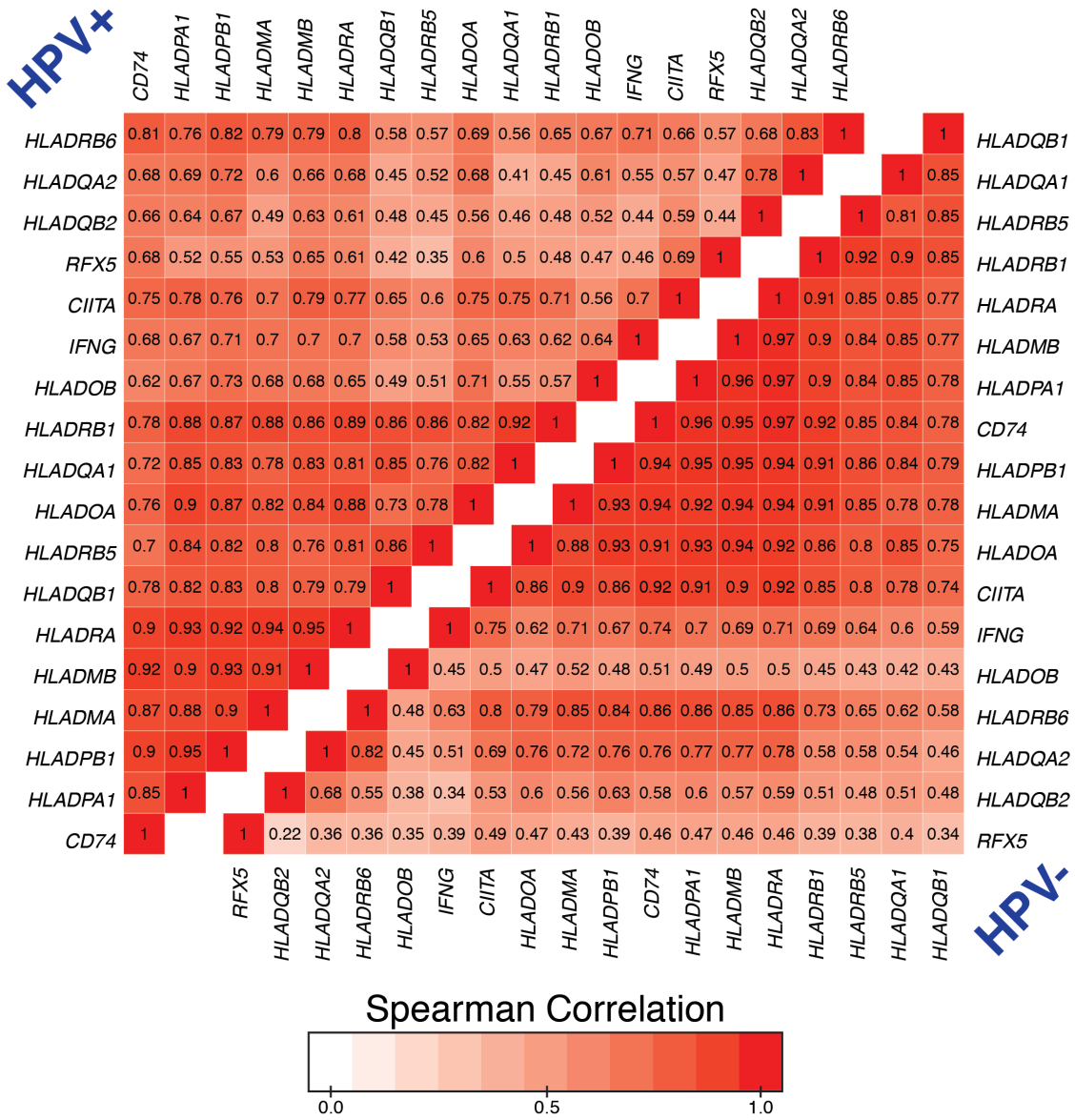

Figure 5.6. Correlation matrix of genes involved in the MHC-II antigen presentation pathway in head & neck carcinomas stratified by HPV status.

RSEM-normalized RNA-seq data for the genes listed above were extracted from the TCGA database for the HNSC cohort for HPV+ (upper triangle) and HPV− samples (lower triangle). Pairwise spearman correlation was performed followed by hierarchical clustering to group based on correlation. Number in boxes indicate Spearman's rank correlation coefficient of analyzed gene pairs.

5.3.4 Impact of HPV status on the expression of T-cell co-stimulatory molecules in HPV+ head & neck carcinomas

Co-stimulation of T-cells occurs through the interaction of its constitutively expressed CD28 receptor with either CD80 or CD86 on APCs (Chen and Flies, 2013). Utilizing RNA expression data for the levels of each of these co-stimulatory molecules, we found higher levels of *CD28* in HPV+ tumors compared to HPV− or normal control tissues (**Figure 5.7**). While the levels of both *CD80* and *CD86* in HPV+ tumors were not significantly different compared to their HPV− counterparts, they were significantly higher compared to normal control tissues (**Figure 5.7**). In addition, we found that the mRNA levels of *CD152*, which encodes for CTLA-4, a marker of T-cell activation (Rudd et al., 2009), was significantly upregulated in HPV+ tumors compared to HPV− and normal control tissues (**Figure 5.7**). Again, these differences were also observed when only considering the expression of these genes in the oropharynx (**Figure 5.2**). These results suggest that, like the MHC-II genes and the genes involved in antigen loading and presentation, co-stimulatory molecules are similarly present at higher levels in HPV+ tumors and this is correlated with a higher level of T-cell activation.

5.3.5 Impact of HPV status on the expression of inducible T-cell survival signal molecules in HPV+ head & neck carcinomas

Utilizing the RNA-seq HNSC dataset from the TCGA, we looked at genes that encode for inducible, T-cell activation-dependent, survival signal molecules and their respective ligands (Beier et al., 2007; Chen and Flies, 2013). We found that *CD137* (4-1BB, TNFRSF9) was significantly upregulated in HPV+ tumors compared to HPV− or normal control tissues (**Figure 5.8**). However, its ligand *TNFSF9* (CD137L, 4-1BBL) was found to be significantly downregulated in HPV+ tumors compared to HPV− and not significantly different compared to normal control tissues (**Figure 5.8**). Next, we looked at the genes that encode for the inducible T-cell co-stimulator (*ICOS*) and its ligand *ICOSLG* and found that both were significantly upregulated in HPV+ tumors compared to HPV−, but only *ICOS* was significantly upregulated in comparison to normal control tissues (**Figure 5.8**). Finally, we looked at OX40 (*TNFRSF4*, CD134) and its ligand OX40L (*TNFSF4*, CD252) and found that both genes were significantly upregulated in HPV+

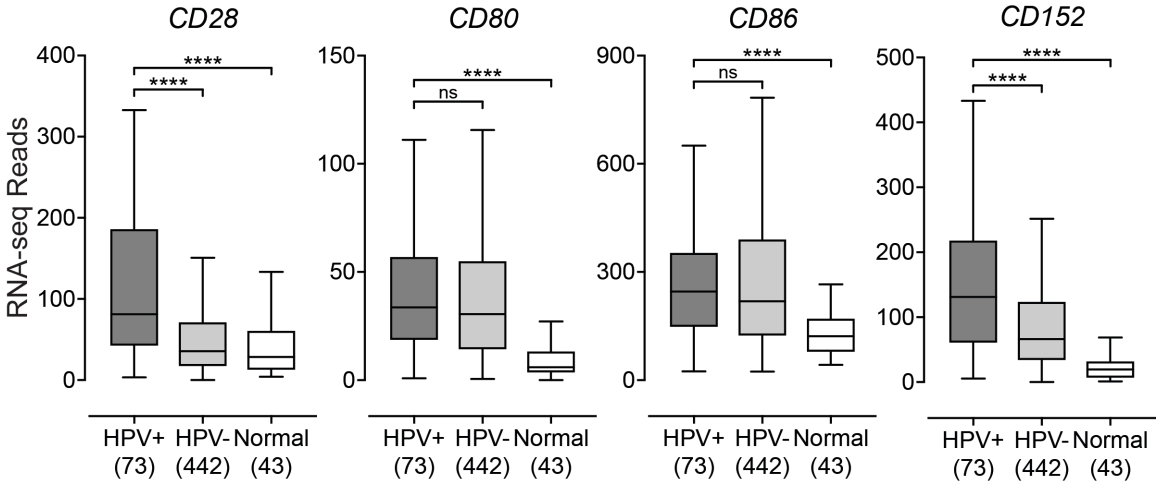

Figure 5.7. Expression of genes that encode for T-cell co-stimulatory molecules in head & neck carcinomas stratified by HPV status.

RSEM-normalized RNA-seq data for genes that encode T-cell specific co-stimulatory molecules was extracted from the TCGA database for the HNSC cohort for HPV+, HPV–, and normal control tissues. Statistical analysis was performed using a two-tailed non-parametric Mann–Whitney U test. Numbers in brackets refer to the number of samples included in each analysis. **** $p \leq 0.0001$, ns – not significant.

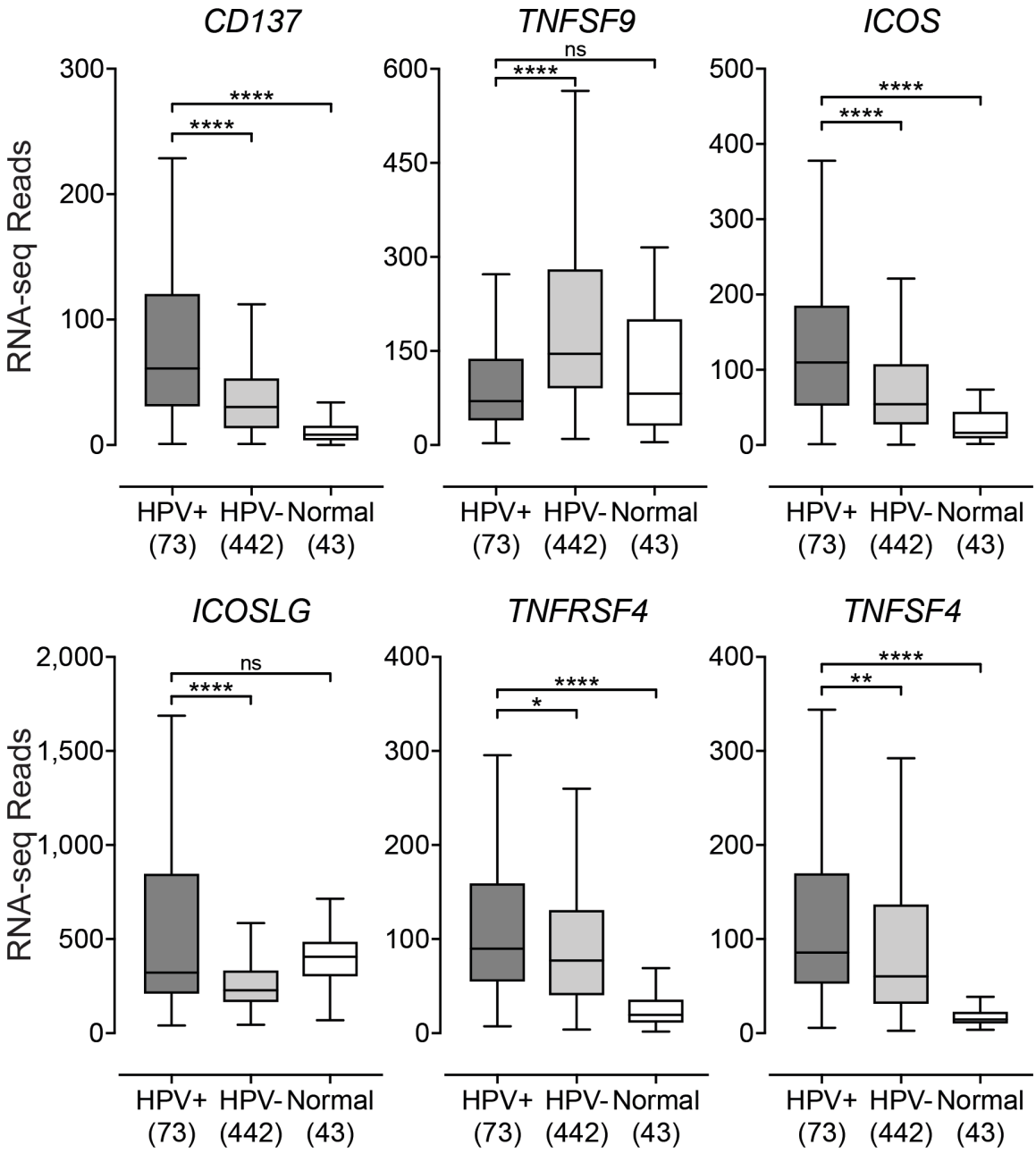

Figure 5.8. Expression of inducible T-cell survival signal molecules in head & neck carcinomas stratified by HPV status.

RSEM-normalized RNA-seq data for inducible genes that encode for T-cell survival molecules was extracted from the TCGA database for the HNSC cohort for HPV+, HPV−, and normal control tissues. Statistical analysis was performed using a two-tailed non-parametric Mann–Whitney U test. Numbers in brackets refer to the number of samples included in each analysis. * $p \leq 0.05$, ** $p \leq 0.01$, **** $p \leq 0.0001$, ns – not significant.

tumors compared to their HPV− counterparts and normal control tissues (**Figure 5.8**). Again, these differences were also observed when only considering the expression of these genes in the oropharynx with the exception of *TNFSF4* (**Figure 5.2**). Taken together, these results suggest that T-cells are activated and proliferating within the HPV+ tumor microenvironment via the observation of an increase in expression of genes that encode for survival signal molecules that are only induced following TCR-mediated antigen-specific T-cell activation and/or CD28 co-stimulation (Beier et al., 2007; Chen and Flies, 2013).

5.4 Discussion

Expression of MHC-II is typically associated with professional APCs, which are considered essential for the initiation of the adaptive immune response. They function by sampling their local environment via phagocytosis, acquiring particles and processing them internally in order to present them on their cell surface to $CD4^+$ T-cells in the context of an antigen-MHC-II complex (Roche and Furuta, 2015). The crosslinking of the $CD4^+$ TCR and antigen-MHC-II complex initiates the T-cell activation protocol that, in conjunction with co-stimulatory signals, can ultimately lead to an effective adaptive immune response against a threat of internal or external origin, such as cancerous cells or bacteria and viruses, respectively (Chen and Flies, 2013).

In non-hematopoietic cells, such as epithelia, MHC-II expression can be induced through exposure to the proinflammatory cytokine IFNγ (Boss and Jensen, 2003; Collins et al., 1984; Steimle et al., 1994). This induction of MHC-II on epithelial cells bestows on them the ability to act as accessory APCs, and this can accentuate the presentation of antigens to $CD4^+$ T-cells (Kim et al., 2009). However, the ability of epithelial cells to function as accessory APCs is generally underappreciated, with most existing information related to the gastrointestinal and respiratory tracts (Wosen et al., 2018). Interestingly, cancerous tissues can retain tumor-specific MHC-II expression, and this has the potential to increase recognition of a tumor by the immune system (Axelrod et al., 2019). Indeed, tumor specific MHC-II expression has been associated with superior prognosis and/or improved response to immune checkpoint inhibitor therapy in several human cancers, as well as increased tumor rejection in murine models (Axelrod et al., 2019; Cioni et al., 2019; Forero et al.,

2016; Johnson et al., 2016; Roemer et al., 2018). The importance of the immune response for successful resolution of cancers cannot be understated. Indeed, mouse models have shown that neither chemotherapy nor radiation treatment functioned effectively in the absence of a functional immune system, at least in HPV+ HNSC (Spanos et al., 2009).

While MHC-II expression has been reported in head and neck tumors (Cioni et al., 2019), existing studies have been limited to individual classical isotypes, such as HLA-DR, based on limitations in available antibodies (Johnson et al., 2018). Cell culture models based on established head and neck cancer lines have also demonstrated MHC-II expression, often in response to IFNγ, or following transfection with CIITA—master regulator of MHC-II transcription (Arosarena et al., 1999; Meissner et al., 2009). However, no existing studies have comprehensively assessed the transcriptional status of the entire MHC-II antigen presentation system in head and neck cancers. In this study, our goal was to determine if MHC-II components were widely expressed in human head and neck cancers and whether expression was influenced by HPV status.

Using data from over 500 primary human head and neck tumors, we provide evidence that HPV+ head and neck carcinomas display high mRNA levels for virtually all MHC-II genes, including the classical and non-classical α- and β-chains, the invariant γ chain, as well as factors required for MHC-II loading and trafficking (**Figures 5.1 and 5.4**). Increased expression of these genes was observed whether the comparison included all head and neck cancer subsites or was restricted to just the oropharynx, where the majority of HPV+ head and neck cancers arise (**Figure 5.2**). These results are in good agreement with the concurrent detection of high levels of expression of *CIITA* and *RFX5*, important global regulators of MHC-II transcription (Boss and Jensen, 2003; van den Elsen, 2011), in HPV+ tumors. HPV+ head and neck carcinomas express significantly higher levels of these genes as compared to normal control tissues, and these levels are generally higher than in HPV– carcinomas (**Figure 5.5**). This likely reflects the T-cell inflamed nature of HPV+ cancers (Gameiro et al., 2018), and specifically the higher levels of IFNγ expressed in these tumors (**Figure 5.5**). This IFNγ-dependent coordinated upregulation of MHC-II genes and related genes involved in antigen processing and presentation was further

illustrated in **Figure 5.6**, where we observed a strong global correlation with all genes analyzed in the MHC-II transcriptional control system.

After generation and programming in the thymus, $CD8^+$ and $CD4^+$ T-cells circulate in the body until they encounter their specific antigen presented on either class I or class II MHC molecules, respectively (Luckheeram et al., 2012; Pennock et al., 2013; Zhang and Bevan, 2011). This interaction between TCR and antigen-loaded MHC complex represents signal 1, which triggers the activation of T-cells. However, in order for the activated T-cell to fully respond to the presented threat, and not enter a state of unresponsiveness, it requires a secondary signal through co-stimulatory molecules (Chen and Flies, 2013). We found higher levels of *CD28* in HPV+ tumors compared to their HPV− counterparts and normal control tissues (**Figure 5.7**). The binding of CD28 with either CD80 or CD86 leads to clonal expansion of the T-cell pool that is specific to the recognized antigen (Beier et al., 2007; Chen and Flies, 2013). In order to attenuate this response, the aforementioned interaction leads to the induction of the co-inhibitory molecule CTLA-4, which is encoded by the gene *CD152*. This co-inhibitory molecule will compete with CD28 for binding to either CD80 or CD86 to attenuate the T-cell response (Chen and Flies, 2013; Rudd et al., 2009). We found that *CD152* was significantly upregulated in the HPV+ cohort (**Figure 5.7**). Collectively, this data indirectly illustrates the higher number of infiltrating T-cells within the tumor microenvironments of HPV+ HNSC through the identification of significantly higher levels of the constitutively expressed T-cell-specific *CD28* marker. In addition, it provides good evidence that the interaction of co-stimulatory molecules in HPV+ HNSC is effective, given that we detected significantly higher levels of expression of *CD152* mRNA, which encodes for the inducible co-inhibitory molecule CTLA-4.

In order for proliferating T-cells to persist and survive after antigen-recognition and subsequent stimulation with co-stimulatory molecules, they require survival signals that are delivered through the cross-linking of various molecules (Beier et al., 2007; Chen and Flies, 2013). Interestingly, unlike other co-stimulatory molecules—such as CD28—that can be found constitutively expressed on T-cells, the molecules that convey these survival signals are encoded by genes that are only expressed following TCR-mediated antigen-specific T-cell activation and/or CD28 co-stimulation (Beier et al., 2007; Chen and Flies,

2013). We found that all inducible T-cell survival genes analyzed, with the exception of *TNFSF9*, were expressed at significantly higher levels in HPV+ tumors compared to HPV− and normal control tissues (**Figure 5.8**). *TNFSF9* was significantly downregulated in HPV+ tumors compared to its HPV− counterpart (**Figure 5.8**). This downregulation of *TNFSF9* is indicative of a mechanistic response to excessive CD137-mediated signaling (Eun et al., 2015; Ho et al., 2013; Kwon, 2015). This data indirectly illustrates that the HPV+ tumor microenvironment contains increased levels of activated and proliferating T-cells via the observation of an increase in expression of genes that encode for survival signal molecules that are induced following TCR-mediated antigen-specific T-cell activation and/or CD28 co-stimulation. These results agree well with previous reports by our group and others that HPV+ tumors contain more T-cells (Chen et al., 2018; Gameiro et al., 2018; Mandal et al., 2016; Nguyen et al., 2016; Solomon et al., 2018), but goes further in that it indirectly provides evidence of productive MHC-II-dependent tumor-antigen recognition.

HPV+ HNSC tumors are remarkably different from their HPV− counterparts in that they express high levels of all components of the MHC-II antigen presentation apparatus. Importantly, while some of this signal can be attributed to professional APCs, the extremely high relative level of expression supports a model whereby the T-cell inflamed environment in HPV+ HNSC induces a functionally effective MHC-II presentation system based on tumor epithelial cells. As MHC-II-dependent antigen presentation is critical for $CD4^+$ help in $CD8^+$ T-cell responses, which are essential for the control and clearance of cancerous cells, it is likely that the expression of non-self-derived viral antigens or tumor-derived neoantigens, combined with intact MHC-II presentation and appropriate co-stimulation, contributes to the markedly better patient outcomes for HPV+ versus HPV– head and neck carcinomas. As immune checkpoint inhibition therapy in other cancers has been reported to be most effective for tumors with high MHC-II levels, suggesting that stratification based on MHC-II levels may help predict those likely to respond to checkpoint inhibition therapy.

5.5 References

Ang KK, Harris J, Wheeler R, et al. (2010) Human papillomavirus and survival of patients with oropharyngeal cancer. *N Engl J Med* 363: 24-35.

Arosarena OA, Baranwal S, Strome S, et al. (1999) Expression of major histocompatibility complex antigens in squamous cell carcinomas of the head and neck: effects of interferon gene transfer. *Otolaryngol Head Neck Surg* 120: 665-671.

Axelrod ML, Cook RS, Johnson DB, et al. (2019) Biological Consequences of MHC-II Expression by Tumor Cells in Cancer. *Clin Cancer Res* 25: 2392-2402.

Banister CE, Liu C, Pirisi L, et al. (2017) Identification and characterization of HPV-independent cervical cancers. *Oncotarget* 8: 13375-13386.

Baruah P, Bullenkamp J, Wilson POG, et al. (2019) TLR9 Mediated Tumor-Stroma Interactions in Human Papilloma Virus (HPV)-Positive Head and Neck Squamous Cell Carcinoma Up-Regulate PD-L1 and PD-L2. *Front Immunol* 10: 1644.

Beier KC, Kallinich T and Hamelmann E. (2007) Master switches of T-cell activation and differentiation. *Eur Respir J* 29: 804-812.

Boss JM and Jensen PE. (2003) Transcriptional regulation of the MHC class II antigen presentation pathway. *Curr Opin Immunol* 15: 105-111.

Bratman SV, Bruce JP, O'Sullivan B, et al. (2016) Human Papillomavirus Genotype Association With Survival in Head and Neck Squamous Cell Carcinoma. *JAMA oncology* 2: 823-826.

Busch R, Rinderknecht CH, Roh S, et al. (2005) Achieving stability through editing and chaperoning: regulation of MHC class II peptide binding and expression. *Immunol Rev* 207: 242-260.

Chen L and Flies DB. (2013) Molecular mechanisms of T cell co-stimulation and co-inhibition. *Nat Rev Immunol* 13: 227-242.

Chen X, Yan B, Lou H, et al. (2018) Immunological network analysis in HPV associated head and neck squamous cancer and implications for disease prognosis. *Mol Immunol* 96: 28-36.

Cioni B, Jordanova ES, Hooijberg E, et al. (2019) HLA class II expression on tumor cells and low numbers of tumor-associated macrophages predict clinical outcome in oropharyngeal cancer. *Head Neck* 41: 463-478.

Collins T, Korman AJ, Wake CT, et al. (1984) Immune interferon activates multiple class II major histocompatibility complex genes and the associated invariant chain gene in human endothelial cells and dermal fibroblasts. *Proc Natl Acad Sci U S A* 81: 4917-4921.

Cresswell P. (1996) Invariant chain structure and MHC class II function. *Cell* 84: 505-507.

Danaher P, Warren S, Dennis L, et al. (2017) Gene expression markers of Tumor Infiltrating Leukocytes. *J Immunother Cancer* 5: 18.

Denzin LK, Fallas JL, Prendes M, et al. (2005) Right place, right time, right peptide: DO keeps DM focused. *Immunol Rev* 207: 279-292.

Doorbar J, Egawa N, Griffin H, et al. (2015) Human papillomavirus molecular biology and disease association. *Rev Med Virol* 25 Suppl 1: 2-23.

Eun SY, Lee SW, Xu Y, et al. (2015) 4-1BB ligand signaling to T cells limits T cell activation. *J Immunol* 194: 134-141.

Fakhry C, Westra WH, Li S, et al. (2008) Improved survival of patients with human papillomavirus-positive head and neck squamous cell carcinoma in a prospective clinical trial. *J Natl Cancer Inst* 100: 261-269.

Faul F, Erdfelder E, Lang A-G, et al. (2007) G*Power 3: a flexible statistical power analysis program for the social, behavioral, and biomedical sciences. *Behavior research methods* 39: 175-191.

Ferris RL. (2015) Immunology and Immunotherapy of Head and Neck Cancer. *J Clin Oncol* 33: 3293-3304.

Forero A, Li Y, Chen D, et al. (2016) Expression of the MHC Class II Pathway in Triple-Negative Breast Cancer Tumor Cells Is Associated with a Good Prognosis and Infiltrating Lymphocytes. *Cancer Immunol Res* 4: 390-399.

Forman D, de Martel C, Lacey CJ, et al. (2012) Global burden of human papillomavirus and related diseases. *Vaccine* 30 Suppl 5: F12-23.

Gall TM and Frampton AE. (2013) Gene of the month: E-cadherin (CDH1). *J Clin Pathol* 66: 928-932.

Gameiro SF, Ghasemi F, Barrett JW, et al. (2018) Treatment-naive HPV+ head and neck cancers display a T-cell-inflamed phenotype distinct from their HPV- counterparts that has implications for immunotherapy. *Oncoimmunology* 7: e1498439.

Gameiro SF, Kolendowski B, Zhang A, et al. (2017a) Human papillomavirus dysregulates the cellular apparatus controlling the methylation status of H3K27 in different human cancers to consistently alter gene expression regardless of tissue of origin. *Oncotarget* 8: 72564-72576.

Gameiro SF, Zhang A, Ghasemi F, et al. (2017b) Analysis of Class I Major Histocompatibility Complex Gene Transcription in Human Tumors Caused by Human Papillomavirus Infection. *Viruses* 9: 252.

Gillison ML, Castellsague X, Chaturvedi A, et al. (2014) Eurogin Roadmap: comparative epidemiology of HPV infection and associated cancers of the head and neck and cervix. *Int J Cancer* 134: 497-507.

Gillison ML, Koch WM, Capone RB, et al. (2000) Evidence for a causal association between human papillomavirus and a subset of head and neck cancers. *J Natl Cancer Inst* 92: 709-720.

Heller C, Weisser T, Mueller-Schickert A, et al. (2011) Identification of key amino acid residues that determine the ability of high risk HPV16-E7 to dysregulate major histocompatibility complex class I expression. *J Biol Chem* 286: 10983-10997.

Ho WT, Pang WL, Chong SM, et al. (2013) Expression of CD137 on Hodgkin and Reed-Sternberg cells inhibits T-cell activation by eliminating CD137 ligand expression. *Cancer Res* 73: 652-661.

Johnson DB, Estrada MV, Salgado R, et al. (2016) Melanoma-specific MHC-II expression represents a tumour-autonomous phenotype and predicts response to anti-PD-1/PD-L1 therapy. *Nat Commun* 7: 10582.

Johnson DB, Nixon MJ, Wang Y, et al. (2018) Tumor-specific MHC-II expression drives a unique pattern of resistance to immunotherapy via LAG-3/FCRL6 engagement. *JCI insight* 3: e120360.

Kim BS, Miyagawa F, Cho YH, et al. (2009) Keratinocytes function as accessory cells for presentation of endogenous antigen expressed in the epidermis. *J Invest Dermatol* 129: 2805-2817.

Kwon B. (2015) Is CD137 Ligand (CD137L) Signaling a Fine Tuner of Immune Responses? *Immune Netw* 15: 121-124.

Luckheeram RV, Zhou R, Verma AD, et al. (2012) CD4(+)T cells: differentiation and functions. *Clin Dev Immunol* 2012: 925135.

Mandal R, Senbabaoglu Y, Desrichard A, et al. (2016) The head and neck cancer immune landscape and its immunotherapeutic implications. *JCI insight* 1: e89829.

Meissner M, Whiteside TL, Kaufmann R, et al. (2009) CIITA versus IFN-gamma induced MHC class II expression in head and neck cancer cells. *Arch Dermatol Res* 301: 189-193.

Network TCGAR. (2015) Comprehensive genomic characterization of head and neck squamous cell carcinomas. *Nature* 517: 576-582.

Network TCGAR. (2017) Integrated genomic and molecular characterization of cervical cancer. *Nature* 543: 378-384.

Nguyen N, Bellile E, Thomas D, et al. (2016) Tumor infiltrating lymphocytes and survival in patients with head and neck squamous cell carcinoma. *Head Neck* 38: 1074-1084.

Pennock ND, White JT, Cross EW, et al. (2013) T cell responses: naive to memory and everything in between. *Adv Physiol Educ* 37: 273-283.

Poluektov YO, Kim A and Sadegh-Nasseri S. (2013) HLA-DO and Its Role in MHC Class II Antigen Presentation. *Front Immunol* 4: 260.

Psyrri A, Rampias T and Vermorken JB. (2014) The current and future impact of human papillomavirus on treatment of squamous cell carcinoma of the head and neck. *Ann Oncol* 25: 2101-2115.

Roche PA. (1995) HLA-DM: an in vivo facilitator of MHC class II peptide loading. *Immunity* 3: 259-262.

Roche PA and Cresswell P. (1990) Invariant chain association with HLA-DR molecules inhibits immunogenic peptide binding. *Nature* 345: 615-618.

Roche PA and Furuta K. (2015) The ins and outs of MHC class II-mediated antigen processing and presentation. *Nat Rev Immunol* 15: 203-216.

Rock KL, Reits E and Neefjes J. (2016) Present Yourself! By MHC Class I and MHC Class II Molecules. *Trends Immunol* 37: 724-737.

Roemer MGM, Redd RA, Cader FZ, et al. (2018) Major Histocompatibility Complex Class II and Programmed Death Ligand 1 Expression Predict Outcome After Programmed Death 1 Blockade in Classic Hodgkin Lymphoma. *J Clin Oncol* 36: 942-950.

Rudd CE, Taylor A and Schneider H. (2009) CD28 and CTLA-4 coreceptor expression and signal transduction. *Immunol Rev* 229: 12-26.

Seiwert TY, Zuo Z, Keck MK, et al. (2015) Integrative and comparative genomic analysis of HPV-positive and HPV-negative head and neck squamous cell carcinomas. *Clin Cancer Res* 21: 632-641.

Sepiashvili L, Bruce JP, Huang SH, et al. (2015) Novel insights into head and neck cancer using next-generation "omic" technologies. *Cancer Res* 75: 480-486.

Solomon B, Young RJ, Bressel M, et al. (2018) Prognostic Significance of PD-L1(+) and CD8(+) Immune Cells in HPV(+) Oropharyngeal Squamous Cell Carcinoma. *Cancer Immunol Res* 6: 295-304.

Spanos WC, Nowicki P, Lee DW, et al. (2009) Immune response during therapy with cisplatin or radiation for human papillomavirus-related head and neck cancer. *Arch Otolaryngol Head Neck Surg* 135: 1137-1146.

Steimle V, Siegrist CA, Mottet A, et al. (1994) Regulation of MHC class II expression by interferon-gamma mediated by the transactivator gene CIITA. *Science* 265: 106-109.

Syrjanen S. (2005) Human papillomavirus (HPV) in head and neck cancer. *J Clin Virol* 32 Suppl 1: S59-66.

van den Elsen PJ. (2011) Expression regulation of major histocompatibility complex class I and class II encoding genes. *Front Immunol* 2: 48.

van den Elsen PJ, Holling TM, Kuipers HF, et al. (2004) Transcriptional regulation of antigen presentation. *Curr Opin Immunol* 16: 67-75.

Wang K, Wei G and Liu D. (2012) CD19: a biomarker for B cell development, lymphoma diagnosis and therapy. *Exp Hematol Oncol* 1: 36.

Worsham MJ, Chen KM, Ghanem T, et al. (2013) Epigenetic modulation of signal transduction pathways in HPV-associated HNSCC. *Otolaryngol Head Neck Surg* 149: 409-416.

Wosen JE, Mukhopadhyay D, Macaubas C, et al. (2018) Epithelial MHC Class II Expression and Its Role in Antigen Presentation in the Gastrointestinal and Respiratory Tracts. *Front Immunol* 9: 2144.

Zaiss M, Hirtreiter C, Rehli M, et al. (2003) CD84 expression on human hematopoietic progenitor cells. *Exp Hematol* 31: 798-805.

Zhang N and Bevan MJ. (2011) CD8(+) T cells: foot soldiers of the immune system. *Immunity* 35: 161-168.

Chapter 6

6 General Discussion

6.1 Thesis Summary

Much of the existing literature that encompasses the foundation for this body of work utilizes relatively artificial *in vitro* model systems. These earlier and current approaches attempt to phenocopy complex malignancies under conditions that can be manipulated, to gain insight into mechanistic processes. Indeed, these approaches have several advantages such as infinite growth, amenability to high-throughput screening, and formation of xenograft tumors for *in vivo* testing. However, their lack of heterogeneity, tumor microenvironment, and infiltrating immune cells severely limit their ability to recapitulate actual human cancers (Namekawa et al., 2019). Therefore, my thesis research capitalizes on genomic and transcriptomic "big" data acquired through next-generation "-omics" technologies from actual human tumors. This *in silico* approach allows for an insightful elucidation of mechanistic processes under the influence of a native heterogeneous environment. Utilizing computational methods, I explored and profiled the epigenetic and immune landscapes between the tumor microenvironments of HPV-positive (HPV+) and HPV-negative (HPV–) carcinomas present in actual human malignancies. True to my proposed hypothesis, my studies have identified strikingly profound differences in the epigenetic and immune landscapes of the tumor microenvironments (TMEs) of these 2 etiologically-distinct carcinomas, regardless of their tissue of origin. Furthermore, they also provided insight into the validity of 2 important models of HR HPV-mediated sabotage of intracellular epigenetic and immune networks that were previously proposed from artificial *in vitro* culture studies. In addition, these studies identified potentially useful therapeutic targets and advocated for the utility of novel immunotherapy treatment modalities. Notably, the expression of immune checkpoint molecules was shown, in HPV+ head and neck patients, to be potentially predictive biomarkers of clinical outcomes that could have implications for treatment deintensification.

6.2 Epigenetic Landscape of HPV+ Tumor Microenvironments

The E7 oncoprotein from HR HPVs have been shown to mediate global changes on the epigenome of the infected host cell (Durzynska et al., 2017). One prime example of an E7-mediated epigenetic change is the global reduction in the levels of tri-methylated lysine 27 on histone 3 (H3K27me3), which is a universal mark of transcriptionally silenced chromatin. (McLaughlin-Drubin et al., 2011; McLaughlin-Drubin et al., 2008; Schwartz and Pirrotta, 2007). Furthermore, HPV has also been shown to increase the expression of the catalytic enzymes responsible for creating and removing methyl groups on lysine 27 of histone 3. Indeed, these *in vitro* studies have shown that HPV induces an increase in the expression level of the EZH2 core component of the PRC2 methyltransferase (Popov and Gil, 2010; Schwartz and Pirrotta, 2007), and the lysine demethylases 6A (KDM6A) and 6B (KDM6B) (Hyland et al., 2011; McLaughlin-Drubin et al., 2011).

Mechanistic studies of HPV-dependent effects on epigenetic regulators have primarily focused on altered expression of the p16 product of the *CDKN2A* locus, which is commonly found to be upregulated in HPV+ carcinomas (Klaes et al., 2001; Sano et al., 1998). Indeed, this HPV-specific upregulation of p16 is a clinically important surrogate marker of HPV status (Burd, 2016; Hoffmann et al., 2010; Klaes et al., 2001). The *CDKN2A* locus encodes for p16 and p14 which are negative regulators of the cell cycle (Zhang et al., 1998). Importantly, transcription from this locus is tightly regulated at the epigenetic level, with the methyltransferase PRC2 serving a key role in its repression by catalyzing the tri-methylation (me3) of H3K27 across the entire genomic region. This is followed by the subsequent recruitment of another methyltransferase, PRC1, that maintains the chromatin in a transcriptionally repressive state by increasing local DNA methylation (Popov and Gil, 2010). Therefore, this well-characterized locus serves as an important model of HPV-induced epigenetic dysregulation (Kanao et al., 2004; Schlecht et al., 2015).

As indicated above, the detailed series of experiments that have mechanistically unraveled the epigenetic changes induced by HPV E7 on the tightly regulated *CDKN2A* and adjacent *CDKN2B* loci have been elucidated in 2-dimensional *in vitro* culture systems (McLaughlin-Drubin et al., 2011; McLaughlin-Drubin et al., 2013). While these cell culture-based experiments have allowed for a detailed elucidation of the biological factors involved in

HPV-mediated upregulation of p16, an analysis of these HPV-specific epigenetic effects has not been done in any HPV+ head and neck carcinomas or on large cohorts of any HPV-induced cancers. Therefore, my objective was to determine if the epigenetic changes involved in p16 upregulation observed in artificial culture systems were recapitulated in actual primary HPV+ tumors from different anatomical locations.

I began this work by developing an initial database of genomic and transcriptomic data that would serve as the basis for this and subsequent studies presented within my thesis. I downloaded normalized RNA expression data for the TCGA head and neck cancer (HNSC) and cervical carcinoma (CESC) cohorts from the Broad Genome Data Analysis Centers Firehose server. Importantly, HPV status was manually curated based on published datasets (Banister et al., 2017; Bratman et al., 2016; The Cancer Genome Atlas Research Network, 2015; The Cancer Genome Atlas Research Network, 2017). Primary patient samples with known HPV status were grouped as HPV+, HPV–, or normal-adjacent control tissue. Patient samples with unknown HPV status were omitted from my calculations, as were samples obtained from secondary metastatic lesions. This resulted in 73 HPV+, 442 HPV–, and 43 normal-adjacent control samples for the HNSC cohort and 278 HPV+, 19 HPV–, and 3 normal-adjacent control samples for the CESC cohort. For all genes analyzed in this thesis, with the exception of *p16* and *p14*, the gene level Firehose dataset was used. For *p16* and *p14*, the gene isoform level Firehose dataset was used to discriminate between these two different products of the *CDKN2A* locus.

In Chapter 2, I began by analyzing the entire *CDKN2A* and adjacent *CDKN2B* loci that encode for the tumor suppressors p16, p14, p15, and the non-coding RNA *CDKN2B-AS*. During normal cell growth and development, expression of genes from this cluster are silenced by PRCs through their catalyzation of methyl groups on lysine 27 of histone 3 (Popov and Gil, 2010). As mentioned above, HPV-induced cancers commonly express high levels of *p16* (Klaes et al., 2001; Sano et al., 1998). In contrast, the expression levels of the other products of this locus, and the adjacent *CDKN2B* locus—*p14*, *p15*, and the non-coding *CDKN2B-AS*—have not been studied as extensively. I therefore utilized my curated database of transcriptomic data from the TCGA to analyze the expression of the 4 genes from the aforementioned loci in both the HNSC and CESC cohorts. As expected,

HPV+ samples from both cohorts had greatly increased levels of *p16* mRNA expression compared to HPV– tumors and normal control tissue. Like *p16*, a similar upregulation of *p14*, *p15*, and *CDKN2B-AS* was observed in HPV+ cancers with respect to their HPV– counterparts. These results led me to conclude that PRC-mediated repression was abrogated across the entire *CDKN2A* and adjacent *CDKN2B* genomic regions as a result of infection by HPV.

Based on the above observations, I wanted to analyze the impact of HPV oncogene expression on the core components of the methyltransferases, PRC2 and PRC1. A straightforward mechanistic explanation of the observed increase of expression from the *CDKN2A* and *CDKN2B* loci in HPV+ cells would be a decreased expression of the core proteins necessary for mediating the methyltransferase activity of PRC2 and PRC1 on H3K27. Interestingly, tissue culture experiments have shown that expression of EZH2 to be increased by the presence of HPV oncogenes, while no significant changes were observed for the EED and SUZ12 core component proteins (Hyland et al., 2011; McLaughlin-Drubin et al., 2011). Furthermore, other cell culture experiments have shown that BMI1, a core component of PRC1, is reduced in human foreskin keratinocytes (HFKs) transduced with E6 and E7. My analysis revealed that all 4 core components of both PRC2 and PRC1 were expressed at levels higher or equivalent to HPV– samples or normal control tissues, with the exception of *BMI1* in the CESC cohort. These results led me to conclude that the increased expression observed in the HPV+ cohorts from the *CDKN2A* and *CDKN2B* loci were not due to a reduction in the overall levels of the core components that form the PRC2 and PRC1 methyltransferases, respectively.

I next looked for an alternative method of activating the *CDKN2A* and *CDKN2B* loci. Since I previously looked at the enzymes responsible for catalyzing the repressive methyl groups onto lysine 27 of histone 3, I therefore wanted to look at the enzymes responsible for the removal of the repressive H3K27me3 modification catalyzed by PRCs. Indeed, these histone modifications are erased by the KDM6A and KDM6B demethylases (Dawson and Kouzarides, 2012). Previous work in tissue culture models established that transduction of HPV E7 into HFKs induced increases in the levels of KDM6A and/or KDM6B mRNA and protein (Hyland et al., 2011; McLaughlin-Drubin et al., 2011). Importantly, siRNA

knockdown of KDM6B antagonized p16 induction by E7, suggesting that upregulation of these demethylases is the mechanism by which HPV reduces global H3K27me3 levels and activates p16 expression (McLaughlin-Drubin et al., 2011; McLaughlin-Drubin et al., 2013). My analysis concluded that *KDM6A* expression was significantly increased in HPV+ samples from both the HNSC and CESC cohorts with respect to their HPV– counterparts and normal control samples. However, this was not the case for *KDM6B*, which was found to be reduced in HPV+ samples compared to HPV– and normal control tissues from both cohorts. These results support the model proposed from tissue culture experiments, in which enhanced expression of KDM6A, but not KDM6B, by HPV is correlated with the dysregulation of H3K27me3 homeostasis and subsequent activation of transcription from the *CDKN2A* and *CDKN2B* loci in both these cancer types.

Since HPV-mediated changes in epigenetic regulation of transcription of genes encoded by *CDKN2A* and *CDKN2B* would be reflected in the methylation-status of CpG dinucleotide sequences in or adjacent to these loci. I therefore sought to analyze the Infinium Human Methylation450 BeadChip array data for the TCGA HNSC and CESC cohorts for consistent alterations in DNA methylation in this region of the genome. My analysis of methylation data revealed that there were two consistent alterations in DNA methylation relative to methylation levels present in HPV– tumors and normal control tissues. Specifically, a region of DNA upstream of the *p14* transcript was consistently identified to be hypomethylated in HPV+ carcinomas of both cohorts. Importantly, genome-wide studies have clearly indicated that methylation in the immediate vicinity of the transcription start site blocks initiation (Jones, 2012). As such, the greatly reduced methylation in HPV+ samples at this region is fully consistent with enhanced *CDKN2A* expression. In contrast, I also observed a hypermethylated region of DNA within the 3'-end of the *CDKN2A* locus in HPV+ tumors regardless of their anatomical origins. Indeed, hypermethylation at this location has been described in other studies of HPV+ head and neck and cervical carcinomas using alternative probes (Ben-Dayan et al., 2017; Schlecht et al., 2015; Wijetunga et al., 2016). These studies have established that *p16* and *p14* expression in a given tumor sample is strongly correlated with increased methylation at this position in the *CDKN2A* locus (Ben-Dayan et al., 2017; Schlecht et al., 2015). Therefore, along with promoter hypomethylation, gene-body methylation correlates well

with the observed enhanced transcription from the *CDKN2A* locus, providing further support for an epigenetic mechanism as the basis for HPV-mediated induction of expression from this locus.

Epigenetic reprogramming induced by HPV should be reversible and could represent a unique and useful therapeutic target. Indeed, cervical carcinoma cell lines or other tumor cell lines expressing HPV E7 from HR HPVs appear to require continuous *p16* expression for survival (McLaughlin-Drubin et al., 2011; McLaughlin-Drubin et al., 2013). Although p16 normally serves as a tumor suppressor, it becomes necessary for continued growth in cells expressing E7. Since HPV+ cells require KDM6 demethylase activity to maintain p16 expression, therefore they are sensitive to small molecule inhibitors of KDM6 in cell culture models (McLaughlin-Drubin et al., 2011; McLaughlin-Drubin et al., 2013). Notably, it has not been determined if actual primary HPV+ head and neck or cervical carcinomas will respond similarly. My analysis of the epigenetic regulators that control *p16* expression finds many commonalities between the hundreds of tumors making up the TCGA HNSC and CESC cohorts compared to *in vitro* cell culture models. Therefore, these observations strongly suggest that testing of KDM6 inhibitors should be aggressively pursued as a novel therapy against HPV+ cancers.

Taken together, my analysis of over 350 HPV+ head and neck or cervical carcinomas in comparison with over 450 HPV– cancers from their respective anatomical sites validates conclusions drawn from artificial 2-dimensional *in vitro* culture models and identifies remarkable similarities between the effects of HPV on gene expression and methylation in large human cohorts from two anatomically distinct regions. Furthermore, these results also showcase the profound differences in the epigenetic landscape between the tumor microenvironments of HPV+ and HPV− carcinomas. In addition, the findings in this study strongly advocate for the testing of KDM6 inhibitors in actual human malignancies caused by infection with HPV.

6.3 Immune Landscape of HPV+ Tumor Microenvironments

6.3.1 Impact of HPV on the MHC-I antigen presentation network

In Chapter 3, I wanted to use the same computational methodology utilized in Chapter 2 to validate another important model of HPV-mediated sabotage that was proposed from artificial *in vitro* tissue culture studies. Indeed, multiple studies have suggested that HPV oncoproteins contribute to the evasion of the adaptive immune response, which supports a model by which the establishment of a persistent HPV infection contributes to the ability of HPV+ cancers to evade antitumor immune responses (Westrich et al., 2017). Specifically, transfection of HR HPV E7 into various cell lines has been shown to repress MHC-I and/or TAP expression (Georgopoulos et al., 2000; Heller et al., 2011; Li et al., 2010). Furthermore, reciprocal studies have also shown that the knockdown of E7 in some HPV+ cervical cancer cell lines increases MHC-I expression (Bottley et al., 2008; Li et al., 2006). Mechanistically, these *in vitro* studies proposed that the reduction of MHC-I and TAP occur at the transcriptional level (Georgopoulos et al., 2000; Heller et al., 2011; Li et al., 2010).

While the majority of published studies using tissue culture models indicate that HPV E7 represses the expression of MHC-I, related studies on the effects of HPV in actual human carcinomas are less consistent. Indeed, conflicting reports have suggested that HPV+ carcinomas and/or precancerous lesions display increased, decreased, or the same levels of MHC-I or TAP when compared to their HPV− counterparts or normal control tissues. (Cromme et al., 1993; Djajadiningrat et al., 2015; Jochmus et al., 1993; Keating et al., 1995; Ramqvist et al., 2015; Ritz et al., 2001; Torres et al., 1993; van Esch et al., 2014). I therefore utilized my curated database of transcriptomic data from over 800 human cervical and head and neck carcinomas, to assess the impact of HPV status on the expression of MHC-I heavy chain genes, the β2 microglobulin light chain gene, and other components of the MHC-I antigen presentation network.

I began by analyzing the expression of both the classical (*HLA-A, -B,* and *-C)* and non-classical (*HLA-E, -F,* and *-G*) heavy chain genes, as well as the invariant *β2 microglobulin light chain* (*B2M*) that comprises the MHC-I heterodimer (Hansen and Bouvier, 2009).

Unexpectedly, the expression levels of the 3 classical heavy chain genes were significantly higher compared to normal control tissues in the HNSC cohort. However, those levels were significantly lower than those observed in the HPV– samples. Furthermore, the expression levels of the non-classical heavy chain genes were higher or comparable to normal control tissues. As noted by others (Cicchini et al., 2017), *HLA-E* was expressed at significantly reduced levels in HPV+ samples compared with HPV− samples in the HNSC cohort only. Moreover, the classical and non-classical heavy chain genes in the CESC cohort were expressed at levels significantly higher in HPV+ samples compared to their HPV– counterparts. However, the comparison between HPV+ and normal control samples in the CESC cohort were insufficiently powered to allow for proper conclusions. In addition, the *B2M* light chain gene in both cohorts was expressed in HPV+ carcinomas at levels higher or comparable to HPV– samples. Collectively, these results indicate that the expression of HPV oncogenes in actual human tumors is not correlated with strong repression of genes encoded by the MHC-I loci, which is in stark contrast to what has been reported in tissue culture-based models. Indeed, the average expression of the mRNA for these genes was consistently higher or equivalent in HPV+ samples versus their respective controls.

Next, I wanted to analyze the expression of key components involved in MHC-I-specific antigen loading and presentation that includes the heterodimer peptide transporter TAP (*TAP1/2*), the bridging factor tapasin (*TAPBP*), the endoplasmic reticulum aminopeptidase (*ERAP1/2*), and the chaperones: calreticulin (*CALR*), calnexin (*CANX*), and ERp57 (*PDIA3*). As mentioned above, several studies have reported the downregulation of TAP in HPV+ cancer cell lines (Georgopoulos et al., 2000; Li et al., 2010). However, much less is known about the effect of HPV on the expression of these other components. In the HNSC cohort, all genes were expressed at higher levels in HPV+ samples with respect to normal control tissues, with the exception of *CANX*. In the CESC cohort, nearly all of these genes were expressed at elevated or comparable levels to HPV– or normal control tissues, although some comparisons were limited due to being insufficiently powered. Therefore, most components of the MHC-I antigen loading and presentation complex were transcribed in HPV+ human tumors at levels that appear similar or significantly higher than normal control tissues. This again contrasts with the reported decreases in *TAP* transcription reported in tissue culture models.

These unexpected results contradict the existing paradigm of HPV-mediated immune evasion and suggest that in the context of an actual human tumor setting, the presence of HPV may actually result in enhanced expression of mRNA encoding MHC-I-specific antigen loading and presentation components. Notably, these results illustrate the limitations of utilizing tissue culture systems to infer on complex networks. The use of *in vitro* 2-dimensional approaches are useful as a launching point into many hypothesis-driven research initiatives; however, their utility in tumor virology—as exposed in this study—can be limited, primarily due to the platforms lack of cellular heterogeneity. Indeed, this cellular heterogeneity that exemplifies tumor microenvironments is a fundamental characteristic of actual human cancers and plays a significant role in influencing the complex interacting biochemical systems of these malignant cells. Specifically, expression of MHC-I and related genes can be induced by proinflammatory mediators that are produced by infiltrating immune cells that create an inflammatory state within the tumor microenvironment (Boehm et al., 1997). However, this would never be recapitulated in studies that simply transfect cell lines with HR HPV oncogenes without exposing them to proinflammatory mediators (Georgopoulos et al., 2000; Heller et al., 2011; Li et al., 2010).

Given my observation that mRNA levels of all MHC-I antigen loading and presentation genes were expressed at higher or at least similar levels in HPV+ tumors compared with HPV− and normal control tissues, I hypothesized that infiltrating lymphocytes producing IFNγ—a proinflammatory cytokine—could be present at higher levels in HPV+ tumors compared to HPV− tumors or normal control tissues. Utilizing an immunogenomic approach with surrogate markers, I found evidence for significant infiltration by T- and NK-cells in both HPV+ and HPV− carcinomas. Indeed, the levels of infiltrating T-cells were significantly higher in HPV+ compared to their HPV– counterparts in both cohorts. In addition, my analysis also revealed significantly higher levels of IFNγ in HPV+ samples in both the HNSC and CESC cohorts. Taken together, these results indicate that HPV+ carcinomas have a significant level of infiltrating lymphocytes that appear to be producing IFNγ, which may explain the upregulated expression of the genes involved in MHC-I antigen loading and presentation observed in these carcinomas.

Taken together, the high absolute levels of mRNAs encoding MHC-I components expressed in HPV+ head & neck and cervical carcinomas provide good evidence that HR HPV E7 is unable to efficiently block the IFNγ induction of transcription of these genes in actual human tumors. Although this contrasts with the results of the studies listed above, my work agrees with other studies showing that various cervical cancer cell lines upregulate MHC-I in response to IFNγ (Bornstein et al., 1997; Evans et al., 2001; Mora-Garcia Mde et al., 2006). Importantly, it should be noted that the levels of MHC-I heavy chain mRNAs are statistically lower in HPV+ compared to HPV− samples in the HNSC cohort, despite the increased levels of IFNγ. This may indicate that HPV is able to modestly impact IFNγ activation in these tissues, but this was not observed in the CESC cohort. In addition, this work differs markedly from my previous study in Chapter 2, in which I showed that tissue culture models faithfully recapitulate what is observed in actual human tumors. This may be due to the intrinsic nature of the pathways analyzed, with the MHC-I network being amenable to influence by immune cells infiltrating into the local environment.

6.3.2 Impact of HPV on the immune status of head and neck tumor microenvironments

Given the observation in Chapter 3 of higher levels of intratumoral IFNγ and increased infiltration by T- and NK-cells into the HPV+ TME, a mechanistic and detailed characterization of immune cell presence and status between the 2 anatomically-similar, etiologically-different head and neck cancer types were warranted. In Chapter 4, I used transcriptional data from my curated dataset of over 500 HNSC samples from the TCGA to compare the immune landscape between HPV+ and HPV– samples. Importantly, the corresponding analysis could not be done in the TCGA CESC cohort because of limitations in the number of HPV– and normal control samples in this dataset. In addition, these samples were treatment-naïve prior to surgical resection, avoiding any confounding effects of exposure to chemotherapy or radiation on the immune-status of these tumors.

Both HPV+ and HPV– HNSC display a similar frequency of somatic mutations, a major source of tumor specific neoantigens that can be recognized and targeted by antitumor immunity (The Cancer Genome Atlas Research Network, 2015). However, unlike HPV–

HNSC, HPV+ carcinomas express exogenous antigenic viral proteins that may contribute to the initial differences observed in Chapter 3 in the levels of infiltrating immune cells between these 2 types of HNSC. Indeed, several studies have compared various immunological parameters between HPV+ and HPV– HNSC and have commonly concluded that HPV+ HNSC are immune "hot" tumors, with markedly more immune infiltration and higher levels of $CD8^+$ T-cell activation than HPV– HNSC (Mandal et al., 2016; Solomon et al., 2018). Importantly, these and other studies suggest that a detailed comparison of the immunological differences between HPV+ and HPV– HNSC provides an opportunity to identify immunological determinants that contribute to successful treatment in HNSC that may be broadly applicable to cancer treatment in general (Feng et al., 2017; Lyford-Pike et al., 2013; Montler et al., 2016).

I began my investigation by comparing the type of immune response generated in HPV+ HNSC compared to its HPV– counterpart. Specifically, $CD4^+$ helper T-cells are instrumental in establishing the type of response triggered by immune activation, whether it be a cell-mediated Th1 response, a humorally-biased Th2 response, or the proinflammatory Th17 response necessary to maintain the immunological integrity of mucosal barriers (Mucida and Salek-Ardakani, 2009). Each of the $CD4^+$ subsets is characterized by a distinct transcriptional program regulated by specific master regulatory transcription factors (Fang and Zhu, 2017). Therefore, I analyzed my HNSC cohort from the TCGA for the expression of the following master regulatory transcription factors and the immune response they dictate: *TBX21* (Th1), *GATA3* and *STAT6* (Th2), and *RORA* and *RORC* (Th17). I found that HPV+ samples had significantly increased levels of *TBX21* compared to HPV– and normal control tissues, which was indicative of a predominant Th1 immune phenotype.

Based on the observation that the HPV+ HNSC tumor microenvironment was characterized by a predominant Th1 cellular-mediated response and the observation in Chapter 3 of increased infiltration by T-cells into the HPV+ TME, I wanted to assess the relative proportion of $CD4^+$ and $CD8^+$ T-cells in these samples. Utilizing an immunogenomic approach, I analyzed the lineage-defining markers *CD4* and *CD8A*/*CD8B*. As expected, HPV+ samples showed significantly increased expression of

all 3 genes compared to HPV– or normal control samples, confirming that enhanced T-cell infiltration is a common feature of HPV+ HNSC. Furthermore, I also observed significantly higher *FOXP3* expression—associated with regulatory T-cells (Tregs)—in HPV+ HNSC. Moreover, analysis of the expression of *CD137* (4-1BB), an activation-induced costimulatory molecule present primarily on $CD8^+$ T-cells, detected significantly higher levels in HPV+ compared to their HPV– counterparts or normal control samples, suggesting a higher overall level of T-cell activation and effector function in HPV+ malignancies. In addition, given the high levels of *CD137* RNA in HPV+ HNSC samples, I expected higher effector cytokine production by T-cells in these samples. Indeed, as previously shown in Chapter 3, HPV+ HNSC expressed significantly higher levels of IFNγ. Furthermore, HPV+ HNSC tumors also expressed significantly higher levels of cytotoxic mediators, including granzyme A (*GRZA*), granzyme B (*GRZB*), and perforin (*PRF1*) compared to both HPV– HNSC or normal control tissues. Taken together, these results indicate that T-cells are not only present at higher levels in HPV+ HNSC, but also appear more active and likely producing effector molecules.

An expected consequence of higher levels of infiltrating $CD8^+$ T-cells producing IFNγ would be induction of expression of interferon-responsive genes in tumor cells in close proximity to the infiltrating T-cells. Indeed, in Chapter 3, I reported that multiple interferon responsive components of the MHC-I antigen presentation apparatus were upregulated in HPV+ HNSC. I therefore wanted to extend my studies to *PDL1* and *IDO1,* which are immunomodulatory genes known to be expressed by tumor cells in response to IFNγ. Both *PDL1* and *IDO1* were significantly upregulated in HPV+ HNSC compared to normal control samples. Notably, these observations provide a scientific rationale for combining immunotherapy of HPV+ HNSC with immune checkpoint and IDO inhibitors in treatment-naïve patients.

Based on the observed increase in the number of infiltrating $CD8^+$ and $CD4^+$ T-cells into the TME of HPV+ HNSC, I hypothesized that this could be explained by the presence of a dendritic cell (DC) signature in these tumors. Indeed, DCs play an important role in migrating into these tumors, phagocytosing antigens, and presenting them to T-cells in the context of MHC-II (Spranger et al., 2015). Therefore, I performed an analysis of DC

signatures in these tumors, utilizing mRNA associated with DCs, as well as molecules expressed by activated DCs that include chemokines that are pivotal in attracting them into the TME. In my analysis, I observed high levels of transcripts from DC-associated genes, but also high levels of molecules expressed by activated DCs, such as chemokines, in HPV+ HNSC. Overall, these results indicate a higher level of DC involvement in HPV+ compared to HPV– HNSC, with higher levels of effector cytokines that could be responsible for the elevated levels of T-cell infiltration into the TME of these samples.

T-cell-inflamed tumors show high levels of immune regulatory genes including *IDO1* and *PDL1*, and high infiltration of FoxP3+ Tregs (Gajewski et al., 2017), secondary to cytotoxic T-cell infiltration into the TME. The presence of these immunosuppressive events in a T-cell-inflamed microenvironment is often accompanied by increased levels of multiple T-cell immune checkpoint molecules indicative of T-cell anergy. Indeed, once activated, T-cells upregulate expression of multiple cell surface receptors that negatively regulate their proliferation and moderate their level of activation. These so-called "exhaustion markers" include LAG3, PD1, TIGIT, and TIM3 (Anderson et al., 2016). Notably, they are important targets for immune checkpoint blockade therapies that are currently approved or under development. My analysis revealed that all 4 of these checkpoint genes were significantly upregulated in HPV+ HNSC compared to HPV– or normal control samples. In addition, I also examined the expression of the immunosuppressive molecule CD39 (Jie et al., 2013), which was recently shown to be exclusively expressed on tumor antigen-specific $CD8^+$ T-cells and not bystander $CD8^+$ T-cells in colorectal and lung tumors (Simoni et al., 2018). My analysis showed significantly higher *CD39* RNA expression levels in HPV+ HNSC tumors compared to HPV– or normal control samples. Collectively, my results indicate that HPV+ HNSC display a markedly different immune signature from HPV– HNSC, revealing sustained $CD8^+$ T-cell activation in HPV+ HNSC. Furthermore, these observations provide a mechanistic insight into the processes that shape the immune structure of HPV+ HNSC as a T-cell-inflamed tumor. Moreover, they also suggest that combined immunotherapy with drugs that target more than one of these inhibitory molecules have potential to be effective in overcoming resistance to antitumor immunity in HPV+ HNSC tumors. Interestingly, there are no such trials currently under way, but these findings strongly indicate that initiation of such

clinical studies are justified once elevated protein levels are confirmed in a secondary validation cohort.

High T-cell infiltration into HNSC, regardless of HPV status, has been reported as a positive prognostic factor (Nguyen et al., 2016). Moreover, expression of checkpoint molecules such as PD1 on circulating $CD8^+$ T-cells is a biomarker of tumor antigen specificity (Gros et al., 2016). I therefore analyzed 5-year overall survival outcomes in both HPV+ and HPV– subsets of patients dichotomized by median expression of *LAG3*, *PD1*, *TIGIT*, *TIM3*, or *CD39*. Furthermore, a second set of survival outcomes were done to compare tumors expressing high levels of each combination of 2 of these markers. I observed that high levels of transcripts from 1 or any combination of 2 genes expressing immune checkpoint molecules (*PD1*, *TIM3*, *TIGIT*, *LAG3*) or *CD39* in HPV+, but not HPV–, HNSC can predict patient survival after surgery. Collectively, these results suggest that the co-expression of high levels of *CD39*, *LAG3*, *PD1*, *TIGIT*, and *TIM3* in HPV+, but not HPV–, HNSC reflect the successful development of T-cell-based antitumor immunity and a T-cell-inflamed phenotype, which contributed to long-term remission. This immune signature could be used as a predictive biomarker of HPV+ HNSC patient outcome after surgery. However, these findings require confirmation by prospective clinical studies to pave the way for the development of immune-predictive biomarkers for HPV+ HNSC patients that may ultimately lead to treatment deintensification in this patient population.

I next applied the Cox Proportional Hazards Model to identify clinical variables (sex, age, smoking history, subsite, T stage, N stage, Overall stage, and HPV type) and immunological markers predictive of overall survival. By univariate analysis, high expression of *TIGIT*, *TIM3*, *PD1*, and *CD39* were correlated with favorable prognosis (HzR = 0.29, 0.24, 0.22, and 0.15 respectively, $p < 0.05$), while an HPV type other than HPV16 was associated with a markedly poorer survival (HzR = 3.22, $p = 0.03$). Furthermore, oral cavity tumors had significantly worse survival compared to those in the oropharyngeal subsite (HzR = 3.05, $p = 0.03$). In addition, stepwise bidirectional multivariate analysis was used to identify the best multivariate model of survival, and the final model included N stage, HPV type, and *CD39*. Notably, *CD39* (HzR = 0.07, $p =$

0.0007), and HPV type (HzR = 9.23, p = 0.001) remained as significant predictors of survival in this multivariate model.

Taken together, this study provides comprehensive evidence that the immune landscape of HPV+ HNSC represents a T-cell-inflamed phenotype that is very different from HPV– HNSC. Importantly, I demonstrate that multiple mechanisms that negatively regulate the antitumor immune response are significantly upregulated in the majority of HPV+ HNSC cases. Furthermore, high levels of gene transcripts from these negative regulators—*CD39, PD1*, *TIM3*, *LAG3*, and *TIGIT*—correlate strongly with improved clinical outcome. Notably, many of these negative regulators of the immune response are targets of clinically-approved immune checkpoint inhibitors or inhibitors currently under investigation in clinical trials. Therefore, HPV+ HNSC has many immunological features that suggest that it would be highly amenable to immune checkpoint inhibition therapy. Based on this study, I propose that HPV+ HNSC is a T-cell-inflamed disease and should be treated differently in the clinic compared to HPV– HNSC, specifically with combinations of immune checkpoint inhibitors.

6.3.3 Impact of HPV on the MHC-II antigen presentation network

In the previous chapters, I have noted significant differences in the epigenetic and immune landscapes between the tumor microenvironments of HPV+ and HPV− carcinomas. Furthermore, other studies have also concluded that HPV+ tumors are distinct from their HPV– counterparts from a molecular perspective, with distinct genetic, epigenetic, and protein expression profiles (Seiwert et al., 2015; Sepiashvili et al., 2015; Worsham et al., 2013). Moreover, in Chapter 4, I have also shown that HPV+ HNSC is a T-cell-inflamed malignancy, with increased infiltration by T-cells that express high levels of *CD39* and multiple exhaustion markers that correlated with improved survival. In order for an effective T-cell-specific antitumor response to occur, a tumor associated antigen must be presented in the context of either MHC-I or MHC-II (Rock et al., 2016). Indeed, in Chapter 3, I reported that HPV+ cancers express high levels of MHC-I and that this observation could be a consequence of the increased levels of intratumoral IFNγ present in the HPV+ TME. While expression of MHC-II molecules is typically restricted to professional APCs, such as DCs, macrophages, and B-cells (van den Elsen et al., 2004), epithelial cells can be

stimulated by IFNγ to express MHC-II and function as accessory APCs to stimulate T-cell responses (Boss and Jensen, 2003; Collins et al., 1984; Kim et al., 2009). In this final chapter, I sought to determine the impact of HPV status on the expression of MHC-II genes and related genes involved in their regulation, antigen presentation, and T-cell co-stimulation by analyzing my large HNSC cohort from the TCGA.

I began by analyzing my large HNSC transcriptomic dataset for expression of the α- and β-chain genes that form the classical MHC-II heterodimers on the cell surface (van den Elsen et al., 2004). Uniformly, all HPV+ patient samples expressed significantly higher levels of mRNA for all MHC-II genes analyzed compared to HPV− patient samples and virtually all normal control tissues. Notably, the normalized read levels of these genes were expressed at levels several orders of magnitude above any lineage-defining markers of professional APCs, such as *CD19* (B-cells) (Wang et al., 2012), *CCL13* (DCs) (Danaher et al., 2017), and *CD84* (macrophages) (Zaiss et al., 2003). However, these normalized read levels were comparable to that of an established epithelial cell marker, E-cadherin (*CDH1*) (Gall and Frampton, 2013). Therefore, it is likely that these MHC-II genes are being expressed by epithelial cells within the actual tumor. Collectively, these results indicate that HPV+ head and neck tumors express high levels of the mRNAs encoding the α- and β-chain heterodimers of the classical MHC-II molecules, providing key evidence that epithelial cells could be functioning as accessory APCs.

Next, I wanted to analyze the genes encoding key components of the MHC-II presentation pathway. Specifically, I analyzed the non-classical α- and β-chains and the invariant γ chain that are required for proper MHC-II antigen loading and trafficking. Similar to the classical MHC-II genes, HPV+ samples expressed significantly higher levels of the invariant chain and MHC-II-like genes compared to their HPV− counterparts and normal control tissues. Collectively, the upregulation of these genes suggests that key components of the MHC-II antigen presentation pathway are transcribed in HPV+ HNSC at levels that are significantly higher than observed in HPV− tumors or normal control tissues. Furthermore, these genes are also expressed at very high levels, indicative of being expressed by epithelial cells within the actual tumor.

Based on the observations that HPV+ head and neck carcinomas display high mRNA levels for virtually all MHC-II genes analyzed above, I wanted to assess the impact of HPV on the expression of transcriptional regulators of MHC-II gene expression. Transcriptional control of MHC-II genes and the related genes that encode key components of the MHC-II antigen presentation pathway is among one of the best understood systems in mammals. It is a complex transcriptional system with a unique method of regulation that is completely dependent on the master transcriptional regulator CIITA (Boss and Jensen, 2003; van den Elsen, 2011). Analysis of the TCGA data revealed significantly higher levels of *CIITA* in HPV+ samples compared to HPV− or normal control tissues. In addition, *RFX5*—another important transcriptional regulator of MHC-II genes (Boss and Jensen, 2003)—was similarly expressed at significantly higher levels in HPV+ samples with respect to HPV− tumors or normal control tissues.

In Chapters 3 and 4, I showed that HPV+ carcinomas had increased levels of intratumoral IFNγ, which as mentioned above, is able to stimulate the expression of MHC-II genes in epithelial cells. To illustrate this IFNγ-specific coordinated upregulation of MHC-II genes and related genes that encode products essential for antigen processing and presentation, I generated a correlation matrix for both HPV+ and HPV− samples. As expected, regardless of HPV status, I found that expression of all MHC-II antigen presentation-specific genes were statistically correlated in a pairwise fashion in each patient sample. Therefore, the upregulated expression of *CIITA*, *RFX5*, and subsequent expression of all the classical MHC-II genes and related genes required for antigen loading and presentation observed in HPV+ head and neck carcinomas are likely a consequence of IFNγ exposure. Furthermore, the correlation matrix illustrates the unique simultaneous coordination of the MHC-II transcriptional control system that has been shown to be dictated by the master transcriptional regulator CIITA (Boss and Jensen, 2003; van den Elsen, 2011).

Next, I wanted to assess the impact of HPV on the expression of T-cell co-stimulatory molecules. After generation and programming in the thymus, $CD8^+$ and $CD4^+$ T-cells circulate in the body until they encounter their specific antigen presented on either class I or class II MHC molecules. (Luckheeram et al., 2012; Pennock et al., 2013; Zhang and Bevan, 2011). This interaction between TCR and antigen-loaded MHC complex represents

signal 1, which triggers the activation of T-cells. However, in order for the activated T-cell to fully respond to the presented threat, it requires a secondary signal mediated by co-stimulatory molecules (Chen and Flies, 2013). My analysis found higher levels of *CD28* in HPV+ tumors compared to their HPV− counterparts and normal control tissues. It is well established that the binding of T-cell-specific CD28 with either CD80 or CD86 leads to the clonal expansion of the T-cell pool that is specific to the recognized antigen (Beier et al., 2007; Chen and Flies, 2013). In order to attenuate this response, the aforementioned interaction leads to the induction of the co-inhibitory molecule CTLA-4, which is encoded by the gene *CD152*. This co-inhibitory molecule will then compete with CD28 for binding to either CD80 or CD86 to attenuate the T-cell response (Chen and Flies, 2013; Rudd et al., 2009). I found that *CD152* was significantly upregulated in the HPV+ cohort. Collectively, this data indirectly illustrates and further confirms what has been shown in previous chapters, that HPV+ tumor microenvironments have a higher number of infiltrating T-cells. In addition, it provides good evidence that the interaction of co-stimulatory molecules in HPV+ HNSC is effective, given that I detected significantly higher levels of expression of *CD152* mRNA, which encodes for the inducible co-inhibitory molecule CTLA-4.

Finally, I wanted to look at the impact of HPV on the expression of activation-inducible T-cell survival molecules. In order for proliferating T-cells to persist and survive after antigen-recognition and subsequent stimulation with co-stimulatory molecules, they require survival signals that are delivered through the cross-linking of various molecules (Beier et al., 2007; Chen and Flies, 2013). Importantly, unlike CD28 that is found constitutively expressed on T-cells, the molecules that convey these survival signals are encoded by genes that are only expressed following TCR-mediated antigen-specific T-cell activation (Beier et al., 2007; Chen and Flies, 2013). Utilizing my HNSC dataset, I looked at these genes that encode for the inducible, T-cell activation-dependent, survival signal molecules. I found that all inducible T-cell survival genes analyzed, with the exception of *TNFSF9*, were expressed at significantly higher levels in HPV+ tumors compared to HPV− and normal control tissues. This data indirectly illustrates that the HPV+ tumor microenvironment contains increased levels of activated and proliferating T-cells via the observation of an increase in expression of genes that encode for survival signal molecules

that are only induced following TCR-mediated antigen-specific T-cell activation. Furthermore, these results agree with my previous work on the immune landscape (Chapters 3 and 4) and with previous reports by others that HPV+ tumor microenvironments contain more T-cells (Chen et al., 2018; Mandal et al., 2016; Nguyen et al., 2016; Solomon et al., 2018).

In summary, this final chapter provided further evidence that the HPV+ HNSC tumor microenvironments are remarkably different from their HPV− counterparts. Importantly, while some of this MHC-II signal can be attributed to professional APCs, the extremely high relative level of expression supports a model whereby the T-cell inflamed environment in HPV+ HNSC induces a functionally effective MHC-II presentation system based on tumor epithelial cells. As MHC-II-dependent antigen presentation is critical for $CD4^+$ help in $CD8^+$ T-cell responses, which are essential for the control and clearance of cancerous cells (Pluhar et al., 2015), it is likely that the expression of non-self-derived viral antigens or tumor derived neoantigens, combined with intact MHC-II presentation and appropriate co-stimulation, contributes to the markedly better patient outcomes observed for those with HPV+ head and neck carcinomas.

Taken together, the aforementioned studies profiled the immune landscape of HPV+ TMEs (Chapters 3–5) and illustrated a microenvironment that consisted of increased MHC-I and MHC-II expression that seemed to be induced from exposure to the proinflammatory cytokine IFNγ that is mainly produced by infiltrating T- and NK-cells. Furthermore, we observed an HPV+ TME that exhibited a strong bias towards a Th1 response which was characterized by increased infiltration with multiple types of immune cells and expression of their effector molecules. In addition, the HPV+ TME also expressed higher levels of multiple T-cell exhaustion markers that were indicative of a T-cell-inflamed phenotype. This predominantly immune “hot” HPV+ tumor microenvironment is summarized in the following proposed schematic model (**Figure 6.1**).

6.4 Limitations of Study Design

The use of transcriptomic “big” data acquired through next-generation “-omics” technologies from bulk tumor samples is a powerful approach that allows for an insightful

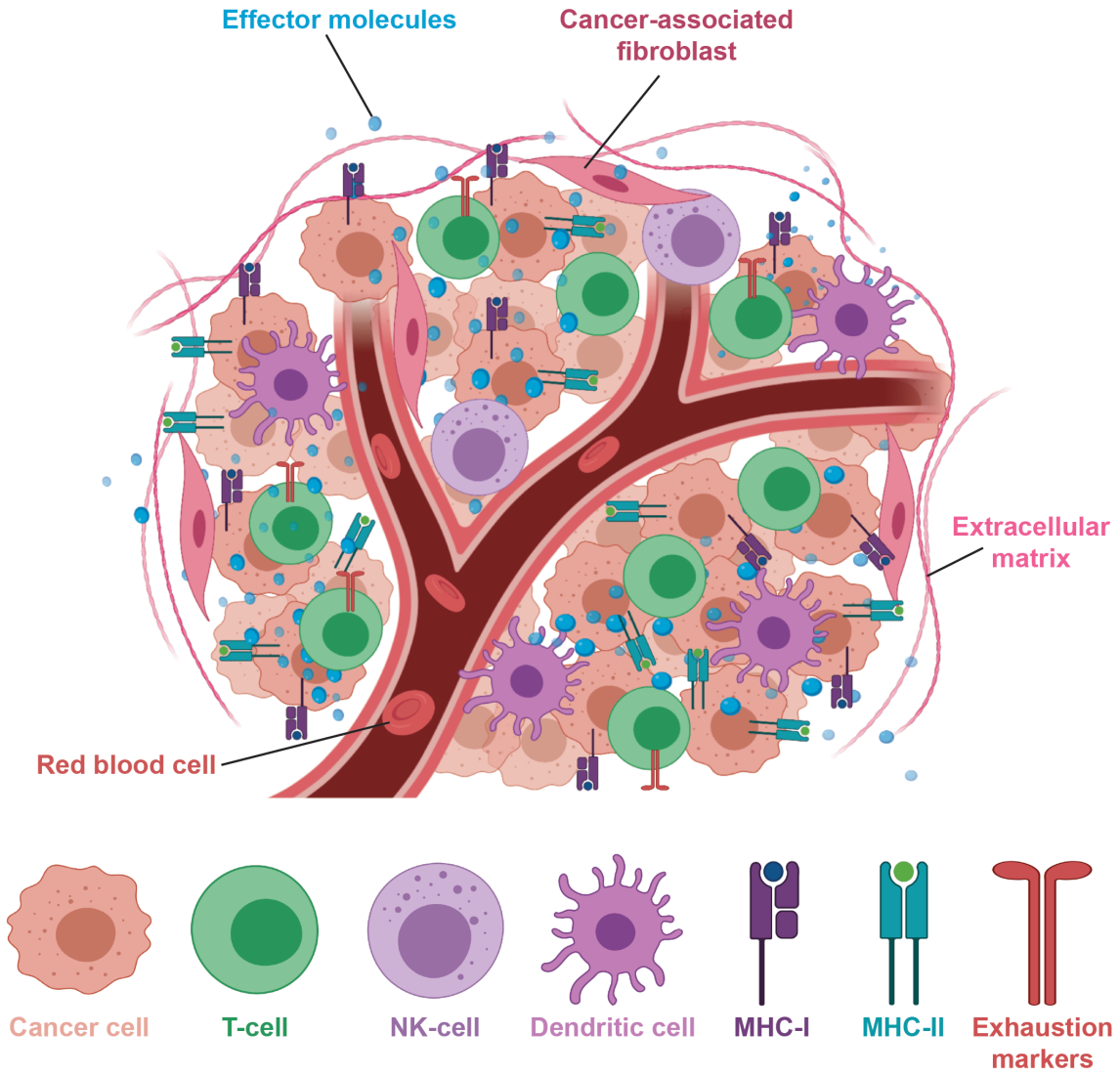

Figure 6.1. Proposed schematic model of an HPV+ tumor microenvironment. Schematic of an immune "hot" HPV+ tumor microenvironment that is characterized by an increase in expression of the MHC-I and MHC-II antigen presentation systems, infiltration with various immune cell subtypes, abundance of effector molecules, and upregulation of T-cell exhaustion markers. Created with BioRender.

elucidation of mechanistic processes under the influence of a native heterogeneous environment. However, this *in silico* method that has been employed in this body of work contains unavoidable limitations. The first limitation is the use of RNA-seq data acquired through bulk tissue RNA sequencing platforms. This bulk tissue method measures the mRNA expression levels of genes from an admixture of cells that include cancerous cells, fibroblasts, immune cells, endothelial cells, and normal-adjacent cells (The Cancer Genome Atlas Research Network et al., 2013). This could lead to confounding results where you have expression of certain genes that can be expressed by different cell types. However, in our study design, we looked at genes that have been shown to be expressed by specific cell types, such as those of the immune system. In terms of tumor purity, the TCGA consortium set a quality threshold that required tumor samples to be composed of at least 60% tumor nuclei, as determined by visual analysis (Aran et al., 2015). Another limitation is the lack of protein data in the TCGA cohorts to corroborate our mRNA analyses, which is important because mRNA expression does not always mirror their respective protein levels (Fortelny et al., 2017). Finally, as with any high throughput analysis, the cohorts used are susceptible to batch effects that result from data processing (Leek et al., 2010).

6.5 Concluding Remarks

In conclusion, these analyses provide significant insight into the validity of epigenetic and immunological models of HPV-mediated sabotage, which have been proposed from experiments conducted on relatively artificial *in vitro* culture systems. Importantly, these studies have illustrated, in great detail, the strikingly profound differences in both the epigenetic and immune landscapes between the tumor microenvironments of HPV+ and HPV– carcinomas. In addition, this body of work has also identified a potentially useful therapeutic target in KDM6A, and strongly advocates for the use of promising immunotherapy strategies in the treatment of HPV+ HNSC. Furthermore, I also show that expression of negative regulators of T-cell responses could potentially serve as predictive biomarkers of clinical outcomes that could allow for treatment deintensification for patients with favorable prognosis. Notably, the novel hypotheses that have been generated by this work can also feedback into the laboratory and allow for further exploration in an

experimental setting where relevant models, based on these studies, can be generated and biologically manipulated. Lastly, it is in my hope that the accumulated knowledge gained from this thesis will help advance the field of tumor virology and provide a positive clinical impact on patients who live their daily lives with the burden of these devastating HPV-induced malignancies.

6.6 References

Anderson AC, Joller N and Kuchroo VK. (2016) Lag-3, Tim-3, and TIGIT: Co-inhibitory Receptors with Specialized Functions in Immune Regulation. *Immunity* 44: 989-1004.

Aran D, Sirota M and Butte AJ. (2015) Systematic pan-cancer analysis of tumour purity. *Nat Commun* 6: 8971.

Banister CE, Liu C, Pirisi L, et al. (2017) Identification and characterization of HPV-independent cervical cancers. *Oncotarget* 8: 13375-13386.

Beier KC, Kallinich T and Hamelmann E. (2007) Master switches of T-cell activation and differentiation. *Eur Respir J* 29: 804-812.

Ben-Dayan MM, Ow TJ, Belbin TJ, et al. (2017) Nonpromoter methylation of the CDKN2A gene with active transcription is associated with improved locoregional control in laryngeal squamous cell carcinoma. *Cancer Med* 6: 397-407.

Boehm U, Klamp T, Groot M, et al. (1997) Cellular responses to interferon-gamma. *Annu Rev Immunol* 15: 749-795.

Bornstein J, Lahat N, Kinarty A, et al. (1997) Interferon-beta and -gamma, but not tumor necrosis factor-alpha, demonstrate immunoregulatory effects on carcinoma cell lines infected with human papillomavirus. *Cancer* 79: 924-934.

Boss JM and Jensen PE. (2003) Transcriptional regulation of the MHC class II antigen presentation pathway. *Curr Opin Immunol* 15: 105-111.

Bottley G, Watherston OG, Hiew YL, et al. (2008) High-risk human papillomavirus E7 expression reduces cell-surface MHC class I molecules and increases susceptibility to natural killer cells. *Oncogene* 27: 1794-1799.

Bratman SV, Bruce JP, O'Sullivan B, et al. (2016) Human Papillomavirus Genotype Association With Survival in Head and Neck Squamous Cell Carcinoma. *JAMA Oncol* 2: 823-826.

Burd EM. (2016) Human Papillomavirus Laboratory Testing: the Changing Paradigm. *Clin Microbiol Rev* 29: 291-319.

Cancer Genome Atlas Research N, Weinstein JN, Collisson EA, et al. (2013) The Cancer Genome Atlas Pan-Cancer analysis project. Nat Genet 45: 1113-1120.

Chen L and Flies DB. (2013) Molecular mechanisms of T cell co-stimulation and co-inhibition. *Nat Rev Immunol* 13: 227-242.

Chen X, Yan B, Lou H, et al. (2018) Immunological network analysis in HPV associated head and neck squamous cancer and implications for disease prognosis. *Mol Immunol* 96: 28-36.

Cicchini L, Blumhagen RZ, Westrich JA, et al. (2017) High-Risk Human Papillomavirus E7 Alters Host DNA Methylome and Represses HLA-E Expression in Human Keratinocytes. *Sci Rep* 7: 3633.

Collins T, Korman AJ, Wake CT, et al. (1984) Immune interferon activates multiple class II major histocompatibility complex genes and the associated invariant chain gene in human endothelial cells and dermal fibroblasts. *Proc Natl Acad Sci U S A* 81: 4917-4921.

Cromme FV, Meijer CJ, Snijders PJ, et al. (1993) Analysis of MHC class I and II expression in relation to presence of HPV genotypes in premalignant and malignant cervical lesions. *Br J Cancer* 67: 1372-1380.

Danaher P, Warren S, Dennis L, et al. (2017) Gene expression markers of Tumor Infiltrating Leukocytes. *J Immunother Cancer* 5: 18.

Dawson MA and Kouzarides T. (2012) Cancer epigenetics: from mechanism to therapy. *Cell* 150: 12-27.

Djajadiningrat RS, Horenblas S, Heideman DA, et al. (2015) Classic and nonclassic HLA class I expression in penile cancer and relation to HPV status and clinical outcome. *J Urol* 193: 1245-1251.

Durzynska J, Lesniewicz K and Poreba E. (2017) Human papillomaviruses in epigenetic regulations. *Mutat Res Rev Mutat Res* 772: 36-50.

Evans M, Borysiewicz LK, Evans AS, et al. (2001) Antigen processing defects in cervical carcinomas limit the presentation of a CTL epitope from human papillomavirus 16 E6. *J Immunol* 167: 5420-5428.

Fang D and Zhu J. (2017) Dynamic balance between master transcription factors determines the fates and functions of CD4 T cell and innate lymphoid cell subsets. *J Exp Med* 214: 1861-1876.

Feng Z, Bethmann D, Kappler M, et al. (2017) Multiparametric immune profiling in HPV-oral squamous cell cancer. *JCI insight* 2: 93652.

Fortelny N, Overall CM, Pavlidis P, et al. (2017) Can we predict protein from mRNA levels? Nature 547: E19-E20.

Gajewski TF, Corrales L, Williams J, et al. (2017) Cancer Immunotherapy Targets Based on Understanding the T Cell-Inflamed Versus Non-T Cell-Inflamed Tumor Microenvironment. *Adv Exp Med Biol* 1036: 19-31.

Gall TM and Frampton AE. (2013) Gene of the month: E-cadherin (CDH1). *J Clin Pathol* 66: 928-932.

Georgopoulos NT, Proffitt JL and Blair GE. (2000) Transcriptional regulation of the major histocompatibility complex (MHC) class I heavy chain, TAP1 and LMP2 genes by the human papillomavirus (HPV) type 6b, 16 and 18 E7 oncoproteins. *Oncogene* 19: 4930-4935.

Gros A, Parkhurst MR, Tran E, et al. (2016) Prospective identification of neoantigen-specific lymphocytes in the peripheral blood of melanoma patients. *Nat Med* 22: 433-438.

Hansen TH and Bouvier M. (2009) MHC class I antigen presentation: learning from viral evasion strategies. *Nat Rev Immunol* 9: 503-513.

Heller C, Weisser T, Mueller-Schickert A, et al. (2011) Identification of key amino acid residues that determine the ability of high risk HPV16-E7 to dysregulate major histocompatibility complex class I expression. *J Biol Chem* 286: 10983-10997.

Hoffmann M, Ihloff AS, Gorogh T, et al. (2010) p16(INK4a) overexpression predicts translational active human papillomavirus infection in tonsillar cancer. *Int J Cancer* 127: 1595-1602.

Hyland PL, McDade SS, McCloskey R, et al. (2011) Evidence for alteration of EZH2, BMI1, and KDM6A and epigenetic reprogramming in human papillomavirus type 16 E6/E7-expressing keratinocytes. *J Virol* 85: 10999-11006.

Jie HB, Gildener-Leapman N, Li J, et al. (2013) Intratumoral regulatory T cells upregulate immunosuppressive molecules in head and neck cancer patients. *Br J Cancer* 109: 2629-2635.

Jochmus I, Durst M, Reid R, et al. (1993) Major histocompatibility complex and human papillomavirus type 16 E7 expression in high-grade vulvar lesions. *Hum Pathol* 24: 519-524.

Jones PA. (2012) Functions of DNA methylation: islands, start sites, gene bodies and beyond. *Nat Rev Genet* 13: 484-492.

Kanao H, Enomoto T, Ueda Y, et al. (2004) Correlation between p14(ARF)/p16(INK4A) expression and HPV infection in uterine cervical cancer. *Cancer Lett* 213: 31-37.

Keating PJ, Cromme FV, Duggan-Keen M, et al. (1995) Frequency of down-regulation of individual HLA-A and -B alleles in cervical carcinomas in relation to TAP-1 expression. *Br J Cancer* 72: 405-411.

Kim BS, Miyagawa F, Cho YH, et al. (2009) Keratinocytes function as accessory cells for presentation of endogenous antigen expressed in the epidermis. *J Invest Dermatol* 129: 2805-2817.

Klaes R, Friedrich T, Spitkovsky D, et al. (2001) Overexpression of p16(INK4A) as a specific marker for dysplastic and neoplastic epithelial cells of the cervix uteri. *Int J Cancer* 92: 276-284.

Leek JT, Scharpf RB, Bravo HC, et al. (2010) Tackling the widespread and critical impact of batch effects in high-throughput data. Nat Rev Genet 11: 733-739.

Li H, Ou X, Xiong J, et al. (2006) HPV16E7 mediates HADC chromatin repression and downregulation of MHC class I genes in HPV16 tumorigenic cells through interaction with an MHC class I promoter. *Biochem Biophys Res Commun* 349: 1315-1321.

Li W, Deng XM, Wang CX, et al. (2010) Down-regulation of HLA class I antigen in human papillomavirus type 16 E7 expressing HaCaT cells: correlate with TAP-1 expression. *Int J Gynecol Cancer* 20: 227-232.

Luckheeram RV, Zhou R, Verma AD, et al. (2012) CD4(+)T cells: differentiation and functions. *Clin Dev Immunol* 2012: 925135.

Lyford-Pike S, Peng S, Young GD, et al. (2013) Evidence for a role of the PD-1:PD-L1 pathway in immune resistance of HPV-associated head and neck squamous cell carcinoma. *Cancer Res* 73: 1733-1741.

Mandal R, Senbabaoglu Y, Desrichard A, et al. (2016) The head and neck cancer immune landscape and its immunotherapeutic implications. *JCI insight* 1: e89829.

McLaughlin-Drubin ME, Crum CP and Munger K. (2011) Human papillomavirus E7 oncoprotein induces KDM6A and KDM6B histone demethylase expression and causes epigenetic reprogramming. *Proc Natl Acad Sci U S A* 108: 2130-2135.

McLaughlin-Drubin ME, Huh KW and Munger K. (2008) Human papillomavirus type 16 E7 oncoprotein associates with E2F6. *J Virol* 82: 8695-8705.

McLaughlin-Drubin ME, Park D and Munger K. (2013) Tumor suppressor p16INK4A is necessary for survival of cervical carcinoma cell lines. *Proc Natl Acad Sci U S A* 110: 16175-16180.

Montler R, Bell RB, Thalhofer C, et al. (2016) OX40, PD-1 and CTLA-4 are selectively expressed on tumor-infiltrating T cells in head and neck cancer. *Clin Transl Immunology* 5: e70.

Mora-Garcia Mde L, Duenas-Gonzalez A, Hernandez-Montes J, et al. (2006) Up-regulation of HLA class-I antigen expression and antigen-specific CTL response in cervical cancer cells by the demethylating agent hydralazine and the histone deacetylase inhibitor valproic acid. *J Transl Med* 4: 55.

Mucida D and Salek-Ardakani S. (2009) Regulation of TH17 cells in the mucosal surfaces. *J Allergy Clin Immunol* 123: 997-1003.

Namekawa T, Ikeda K, Horie-Inoue K, et al. (2019) Application of Prostate Cancer Models for Preclinical Study: Advantages and Limitations of Cell Lines, Patient-Derived Xenografts, and Three-Dimensional Culture of Patient-Derived Cells. *Cells* 8.

Network TCGAR. (2015) Comprehensive genomic characterization of head and neck squamous cell carcinomas. *Nature* 517: 576-582.

Network TCGAR. (2017) Integrated genomic and molecular characterization of cervical cancer. *Nature* 543: 378-384.

Nguyen N, Bellile E, Thomas D, et al. (2016) Tumor infiltrating lymphocytes and survival in patients with head and neck squamous cell carcinoma. *Head Neck* 38: 1074-1084.

Pennock ND, White JT, Cross EW, et al. (2013) T cell responses: naive to memory and everything in between. *Adv Physiol Educ* 37: 273-283.

Pluhar GE, Pennell CA and Olin MR. (2015) CD8(+) T Cell-Independent Immune-Mediated Mechanisms of Anti-Tumor Activity. *Crit Rev Immunol* 35: 153-172.

Popov N and Gil J. (2010) Epigenetic regulation of the INK4b-ARF-INK4a locus: in sickness and in health. *Epigenetics* 5: 685-690.

Ramqvist T, Mints M, Tertipis N, et al. (2015) Studies on human papillomavirus (HPV) 16 E2, E5 and E7 mRNA in HPV-positive tonsillar and base of tongue cancer in relation to clinical outcome and immunological parameters. *Oral Oncol* 51: 1126-1131.

Ritz U, Momburg F, Pilch H, et al. (2001) Deficient expression of components of the MHC class I antigen processing machinery in human cervical carcinoma. *Int J Oncol* 19: 1211-1220.

Rock KL, Reits E and Neefjes J. (2016) Present Yourself! By MHC Class I and MHC Class II Molecules. *Trends Immunol* 37: 724-737.

Rudd CE, Taylor A and Schneider H. (2009) CD28 and CTLA-4 coreceptor expression and signal transduction. *Immunol Rev* 229: 12-26.

Sano T, Oyama T, Kashiwabara K, et al. (1998) Expression status of p16 protein is associated with human papillomavirus oncogenic potential in cervical and genital lesions. *Am J Pathol* 153: 1741-1748.

Schlecht NF, Ben-Dayan M, Anayannis N, et al. (2015) Epigenetic changes in the CDKN2A locus are associated with differential expression of P16INK4A and P14ARF in HPV-positive oropharyngeal squamous cell carcinoma. *Cancer Med* 4: 342-353.

Schwartz YB and Pirrotta V. (2007) Polycomb silencing mechanisms and the management of genomic programmes. *Nat Rev Genet* 8: 9-22.

Seiwert TY, Zuo Z, Keck MK, et al. (2015) Integrative and comparative genomic analysis of HPV-positive and HPV-negative head and neck squamous cell carcinomas. *Clin Cancer Res* 21: 632-641.

Sepiashvili L, Bruce JP, Huang SH, et al. (2015) Novel insights into head and neck cancer using next-generation "omic" technologies. *Cancer Res* 75: 480-486.

Simoni Y, Becht E, Fehlings M, et al. (2018) Bystander CD8(+) T cells are abundant and phenotypically distinct in human tumour infiltrates. *Nature* 557: 575-579.

Solomon B, Young RJ, Bressel M, et al. (2018) Prognostic Significance of PD-L1(+) and CD8(+) Immune Cells in HPV(+) Oropharyngeal Squamous Cell Carcinoma. *Cancer Immunol Res* 6: 295-304.

Spranger S, Bao R and Gajewski TF. (2015) Melanoma-intrinsic beta-catenin signalling prevents anti-tumour immunity. *Nature* 523: 231-235.

Torres LM, Cabrera T, Concha A, et al. (1993) HLA class I expression and HPV-16 sequences in premalignant and malignant lesions of the cervix. *Tissue Antigens* 41: 65-71.

van den Elsen PJ. (2011) Expression regulation of major histocompatibility complex class I and class II encoding genes. *Front Immunol* 2: 48.

van den Elsen PJ, Holling TM, Kuipers HF, et al. (2004) Transcriptional regulation of antigen presentation. *Curr Opin Immunol* 16: 67-75.

van Esch EM, Tummers B, Baartmans V, et al. (2014) Alterations in classical and nonclassical HLA expression in recurrent and progressive HPV-induced usual vulvar intraepithelial neoplasia and implications for immunotherapy. *Int J Cancer* 135: 830-842.

Wang K, Wei G and Liu D. (2012) CD19: a biomarker for B cell development, lymphoma diagnosis and therapy. *Exp Hematol Oncol* 1: 36.

Westrich JA, Warren CJ and Pyeon D. (2017) Evasion of host immune defenses by human papillomavirus. *Virus Res* 231: 21-33.

Wijetunga NA, Belbin TJ, Burk RD, et al. (2016) Novel epigenetic changes in CDKN2A are associated with progression of cervical intraepithelial neoplasia. *Gynecol Oncol* 142: 566-573.

Worsham MJ, Chen KM, Ghanem T, et al. (2013) Epigenetic modulation of signal transduction pathways in HPV-associated HNSCC. *Otolaryngol Head Neck Surg* 149: 409-416.

Zaiss M, Hirtreiter C, Rehli M, et al. (2003) CD84 expression on human hematopoietic progenitor cells. *Exp Hematol* 31: 798-805.

Zhang N and Bevan MJ. (2011) CD8(+) T cells: foot soldiers of the immune system. *Immunity* 35: 161-168.

Zhang Y, Xiong Y and Yarbrough WG. (1998) ARF promotes MDM2 degradation and stabilizes p53: ARF-INK4a locus deletion impairs both the Rb and p53 tumor suppression pathways. *Cell* 92: 725-734.

Curriculum Vitae

Steven F. Gameiro, B.Sc. (Hon.)

EDUCATION

Doctor of Philosophy (Ph.D.) **September 2013 – November 2019**
Supervisor: Dr. Joseph Mymryk
Department of Microbiology and Immunology
Schulich School of Medicine and Dentistry
The University of Western Ontario

Bachelor of Science (Hon.) **September 2007 – April 2013**
Major in Biology and Major in Medical Sciences
The University of Western Ontario

SCHOLARSHIPS AND AWARDS

2019 PSAC GTA Scholarship for Outstanding Research Contributions **November 2019**
- valued at $500

Morris Kroll Memorial Scholarship in Cancer Research **July 2019**
(Schulich School of Medicine and Dentistry wide competition for an outstanding cancer research trainee)
- valued at $500

Dr. FW Luney Graduate Travel Award in Microbiology & Immunology **July 2018**
- valued at $2,000

Oncology Research and Education Day Top Poster Presentation Award **June 2018**
- valued at $100

Dr. RGE Murray Graduate Scholarship **September 2017**
(Awarded annually to students in the Microbiology & Immunology Graduate Program, based on academic achievement and research merit)
- valued at $10,000

Cancer Research and Technology Transfer Scholar **September 2017 – August 2018**
(Competitive program that provides trans-disciplinary training links among basic and clinical researchers)
- valued at $18,000 over one year

Dr. FW Luney Graduate Travel Award in Microbiology & Immunology **July 2017**
- valued at $2,000

American Society for Virology Travel Award **June 2017**
- valued at $500 (USD)

Oncology Research and Education Day Poster Presentation Award **June 2016**
- valued at $100

Dr. FW Luney Graduate Travel Award in Microbiology & Immunology **June 2016**
- valued at $2,000

Ontario Graduate Scholarship **May 2016 – May 2017**
(Awarded annually to graduate students in Ontario, based on academic achievement and research merit)
- valued at $15,000 over one year

Schulich Graduate Scholarship **May 2015 – May 2018**
(Awarded annually to graduate students registered in the Schulich School of Medicine and Dentistry)
- valued at $2,000 over one year

Western Graduate Research Scholarship-M&I **September 2013 – September 2018**
(Awarded annually to students in the Microbiology & Immunology Graduate Program)
- valued at $4,500 over one year

Cancer Research and Technology Transfer Scholar **September 2013 – August 2014**
(Competitive program that provides trans-disciplinary training links among basic and clinical researchers)
- valued at $18,100 over one year

Robert and Ruth Lumsden Undergraduate Award **September 2012 – April 2013**
- valued at $1,000 over one year

Cancer Research and Technology Transfer Studentship **May 2012 – August 2012**
- valued at $6,500 over 4 months

Dean's Honor List **2011 – 2013**

ACADEMIC POSITIONS

Teaching Assistantship **September 2018 – December 2018**
MICROIMM 2500A: Biology of Infection and Immunity
Course Coordinator: Dr. Kelly Summers

Teaching Assistantship (2) **January 2017 – April 2017; January 2018 – April 2018**
MICROIMM 4200B: Molecular Virology
Course Coordinator: Dr. Joseph Mymryk

Teaching Assistantship (2) **January 2015 – April 2015; January 2016 – April 2016**
MICROIMM 3620G: Immunology Laboratory
Course Coordinator: Dr. Kelly Summers

Laboratory Manager/Ordering Technician **June 2013 – Present**
Mymryk Laboratory
Summer Research Assistant **May 2013 – September 2013**
Mymryk Laboratory

Research Assistant—CaRTT Summer Studentship **January 2012 – April 2013**
Turley Laboratory

GUEST LECTURER

Fanshawe College: Current Topics in Biotechnology **April 12, 2019**
Course Coordinator: Dr. Pieter Anborgh

MICROIMM 3820A: Nursing Students Course **November 9, 2018**
Fungi Lecture
Course Coordinator: Dr. Kelly Summers

SUPERVISORY EXPERIENCE

4th year Honors Research Project Student Supervisor **October 2017 – April 2018**
Trainee: Matt Wong

Partners in Experiential Learning Student Supervisor **October 2015 – June 2016**
Trainee: Bowen Zhang

Partners in Experiential Learning Student Supervisor **March 2014 – June 2014**
Trainee: Estefani Romero

4th year Honors Research Project Student Supervisor **October 2013 – April 2014**
Trainee: Lisa Newhook

PEER-REVIEWED PUBLICATIONS (*co-first authorship)

1. Sitz J, Blanchet SA, **Gameiro SF**, Biquand E, Morgan TM, Lavoie EG, Blondeau A, Smith BC, Mymryk JS, Moody CA, and Fradet-Turcotte A. Human papillomavirus E7 oncoprotein targets RNF168 to hijack the host DNA damage response. *PNAS.* 2019; 116(39): 19552–19562 **[IF – 9.580]**

2. **Gameiro SF**, Ghasemi F, Barrett JW, Nichols AC, Mymryk JS. High Level Expression of MHC-II in HPV+ Head and Neck Cancers Suggests that Tumor Epithelial Cells Serve an Important Role as Accessory Antigen Presenting Cells. *Cancers*. 2019; 11(8): 1129 **[IF – 6.162]**

3. **Gameiro SF**, Ghasemi F, Barrett JW, Koropatnick J, Nichols AC, Mymryk JS, and Maleki Vareki S. DIY: Visualizing the immune landscape of tumors using transcriptome and methylome data. *Methods in Enzymology*. 2019; (In Press) **[IF – 1.862]**

4. Ghasemi F, Prokopec SD, MacNeil D, Mundi N, **Gameiro SF**, Howlett CJ, Stecho W, Plantinga P, Pinto N, Ruicci KM, Khan MI, Yoo J, Fung K, Sahovaler A, Palma DA, Winquist E, Mymryk JS, Barrett JW, Boutros PC, Nichols AC. Mutational analysis of Head and Neck Squamous Cell Carcinoma stratified by smoking status. *JCI Insight*. 2019; 4 (1): e123443. **[IF – 6.014]**

5. Zhang A, Tessier TM, Galpin KJC, King CR, **Gameiro SF**, Anderson WA, Yousef AF, Qin WT, Li SSC, and Mymryk JS. The transcriptional repressor BS69 is a conserved target of the E1A proteins from multiple human adenovirus species. *Viruses*. 2018; 10(12): E662. **[IF – 3.811]**

6. **Gameiro SF**, Ghasemi F, Barrett JW, Koropatnick J, Nichols AC, Mymryk JS, and Maleki Vareki S. Treatment-naïve HPV+ head and neck cancers display a T-cell-inflamed phenotype distinct from their HPV- counterparts that has implications for immunotherapy. *OncoImmunology*. 2018; 7(10): e1498439 **[IF – 5.333]**

7. King CR, Zhang A, Tessier TM, **Gameiro SF**, and Mymryk JS. Hacking the cell: Network intrusion and exploitation by adenovirus E1A. *mBio*. 2018; 9(3): e00390-18. **[IF – 6.747]**

8. King CR, **Gameiro SF**, Tessier TM, Zhang A, and Mymryk JS. Mimicry of cellular A kinase anchoring proteins is a conserved and critical function of E1A across various human adenovirus species. *Journal of Virology*. 2018; 92(8): e01902-17. **[IF – 4.324]**

9. **Gameiro SF**, Zhang A, Ghasemi F, Barrett JW, Nichols AC, and Mymryk JS. Analysis of class I major histocompatibility complex gene transcription in human tumors caused by human papillomavirus infection. *Viruses.* 2017; 9(9): E252. **[IF – 3.811]**

10. **Gameiro SF***, Kolendowski B*, Zhang A, Barrett JW, Nichols AC, Torchia J, and Mymryk JS. Human papillomavirus dysregulates the cellular apparatus controlling the methylation status of H3K27 in different human cancers to consistently alter gene expression regardless of tissue of origin. *Oncotarget*. 2017; 8(42): 72564-72576. **[IF – 5.168]**

MEDIA PUBLICATIONS

Steven F. Gameiro. Promise in Cancer Research—Young Researcher Series. Published in *The Londoner.* Research Information Outreach Team Article Series. Thursday, November 16, 2017.

Steven F. Gameiro and Joseph S. Mymryk. HPV-Induced Cancers—A Warty Problem! Published in *The Londoner.* Research Information Outreach Team Article Series. Thursday, May 26, 2016.

ORAL PRESENTATIONS

Treatment-naïve HPV+ head and neck cancers display a T-cell-inflamed phenotype distinct from their HPV- counterparts that has implications for immunotherapy. *Presented at the Infection and Immunity Research Forum (IIRF), held in Stratford, Ontario, Canada. November 11, 2018*

Treatment-naïve HPV+ head and neck cancers display a T-cell-inflamed phenotype distinct from their HPV- counterparts that has implications for immunotherapy. *Presented at the Molecular Biology of DNA Tumor Viruses Conference, held in Madison, Wisconsin, USA. July 31-August 4, 2018*

Human papillomavirus dysregulates the cellular apparatus controlling the methylation status of H3K27 in different human cancers to consistently alter gene expression regardless of tissue of origin. *Presented at the Infection and Immunity Research Forum (IIRF), held in London, Ontario, Canada. October 27, 2017*

Human papillomavirus dysregulates the cellular apparatus controlling the methylation status of H3K27 in different human cancers to consistently alter gene expression regardless of tissue of origin. *Presented at the Molecular Biology of DNA Tumor Viruses Conference, held in Birmingham, England. July 17-22, 2017*

HPV16 intratypic variants in head & neck cancers: A Southwestern Ontario perspective. *Presented at the American Society for Virology Annual Meeting, held in Madison, Wisconsin, USA. June 24-28, 2017*

HPV16 intratypic variants in head & neck cancers: A Southwestern Ontario perspective. *Presented at the Molecular Biology of DNA Tumor Viruses Conference, held in Montreal, Quebec, Canada, July 18-23, 2016*

Reduction of MHC I by HPV16 E7 and its role in head & neck cancers. *Presented at the Molecular Biology of DNA Tumor Viruses Conference, held in Madison, Wisconsin, USA. July 21-26, 2014*

INVITED ORAL PRESENTATIONS

HPV-induced Cancers. *Presented at World Cancer Day, held at the Covent Garden Market, London, Ontario, Canada. February 4, 2018*

The Epigenetic dysregulation of p16 by HPV in head and neck cancers is a potential target for therapy. *Presented at the Oncology Grand Rounds, held at Victoria Hospital, London Regional Cancer Program, London, Ontario, Canada. December 5, 2017*

Surgical Management of Aortic Dissection—A Patient's Perspective. *Presented at the Canadian Society of Vascular Nursing (London Chapter) held at the Four Points Sheraton in London, Ontario, Canada. November 2, 2011*

POSTER PRESENTATIONS

Human papillomavirus-positive head and neck cancers express high levels of class II major histocompatibility complex. *Abstract and poster presented at the Molecular Biology of DNA Tumor Viruses Conference, held in Trieste, Italy. July 9-14, 2019*

*Treatment-naïve HPV+ head and neck cancers display a T-cell-inflamed phenotype distinct from their HPV- counterparts that has implications for immunotherapy. *Abstract and poster presented at Oncology Research and Education Day, held in London, Ontario, Canada. June 8, 2018*

*HPV16 intratypic variants in head & neck cancers: A Southwestern Ontario perspective. *Abstract and poster presented at Oncology Research and Education Day, held in London, Ontario, Canada. June 17, 2016*

HPV16 intratypic variants in head & neck cancers: A Southwestern Ontario perspective. *Abstract and poster presented at the Infection and Immunity Research Forum (IIRF), held in London, Ontario, Canada. November 6, 2015*

Reduction of MHC I by HPV16 E7 and its role in head & neck cancers. *Abstract and poster presented at the Molecular Biology of DNA Tumor Viruses Conference, held in Trieste, Italy. July 21-26, 2015*

Reduction of MHC I by HPV16 E7 and its role in head & neck cancers. *Abstract and poster presented at the Infection and Immunity Research Forum (IIRF), held in London, Ontario, Canada. November 6, 2014*

Reduction of MHC I by HPV16 E7 and its role in head & neck cancers. *Abstract and poster presented at the Molecular Biology of DNA Tumor Viruses Conference, held in Madison, Wisconsin, USA. July 21-26, 2014*

Elucidating the mechanism by which HPV16 E7 modulates MHC I and defining its role in OSCC. *Abstract and poster presented at the London Health Research Day (LHRD), held in London, Ontario, Canada. March 18, 2014*

Elucidating the mechanism by which HPV16 E7 modulates MHC I and defining its role in OSCC. *Abstract and poster presented at the Infection and Immunity Research Forum (IIRF), held in London, Ontario, Canada. November 1, 2013*

***Denotes award-winning presentation**

SCHOLARLY ACTIVITIES

Chair **October 2017 – August 2018**
Translational Seminar Speaker Selection Committee
Cancer Research and Technology Transfer Program

- Act as liaison between the selection committee and administrative staff

Student Representative **September 2017 – August 2019**
American Society for Virology
Department of Microbiology and Immunology

- Convey information regarding the annual general meeting, funding opportunities, and other relevant information from the society to M&I graduate students

Student Representative **September 2015 – August 2017**
Seminars Committee
Department of Microbiology and Immunology

- Responsible for attending meetings throughout the year to discuss potential speakers for the R.G.E Murray Seminar Series

Grad Coordinator **January 2014 – May 2015**
Microbiology & Immunology Student Association (MISA)

- Mentor in the MISA mentorship program
- Aid in organizing events to educate undergraduate students about graduate studies in the Microbiology and Immunology program at The University of Western Ontario

Organizing Committee Member **November 2013 – August 2018**
Infection and Immunity Research Forum (IIRF)

- The IIRF is an annual scientific conference that is organized and run by the graduate students of The University of Western Ontario in the department of Microbiology and Immunology. This conference showcases undergraduate, graduate, and post-doctoral research in the fields of microbiology, immunology, and virology

Committee Member **October 2013 – August 2016**
Microbiology and Immunology Social Committee

- Organizing and running social events, including fundraising for the department of Microbiology and Immunology

MEMBERSHIPS

American Society for Virology Student Member **February 2017 – Present**

VOLUNTEER WORK

Research Information Outreach Team **September 2017 – Present**
Canadian Cancer Society—London Chapter

- Help plan and organize annual activities such as: World Cancer Day and Let's Talk Cancer
- Spread the word about progress and promise in cancer research through a monthly column in *The Londoner* and through social media postings

Undergraduate Science Case Competition Judge **March 2016**
SciNapse Science—The University of Western Ontario

- Evaluated undergraduate poster presentations and their understanding of the research project

The American Society for Virology (ASV) Volunteer **June 2015**
34th annual ASV meeting—The University of Western Ontario

- Organized and ran oral presentation workshops

Outreach Volunteer **December 2012 – January 2015**
Let's Talk Science -The University of Western Ontario

- Deliver science learning programs and services that turn children and youth on to science

Volunteer Speaker **December 2012 – March 2014**
Canadian Blood Services Volunteer Speakers' Bureau Program

- Share my personal story at organized events to expand Canadian Blood Services' capacity to recruit blood donors and help raise awareness of the increasing need for blood and new blood donors

In-Community Volunteer **November 2012 – May 2013**
Canadian Blood Services

- Sign up blood donors for upcoming clinics
- Monitor donors after they have given blood
- Promote public awareness about the importance of blood donation through handing out flyers